COMMUNAUTE FRANCAISE DE BELGIQUE

FACULTE UNIVERSITAIRE DES SCIENCES
AGRONOMIQUES DE GEMBLOUX

ETUDE DE L'IMPACT DES CONDITIONS HYDRODYNAMIQUES DU BIO-REACTEUR SUR LA CONDUITE ET L'EXTRAPOLATION DES BIOPROCEDES

Frank DELVIGNE

Dissertation originale présentée en vue de
l'obtention du grade de docteur en sciences
agronomiques et ingénierie biologique

Promoteur : Prof. P. Thonart

2006

Remerciements

Au terme de ce travail, je voudrais remercier les personnes suivantes :

Mr Thonart, promoteur de ce travail pour m'avoir permis d'aborder des matières très intéressantes dans un contexte très dynamique. Grâce à lui, je ne crois pas m'être ennuyé depuis ma sortie des études en 2000

Mr Béra et Mr Crine, rapporteurs, pour leur lecture attentive du travail et leurs remarques judicieuses qui ont contribué à améliorer la qualité de ce travail

Monsieur G. Lognay, pour une relecture attentive de ce travail malgré un emploi du temps très chargé

Mr Bruxelmane, pour les nombreux renseignements sur « l'opération de mélange »

Madame M.F. Destain et Monsieur Lebeau pour m'avoir permis d'accéder au logiciel MatLab

Les reviewers des articles inclus dans cette thèse pour leurs remarques très judicieuces

Monsieur Samuel « Zam » Telek, pour la réalisation des tests de fermentation et en général pour son aide très précieuse

Messieurs J.C. Bougelet et J.M. Ista pour la conception de la cuve agitée expérimentale m'ayant permis d'effectuer mes premières expériences

Monsieur Guy Delimme pour son aide lors de la réalisation des tests de temps de mélange

Mes collègues Jacqueline et Jean-Marc pour la très bonne ambiance de travail et les nombreux « Cappu »

Les deux secrétaires de choc Marina et Margue

Les étudiants ayant participé à ce travail : Annick, Cédric et Jean-Michel

D'une manière générale, l'ensemble du personnel et des étudiants de l'unité de bio-industries pour la bonne ambiance de tous les jours

Un merci particulier à ma compagne Marjorie pour sa patience et ses encouragements durant toute la durée de ce travail

Mes parents, pour m'avoir permis de réaliser mes études à la Faculté

DELVIGNE Frank (2006) Etude de l'impact des conditions hydrodynamiques du bio-réacteur sur la conduite et l'extrapolation des bioprocédés (Thèse de doctorat). Gembloux, Faculté Universitaire des Sciences Agronomiques

Résumé : à l'heure actuelle, les règles d'extrapolation des bio-réacteurs agités sont basées sur des paramètres globaux du génie chimique relatif à l'opération de mélange. L'objectif du travail est de proposer des règles d'extrapolation et de dimensionnement des bio-réacteurs intégrant à la fois les notions du génie chimique et les contraintes afférentes aux micro-organismes. A cette fin, trois composantes ont été identifiées : une première composante hydrodynamique pour l'homogénéisation du réacteur, une seconde composante hydrodynamique pour décrire le déplacement ou la circulation des micro-organismes à l'intérieur du bio-réacteur et une troisième composante pour la description de l'impact hydrodynamique au niveau de la physiologie des micro-organismes. La superposition des deux premières composantes permet d'obtenir les profils de concentration rencontrés par les micro-organismes lors de leur séjour dans le réacteur et la dernière composante permet de décrire la réaction des micro-organismes vis-à-vis du profil de concentration rencontré.

Chacune des composantes à fait l'objet d'une modélisation mathématique structurée et stochastique. La formulation stochastique des modèles a été choisie du fait des nombreux phénomènes aléatoires entrant en ligne de compte.

Lors du travail, le concept de réacteur *scale-down* a été utilisé afin d'étudier l'impact des conditions hydrodynamiques sur la physiologie microbienne. Ce réacteur comprend une partie agitée et une partie non agitée et permet de reproduire à l'échelle du laboratoire les conditions d'écoulement rencontrées dans les réacteurs industriels.

Ce dispositif à permis d'observer des chutes de rendement de croissance dues aux conditions hydrodynamiques dans le cas de procédés *fed-batch* de production de *Escherichia coli* et de *Saccharomyces cerevisiae*. Ces résultats expérimentaux ont permis de valider les modèles mathématiques décrits précédemment, soulignant le fait que ceux-ci peuvent être utilisés comme outils de dimensionnement et d'extrapolation fiables.

DELVIGNE Frank (2006) Study of the bioreactor hydrodynamic impact on bioprocesses scale-up and design (Thèse de doctorat). Gembloux, Faculté Universitaire des Sciences Agronomiques

Summary : until now, the stirred bioreactor scale-up and design rules are based entirely on physical parameters. The aim of this work is to propose new scale-up rules taking into account the micro-organisms physiological constraints. In this perspective, three components have been identified : a first component linked to the homogenisation efficiency of the reactor, a second component for the description of the microorganisms circulation inside the reactor, and a third component for the description of the hydrodynamic impact on the microorganisms. The superimposition of the two first components allows to describe the concentration profile experienced by the microorganisms during their sojourn in the bioreactor, whereas the last component allows the description of the microorganisms responses in front of these profiles.

Each of these components have been mathematically modelled. A stochastic formulation has been chosen because of the great proportion of random phenomena governing the processes studied.

A scale-down reactor has been designed in order to study the impact of the hydrodynamics on the microbial physiology. This reactor comprises a stirred part and a non-stirred part and is able to reproduce at small scale the industrial fluid dynamics.

This apparatus have allowed us to observe microbial yield drop induced by the bioreactor hydrodynamics in the case of fed-batch processes for the production of *Escherichia coli* and *Saccharomyces cerevisiae*. These experimental data permit to validate the above mentioned mathematical models as efficient tools for the bioreactors design and scale-up.

Table des matières

Symboles et notations

Cette liste reprend les symboles et notations les plus souvent utilisés. Des notations plus particulières peuvent être trouvées pour les chapitres 2 à 8

a : aire interfaciale spécifique (m^2/m^3)

b : largeur des contre-pales (m)

C_L : concentration en oxygène dissous (kg/m^3)

C^0_L : concentration en oxygène dissous à saturation (kg/m^3)

CTD : circulation time distribution – distribution des temps de circulation

d : diamètre de l'agitateur (m)

D : diamètre de la cuve (m)

e : épaisseur des contre-pales (m)

Fr : nombre de Froude (adimensionnel)

g : accélération de la pesanteur (m^2/s)

G : débit gazeux (m^3/s)

H : hauteur de la cuve (m)

k_l : coefficient de transfert de masse en phase liquide (kg/s)

k_la : coefficient volumique de transfert d'oxygène (s^{-1})

K_s : constante d'affinité du micro-organisme pour le substrat (kg/m^3)

l : longueur de la pale (m)

M : torsion subie par l'axe (N m)

N : vitesse d'agitation (s^{-1})

NOZ : network-of-zones (modèle en réseau de zones)

n_p : nombre de pales

N_p : nombre de puissance (adimensionnel)

N_{qp} : nombre de pompage (adimensionnel)

N_{qc} : nombre de circulation (adimensionnel)

P ou P_o : puissance dissipée en milieu non aéré (W)

P_g : puissance dissipée en milieu aéré (W)

P_{indice} : probabilité d'occurrence d'un événement (l'indice spécifie le type d'événement)

Q_0 : consommation de l'oxygène dissous par les micro-organismes (kg/l.h)

Q_c : débit de circulation (m^3/s)

Q_e : débit d'entraînement (m^3/s)

Q_p : débit de pompage (m^3/s)

Re : nombre de Reynolds (adimensionnel)

rpm : tours par minute

S : concentration en substrat (kg/m^3)

S_i : vecteur d'état à l'instant i

T : matrice de transition

t_c : temps de circulation (s)

t_m = temps de mélange (s)

t_p : temps de pompage (s)

TD4 : turbine à disque à 4 pales droites

TD6 : turbine à disque à 6 pales droites
V_L : volume de liquide du réacteur (m³)
w : largeur de la pale (m)
We : nombre de Weber (adimensionnel)
X : concentration cellulaire (kg/m³)
Y : distance entre l'agitateur et le fond de la cuve (m)

ρ : masse volumique (kg/m³)
μ : viscosité dynamique (Pa s)
μ_{max} : taux de croissance maximum du micro-organisme (s^{-1})
σ : tension de surface (N/m)

CHAPITRE 1
Introduction générale et analyse bibliographique

1.1. <u>Aperçu de la problématique abordée dans ce travail</u>

La thèse a pour thème l'étude de l'impact des conditions hydrodynamiques du bio-réacteur sur la conduite et l'extrapolation des bioprocédés. Vu la grande diversité des bioprocédés, et afin de limiter l'étude des phénomènes se déroulant à l'intérieur des réacteurs, seuls les procédés *fed-batch* ont été envisagés. Ces procédés sont effectués en ajoutant progressivement une solution concentrée en substrat carboné en cours de culture. Ce mode de conduite du réacteur favorise l'apparition de gradients de concentration du fait de l'ajout intermittent de la source de carbone (généralement effectué par le dessus du réacteur). La représentation schématique de l'apparition d'un gradient de concentration dans le plan axial d'un réacteur est présentée à la figure 1. Il est important de noter que cette représentation n'est pas figée dans le temps, mais évolue en fonction des performances de mélange du système, de la fréquence d'impulsion de la pompe d'ajout et de la consommation en substrat par les microorganismes. De ce fait, la caractérisation de ces phénomènes nécessite l'emploi de modèles hydrodynamiques plus élaborés que l'approche classique du génie chimique qui se base principalement sur des corrélations empiriques globales.
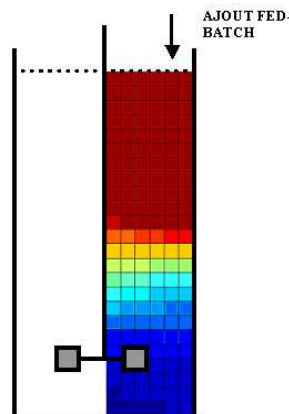
Figure 1 : représentation schématique de l'apparition de gradient de concentration dans le plan axial d'un réacteur agité opérant en mode *fed-batch* (les zones rouges représentent les zones fortement concentrées et les zones bleues les zones faiblement concentrées)

Ce phénomène d'apparition de gradient de substrat au sein des réacteurs sera amplifié au cours de l'extrapolation du procédé à des volumes de cuve industriels. En effet, la figure 2 montre que l'augmentation d'échelle du réacteur entraîne une augmentation irrémédiable du temps mis par le système pour revenir à un degré d'homogénéité acceptable (exprimé par le temps de mélange t_m). Cette augmentation du temps de mélange peut être expliquée comme suit : quand l'échelle du réacteur augmente, les éléments fluides doivent être transportés sur de plus longues distances. Leur vitesse de déplacement doit donc être augmentée afin d'assurer le même degré d'homogénéisation par rapport aux réacteurs de plus petites tailles. Malheureusement, cette vitesse est directement proportionnelle à la puissance volumique (puissance dissipée par l'opération d'agitation rapportée au volume utile du réacteur), ce qui contraint d'augmenter celle-ci en fonction de l'échelle du réacteur. Au niveau industriel, de telles puissances volumiques sont généralement impossible à mettre en œuvre du fait des contraintes mécaniques. Tous ces phénomènes conduisent donc à une diminution de l'efficacité de mélange des réacteurs au fur et à mesure du processus d'extrapolation.
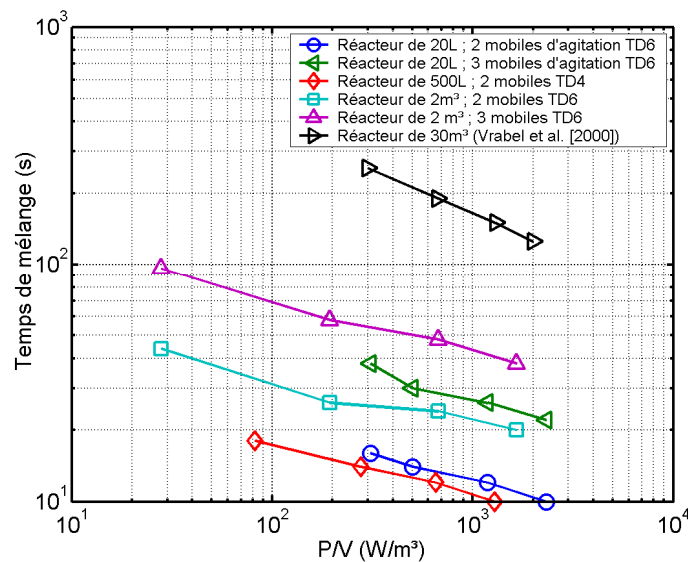
Figure 2 : évolution du temps de mélange en fonction de la puissance d'agitation requise par unité de volume P/V pour des réacteurs agités de différents volumes et

munis de différentes combinaisons de mobiles d'agitation. Les résultats relatifs au réacteur de 30 m³ ont été extraits de la littérature [1]

La formation de gradient axial à l'intérieur des réacteurs n'est pas la seule composante à prendre en compte dans le cadre du génie chimique. En effet, les micro-organismes se déplacent à l'intérieur du réacteur selon un mouvement de circulation dépendant de l'action des agitateurs. Les micro-organismes ne sont donc pas statiques par rapport au gradient de concentration. Lors de son évolution dans le bio-réacteur, une cellule microbienne sera soumise à des fluctuations de concentration dont l'intensité et la fréquence dépendront des conditions opératoires et du volume de culture. Il est important de caractériser ces fluctuations de concentration et de connaître leurs effets sur la physiologie microbienne. Ces deux aspects constituent la toile de fond du présent travail. La circulation d'un micro-organisme à l'intérieur d'un réacteur agité à été représentée à la figure 3 et montre que le déplacement du micro-organisme va conditionner le profil temporel des concentrations extracellulaires auxquelles il sera soumis.
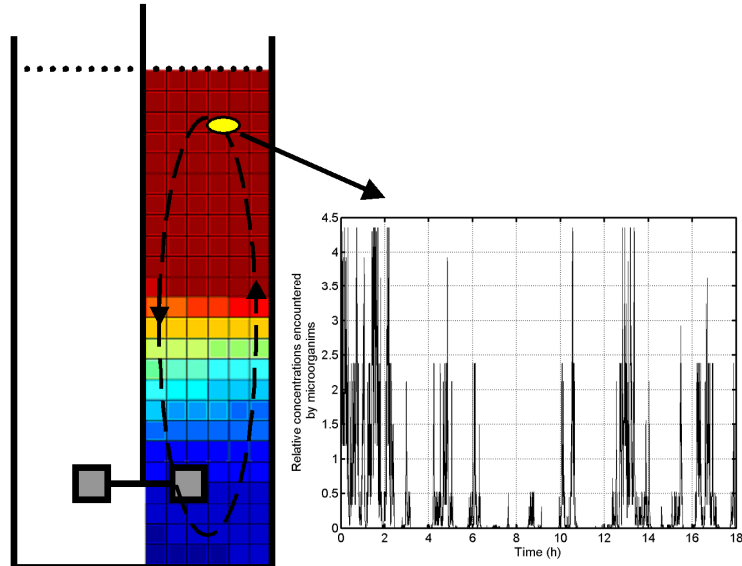
Figure 3 : représentation schématique du déplacement d'un micro-organisme dans un réacteur agité sous l'action des flux de circulation engendrés par le mobile d'agitation (à gauche). Le profil de concentration résultant auquel est soumis le

micro-organisme durant son déplacement dans le réacteur est également représenté (à droite)

La complexité du problème traité au cours de ce travail réside dans les interactions qui existent entre la population microbienne et le réacteur. Ces deux composantes feront l'objet d'une étude bibliographique approfondie dans les deux paragraphes qui suivent.

1.2. <u>Notions relatives aux aspects du génie chimique : dimensionnement du bio-réacteur</u>

Le dimensionnement des bio-réacteurs est la première étape à envisager pour résoudre la problématique précédemment exposée. Selon l'approche classique du génie chimique, le dimensionnement d'un réacteur agité est réalisé en plusieurs étapes [2] :

- Utilisation d'un réacteur de géométrie standard
- Calcul des paramètres de base de l'opération des mélange (nombre de Reynolds, puissance, débit de pompage et de circulation) obtenus par l'analyse dimensionnelle.
- Estimation des paramètres de performances en relation avec le but de l'opération de mélange considéré. Dans ce travail, les deux types d'opération de mélange considérées sont l'homogénéisation et le transfert d'oxygène.

Ces notions de base pour le dimensionnement d'un réacteur agité seront détaillées au cours des paragraphes 1.2.1. et 1.2.2. Néanmoins, il sera montré au cours des chapitres suivants que l'approche classique du génie chimique n'est pas suffisante pour un dimensionnement correct du bio-réacteur en accord avec les contraintes du micro-organisme.

1.2.1.   Géométrie standard et analyse dimensionnelle d'un réacteur agité

La considération de rapports géométriques prédéterminés au niveau du système cuve-mobile d'agitation est très importante pour la réalisation d'expériences relatives au dimensionnement du bio-réacteur. En effet, cela permet de comparer les résultats obtenus dans d'autres systèmes respectant également cette standardisation de géométrie, mais cela permet surtout d'extrapoler ces résultats à l'échelle industrielle. Les cuves agitées sont donc conçues de manière à respecter une géométrie dite « standard ». La figure 4 reprend les critères recommandés pour qu'une cuve mécaniquement agitée réponde à la géométrie standard du point de vue de ses dimensions [2]. Les cuves standards sont cylindriques, comprennent un axe d'agitation sur lequel sont fixés un ou plusieurs mobiles d'agitation et leur paroi est munie de contre-pales permettant d'éviter la mise en rotation du fluide agité. Toutes les cuves agitées utilisées au cours de ce travail répondent aux conditions standards de géométrie ou s'en approchent fortement.

$$H = D$$
$$Y = D/3$$
$$e = D/10$$
$$0.3\,D < d < 0.5D$$
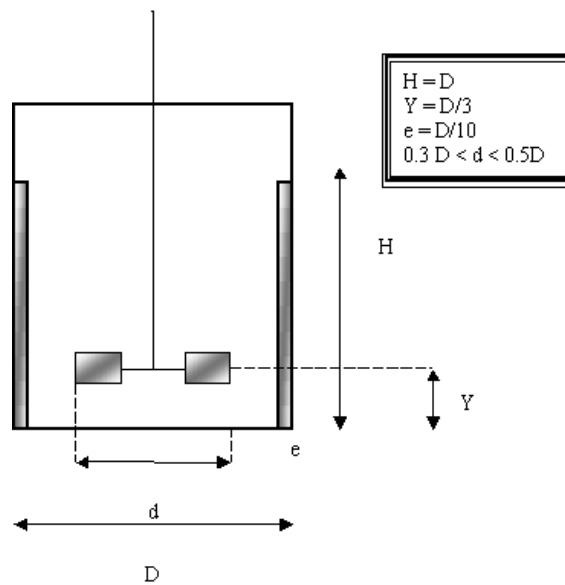
Figure 4 : schéma reprenant les principaux paramètres géométriques nécessaires pour respecter la configuration standard (H : hauteur de liquide ; D : diamètre de la

cuve ; d : diamètre du mobile d'agitation ; e : épaisseur des contre-pales ; Y : éloignement du mobile par rapport au fond de la cuve)

La puissance dissipée au niveau de l'élément mélangeur est un élément important dans la caractérisation de l'efficacité de l'opération de mélange. En effet, la dissipation de puissance d'un mobile d'agitation est directement liée à son efficacité à réaliser une opération de mélange donnée. Dans les considérations suivantes, le terme puissance ou puissance dissipée sera adopté pour quantifier l'énergie fournie par l'élément mélangeur au fluide agité. La relation permettant de calculer la puissance en milieu non aéré a été mise au point grâce à l'analyse dimensionnelle du problème. Cette analyse est réalisée en utilisant le théorème de Vaschy-Buckingham [3].

L'analyse dimensionnelle permet de réduire les 16 variables impliquées dans le problème d'agitation à 16 - n = 13 (n étant le nombre de dimensions impliquées, celles-ci étant la longueur, la masse et le temps). Parmi ces 13 nombres adimensionnels, 9 sont des rapports géométriques ne présentant pas d'intérêt si la géométrie standard de la cuve est respectée. Les 4 autres nombres sont :

- Le nombre de Reynolds (Re) = $\rho N d^2/\mu$. Celui-ci caractérise l'action des forces de viscosité et est utilisé pour déterminer le type de régime d'écoulement pour un liquide de masse volumique ρ (kg/m³) et de viscosité dynamique μ (Pa.s), dans une cuve de géométrie standard, pour un diamètre de mobile d'agitation d (m) donné et pour une vitesse d'agitation N (s^{-1}) donnée.

- Le nombre de puissance ou de Newton (N_p) = $P/\rho N^3 d^5$, caractérisant le rapport des forces d'entraînement du fluide par différence de pression (avec P (W) représentant la puissance dissipée par le mobile d'agitation) sur les forces d'inertie. Ce rapport est mieux connu sous le terme de coefficient de traînée du système d'agitation [2]. Nous verrons par après que ce nombre est fonction de la géométrie du système d'agitation et prend des valeurs particulières en fonction nombre de Reynolds.

- Le nombre de Weber (We) = $\rho N^2 d^3/\sigma$, caractérisant le rapport des forces de cisaillement sur les forces de tension superficielle σ (N/m).

- Le nombre de Froude (Fr) = $N^2 d/g$, caractérisant l'action des forces d'inertie sur les forces de gravité (avec g (m/s²) représentant l'accélération de la pesanteur).

Parmi l'ensemble des 13 nombres adimensionnels obtenus, l'expérience montre qu'il vaut mieux choisir N_p comme variable indépendante [2]. On obtient alors une relation entre N_p et un produit de nombres sans dimensions (avec les puissances x, y, z, x_1, x_2,…) :

$$N_p = k \cdot Re^x \cdot Fr^y \cdot We^z \cdot (H/d)^{x1} \cdot (D/d)^{x2} \ldots$$

Pour une cuve d'agitation standard munie de contre-pales, cette équation peut être simplifiée et se résume à une simple relation entre le nombre de puissance et le nombre de Reynolds [2]. Cette relation est généralement déterminée pour un mobile d'agitation donné et est présentée sous la forme d'une courbe caractéristique de puissance (figure 5).
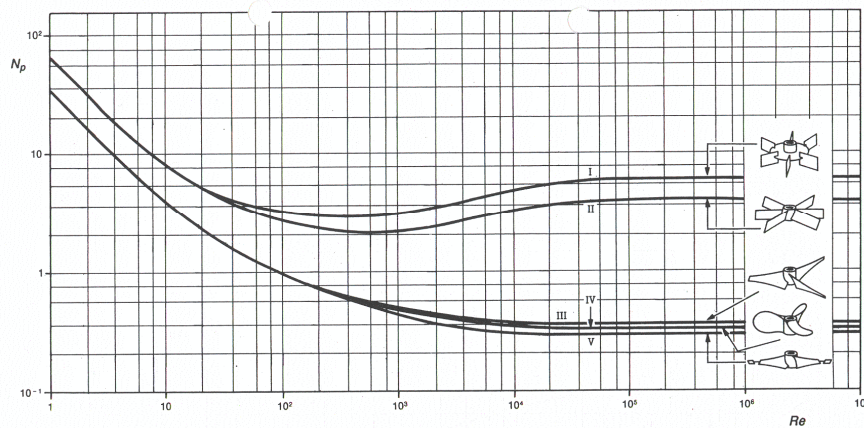
Figure 5 : courbe caractéristique de puissance N_p = f(Re). Selon l'analyse dimensionnelle, cette courbe ne dépend que du type de mobile d'agitation [4].

La figure 5 montre que pour la région de flux turbulent (Re > 10^4 à 10^5, en fonction du type de mobile utilisé) le nombre de puissance N_p est indépendant du nombre de Reynolds Re. A partir de là, la puissance dissipée peut être facilement calculée à partir du nombre de puissance :

$$P = N_p \cdot \rho \cdot N^3 \cdot d^5$$

La valeur du nombre de puissance est donnée par le constructeur du mobile d'agitation et peut être trouvée dans des tables.

7

D'autres paramètres de l'opération de mélange peuvent être déterminés par un raisonnement analogue et des courbes caractéristiques de pompage et de circulation peuvent être définies pour un système d'agitation donné. En régime turbulent, les nombres adimensionnels relatifs aux actions de pompage et de circulation du mobile considéré ne dépendent plus du nombre de Reynolds et sont seulement fonction du type de mobile [2]. Le débit de pompage Q_p (m³/s) est défini comme étant le débit de liquide qui passe effectivement par le mobile d'agitation. Il peut être déterminé par l'équation :

$$Q_p = N_{qp} \, N \, d^3$$

Le coefficient N_{qp} est le nombre de pompage, N la vitesse d'agitation (s^{-1}) et d le diamètre du mobile d'agitation (m). Celui-ci dépend du type de mobile d'agitation et est constant en régime turbulent.

A partir de là, un temps de pompage moyen, correspondant au temps qui s'écoule entre deux passages successifs au niveau de l'agitateur, peut être défini :

$$t_p = V_l / Q_p$$

Avec V_l (m³) correspondant au volume effectif de liquide dans la cuve. Ce paramètre peut être pour calculer la fréquence de passage des micro-organismes au niveau de zones de fluide particulières à l'intérieur du bio-réacteur, comme par exemple, la zone d'ajout d'une solution *fed-batch* [5], les zones enrichies en oxygène dissous [5-8]. Le passage au niveau de ces zones de fluide est souvent associé à l'induction d'un stress physiologique et est donc un paramètre important pour le dimensionnement d'un bio-réacteur.

Le débit de pompage induit, par transfert de quantité de mouvement, un débit d'entraînement. Le débit de circulation dans la cuve est la somme du débit de pompage et du débit d'entraînement :

$$Q_c = Q_e + Q_p$$

Par analogie avec le débit de pompage :

$$Q_c = N_{qc} \, N \, d^3$$

Avec N_{qc} étant le nombre de circulation.

A partir de là, un temps de circulation moyen peut être défini :

$$t_c = V_l / Q_c$$

Dans ce paragraphe, plusieurs paramètres relatifs à l'opération de mélange ont été définis. Ces paramètres sont faciles à calculer pour une cuve d'agitation standard, mais leur application reste globale et ne permet pas d'obtenir de renseignement sur l'hétérogénéité régnant dans un bio-réacteur. Au cours du travail, ces paramètres (puissance, débit de pompage et débit de circulation) seront utilisés pour l'élaboration de modèles hydrodynamiques structurés permettant de caractériser cette hétérogénéité (pour plus de détails, voir paragraphe 1 .2.3.).

Le calcul du temps de circulation réel peut être employé afin d'illustrer cette notion d'hétérogénéité des paramètres au sein d'un réacteur. En effet, dans la réalité, le micro-organisme peut emprunter une série de chemins de circulation dont la diversité et la longueur dépendent des dimensions du réacteur. Il n'existe pas un chemin unique de circulation moyen, mais bien une distribution de chemin de circulation ou de temps de circulation. Dans le cas des réacteurs de petit volume, le calcul du temps de circulation par l'analyse dimensionnelle est une bonne estimation du temps moyen mis par un micro-organisme pour être transporté au sein du volume réactionnel. Néanmoins, les dimensions du réacteur augmentant, l'écart-type de la distribution des temps de circulation augmente et le calcul du temps moyen de circulation par analyse dimensionnelle ne constitue plus une bonne estimation du comportement global des micro-organismes à l'intérieur du réacteur. L'estimation de la distribution des temps de circulation peut être effectuée par mesure, ou par modélisation mathématique de l'écoulement au sein des réacteurs [9].

Dans le paragraphe qui suit, l'opération de mélange sera abordée pour les cas particuliers de l'homogénéisation et du transfert d'oxygène. Ces deux opérations ont en effet beaucoup d'importance dans le cadre des bioprocédés du fait de la sensibilité des micro-organismes face aux fluctuations des conditions environnementales et aux disponibilités en oxygène dissous.

1.2.2. Opération de mélange appliquée à l'homogénéisation et au transfert d'oxygène

Les buts de l'opération de mélange peuvent être analysés sur base de paramètres de performance. Un paramètre de performance est une grandeur qui permet de

quantifier l'efficacité d'une opération de mélange dans un but bien précis. Le paramètre de performance utilisé pour quantifier l'efficacité d'homogénéisation d'un système d'agitation est le temps de mélange. Le concept de temps de mélange est illustré à la figure 6 par un l'injection d'un traceur coloré dans une cuve agitée. Dans ce cas, l'estimation du temps de mélange peut être effectuée en suivant visuellement l'homogénéisation du colorant après ajout de celui-ci dans un système d'agitation. La valeur du temps de mélange correspond au temps écoulé entre l'injection du traceur et son homogénéisation dans le volume de la cuve.

Figure 6 : répartition d'un colorant dans une cuve agitée pour l'estimation du temps de mélange [10]

En pratique, le temps de mélange est estimé par des méthodes plus précises [11]. Celles-ci mettent en œuvre un traceur de nature particulière et une sonde adaptée : sonde pH dans le cas d'un traceur acido-basique [12], sonde de conductivité dans le cas d'un traceur salin [13], thermocouple dans le cas d'un traceur thermique [14].

Ces trois méthodes sont celles qui sont le plus couramment rencontrées dans la littérature, mais il en existe encore bien d'autres (traceurs radioactifs,…).

Le temps de mélange est un paramètre de performance important à considérer pour le dimensionnement d'un bio-procédé, spécialement si celui-ci est effectué en mode *fed-batch* (c'est-à-dire avec un apport externe en nutriments). En effet, dans ce cas, la source de carbone est ajoutée de manière ponctuelle au cours de la culture. Si le temps de mélange est trop important, des gradients de concentration en substrat se forment à l'intérieur du bio-réacteur. Suivant l'intensité de ce gradient et la nature du micro-organisme cultivé, les rendements du bio-procédé peuvent en être affectés. Comme la figure 2 le montre, les performances d'homogénéisation du réacteur vont

se détériorer au cours de son extrapolation, principalement à cause de limitations au niveau de la puissance pouvant être fournie par le système d'agitation.

Le transfert d'oxygène est également un processus important qui dépend de l'opération de mélange. Cette opération est particulièrement limitante pour les cultures de micro-organismes aérobies. En effet, la solubilité de l'oxygène dans les milieux aqueux est très faibles, environ 7 à 8 mg/l dans la gamme de pression et de température courante, la demande moyenne des micro-organisme dépassant plusieurs fois cette valeur. Ce n'est donc pas sur la quantité d'oxygène transféré que va se baser le dimensionnement du bio-réacteur, mais plutôt sur la vitesse de transfert de l'oxygène. Le paramètre de performance qui est utilisé pour l'opération de transfert d'oxygène est le taux de transfert d'oxygène $k_l a$ (s^{-1}). De nouveau, cette opération est particulièrement limitante dans le cas des procédés *fed-batch* pour lesquels la densité cellulaire peut atteindre des valeurs très importantes. Une augmentation de la densité cellulaire nécessite de pousser au maximum la capacité de transfert d'oxygène du système.

En pratique, l'évolution de la concentration en oxygène dissous dans un réacteur peut être décrite par plusieurs types d'équation. L'équation la plus couramment utilisée est celle qui découle du modèle du double film [15] :

$$\frac{dC_L}{dt} = k_l\, a \cdot \left(C_L^0 - C_L\right) - Q_O$$

Où dC_L/dt représente l'évolution de la concentration en oxygène dissous dans la phase liquide C_L (g/l) au cours du temps ; $k_l a$ (h^{-1}) est le coefficient volumique de transfert d'oxygène ; C_L^0 (g/l) est la concentration en oxygène dissous maximale pouvant être atteinte à saturation du milieu ; Q_0 est la consommation de l'oxygène dissous par les micro-organismes (g/l.h)

Ce modèle se concentre sur le transfert de masse au travers du film gazeux et du film liquide situés de part et d'autre de l'interface gaz-liquide. Dans le cas de l'oxygène, il a été démontré que le film liquide est l'élément limitant du processus de transfert de masse. Dans ce cas, l'équation de l'évolution en oxygène dissous au cours du temps dC_L/dt est formulée uniquement à partir de ce film liquide et est

proportionnelle au $k_l a$ (coefficient volumique de transfert d'oxygène) et au gradient de concentration ($C_L^0 - C_L$).

Une grande diversité de techniques expérimentales sont disponibles pour la détermination du $k_l a$ [16, 17]. Ces techniques ne permettent néanmoins qu'une estimation globale de la capacité de transfert d'oxygène d'un réacteur.

1.2.3.   Vers une approche structurée de l'opération de mélange

Les notions abordées dans les paragraphes précédents permettent d'étudier le bio-réacteur en lui attribuant des paramètres représentant une tendance globale (par exemple, le temps de circulation représente le temps moyen mis par un micro-organisme pour traverser le volume du réacteur). Au vu de la sensibilité des micro-organismes face aux contraintes physiques, il est important de bien maîtriser les connaissances de dimensionnement des réacteurs. De ce fait, de nombreuses études ont porté sur une amélioration des performances des réacteurs :

- Optimisation de la géométrie du réacteur : dimensionnement de nouveaux systèmes d'agitation, d'aération,… [18, 19]
- Mise au point de techniques sophistiquées pour l'estimation des performances du réacteur : techniques de tomographie [20], d'anémométrie laser [21, 22],…
- Amélioration des systèmes de régulation de paramètres opératoires, tel que le pH, la quantité d'oxygène dissous, la concentration en glucose dans le cas d'un réacteur fonctionnant en *fed-batch*,… [23, 24]

Malgré ces études, l'hétérogénéité spatiale des propriétés physiques, chimiques et biologiques du contenu des réacteurs constitue toujours un écueil à leur bon fonctionnement et à leur optimisation. Les paramètres temporels sont également importants et sont représentés sous la forme d'une analyse des temps caractéristiques de procédé [25] à la figure 7.
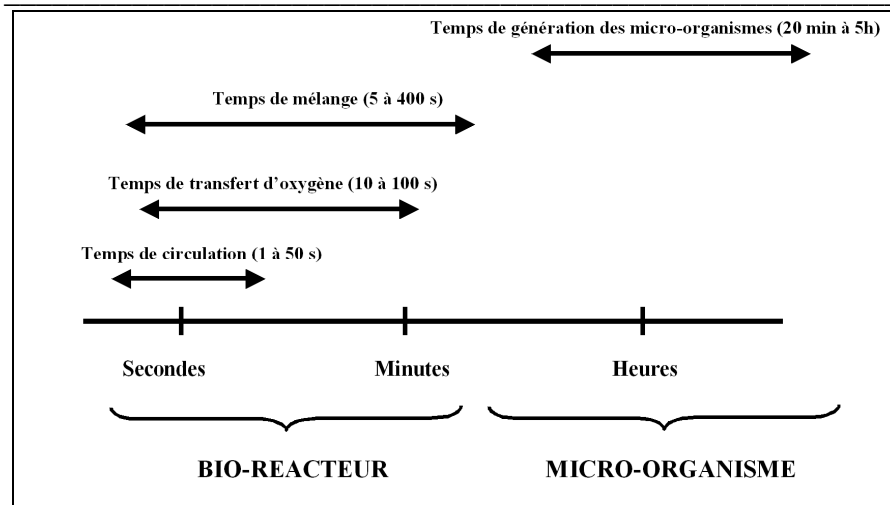
Figure 7 : analyse des temps caractéristiques liés aux bioprocédés

Les temps moyens pour la croissance des micro-organismes étant très longs, les temps de réaction requis au niveau des systèmes de régulation ne sont pas problématiques. Néanmoins, les micro-organismes peuvent répondre à certaines perturbations par des réponses métaboliques rapides. Par exemple, *Saccharomyces cerevisiae* réagit en quelques secondes face à une concentration trop importante en glucose par le passage d'un métabolisme respiratoire à un métabolisme fermentaire (effet Crabtree) [5]. Ces phénomènes métaboliques rapides peuvent être imputés aux temps relativement courts pour l'induction des gènes impliqués et la synthèse des ARN messagers [26]. La figure 8 permet d'illustrer l'impact des réponses métaboliques rapides sur les systèmes de régulation des bio-réacteurs. Cette figure met en œuvre le suivi de la concentration en oxygène dissous lors de la culture *fed-batch* d'une levure. Le système de régulation intervient pour maintenir un niveau en oxygène dissous supérieur à 30% (100% correspondant à la saturation du milieu). La figure 8 montre que des perturbations sont observées. Celles-ci peuvent être attribuées à l'ajout ponctuel de glucose dans le réacteur. En effet, suite à cet ajout, la levure consomme le glucose de manière aérobie, ce qui entraîne une chute au niveau de l'oxygène dissous. Cette réaction de respiration de glucose étant trop rapide, le temps de relaxation du bio-réacteur est trop important pour équilibrer le niveau d'oxygène dissous à 30%.

_____
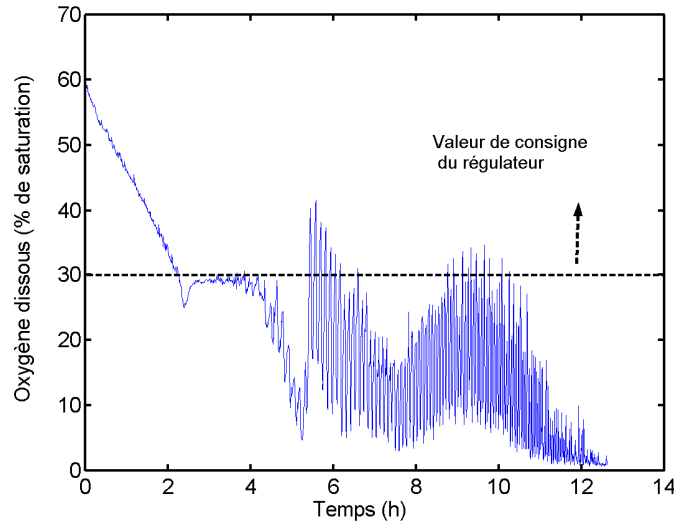
Figure 8 : profil en oxygène dissous lors de la culture *fed-batch* de *Pichia pastoris*. Le système de régulation est programmé pour maintenir le niveau d'oxygène dissous au-dessus des 30% en modulant la vitesse d'agitation du système

Outre le temps de réponse parfois insuffisant, un autre type de problème peu affecter les systèmes de régulation. En effet, leur fonctionnement est souvent lié à la réponse d'une sonde ou d'un capteur (sonde de température, sonde pH, analyseur de gaz, sonde à oxygène dissous,…). Néanmoins, ce capteur est placé à un endroit donné du réacteur et ne scrute qu'une petite partie du volume de celui-ci. Si le temps de mélange du système est court, le réacteur peut être considéré comme une boîte noire dont les paramètres peuvent être mesurés par une sonde placée à n'importe quel endroit du système (celui-ci étant homogène). Néanmoins, pour les réacteurs de taille plus imposante, le système est généralement hétérogène, et la sonde ou le capteur peut induire en erreur le système de régulation.

Le même raisonnement peut être effectué à partir du développement des techniques d'estimation des performances des réacteurs. En effet, le fait que les réacteurs ne soient plus considérés comme des systèmes homogènes a conditionné le développement de techniques expérimentales permettant d'étudier la distribution spatiale des paramètres de performance au sein du volume réactionnel [20].

Ces considérations sont particulièrement importantes dans le cas des bio-réacteurs, l'hétérogénéité pouvant gravement affecter certaines voies métaboliques. Il y a donc un intérêt de plus en plus grand pour les modèles de bio-réacteur permettant de simuler certains paramètres de performance à l'échelle locale. De tels modèles sont appelés modèles structurés ou modèles boîte grise, par rapport aux modèles considérant le réacteur comme une simple boîte noire.

Dans la méthodologie développée dans ce travail, deux aspects du génie chimique interviennent dans le cadre du dimensionnement des bio-réacteurs : l'apparition du gradient de concentration et le déplacement du micro-organisme par rapport à ce gradient. Plusieurs modèles structurés sont disponibles dans la littérature pour caractériser l'intensité du gradient de concentration au sein du réacteur. Ces modèles structurés (c'est-à-dire prenant en compte les caractéristiques locales du système) sont basés sur le concept de réacteurs parfaitement agités placés en série [27, 28]. Dans cette approche, le volume du réacteur est délimité par l'esprit en une série de réacteurs pour lesquels le mélange est considéré comme parfait. Ces réacteurs, encore appelés zones ou compartiments sont reliés les uns aux autres par des flux dont l'intensité et l'orientation permettent de représenter les écoulements au sein du réacteur considéré. Le concept de « compartimentation » d'un réacteur agité est illustré à la figure 9. La figure 9A met en évidence la dynamique interne de la cuve agitée. La figure 9B montre l'agencement des flux (ou débits) entre les compartiments de manière à respecter les écoulement générés par l'agitateur. On distingue :

- les flux de circulation qui proviennent du fluide entraîné par le mobile d'agitation. Ces flux de circulation Q_c (m³/s) peuvent être calculés grâce aux corrélations présentées au paragraphe 1.2.1.
- les flux de turbulence qui représentent le fluide entraîné sous l'action des forces de turbulence. Ces flux, représentés sur la figure 9B par des flèches à double sens, expriment le rétro-mélange engendré par la turbulence. Ces flux ne peuvent pas être calculés à partir de corrélation et doivent être estimés par expérimentation (par exemple, en effectuant des tests de temps de mélange).
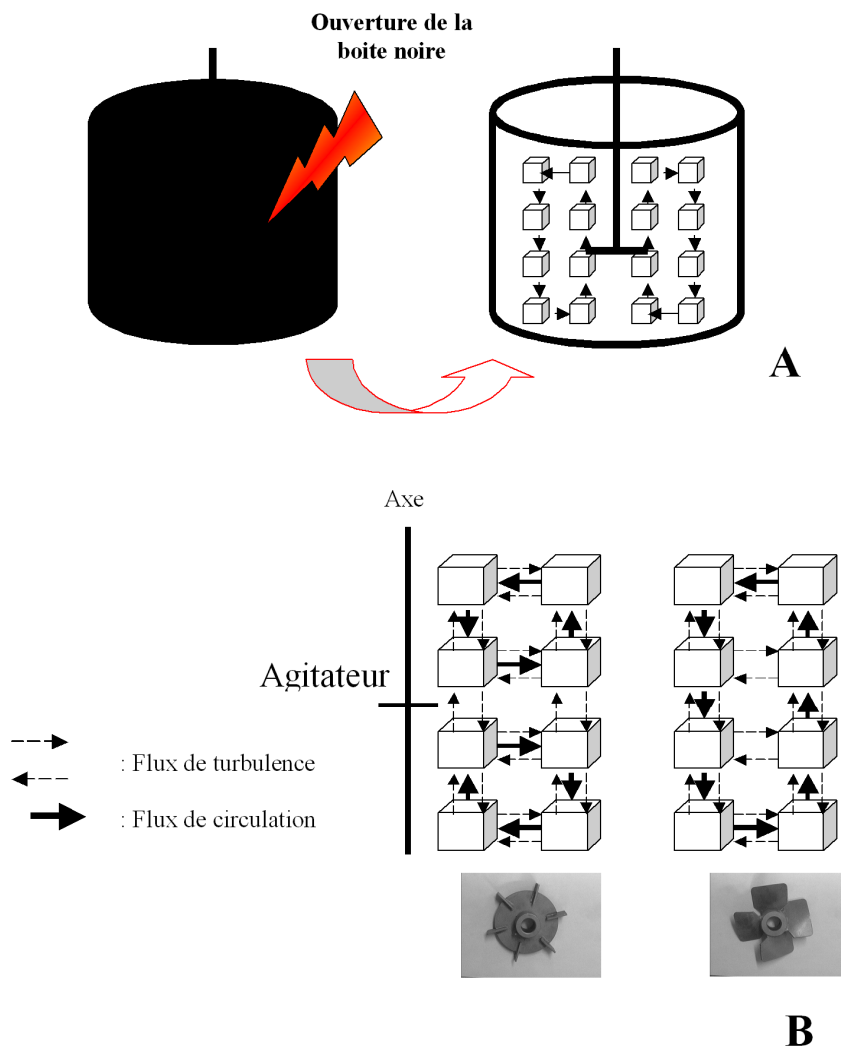
Figure 9 : illustration du principe de « compartimentation » d'un réacteur agité. A : ouverture de la boîte noire. B : orientation des flux de circulation et des flux de turbulence en fonction du type d'agitateur choisi

La compartimentalisation permet d'obtenir un modèle mathématique de l'hydrodynamique du réacteur, exprimé sous la forme d'un système d'équations différentielles exprimant le bilan de matière au niveau des compartiments. Il y a autant d'équations que de compartiments délimités dans le modèle. Par exemple, pour un compartiment donné n, l'évolution de la concentration (par exemple, en traceur, si on désire simuler une expérience de temps de mélange) est donnée par :

$$\frac{dC_n}{dt}=Q_{c,in}C_{n-1}-Q_{c,out}C_n+Q_{e,in}C_{n-1}-Q_{e,out}C_n$$

Où $Q_{c,out}$ et $Q_{e,out}$ (m³/s) représentent respectivement les débits de circulation et les débits de turbulence sortant du compartiment n considéré et $Q_{e,in}$ et $Q_{c,in}$, les débits de turbulence et les débits de circulation provenant du ou des compartiments adjacents n-1. C représente la concentration de la substance à homogénéiser.

Ce genre d'équation peut être modélisé pour simuler l'évolution d'une concentration C au cours du temps dans un compartiment donné du réacteur, cette concentration pouvant être liée à un traceur ou à un substrat utilisé par les micro-organismes. La résolution (c'est-à-dire les différences spatiales de concentration pouvant être mises en évidence) obtenue avec un modèle compartimenté dépend du nombre de compartiments considéré et est généralement acceptable si ce dernier est suffisamment élevé (on peut trouver dans la littérature des modèles compartimentés complexes composés de plusieurs centaines de compartiments [20, 29]). Un résolution plus élevée peut être obtenue avec les modèles de mécanique des fluides numérique [30]. Néanmoins, ce type de modèle est beaucoup plus difficile à manipuler du point de vue mathématique.

Au cours de ce travail, plusieurs modèles structurés ont été développés pour représenter l'hydrodynamique de la composante bio-réacteur de la problématique. Ces modèles ont été exprimés de manière stochastique de manière à pouvoir non seulement représenter les phénomènes de mélange, mais aussi les phénomènes de circulation des micro-organismes au sein du réacteur. Ces modèles hydrodynamiques stochastiques sont basés sur la notion de probabilité de passage d'une particule d'un compartiment à un autre et seront décrits plus en détail au chapitre 3. Les principes généraux de construction des modèles hydrodynamiques stochastiques sont abordés en détail en annexe de ce travail.

1.3. Notions relatives au génie biochimique : croissance microbienne

Afin d'aborder la culture d'un micro-organisme en bio-réacteur, il est important de connaître :

- Les performances hydrodynamiques du bio-réacteur (celles-ci ont été abordées au cours du paragraphe précédent).
- La vitesse de la réaction considérée, c'est-à-dire dans notre cas la vitesse de croissance du micro-organisme ou la vitesse de production d'un métabolite (celle-ci étant liée à la croissance du micro-organisme).

Ce paragraphe à pour but de décrire l'aspect « cinétique microbienne » de la problématique en relation avec les contraintes du bio-réacteur.

1.3.1. Expression classique de la cinétique microbienne

La vitesse de croissance des micro-organismes est généralement exprimée à partir de l'équation de Monod [31, 32] :

$$\mu = \mu_{max} \cdot \frac{S}{S + K_S}$$

L'équation de Monod exprime l'évolution du taux de croissance μ (s^{-1}) en fonction de la concentration en substrat S (g/l). Si la concentration en substrat est de loin supérieure à K_s, le micro-organisme se développe à son taux de croissance maximum μ_{max}. Par contre, si la concentration en substrat dans le réacteur est inférieure à K_s, le taux de croissance du micro-organisme varie en fonction de la concentration en substrat selon une loi de premier ordre (linéaire). K_s (g/l) est la constante d'affinité du micro-organisme et correspond à la concentration en substrat pour laquelle le micro-organisme se développe selon un taux de croissance égal à la moitié du taux de croissance maximal μ_{max}. Plus la constante d'affinité est faible et plus le micro-organisme aura la capacité de capter de faibles concentrations en substrat dans le milieu de culture. Connaissant l'évolution du taux de croissance, la vitesse de développement d'une population microbienne répond à l'équation suivante :

$$\frac{dX}{dt} = \mu.X$$

Avec X étant la concentration cellulaire (g/l) au temps t. Cette équation est uniquement valable dans le cas d'un réacteur fermé (*batch*). Dans le cas des réacteurs continus ou semi-ouverts (*fed-batch*), des termes doivent être ajoutés à cette équation, mais le principe général reste le même.

L'utilisation de cette équation pour décrire l'évolution d'une population microbienne dans un réacteur a rencontré un franc succès et reste encore utilisée de nos jours (de nombreuses variantes ayant fait leur apparition). Néanmoins, de nombreuses hypothèses ont été émises pour établir cette équation [31, 32]. Citons, parmi celles-ci :

- Le réacteur est considéré comme parfaitement mélangé
- La source de carbone S est le seul élément limitant la croissance
- L'oxygène est apporté en excès
- La mortalité cellulaire est négligée

Ces hypothèses entraînent un biais par rapport à la réalité, ce biais étant plus ou moins important suivant le procédé considéré. Dans la problématique qui constitue la toile de fond de ce travail, le fait de considérer le réacteur comme parfaitement agité constitue un écart important par rapport à la réalité. Il est donc nécessaire d'adapter la loi de Monod, voire de considérer un autre type de modèle de cinétique microbienne plus élaboré. Avant de passer au paragraphe suivant qui traite de ces modèles plus élaborés, il est utile de dresser une classification des modèles de croissance microbienne pouvant être trouvés dans la littérature [32]. En effet, les modèles peuvent être qualifiés d'une part de :

- ***Non structurés*** : ce type de modèle considère la cellule de manière globale, sans se soucier des réactions internes à celle-ci (modèle de type boîte noire). Le modèle de Monod constitue un exemple de modèle non structuré.
- ***Structurés*** : pour certaines applications, il est intéressant d'observer une ou plusieurs voies métaboliques particulières. Les modèles structurés ne considèrent plus la cellule microbienne comme une boîte noire, mais comme un ensemble plus ou moins complexe de réactions biochimiques.

Et, d'autre part, de :

- *Non ségrégés* : ce type de modèle considère que toutes les cellules de la population microbienne sont identiques.
- *Ségrégés* : dans la réalité, les cellules microbiennes constituant une population donnée sont dans des stades de croissance ou des stades physiologiques différents. Les modèles ségrégés permettent de distinguer plusieurs sous-populations, caractérisées par des états physiologiques différents, au sein d'une même population.

Les modèles à la fois structurés et ségrégés sont bien sûr les modèles de croissance microbienne les plus élaborés.

1.3.2. Vers un modèle plus réaliste de la croissance microbienne en réacteur

Le développement de modèles de croissance microbienne plus élaborés a été rendu possible grâce au développement de techniques expérimentales fines permettant leur validation. Dans le cas des modèles structurés, ce sont des techniques de marquage moléculaire, de génomique, de puce à ADN,… qui sont utilisées pour la mise en évidence des flux métaboliques [33]. En effet, ces techniques performantes permettent la mise en évidence de nombreuses voies métaboliques, ce qui permet par la suite leur inclusion dans un modèle structuré pouvant simuler des métabolismes très complexes [34]. Ces modèles structurés peuvent trouver des applications très importantes dans la problématique qui fait l'objet de ce travail. En effet, dans les réacteurs hétérogènes, les cellules microbiennes sont soumises à des variations environnementales, notamment au niveau des concentrations en glucose. Certains micro-organismes réagissent différemment en fonction de la concentration en glucose environnante. Par exemple, dans le cas d'*Escherichia coli*, le passage de faibles concentrations à de fortes concentrations en glucose entraîne l'induction de nouvelles voies métaboliques et le passage d'un métabolisme de type respiratoire avec production de biomasse à un métabolisme « surverse » dans lequel le glucose excédentaire est converti en acétate [35, 36]. Le même raisonnement peut être effectué dans le cas de *Saccharomyces cerevisiae* [37]. Ces phénomènes sont

impossibles à reproduire à l'aide d'un simple modèle de type Monod et un modèle structuré devient nécessaire.

Dans le cas des modèles ségrégés, la validation a été effectuée grâce à des techniques expérimentales permettant d'estimer très rapidement l'état physiologique d'un grand nombre de cellules microbiennes, comme par exemple la cytométrie en flux [38, 39]. Les modèles ségrégés sont également importants dans le cadre de ce travail. En effet, du fait de l'hétérogénéité du réacteur (surtout dans le cas des réacteurs de taille industrielle), plusieurs états physiologiques peuvent être distingués au sein d'une même population. De nouveau, le modèle simple de Monod ne permet pas de représenter ce phénomène. L'utilisation de modèles ségrégés permet de quantifier l'impact du réacteur en simulant les proportions prises par les différentes sous-populations présentant des états physiologiques différents.

Au cours de ce travail, le modèle ségrégé a été choisi pour étudier la composante microbienne de la problématique. La plupart des modèles ségrégés utilisés pour décrire l'évolution des populations microbiennes dans les réacteurs sont exprimés sous formes d'équations déterministes [40]. Nous avons choisi dans notre cas d'exprimer le modèle ségrégé sous forme d'équations stochastiques, le passage des cellules d'un état à une autre étant gouverné par des probabilités (ces modèles seront développés au cours du chapitre 8).

1.4. <u>Stratégie de recherche</u>

La complexité des opérations d'extrapolation des bio-réacteurs provient de l'hétérogénéité à la fois au niveau du bio-réacteur, mais aussi au niveau de la population microbienne considérée. Cette complexité est encore accrue par les interactions entre les micro-organismes et le bio-réacteur. Afin de simplifier l'étude des systèmes complexes, des outils de modélisation mathématique peuvent être employés. Ces techniques permettent de mieux visualiser la dynamique interne des systèmes complexes tels que l'hydrodynamique du bio-réacteur ou la dynamique d'une population microbienne. Le système est d'autant plus complexe à analyser si il est composé de plusieurs processus en interaction. Dans notre cas, 3 processus doivent être considérés (figure 10). Le premier processus est le gradient de

concentration se développant dans le réacteur. Le second processus est la circulation du micro-organisme dans le réacteur. La superposition des deux premiers processus permet d'obtenir les fluctuations environnementales encourues par les micro-organismes lors de leur séjour dans le réacteur. Enfin, le troisième et dernier processus est relatif à la croissance microbienne elle-même.
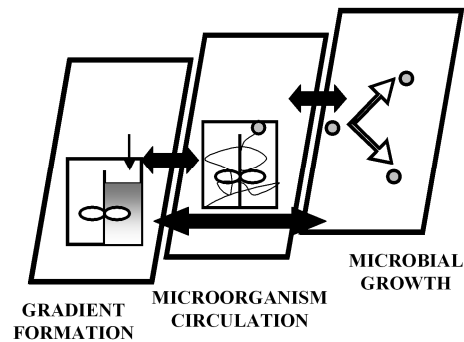
Figure 10 : présentation schématique des 3 processus intervenant dans l'étude d'un bioprocédé. Un modèle est requis pour prendre en compte chacun de ces processus.

La modélisation mathématique de ces processus permet de faciliter leur compréhension. L'originalité provient de la formulation stochastique des modèles employés, ce qui permet de prendre en compte les facteurs aléatoires (comme, par exemple le déplacement d'un micro-organisme au sein du réacteur). En effet, l'expression stochastique des 3 composantes et de leurs interactions a permis :

-   de caractériser les fluctuations de concentration subies par les micro-organismes lors de leur séjour dans le réacteur.
-   d'évaluer l'impact des contraintes liées au réacteur sur la cinétique microbienne.

Les résultats expérimentaux relatifs à la cinétique microbienne ont été obtenus grâce à la mise en place d'un réacteur *scale-down*. Ce type de réacteur est conçu de manière à reproduire à petite échelle l'hydrodynamique des réacteurs industriels. Le concept de réacteur *scale-down* est illustré à la figure 11. Dans les réacteurs industriels, les éléments fluides sont transportés par le flux de circulation provenant du mobile d'agitation, le flux de circulation formant une boucle de mélange. Le temps mis pour homogénéiser une perturbation sera proportionnel à la fréquence de passage au niveau du mobile d'agitation, et donc au débit de fluide dans la boucle de

circulation. Lors de l'extrapolation, le temps de circulation (temps mis par une particule fluide pour traverser consécutivement deux fois le même plan du réacteur) va augmenter avec l'échelle du réacteur, induisant de ce fait une détérioration de l'efficacité d'homogénéisation du système. Le réacteur *scale-down* a pour but de reproduire ces phénomènes en couplant un réacteur agité de petit volume à une section non agitée en écoulement piston censée représenter la boucle de circulation. Une pompe permet de faire circuler le liquide entre la section agitée et la section en écoulement piston. Le réglage du débit de la pompe permet de simuler toute une série de conditions hydrodynamiques proches de celles rencontrées au niveau industriel.
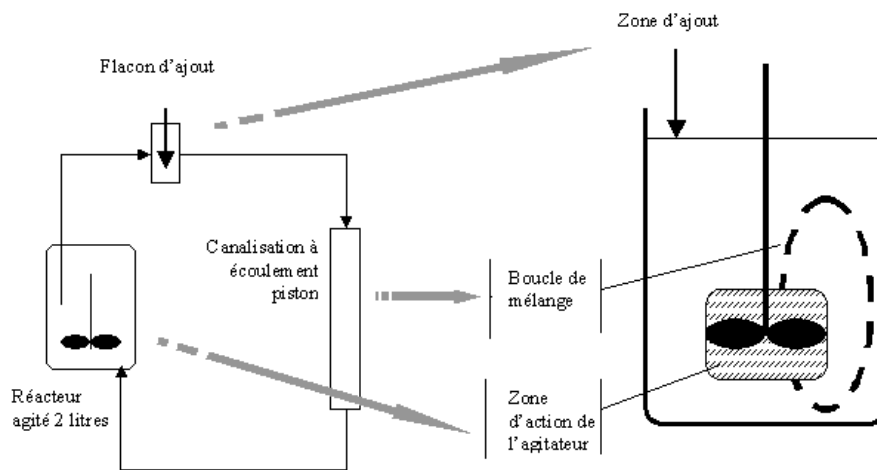
Figure 11 : illustration du concept de réacteur *scale-down* (à gauche) par comparaison avec un réacteur industriel (à droite)

La stratégie de recherche mise en œuvre pour répondre à la problématique présentée au paragraphe 1.1. (c'est-à-dire la compréhension des mécanismes d'interaction entre les micro-organismes et l'hydrodynamique du réacteur dans un contexte d'extrapolation de procédé) comprend plusieurs étapes qui seront abordées comme suit :

- Développement des outils de modélisation de l'hydrodynamique du réacteur : étapes **1** et **2**.

23

- Dimensionnement d'un réacteur *scale-down* permettant de reproduire en laboratoire les conditions d'écoulement industrielles : étape **3**.
- Etude de l'impact des conditions hydrodynamiques sur plusieurs types de micro-organisme : étapes **4**, **5** et **6**.
- Inclusion des données hydrodynamiques dans un modèle de croissance microbienne prenant en compte les différents états physiologiques des micro-organismes : étape **7**.

Les différentes étapes de cette stratégie de recherche constituent les chapitres relatifs aux résultats et discussion de ce travail, chacun de ces chapitres ayant fait l'objet d'une publication.

Afin de faciliter la lecture du document, le tableau 1 reprend les différentes étapes de la stratégie de recherche en mettant l'accent sur les résultats attendus et la correspondance avec les chapitres de la thèse. Ce tableau est suivi d'une série de paragraphes reprenant chacun de manière détaillée une des étapes du travail.

Tableau 1 : résumé de la stratégie de recherche mise en œuvre au cours de ce travail

Etape de la stratégie de recherche	Composante(s) étudiée(s)	Type(s) de modèle employé(s)	Micro-organisme étudié	Résultats attendus	Chapitre de la thèse correspondant
1	Bio-réacteur + micro-organisme	Déterministe	*Pichia pastoris*	Comparaison de l'approche globale et de l'approche structurée pour le dimensionnement des bio-réacteurs	Chap. 2
2	Bio-réacteur	Déterministe + stochastique	–	Comparaison de la formulation déterministe et stochastique des modèles structurés hydrodynamique de bio-réacteur	Chap. 3
3	Bio-réacteur	Stochastique	–	Dimensionnement de réacteurs *scale-down* représentatifs de réacteurs industriels à l'aide des modèles stochastiques	Chap. 4
4	Bio-réacteur + micro-organisme	Stochastique	*Escherichia coli*	Mise en évidence de l'impact de l'hydrodynamique des bio-réacteurs sur *E. coli*	Chap. 5
5	Bio-réacteur + micro-organisme	Stochastique	*Saccharomyces cerevisiae*	Mise en évidence de l'impact de l'hydrodynamique des bio-réacteurs sur *S. cerevisiae*	Chap. 6
6	Bio-réacteur + micro-organisme	Stochastique	*Saccharomyces cerevisiae*	Standardisation de l'approche de modélisation stochastique du bio-réacteur afin de considérer l'impact de l'hydrodynamique sur une population microbienne de taille donnée	Chap. 7
7	Bio-réacteur + micro-organisme + interactions	Stochastique	*Escherichia coli*	Mise au point d'un modèle stochastique de croissance microbienne et couplage de celui-ci avec les modèles hydrodynamiques étudiés précédemment	Chap. 8

Il est important de noter que, d'après le tableau 1, le travail met en œuvre plusieurs micro-organismes appartenant à des genres différents : *Pichia pastoris, Saccharomyces cerevisiae, Escherichia coli*. Le choix de ces micro-organismes comme modèle d'étude pour l'influence des conditions hydrodynamiques du réacteur sur la physiologie microbienne a été conditionné par les aspects suivants :

- ces micro-organismes sont fortement utilisés dans des applications industrielles (pour la production de métabolites, de biomasse, ou encore comme vecteur d'expression)
- ils produisent des métabolites secondaires défavorables à la croissance lorsqu'ils sont soumis à de trop fortes concentrations en substrat.
- de nombreuses données (physiologiques, génétiques,…) sont disponibles dans le cas de *E. coli* et *S. cerevisiae*, ce qui permet de faciliter par la suite l'intégration de celles-ci pour la construction d'un modèle de croissance microbienne en relation avec les performances du réacteur
- l'utilisation de *E. coli* et de *S. cerevisiae* pour la réalisation des expériences nous permet de comparer le comportement des organismes procaryote et eucaryote face aux stress induits par le bio-réacteur, ce qui permettra de généraliser les résultats obtenus au cours de ce travail

1.4.1. Description de la première étape de la stratégie de recherche

Intitulé : approche classique et structurée pour l'étude des paramètres du génie chimique en relation avec un bio-procédé

Bref descriptif des travaux effectués : des cultures en réacteur *fed-batch* de *Pichia pastoris* ont été effectuées pour différents systèmes d'agitation :

- TD6-TD6 : deux turbines de rushton à écoulement radial.
- TD6-A340 : une turbine de rushton à écoulement radial dans le bas de la cuve combinée avec une hélice à effet axial « pompe bas » dans la partie supérieure de la cuve.

- A315-A340 : une hélice à effet axial « pompe haut » en bas de cuve combinée avec une hélice axiale « pompe bas » dans la partie supérieure de la cuve.

Les systèmes d'agitation ont été testés du point de vue de leur performances d'homogénéisation et de transfert d'oxygène. Les essais de traceur effectués pour la détermination du temps d'homogénéisation ont montrés des comportements hydrodynamiques très différents selon le système d'agitation testé. Les tests de traceur ont été exploités de deux manières différentes :

- Tout d'abord pour le calcul du temps d'homogénéisation, afin de chiffrer l'efficacité de mélange d'un système d'agitation. Cette méthodologie est caractéristique de l'approche classique du génie chimique qui consiste à décrire une caractéristique d'un système d'agitation donné par un paramètre chiffré. Cette approche considère le système d'agitation comme une boîte noire et ne prend pas en compte la dynamique interne du procédé. Dans le cas d'un bio-procédé mettant en œuvre des micro-organismes sensibles aux fluctuations de concentration en substrat, cette approche n'est pas satisfaisante.

- Ensuite, les courbes de traceur ont été exploitées pour la mise au point d'un modèle hydrodynamique structuré (ces modèles ont été décrits au cours du paragraphe 1.2.3.). Ce modèle hydrodynamique a été couplé à une réaction de croissance microbienne de type Monod (voir paragraphe 1.3.1.) afin de calculer l'évolution du gradient de concentration au cours du procédé *fed-batch* en fonction du système d'agitation utilisé.

Résumé des principaux résultats obtenus et des perspectives : l'utilisation du modèle hydrodynamique structuré couplé à une réaction de croissance microbienne a permis de comparer de manière objective l'efficacité des systèmes d'agitation dans le cadre d'un bio-procédé. Les simulations ont montré une chute de l'efficacité d'homogénéisation du système lors de l'utilisation d'un système d'agitation TD6-TD6 et lors du passage d'un volume de cuve de 20 litres à 500 litres. Les simulations ont également montré l'intérêt de la combinaison TD6-A340,

qui permet d'atténuer le gradient de concentration lors du procédé *fed-bacth* tout en assurant un apport en oxygène satisfaisant. En réacteur de 20 litres, les résultats d'efficacité de mélange n'ont pas pu être corrélé au rendement correspondant en biomasse. En effet, à cette échelle relativement modeste, l'impact des conditions hydrodynamiques sur la croissance microbienne n'est pas très marqué. Néanmoins, d'un point de vue économique, la réalisation de tests de fermentation dans des cuves industrielles est irréalisable. Il serait donc intéressant de mettre au point un système permettant de reproduire à petite échelle les conditions d'écoulement rencontrées dans les réacteurs industriels. En conclusion, l'approche de modélisation structurée développée au cours de ce chapitre permet de caractériser avec précision l'efficacité de mélange du système d'agitation en relation avec les contraintes d'un bio-procédé (dans notre cas, la culture *fed-batch* d'une levure sensible aux gradients de concentration).

1.4.2. Description de la seconde étape de la stratégie de recherche

Intitulé : expression déterministe et stochastique d'un modèle hydrodynamique structuré de bio-réacteur

Bref descriptif des travaux effectués : la première étape de la stratégie de recherche (paragraphe 1.4.1.) a démontré l'intérêt des modèles hydrodynamiques structurés pour l'étude de l'impact de l'opération de mélange sur la cinétique microbienne. Le but de la seconde étape est de reformuler ces modèles structurés de manière stochastique. Dans cette optique des modèles stochastiques ont été formulés de manière équivalente aux modèles structurés déterministes préalablement utilisés. Premièrement, le même nombres d'états stochastiques ou de compartiments déterministes ont été utilisés, chaque état ou compartiment correspondant à une zone de volume donné du réacteur agité. Deuxièmement, les probabilités de transition entre états du modèle stochastique ont été calculées sur base des flux de circulation et de turbulence du modèle stochastique. La probabilité pour un élément fluide de passer d'un état à un autre a été définie comme étant égale au rapport des flux responsables du mouvement sur la totalité des flux s'exerçant sur l'état considéré.

Cette manière de procéder implique l'intervention d'un paramètre Δt représentant l'intervalle de temps correspondant à une transition.

Résumé des principaux résultats obtenus et des perspectives : la comparaison des formulations stochastique et déterministe des modèles hydrodynamiques de réacteur a montré l'équivalence des deux approches au niveau de leur résolution du phénomène d'homogénéisation en cuve agitée. Néanmoins, les modèles stochastiques présentent l'avantage de posséder une formulation mathématique moins compliquée que leurs homologues déterministes exprimés sous forme d'équations différentielles. De plus, les modèles stochastiques permettent de simuler le déplacement de particules à l'intérieur du réacteur. Cette propriété importante sera exploitée dans la suite du travail pour simuler le déplacement des micro-organismes dans les bio-réacteurs.

1.4.3.   Description de la troisième étape de la stratégie de recherche

Intitulé : utilisation des modèles stochastiques pour le dimensionnement d'un réacteur *scale-down* représentatif.

Bref descriptif des travaux effectués : afin d'étudier l'impact des conditions hydrodynamiques industrielles sur les performances d'un bio-procédé, il est nécessaire de développer des outils d'étude permettant de reproduire ces conditions en laboratoire. Le réacteur *scale-down* représente un bonne alternative à cette problématique (voir figure 11). Afin de faire correspondre au mieux ce type de réacteur aux écoulements industriels envisagés, une méthodologie de dimensionnement est proposée sur base des modèles hydrodynamiques stochastiques. Les simulations permettent en effet d'obtenir l'intensité relative des gradients de concentration se développant dans le réacteur, mais aussi le déplacement des micro-organismes sous l'effet des flux engendrés par les agitateurs. La superposition de ces deux phénomènes permet d'obtenir le profil temporel des concentrations rencontrées par le micro-organisme lors de son déplacement au sein du fluide agité.

Résumé des principaux résultats obtenus et des perspectives : l'intervalle de temps Δt entre deux transitions lors d'une simulation stochastique a été choisi comme base de comparaison pour le processus d'extrapolation des réacteurs et pour la comparaison de l'hydrodynamique des réacteurs industriels et des réacteurs *scale-down*. En effet, l'extrapolation ou l'augmentation de volume du réacteur, affecte de manière notable l'échelle de temps du procédé. Dans notre cas, les temps de mélange et de circulation (voir paragraphes 1.2.1 et 1.2.2. pour la définition de ces paramètres) seront considérés. Les simulations réalisées de cette manière ont permis de mettre en évidence l'importance de l'arrangement géométrique des états spatiaux du modèle, de manière à représenter de manière précise l'écoulement des réacteurs. En effet, selon le type de réacteur *scale-down*, l'arrangement des états au sein de la partie non agitée du réacteur doit être effectué de manière a représenter un écoulement piston plus ou moins prononcé. D'une manière plus générale, le nombre d'états doit être augmenté pour représenter le phénomène de circulation lors d'un processus d'extrapolation. Mis a part la contrainte quand à la spécification de l'arrangement spatial et du nombre d'états devant être considérés dans le modèle, l'approche proposée permet de comparer l'efficacité d'homogénéisation des réacteurs *scale-down* et des réacteurs industriels. Cette approche pourra être utilisée pour dimensionner des réacteurs *scale-down* représentatifs des conditions rencontrées à l'échelle industrielle.

1.4.4. Description de la quatrième étape de la stratégie de recherche

Intitulé : impact des performances d'homogénéisation du bio-réacteur sur la cinétique microbienne : cas de *Escherichia coli*

Bref descriptif des travaux effectués : des expériences de cultures de *E. coli* en réacteur *scale-down* ont été effectuées afin de déterminer l'impact de l'hydrodynamique du réacteur sur la croissance de ce micro-organisme. Le modèle hydrodynamique stochastique, mis au point au cours des deux étapes précédentes, a été utilisé afin de simuler les gradients de concentration se développant au sein des réacteurs *scale-down* et la circulation des micro-organismes.

Résumé des principaux résultats obtenus et des perspectives : en examinant les courbes de cinétiques microbiennes obtenues à partir de réacteur *scale-down*, il a été déterminé que ces réacteurs ne reproduisent pas les conditions d'écoulement rencontrées à l'échelle industrielle. Premièrement, le débit d'alimentation en source de carbone est trop important et induit une accumulation de glucose dans l'ensemble du système, ce qui rend difficile l'observation de l'effet hydrodynamique du gradient de concentration. Deuxièmement, la section non mélangée du réacteur *scale-down* présente une géométrie propice à générer un écoulement de type piston, ce qui s'éloigne relativement des conditions d'écoulement industrielles. Afin d'améliorer la représentativité des expériences en réacteur *scale-down* (concevoir des expériences en réacteur *scale-down* représentatives des conditions industrielles), cette étude a montré l'intérêt de travailler avec un débit d'ajout *fed-batch* limitant l'accumulation de glucose dans l'ensemble du réacteur, ainsi que de considérer des sections non mélangées de géométries différentes. Les résultats de croissance de *Escherichia coli* dans différentes conditions de réacteur *scale-down* ont pu être expliqués par les simulations hydrodynamiques réalisées à partir du modèle stochastique.

1.4.5. Description de la cinquième étape de la stratégie de recherche

Intitulé : impact des performances d'homogénéisation du bio-réacteur sur la cinétique microbienne : cas de *Saccharomyces cerevisiae*

Bref descriptif des travaux effectués : la stratégie expérimentale est la même que celle de l'étape 4 et est basée sur l'étude de l'influence des conditions hydrodynamiques sur la croissance de *Saccharomyces cerevisiae* en réacteur *scale-down*. Les défauts relevés lors de l'étape 4 ont été intégrés, et un intérêt particulier a été porté sur la méthode d'ajout *fed-batch* et sur la géométrie de la partie non mélangée du réacteur *scale-down*.

Résumé des principaux résultats obtenus et des perspectives : les tests de croissance de *S. cerevisiae* ont montré un impact significatif de l'hydrodynamique du réacteur. Une chute du rendement en biomasse (nombre de grammes de biomasse produits sur nombre de grammes de glucose consommés) a été notée lorsque le débit

de recirculation du réacteur *scale-down* est diminué. Le modèle hydrodynamique stochastique a été utilisé pour calculer les concentrations en glucose rencontrées par les micro-organismes lors de leur séjour dans le réacteur *scale-down*. Pour cela, les chemins de circulation de 3500 cellules microbiennes ont été superposés au gradient de concentration. Le calcul des chemins de circulation et du gradient de concentration ont été effectués sur base du même modèle stochastique. Les profils de concentration en glucose rencontrés par les cellules de levure ont été exploités de manière a calculer la concentration moyenne rencontrée par chaque micro-organisme lors de son séjour dans le réacteur. La comparaison des distributions de fréquence obtenues montre un étalement plus important dans le cas des réacteurs *scale-down* fonctionnant à un débit de recirculation moins important. Cet étalement signifie qu'une partie de la population microbienne est soumise à des concentrations plus importantes en glucose, ce qui explique les chutes de coefficient de rendement en biomasse.

1.4.6.   Description de la sixième étape de la stratégie de recherche

Intitulé : étude de l'impact du bio-réacteur sur une population microbienne de taille limitée

Bref descriptif des travaux effectués : le but de cette étape de la stratégie de recherche est de standardiser l'approche de modélisation mise au point lors de l'étape 5. Pour rappel, cette approche consiste à superposer le gradient de concentration en substrat et les chemins de circulation suivis par les micro-organismes lors de leur séjour dans le réacteur. Plusieurs paramètres numériques ont été observés : la taille ou le nombre de cellules de la population microbienne, la position initiale de ces cellules dans le réacteur, le temps de simulation et l'effet de la fréquence d'impulsion de la pompe d'ajout *fed-batch*.

Résumé des principaux résultats obtenus et des perspectives : les simulations ont montré que chacun des paramètres numériques observés ont une influence sur la distribution des concentration en substrat rencontrées par les micro-organismes lors de leur séjour dans le réacteur. Les valeurs optimales pour chacun de ces paramètres ont été déterminées. Les simulations effectuées avec ces valeurs de paramètres ont

permis de comparer différents types de réacteurs *scale-down* , ainsi que différents types de bio-réacteurs industriels.

1.4.7. Description de la septième étape de la stratégie de recherche

Intitulé : vers un modèle de cinétique microbienne prenant en compte les contraintes liées aux bio-réacteurs et à leur extrapolation

Bref descriptif des travaux effectués : le but de cette septième étape est d'élaborer un modèle représentatif de la deuxième composante de la problématique de ce travail : la population microbienne. L'utilisation du modèle hydrodynamique stochastique a montré une diversité au niveau du stress encouru par les cellules d'une même population microbienne (étapes 5 et 6). Le modèle de cinétique microbienne doit pendre en compte cette diversité et doit donc être formulé de manière ségrégée (voir chapitre 1, paragraphe 1.3.1., un modèle ségrégé est un modèle qui prend en compte une ou plusieurs caractéristiques individuelles des cellules d'une population). Afin de respecter la philosophie du travail, le modèle de cinétique microbienne doit être formulé de manière stochastique. Cela permet de faciliter par la suite la connexion entre le modèle hydrodynamique et le modèle de cinétique microbienne. Un modèle stochastique de croissance microbienne a donc été élaboré. Dans ce modèle, les temps de génération individuels des cellules sont générés de manière aléatoire à partir d'une distribution log-normale. Au terme de son temps de génération, la cellule considérée se divise et donne naissance à une nouvelle cellule. Par ce processus mathématique, l'évolution du nombre de cellules au cours du temps peut être simulée, chaque cellule étant considérée de manière individuelle.

Résumé des principaux résultats obtenus et des perspectives : la loi log-normale s'est avérée efficace pour l'obtention des temps de génération individuels. Les courbes de croissance microbienne en réacteur *scale-down* fonctionnant en mode *fed-batch* ont pu être reproduites. Les paramètres de la distribution log-normale doivent néanmoins être modifiés de manière continue au cours de la phase *fed-batch* du procédé afin d'obtenir des courbes de croissance en accord avec l'expérience.

Cette modification correspond concrètement aux changements environnementaux perçus par les cellules microbiennes au cours du procédé *fed-batch*.

Références

1.   Vrabel P., van der Lans R.G.J.M., Luyben K.Ch.A.M., Boon L., Nienow A.N., *Mixing in large-scale vessels stirred with multiple radial or radial and axial up-pumping impellers : modelling and measurements.* Chemical engineering science, 2000. **55**: p. 5881-5896.
2.   Bruxelmane M., Delvosalle C., *Mixing in biological treatment systems.* Global bioconversions, ed. D.L. Wise. Vol. 4. 1986, Roca Baton: CRC press. 1-138.
3.   Perry R.H., Green D.W., *Perry's chemical engineers' handbook.* 7th ed. 1997: Mac Graw and Hill.
4.   Roustan M., Pharamond J.C., *Agitation-Mélange*, in *Fascicule A 5900*, T.d. l'ingénieur, Editor.
5.   Namdev P.K., Thompson B.G., Gray M.R., *Effect of feed zone in fed-batch fermentations of Saccharomyces cerevisiae.* Biotechnology and bioengineering, 1992. **40**(2): p. 235-246.
6.   Oosterhuis N.M.G., Kossen N.W.F., Olivier A.P.C., Schenk E.S., *Scale-down and optimization studies of the gluconic acid fermentation by Gluconobacter oxydans.* Biotechnology and bioengineering, 1985. **27**: p. 711-720.
7.   Vlaev D., Mann R., Lossev V., Vlaev S.D., Zahradnik J., Seichter P., *Macro-mixing and Streptomyces fradiae : modelling oxygen and nutrient segregation in an industrial bioreactor.* Trans IChemE, 2000. **78**: p. 354-362.
8.   Namdev P.K., Yegneswaran P.K., Thompson B.G., Gray M.R., *Experimental simulation of large-scale bioreactor environments using a monte carlo method.* Canadian journal of chemical engineering, 1991. **69**: p. 513-519.
9.   Davidson K.M., Sushil S., Eggleton C.D., Marten M.R., *Using computational fluid dynamics software to estimate circulation time distribution in bioreactors.* Biotechnology progress, 2003. **19**: p. 1480-1486.
10.   Bakker A., *The colorful fluid mixing gallery*. 2003, www.bakker.org.
11.   Caçaval D., Oniscu C., Galaction A.I., Dumitru I.F., *Characterisation of mixing efficiency in bioreactors.* Roum. biotechnol. lett., 2001. **6**(4): p. 281-291.
12.   Poulsen B.R., Iversen J.J.L., *Mixing determinations in reactor vessels using linear buffers.* Chemical engineering science, 1997. **52**(6): p. 979-984.

13. Gogate P.R., Pandit A.B., *Mixing of miscible liquids with density differences : effect of volume and density of the tracer fluid.* Canadian journal of chemical engineering, 1999. **77**: p. 988-996.

14. Mayr B., Horvat P., Moser A., *Engineering approach to mixing quantification in bioreactors.* Bioprocess engineering, 1992. **8**: p. 137-143.

15. Levenspiel O., *Modeling in chemical engineering.* Chemical engineering science, 2002. **57**: p. 4691-4696.

16. Rainer B.W., *Determination methods of the volumetric oxygen transfer coefficient kla in bioreactors.* Chem. Biochem. Eng. Q., 1990. **4**(4): p. 185-196.

17. Gogate P.R., Pandit A.B., *Survey of the measurement techniques for gas-liquid mass transfer coefficient in bioreactors.* Biochemical engineering journal, 1999. **4**: p. 7-.

18. Gogate P.R., Beenackers A.A.C.M., Pandit A.B., *Multiple-impeller systems with a special emphasis on bioreactors : a critical review.* Biochemical engineering journal, 2000. **6**: p. 109-144.

19. Doran P.M., *Design of mixing systems for plant cell suspensions in stirred reactors.* Biotechnology progress, 1999. **15**: p. 319-335.

20. Mann R., Williams R.A., Dyakowski T., Dickin F.J., Edwards R.B., *Development of mixing models by using electrical resistance tomography.* Chemical engineering science, 1997. **52**(13): p. 2073-2085.

21. Zhou G., Kresta S.M., *Impact of tank geometry on the maximum turbulence energy dissipation rate for impellers.* AIChE journal, 1996. **42**(9): p. 2476-2490.

22. Moore I.P.T., Cossor G., Baker M.R., *Velocity distributions in a stirred tank containing a yield stress fluid.* Chemical engineering science, 1995. **50**(15): p. 2467-2481.

23. Lee J., Lee S.Y., Park S., Middelberg A.P.J., *Control of fed-batch fermentations.* Biotechnology advances, 1999. **17**: p. 29-48.

24. Cannizzaro C., Valentinotti S., von Stockar U., *Control of yeast fed-batch process trough regulation of extracellular concentration.* Bioprocess biosyst. eng., 2004. **26**: p. 377-383.

25. Sweere A.P.J., Luyben K.C.A.M., Kossen N.W.F., *Regime analysis and scale-down : tools to investigate the performance of bioreactors.* Enzyme and microbial technology, 1987. **9**: p. 386-398.

26. Schweder T., Krüger E., Xu B., Jürgen B., Blomsten G., Enfors S.O., Hecker M., *Monitoring of genes that respond to process related stress in large-scale bioprocesses.* Biotechnology and bioengineering, 1999. **65**(2): p. 151-159.

27. Mayr B., Horvat P., Nagy E., Moser A., *Mixing models applied to industrial batch reactor.* Bioprocess engineering, 1993. **9**: p. 1-12.

28. Mayr B., Nagy E., Horvat P., Moser A., *Scale-up on basis of structured mixing models : a new concept.* Biotechnology and bioengineering, 1994. **43**: p. 195-206.

29. Mann R., Pillai S.K., El-Hamouz A.M., Ying P., Togatorop A., Edwards R.B., *Computational fluid mixing for stirred vessels : progress from seeing to believing.* Chemical engineering journal, 1995. **59**: p. 39-50.

30. Schmalzriedt S., Jenne M., Mauch K., Reuss M., *Integration of physiology and fluid dynamics.* Advances in biochemical engineering, 2003. **80**: p. 19-68.

31. Blanch H.W., Clark D.S., *Biochemical engineering.* first ed, ed. M. Dekker. 1997, New-York: Marcel Dekker. 702.

32. Dunn I.J., Heinzle E., Ingham J., Prenosil J.E., *Biological reaction engineering.* 2003, Mörlenbach, Germany: Wiley-VCH. 508.

33. Mahadevan R., Edwards J.S., Doyle F.J., *Dynamic flux analysis of diauxic growth in Escherichia coli.* Biophysical journal, 2002. **83**: p. 1331-1340.

34. Holms H., *Flux analysis and control of the central metabolic pathways in Escherichia coli.* FEMS microbiology reviews, 1996. **19**: p. 85-116.

35. Xu B., Jahic M., Blomsten G., Enfors S.O., *Glucose overflow metabolism and mixed-acid fermentation in aerobic large-scale fed-batch processes with Escherichia coli.* Applied microbiology and biotechnology, 1999. **51**: p. 564-571.

36. Xu B., Jahic M., Enfors S.O., *Modeling of overflow metabolism in batch and fed-batch cultures of Escherichia coli.* Biotechnology progress, 1999. **15**: p. 81-90.

37. Sonnleitner B., Käppeli O., *Growth of Saccharomyces cerevisiae is controlled by its limited respiratory capacity : formulation and verification of a hypothesis.* Biotechnology and bioengineering, 1986. **28**: p. 927-937.

38. Müller S., Lösche A., *Population profiles of a commercial yeast strain in the course of brewing.* Journal of food engineering, 2004. **63**: p. 375-381.

39. Srienc F., *Cytometric data as the basis for rigorous models of cell population dynamics.* Journal of biotechnology, 1999. **71**: p. 233-238.

40. Henson M.A., *Dynamic modeling of microbial cell populations.* Current opinion in biotechnology, 2003. **14**: p. 460-467.

CHAPITRE 2

Approche classique et structurée pour l'étude des paramètres du génie chimique en relation avec un bio-procédé

Abstract

In this article, two theories are unified to investigate the effect of hydrodynamics on a specific bioprocess : the network-of-zones (NOZ) hydrodynamic structured modelling approach (developed by several authors but only applied to a few bioprocesses (17) (20)) and the effectiveness factor η approach (4) (15). Two process scales have been investigated (20 and 500 liters) and for each, hydrodynamics have been quantified by the use of a NOZ validated by homogeneity time measurements. Several impeller combinations inducing very different hydrodynamics were tested at 20L scale. After this step, effectiveness factors were determined for each fermentation run. To achieve this, a perfectly mixed microbial kinetic model was evaluated by using simple Monod kinetics with a fed-batch mass balance. This methodology permitted determination of the effectiveness factor with more accuracy because of the relation with the perfect case deduced from the Monod kinetic. It appears that for small scale, η decreases until reaching a value of approximately 0.7 (30% from ideal case) for the three impeller systems investigated. However, stirring systems which include hydrofoils seem to maintain higher effectiveness factors during the course of the fermentation. This effect can be attributed to oxygen transfer performance or to homogenisation efficiency exhibited by hydrofoils. In order to distinguish the oxygen transfer from the homogenisation component of the effectiveness factor, these phenomenon were analysed separately. After determination of the evolution of η_{O2} linked to oxygen transfer for each of the fermentation runs, NOZ model was employed to quantify substrate gradient appearance.

After this step another effectiveness factor η_{mix} related to mixing was defined. By this way, it is possible to distinguish relative importance of mixing effect and oxygen transfer on a given bioprocess.

Results have highlighted an important scale effect on the bioprocess which can be analysed by the use of the NOZ model.

_____

1. **Introduction**

Microorganisms are very sensitive to environmental conditions such as pH level, substrate concentration and dissolved oxygen level. These considerations have led to the design of stirred bioreactor for large scale manipulation of micro-organisms. Indeed, impeller systems tend to generate a high turbulence in the bulk of the stirred liquid and thus to enhance transfer processes such as mass transfer, heat transfer and kinetic energy transfer. Nevertheless, limitations to these actions appear when operating at large scale or with viscous broth.

Bioreactor efficiency is important at several levels. First, to ensure a good homogeneity of the broth, and second, to enhance the transfer efficiency such as oxygen transfer from the gas phase to the liquid phase and heat transfer. This paper deal with the impact of chemical engineering parameters on the growth of a *Pichia pastoris* wild strain in a fed-batch stirred bioreactor. This micro-organism is sensitive both to oxygen transfer and substrate homogenisation (due to Pasteur effect at high substrate concentration). Traditional chemical engineering approaches involve the use of specific performance criteria in order to quantify the efficiency of these two phenomena : $k_l a$ for oxygen transfer and mixing time or homogeneity time for mixing efficiency. However, these performance criteria are not characteristic of the bioprocess because they are only linked with physical performance of the stirring system and not with the dynamics of the process.

In order to quantify the efficiency of bioreactor, a practical approach consist to employ an effectiveness factor η (4). This factor represent the ratio of the reaction rate $r_{process}$ of the process considered to the reaction rate $r_{perfect}$ of a process without mixing and transport limitations :

$$\eta = r_{process}/ r_{perfect}$$

When there is no problem associated with mixing or mass transfer, the biochemical reaction rate is only limited by the biological system itself and $\eta = 1$.

In this paper we propose to use a theoretical kinetic in order to fix the denominator of η at a reliable value. Indeed, the traditional approaches have not considered a real fermentation run to fix the reaction rate of the supposed perfect process. However, this run does not correspond to an ideal case because it is performed in real

conditions and some uncertainties related to this assumption remain when calculating η.

When $\eta < 1$, mixing operation becomes limiting for the process reaction rate and problems due to gradient appearance and oxygen transfer appear.

The process considered here is particularly sensitive to gradient formation and oxygen limitation. Indeed, *P. pastoris* is sensitive to glucose effects (shift from a respiratory to a fermentative metabolism, even in aerobic conditions, which lead to a lower cell yield) and fed-batch regulation must be tuned in this way. Nevertheless, substrate addition at the top of the bioreactor leads to gradient formation with an intensity depending of the mixing efficiency of the agitation system. We can thus describe the effectiveness factor as a function of two components :

$$\eta = f(\eta_{mix}, \eta_{O2})$$

With η_{mix} being the component of the η factor associated with the homogenisation efficiency of the impeller system and η_{O2} being the oxygen transfer performance component of the impeller system. Distinction between the two components is important in order to orientate the stirring system design and operating conditions.

At this stage of knowledge, we need reliable methods to predict mixing efficiency of a bioreactor. Simplest method consist of a mixing time measurement. This can be achieved by injecting a non-reactive tracer and following it in the vessel studied. But experiments involving several probes are best to conduct homogeneity time measurements (10).

Improvements have been accomplished with the appearance of structured hydrodynamic models. These models are based on tank-in-series concept in which the vessel is separated into several compartments which are individually considered as perfectly mixed. Figure 1 give example of a fed-batch process. By using traditional approach which consist to consider the vessel as perfectly mixed, gradient formation is neglected. It as been showed that these gradients have a great impact on microbial kinetics (2) (6) (7) (11). The structured approach will take into account gradient appearance along the vessel by breaking the black box (figure 1). By this approach, it is possible to see what happen inside the vessel and to follow several parameters at several locations. In the case of a fed-bacth process, it permits detection of gradient appearance along the vessel height. Great interest has been

given to this approach and several variants can be found in the literature in function of type of impeller used (axial or radial), number of agitation stages, number of perfectly mixed cells (this parameter being given in the case of a batch bioreactor). Complexity of hydrodynamic model varies from considering single or a few perfectly mixed cells per agitation stage (3) (8) (16) (18) to a network of interconnected cells per agitation stage (9) (17) (20).
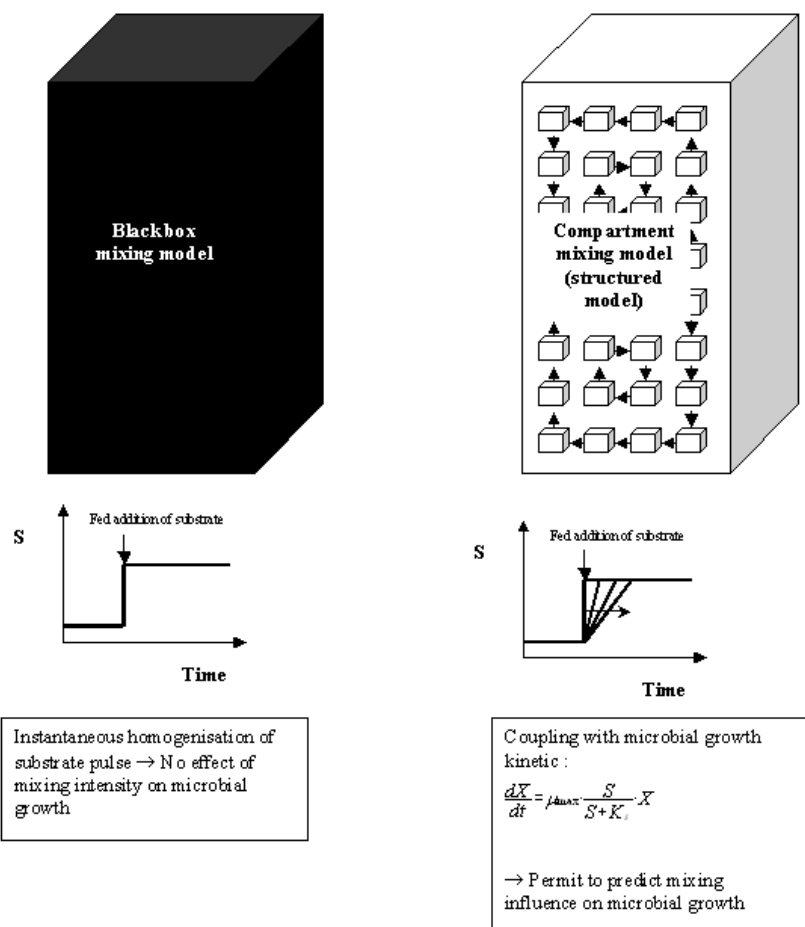

Figure 1 : comparison of an hydrodynamic black box (unstructured) model with a structured network-of-zones model. The first model consider that a pulse of substrate fed to the top of the vessel is instantaneously mixed and thus substrate concentration is automatically homogenized after injection. The second model

consider the internal dynamic of mixing by dividing the whole tank into a series of perfectly mixed elements. This second approach permit to consider substrate gradient appearance during a fed-batch process.

In this study, the efficiency of a fed-batch process involving a *P. pastoris* strain cultivation was studied. Several impeller combinations were tested and fermentation at pilot scale was also performed in order to investigate scaling effect. A network-of-zones model has been constructed to estimate mixing efficiency for each of agitation systems and the oxygen transfer coefficient was followed during fermentation runs. In a second step effectiveness factor was calculated on the basis of the theoretical microbial curve obtained by the use of a Monod kinetic adapted to *P. pastoris* cultivation in fed batch mode. Estimation of effectiveness factor permitted determination of the appearance of mixing or transport limitations. On the basis of the NOZ model, a method to distinguish mixing efficiency from oxygen transfer efficiency will be discussed.

2. __Material and methods.__

Experimental strategy.

During a first experimental step, chemical engineering experiments of homogeneity time were performed. Mixing curves obtained were used to validate the turbulent flow rate component (q_e) of the network-of-zones model .

During a second experimental step, several fermentation runs with varying impeller system and scale were performed. Effectiveness factor was calculated in function of time for each fermentation run.

At this stage NOZ simulations with fermentation stirring conditions permit to quantify heterogeneity magnitude. On this basis, it is possible to distinguish heterogeneity problems from oxygen transfer problem, this distinction being useful to improve bioreactor efficiency.

_____

P. pastoris cultivation.

P pastoris CWBI F383 wild strain were grown on rich medium. Precultures were performed on 863 broth (20 g/l glucose ; 10 g/l yeast extract ; 10 g/l casein pepton) in 150 and 500 ml shake flasks. The 500 ml flasks were used to inoculate fermentors. *P pastoris* CWBI F383 wild strain were grown on rich medium.

Bioreactors.

Stainless steel strirred bioreactors (Biolaffite-France) of 20 liters (D = 0.22 m) and 500 liters (D = 0.62 m) were used in this study. Temperature, dissolved oxygen and pH were regulated by an automate (ABB). During the culture, pH was maintained at 5.5, temperature at 30°C and dissolved oxygen was maintain as longer as possible above 30% from saturation by varying stirrer speed (initial rotational speed of 150 rpm and maximum rotational speed of 450 rpm). Substrate (glucose) is fed at the top of the bioreactor with an exponential flow rate $F = F_0 . exp^{ex.(t-tstart)}$ (maximum flow rate F_{max}). Off-gas analysis was performed by a CO_2 infrared analyser (Servomex) and an oxygen paramagnetic analyser (Servomex). Data were collected and managed to compute the volumetric oxygen transfer coefficient ($k_l a$).
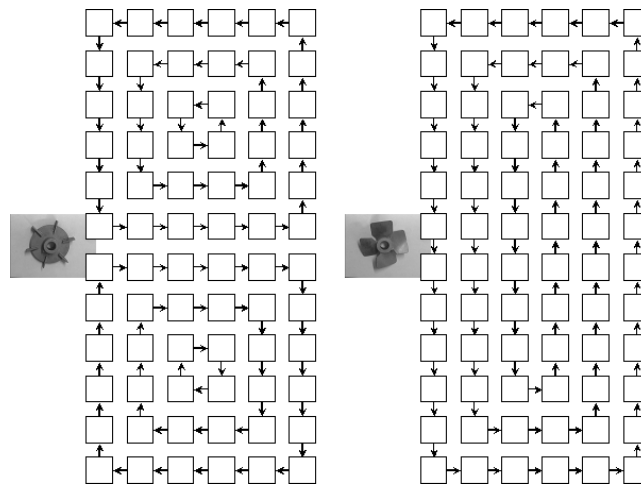
Figure 2 : distinction between a radial flow pattern (left) induced by a rushton turbine and an axial flow pattern (right) induced by an A315 hydrofoil. Only the qc circulation component is represented on this figure.

_____

In the case of 500 L vessel, only TD6-TD6 stirring system were used. For experiments conducted in 20L vessel, several impeller combinations were tested (see figure 2 for details). Mixing efficiency of these impellers were previously tested in an experimental perspex stirred vessel. Microbial growth was followed by optical density measurements at a wavelength of 540 nm. Plate count and final dry matter measurements were also performed in order to convert OD measurements in grams of biomass per litter.

Experimental vessel.

Homogeneity time experiments were performed in a Perspex vessel (D = 0.24 m). Air is injected trough a pipe sparger (2 mm holes). Two experimental fluids of varying rheological properties were used : water and aqueous solutions of carboxymethylcellulose (Fluka). CMC solutions were made at weak concentration in order to show the impact of a slight increase of the viscosity on the mixing process, as can be observed when operating with a high cell density fermentation like a *Pichia pastoris* fed-batch process. A pulse of heated fluid (100 ml) was added at the top of the vessel near a baffle in order to produce a temperature fluctuation of approximately 0.3°C. The temperature curves were recorded by several thermosensors disposed on the baffle. Data were recorded each second by a labview 3.1. station.
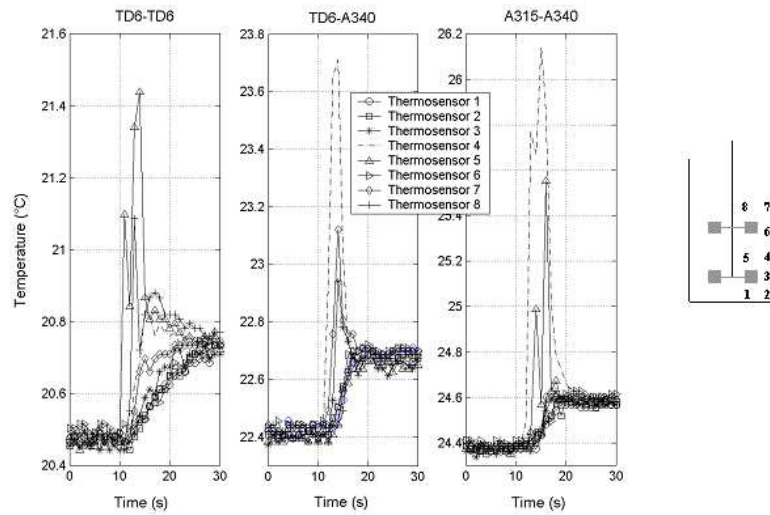
Figure 3 : Comparison of mixing curve obtained for different impeller combinations tested (Working fluid : water ; N = 270 rpm). Figure on the right side show the location of the thermosensors in the vessel.

Thermosensors are made of copper–constantan (response time of 0.45 s.). Typical mixing curves can be seen on figure 3. Homogeneity time was calculated as described in the literature (10). Mixing curves were used to adjust parameter of the NOZ model. Mixing time experiments were also perfomed on the 500L vessel by using the conductivity technique (Conducell electrode with acquisition interval of 2 s).

3. Network-of-zones mathematical model design.

The model contain a constant number of perfectly mixed zones (72) per stirring stage. The number of zones is justified by a geometrical network of 2 cm sided cells. The adjustable parameters are : the circulation flux between cells q_c and turbulence flow q_e (this parameter also include the pneumatic component of mixing in the case of aeration). The circulating floware oriented depending on the global pattern generated by the impeller type used (radial or axial) as can be seen on figure 2. NOZ model consist of a mass balance on the perfectly mixed cells interconnected by

circulating and/or turbulence flows. For a given zone n, mass balance equation have the following form :

$$V \cdot \frac{dC_n}{dt} = Q_c \cdot (C_{n+i} - C_n) + Q_e \cdot (C_{n+i} + C_{n-j} - 2C_n)$$

It result a set of ordinary differential equations (one for each cell or zone) that can be resolved numerically by a Runge-Kutta routine.

Turbulence flow q_e is modelled by backmixing flow between each adjacent zones in the vertical direction. The value of this parameter is estimated by adjustment on experimental homogeneity curve.

The circulation flow q_c is determined by the use of the following correlation which come from dimensional analysis :

$$Q_c = N_{qc}.N.d^3$$

For turbulent flow (Re > 10000), circulating number N_{qc} remain constant. In the case of an aerated vessel, gaseous cavities formation at the back of impeller blades induce a drop of the pumping capacity of the agitation system. This drop is similar to the power drop and can be estimated by computing the aerated power by the use of correlations found in the literature (17) (20).

For transitional flow, influence of viscosity on circulation capacity of the impeller must be taken into account. For TD6 impeller Meztner and Norwood (13) correlation can be employed (this correlation was previously validated for several working fluids such as CMC and xanthan solutions(17)).

4. <u>Results and discussion.</u>

Chemical engineering experiments.

The three impeller systems were first tested for mixing efficiencies. To achieve this, homogeneity time measurements were made as described earlier. As shown at figure 4, radial impeller combination showed a larger time to achieve a given homogeneity degree (here, 85%). Previous studies have shown similar results (1). This was due to the compartmentalisation effect induced by radial projection of liquid by the turbine.

_____
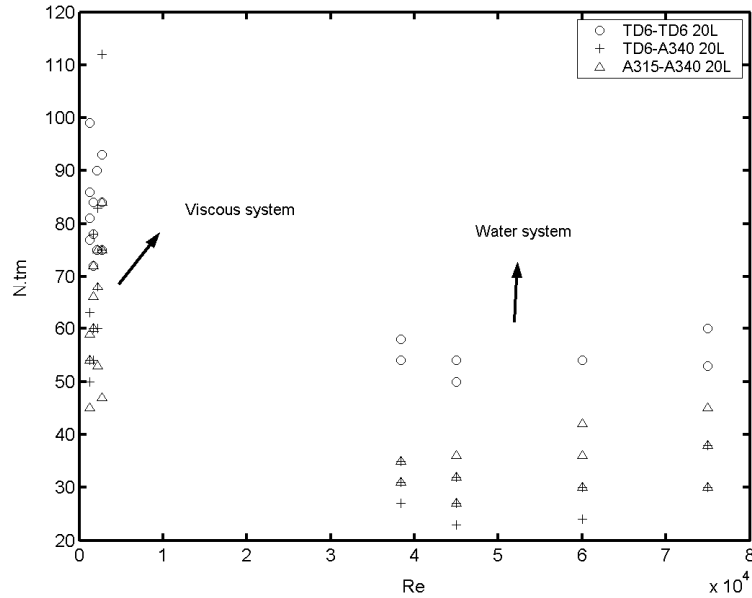
Figure 4 : dimensionless plot synthesizing homogeneity time results obtained for Water and CMC solution (viscous system) under varying operating conditions for the three impeller combinations tested.

Replacement of the upper impeller by a propeller (axial) avoided this effect and reduced the homogeneity time. We can see that the three impeller combinations tested showed different hydrodynamic behaviours and mixing experiments highlight only the impact of these differences on the homogenisation efficiency. Indeed, analysis of typical mixing curves show pronounced divergence between fluid mechanics induced by the impeller combinations (figure 3). These differences have been interpreted by several authors as an exchange flow between agitation stages, this exchange flow being more pronounced in the case of axial impeller (8).

We can thus conclude that the radial or axial behaviour exerted by the impeller greatly influences the hydrodynamic, differences being induced by the balance between recirculating and turbulence component of the impeller. These a priori knowledge will be exploited for the elaboration of the NOZ model firstly by representing the circulation flows following a radial or an axial pathway, and secondly by considering a circulating component (q_c) and a turbulence component (q_e).

46

Values of homogeneity time are used to adjust the q_e parameter of the NOZ model for different operating conditions and for different impeller combinations. This model will be used to operate simulations in order to estimate substrate gradient magnitude for each agitation system tested. To achieve this, the NOZ model will be coupled with a simple Monod kinetic in order to take into account the impact of the substrate consumption rate.

Biochemical engineering experiments.

The use of an effectiveness factor is an original way to investigate impact of mixing operation on microbial processes. Referring to the definition of η, microbial kinetic corresponding to a perfectly mixed case can be defined with a stronger theoretical basis by employing a simple Monod kinetic coupled with mass balance equations corresponding to a fed-batch operation (5). Parameters related to the calculation of theoretical microbial kinetic are given in table 1 and were obtained during previous batch experiment.

Table 1 : list of kinetic parameters used to determine the theoretical microbial growth curve in perfectly mixed condition for the calculation of η.

μ_{max}	$0.32\ h^{-1}$
K_s	$0.025\ g/l$
m_s	$0.013\ h^{-1}$
$Y_{x/s}$	0.42
S_a	$370\ g/l$
Q_o	$0.005\ l/h$
Q_{max}	$0.25\ l/h$
exp	0.32
t_{start}	$9\ h$

We obtain by this way a theoretical microbial growth curve which correspond to the following ideal assumptions : bioreactor is perfectly mixed, oxygen is in excess and only carbon source is limiting. Thus, effectiveness factor calculated on the basis of this theoretical growth curve is representative of the mixing and mass transfer

efficiency of the apparatus chosen to achieve a given bioprocess. Figure 5 compare microbial kinetics obtained on a theoretical basis and those obtained during fermentation experiments.
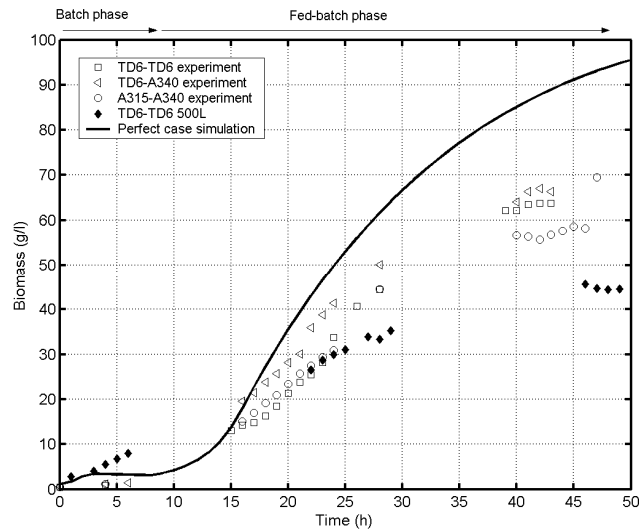
Figure 5 : microbial growth curves obtained during fermentation runs at 20L and 500L scales and comparison with theoretical growth curve.

We can see that after the initial batch phase (10 hours), there is a divergence from ideal case for all mixing system considered.

Figure 6 show the evolution of the effectiveness factor along each fermentation run performed for different hydrodynamic conditions. After the initial batch step (feed pump is only activated after 10 hours), η tend to decrease. This can be attributed by mixing limitation which is traduced by substrate gradient appearance and by oxygen depletion.
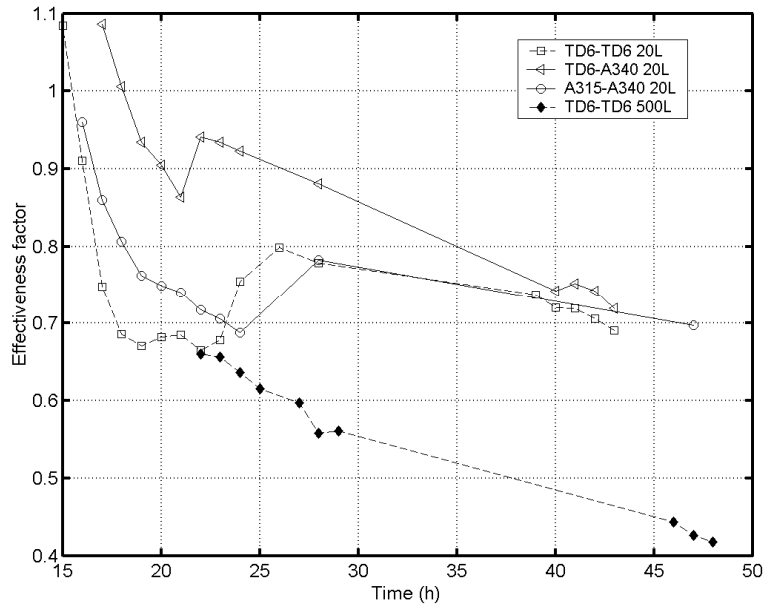
Figure 6 : variation of the effectiveness factor η with time for each stirring system considered.

We need thus a new parameter to make the distinction between mixing and mass transfer phenomena.

The first step for going in this way is to manage oxygen transfer coefficient obtained by gas balance analysis in order to define an effectiveness factor related to mass transfer only. We can thus define :

$$\eta_{O2} = k_l a / k_l a_{perfect}$$

With being the oxygen transfer coefficient permitting to ensure no oxygen limitation during the culture. It can be easily calculated knowing that in a perfect situation, 1 g of oxygen must be used to assimilate 1 g of glucose. Taking into account the time and the volume of culture, we obtain $k_l a_{perfect} = 900 \ h^{-1}$. Figure 7 show the evolution of η_{O2} for all the fermentation runs. Dissolved oxygen regulation by controlling stirring speed improves the η_{O2} (shift from 0,2 to 0,4 for the 20L scale), this impact being less pronounced at 500L scale. Indeed, in this case oxygen becomes limiting faster than for the 20 litters vessel due to the lower aeration capacity of the larger system as can be seen at figure 7. In this figure, it can be also seen that the TD6-TD6

system at 20 litters scale show a drop of performance at 16 h. At this time, growth was exponential and the dissolved oxygen requirement was maximal. The drop recorded for the TD6-TD6 system is due to a lack in the capability of reaction of the dissolved oxygen regulation system based on agitation speed (this phenomenon can be visualised at the top part of figure 7 which show the stirrer speed evolution during the culture).
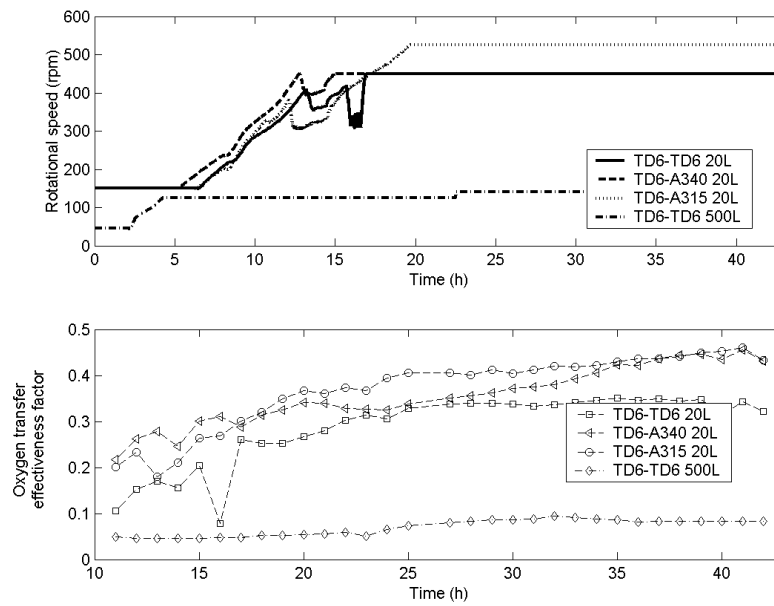
Figure 7 : variation of the oxygen transfer effectiveness factor η_{O2} with time for each stirring system considered. Upper graphic show the increase of stirring speed induced by he regulator in order to maintain dissolved oxygen level at 30% from saturation.

In general, η_{O2} stays at a low value and dissolved oxygen is irremediably a limiting factor of *P. pastoris* growth, and in general for high cell density cultures.

Computation of an effectiveness factor related to homogenisation by the use of the NOZ model.

The effectiveness factor does not permit to distinguish directly mixing effects from mass transfer effect. In our case, mixing effect is very important because substrate is added continuously during the culture. We need thus a parameter to estimate mixing efficiency in the particular case of a fed-batch process. By using NOZ coupled with a simple Monod microbial kinetic, it is possible to evaluate glucose gradient in bioreactor. But it is a purely subjective method, because the microbial growth is directly influenced by substrate repartition into bioreactor. Indeed, if we take a given value of growth rate to compare mixing efficiency of different apparatus, the results don't depend on the microbial activity but are only influenced by homogenisation efficiency of the apparatus. It is an artefact created by the coupling of NOZ and microbial growth model. In order to obtain a realistic model coupling microbial growth and fluid mechanic, we need an equation relating the influence of substrate concentration fluctuation on specific growth rate. This is a very ambitious task going out of the context of this paper. At this stage, attention will be focused on the fluid mechanic part of the problematic.
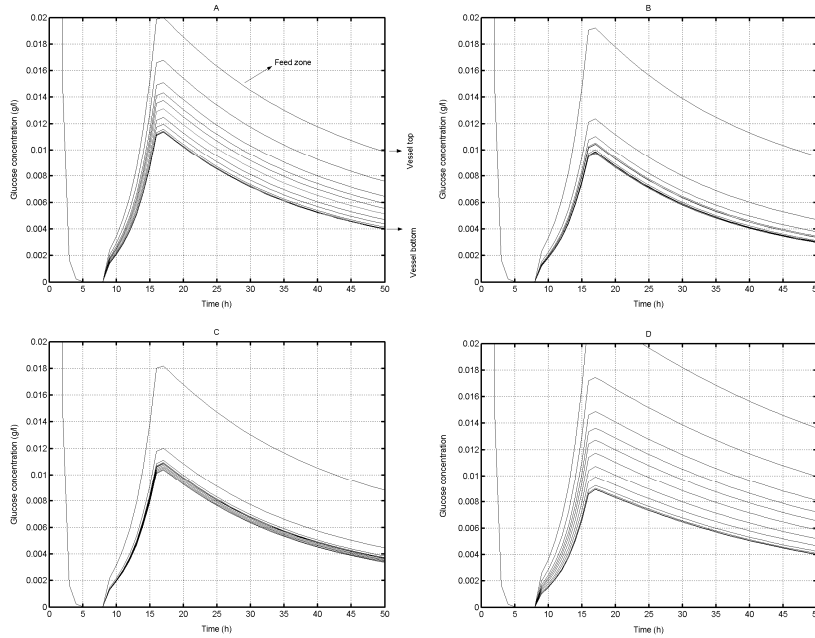
Figure 8 : substrate gradients observed for each stirring systems when coupling NOZ model to a simple Monod microbial growth model (A : TD6-TD6 system at 20L scale ; B : TD6-A340 system at 20L scale ; C : A315-A340 system at 20L scale ; D : TD6-TD6 system at 500L scale).

Microbial kinetic can thus be coupled to the NOZ model, the growth rate being the same for all the experiments. Results obtained depend only on the chemical engineering performance of the impeller systems and are not influenced by the microbial growth.

Simulations performed for each stirring system are shown at figure 8. It can be seen that systems including hydrofoils (A340 or A315) are more efficient to minimise the substrate gradient inside the vessel. For all the simulations, the zone receiving directly substrate pulse is constantly subjected to higher substrate concentration than in the bulk of the vessel.

An objective way to define the effectiveness factor related to the mixing component is to consider the inhomogeneity curve (10). On this basis, a parameter specific to the homogenisation of the system at a given microbial reaction rate can be defined :

$$\eta_{mix} = 1 - i$$

With i being the inhomogeneity degree as described in the literature (10). Modification have been performed on this parameter in order to be specific of the microbial process :

$$i = s \,/\, \text{acceptable gradient}$$

With s being the mean absolute deviation of the different zones of the model from a homogenous substrate concentration. Here, the originality comes from the fact that the inhomogeneity degree is calculated on the basis of an acceptable gradient for the bioprocess. We obtain a parameter more reliable than the traditional performance criteria used to quantify mixing efficiency (mixing time) because related to the dynamic of a fed-batch bioprocess.

Evolution of the inhomogeneity degree is shown at figure 9. During the exponential phase of the feed, gradient formation tendency is greater for all the system tested. Working at 500L scale implies a degree of inhomogeneity of 16%, which is 4 time greater than the 20L scale with the same impeller system. At this scale system comprising hydrofoil presents a slightly lower inhomogeneity degree than the double turbine (TD6-TD6) system. This effect can be attributed to the well known compartmentalization effect induced by radial impeller such as TD6.
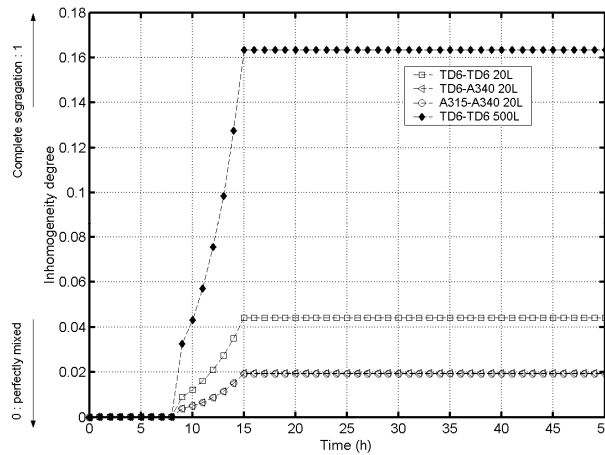
Figure 9 : evolution of the inhomogeneity degree compute by he use of NOZ model for each stirring system considered. Calculations performed on the basis of an acceptable gradient of 10 mg/l.

Figure 10 present the evolution of for each of the system tested. It can be seen that this factor is acceptable from a biochemical engineering point of view for each scale considered ($> 80\%$). However, sensitivity of *P. pastoris* to gradient exposure is not known , and it is not possible to obtain maximal tolerable gradient to compute the η_{mix} value limiting for the bioprocess. Further research must then be necessary to investigate this effect.
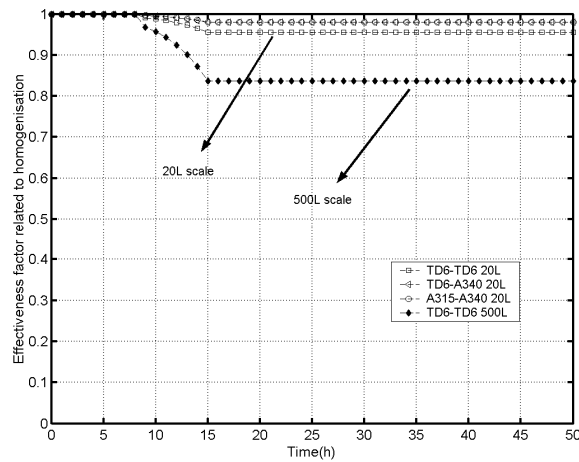
Figure 10 : variation of the homogenisation effectiveness factor η_{mix} with time for each stirring system considered.

Conclusions.

Experiments conducted in this study highlight the influence of the homogenisation efficiency and mass transfer on a bioprocess conducted in a stirred vessel operating with a low viscosity broth. To achieve this, a NOZ model has been elaborated to integrate fluid dynamic in the microbial process and thus to facilitate study of mixing and mass transfer for a given set of operating conditions. Indeed, these two factors are implied in the efficiency of bioreactors and a method is necessary to distinguish them. A method has been developed in this paper and involve the concept of effectiveness factor developed by (4). The effectiveness factor has been divided into two components to deal separately with oxygen transfer and

homogenisation. These factors have been expressed in comparison with a perfectly mixed simulated growth curve. This approach permit to obtain results on a more reliable basis.

The effectiveness factor related to the homogenisation efficiency is more difficult to express. To facilitate its implementation, a NOZ model has been used to express substrate gradient concentration in stirred vessel. NOZ model has been extensively studied in the literature, but only a few papers deal with application to bioprocesses. The methodology presented here permit to make this link by the use of an integrated effectiveness factor.

Experiments and simulations with NOZ have demonstrated very different hydrodynamic behaviours between impeller combinations tested. Chemical engineering data obtained are in accordance with related literature (1). Scale-up has shown a significant decrease in microbial growth which can be attributed to hydrodynamic and oxygen transfer. At this stage of the study, it is recommended to try hybrid radial-axial (TD6-A340) or complete axial (A315-A340) impeller combinations at larger scale, these configurations promoting better mixing efficiency.

However, during the scaling-up, heterogeneity will become more and more important leading to substrate gradient accompanied by an oxygen gradient. Comparison of experiments conducted in 500L and in 20L have highlighted this effect. The structured component of the effectiveness factor related to homogeneity will thus have a critical importance at large scale because both carbon substrate and oxygen have to be homogenised (14). NOZ have proven to be an efficient tool for the estimation of gradient appearance and can be used for estimating the mixing part of the effectiveness factor.

Analysis of effectiveness factor components have lead to the conclusion that stirring systems composed of hydrofoil(s) present better oxygen transfer effectiveness factor and homogenisation effectiveness factor. Results obtained in this study show a slightly positive impact on microbial growth. It implies that hydrofoils could be used to design a stirring system at a greater scale were mixing efficiency is necessary to

ensure a good homogenisation of both dissolved oxygen concentration and substrate concentration.

In order to obtain more reliable η_{mix} value, acceptable gradient intensity must be know. To achieve this, it is necessary to know the substrate gradient sensitivity of P. pastoris. Apparatus for such experiments is described in the literature (6) (11) and more work must be conducted in this way.

In conclusion, a method for comparing the impact of homogenisation and oxygen transfer on bioprocesses has been proposed. Efficiency of such a methodology has been tested on a *Pichia pastoris* fed-batch process and has lead to a reliable basis for comparison of processes performances (several impeller combinations and two scales have been investigated). The great advantage of this approach is to make a direct link between chemical engineering variables and microbial kinetic.

References

1. Bouaiffi M., Roustan M. (2001), *Chemical engineering and processing*, **40**, 87-95.
2. Bylund F., Collet E., Enfors S.O., Larsson G. (1998), *Bioprocess engineering*, **18**, 171-180.
3. Cui Y.Q., van der Lans R.G.J.M., Noorman H.J., Luyben K. (1996), *Trans. IchemE*, **74**, 261-271.
4. Diaz M., Garcia A.I., Garcia L.A. (1996), *Biotechnology and bioengineering*, **51**, 131-140.
5. Dunn I.J., Heinzle E., Ingham J., Prenosil J.E. (2003), *Biological reaction engineering*, Wiley-VCH Verlag, Weinheim, pp.77-116.
6. Enfors S.O., Jahic M., Rozkov A., Xu B., Hecker M., Jürgen B., Krüger E., Schweder T., Hamer G., O'Beirne D., Noisommit-Rizzi N., Reuss M., Boone L., Hewitt C., McFarlane C., Nienow A., Kovacs T., Trägardh C., Fuchs L., Revstedt J., Friberg P.C., Hjertager B., Blomsten G., Skogman H., Hjort S., Hoeks F., Lin H.Y., Neubauer P., van der Lans R., Luyben K., Vrabel P., Manelius A. (2001), *Journal of biotechnology*, **85**, 175-185.
7. Lin H.Y., Neubauer P. (2000), *Journal of biotechnology*, **79**, 27-37.
8. Machon V., Jahoda M. (2000), *Chemical engineering technology*, **23**, 869-876.
9. Mann R., Williams R.A., Dyakowski T., Dickin F.J., Edwards R.B. (1997) *Chemical engineering science*, **52**(13), 2073-2085.
10. Mayr B., Horvat P., Moser A. (1992), *Bioprocess engineering*, **8**, 137-143.

11. Neubauer P., Häggström L., Enfors S.O. (1995), *Biotechnology and bioengineering*, **47**, 139-146.
12. Nienow A.W. (1997), *Chemical engineering science,* **52**(15), 2557-2565.
13. Norwood K.W., Metzner A.B. (1960), *AIChE journal*, **6**(3), 432-437.
14. Oosterhuis N.M.G., Kossen N.W.F. (1983), *Biotechnology and bioengineering*, **26**, 546-550.
15. Pena C., Galindo E., Diaz M. (2002), *Journal of biotechnology*, **95**, 1-12.
16. Vasconcelos J.M.T., Alves S.S., Barata J.M. (1995), *Chemical engineering science*, **50**(14), 2343-2354.
17. Vlaev D., Mann R., Lossev V., Vlaev S.D., Zahradnik J., Seichter P. (2000), *Trans. IchemE*, **78**, 354-362.
18. Vrabel P., van der Lans R.G.J.M., Luyben K.Ch.A.M., Boon L., Nienow A.W. (2000), *Chemical engineering science*, **55**, 5881-5896.
19. Vrabel P., van der Lans R.G.J.M., van der Schot F.N., Luyben K.Ch.A.M., Xu B., Enfors S-O. (2001), *Chemical engineering journal*, **84**, 463-474.
20. Zahradnik J., Mann R., Fialova M., Vlaev D., Vlaev S.D., Lossev V., Seichter P. (2001), *Chemical engineering science*, **56**, 485-492.

Nomenclature

CMC : carboxymethylcellulose

d : impeller diameter (m)

ex : exponential factor of the substrate feed pump

F : fed-batch pump feed rate (m³/s)

F_o : initial fed-batch feed rate (m³/s)

F_{max} : maximum feed rate (m³/s)

i : inhomogeneity degree

K_s : affinity constant (g/l)

N : impeller rotational speed (s^{-1})

n : number of circulation loops of NOZ model

N_{qc} : circulation number (dimensionless)

NOZ : network-of-zones

Q_c : circulating flow rate (m³/s)

q_c : circulating flow rate of NOZ model ($q_c = Q_c/n$) (m³/s)

q_e : turbulence backmixing flow rate of NOZ model (m³/s)

Re : Reynolds number (dimensionless)

rpm : round per minute (s^{-1})

_____

s : mean absolute deviation

S : substrate concentration (g/l)

Sa : substrate concentration in the feed (g/l)

X : biomass concentration (g/l)

Y_{xs} : substrate to biomass conversion yield

μ : viscosity (Pa.s)

μ_x : growth rate (h^{-1})

μ_{xmax} : maximum growth rate (h^{-1})

η : effectiveness factor (%)

η_{mix} : homogenisation component of the effectiveness factor (%)

η_{O2} : oxygen transfer component of the effectiveness factor (%)

Acknowledgements

CHAPITRE 3
Expression déterministe et stochastique d'un modèle hydrodynamique structuré de bio-réacteur

_____

Abstract

The potentiality of a stochastic approach is examined in the case of a mixing model for stirred vessels. This model is interesting due to the probabilistic and discrete properties that can be used further to facilitate the implementation of a hydrodynamic model into complex reacting systems, such as those encountered in bioprocesses. Stochastic model performances are compared to well known deterministic compartment mixing models (CM). It appears that parameters coming from CM can be used in the stochastic approach and that they give equivalent results. A methodology is elaborated that simplifies the determination procedure of the adjustable parameters of the stochastic model. The most important parameter to determine is the time step of a simulation performed by the aim of the stochastic model. Indeed, the time step is not explicitly given by the model and a correlation is necessary to translate simulation intervals into real time increments. After an appropriate analysis of several mixing systems (single or multi-agitated) it appears that a simple correlation involving circulation time could be used to perform this translation. The correlation contains an adjustable parameter, which has been quantified for the operating conditions covered in the study. The circulation of micro-organisms was also simulated simply by using the transition matrix coming from the stochastic model, which shows the potentiality of this kind of model in the field of complex reacting systems, such as those encountered in bioprocesses.

Introduction

The elaboration of a probabilistic mixing model from the well known structure of a compartment model (CM) has been investigated in this study. CM has been widely described in the literature and allows the representation of mixing phenomena with a relatively good resolution (depending of the model structure). Nevertheless, only a few number of compartment models have been applied to the description of mixing problems in bioprocesses [1-3].

The idea is to extend this kind of model to a stochastic approach in which the passage of particles from one flow region to another is governed by probabilities. Interest in this kind of model comes from its probabilistic and discrete properties, which facilitate implementation with complex reacting systems, such as fermentation processes. In addition, the stochastic model is very simple to compute and does not require large computation space or time. This low computational requirement is an additional reason allowing the inclusion of this model within more complex ones, such as microbial kinetic models.

In order to understand the working principles of these models, a short literature review is necessary. As stated previously, a large number of compartment mixing models are available in the literature. The first structures were very simple and comprised a single compartment per agitation stage, a compartment corresponding to a volume element of the reactor considered to be perfectly mixed [4-10]. The structures then evolved and were applied to stirred bioreactors. This led to very complex model structures, such as the network-of-zones (NOZ), which comprises a large number of interconnected compartments [11, 12]. These NOZ models have a higher resolution but require more computation space because of the large number of differential equations involved.

In terms of similarity, the compartment network of a classical CM can be used in a stochastic context. Indeed, this model consists of several states that can be assimilated into the compartments of the CM. The structures are therefore very similar and differences between the two approaches come from the mathematical formulation of the models. Stochastic mathematical expression does not involve ordinary differential equations, but a transition probability matrix that orientates the evolution of the system. This system comprises several states that correspond in our application to the concentrations in several delimited zones in the stirred vessel. The CM principle, having been greatly improved upon, is useful to take as a basis from which to elaborate stochastic models that are not widely applied in the area of fluid mixing, except in the case of some theoretical considerations [13-15]. Of interest is the fact that stochastic models have properties that can be used to study special mixing phenomena, which are important, notably in bioprocesses.

The first property is the stochastic aspect of the model that can be used to make particle following studies [14]. This aspect is very important in bioprocesses because it enables the easy description of circulation paths taken by microorganisms inside a stirred bioreactor, and allows the determination of, for example, the frequency at which microbes are exposed to high nutrient concentrations or high shear stress [2, 16]. Circulation simulation will be investigated in the last section of this paper.

The second property is the discrete aspect of the model that can be interesting when coupling hydrodynamics with complex reactions, such as microbial kinetics [17]. This property will be investigated in further studies. There are many other properties that can be usefully exploited. One example is the absorbing property, which will be investigated in this study.

Material and methods

Experimental stirred vessel

Two impellers were used: rushton disk turbines (RDT6) and lightning hydrofoils A315 (pumping downward), both having a diameter of 0.1 m. Some combinations were particularly investigated: RDT6-RDT6, RDT6-A315 (the first cited impeller was placed at the lower part of the vessel and the second one at the upper part ; impeller clearance from the bottom of the vessel : 0.1 m ; inter-impeller clearance : 0.2 m). Photographs of these impellers are shown in Figure 2. All experiments were performed in a Perspex stirred vessel (D = 0.22 m) equipped with four baffles.

Mixing time experiments

Three kinds of mixing experiments were employed in this study, each kind permitting the investigation of a specific aspect of mixing behaviour.

The first kind of experiment consisted of measuring the mixing time in a vertical plane of the stirred vessel. To achieve this, a series of thermocouples attached onto a baffle of the vessel were used. The small dimension of these probes (0.45 mm diameter) allows the control of only a restricted volume element in the vessel. It can

thus be assumed that only a vertical plane in the vessel was involved in the experiments facilitating the implementation of the results in a CM.

The second kind of experiment was also a mixing time measurement, but here we used conductivity probes. In this case, due to the larger dimensions of the probes (1 cm diameter), the volume elements are bigger and must be considered in a three-dimensional context. Experiments conducted in this way were used to implement three-dimensional models. The positions of the probes for these two kinds of experiment are presented in Figure 1.
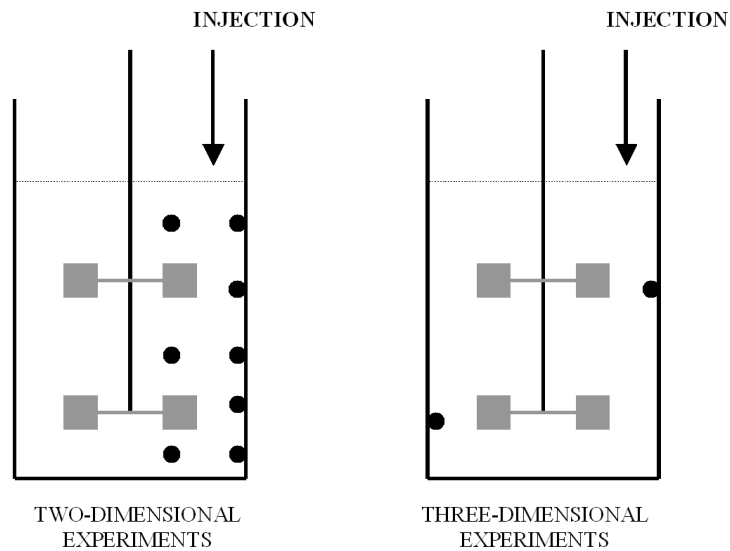
Figure 1: Locations of thermosensors (on the left) and conductivity probes (on the right) in the stirred vessel

The third kind of experiment was a residence time distribution (RTD) measurement. The apparatus is the same as for the previous one, but here fluid is continuously fed and extracted from the vessel at a flow rate of 50 ml/s. Conductivity probes allow the on-line measurement of the decreasing concentration of the injected tracer. These experiments allowed for an improvement of the stochastic model, by analysing the absorbing state property.

For the first and second kind of experiment, the mixing time (corresponding to a degree of mixing of 85%) was calculated from tracer curves using the method

presented by Mayr *et al.* [18]. In this method, an ideal response function corresponding to the tracer curve of a pulse added in a perfectly mixed reactor must be first determined. The standard deviations of each experimental tracer curve (5 or 8 for the thermal method and 1 or 2 for the conductivity method) from this ideal response function are then calculated. The standard deviations are summed and divided by the number of sensors to give an inhomogeneity function varying from 0 (total homogeneity) to 1 (total inhomogeneity). In this study, the mixing time corresponded to the time at which the value of the inhomogeneity function dropped to 0.15, or in other words a degree of mixing of 85%. The inhomogeneity degree was chosen at a high enough level to make the fluctuation signal of the probes negligible.

A large amount of data were collected in this way and were used to elaborate a mixing database containing the experimental conditions, the mixing time results and the parameter estimation for each model. In order to limit the experimental field and to concentrate our attention on stochastic model development, only the results performed in water in non-aerated conditions will be considered in this paper. Indeed, aeration and viscosity led to a modification of the parameters of the model (e.g., circulation flow drop with increasing aeration and/or viscosity). This requires extensive discussion, which cannot be included in the space allowed.

Mathematical models: CM and stochastic approaches

The aim of this paper is to translate compartment mixing model knowledge into a stochastic context. Advantages of such an approach have been briefly discussed in the introduction and will be reviewed at the end of this study.

It is of practical importance to begin with a brief description of the two models presented here and to discuss their differences. In the case of the compartment mixing (CM) approach, the flows between the interconnected compartments are responsible for homogenisation. In the case of a stochastic model, it is a series of probabilistic transitions between states that are responsible for the repartition of the tracer in the whole vessel. The CM approach consists of a set of ordinary differential equations (one for each compartment), which are resolved in a continuous manner

with an appropriate numerical method (in our case a Runge-Kutta routine was used). More details about CM construction can be found in [6, 11]. The stochastic model consists of an initial state vector S_0, which is multiplied with a transition matrix T to give a new state, S_1. This procedure can be represented by the following equation:

For the first transition: $S_1 = T . S_0$ (1)

The next step involves the multiplication of the new state vector S_1 with the same transition matrix T until a steady-state is reached:

For the second transition: $(S_2 = T . S_1)$ or $(S_2 = T^2 . S_0)$ (2)

For the ith transition: $(S_i = T . S_{i-1})$ or $(S_i = T^i . S_0)$ (3)

In our case, the state vector contained the tracer concentrations for all states, a state corresponding to a region of the agitated vessel (or a compartment in the CM context).

The numerical implementation of a stochastic simulation is thus very simple because it involves only matrix multiplication. An important fact is that the stochastic model is a discrete-space and discrete-time model, whereas CM is a continuous-time and discrete-space model. It thus appears that the two models work on a very different basis. The dissimilarities between the CM and the stochastic mixing models need to be analysed in order to facilitate the translation of knowledge between the two approaches.

In order to stay within the same referential for all the models constructed in this paper, the number of compartments per agitation stage was always 8. This is the minimum number of compartments that allow for differentiation between axial and radial impellers.

The impellers used (RDT6 and A315) exhibit three different flow patterns that influence the orientation of the circulation flow rates in the CM model. RDT6 exhibits a radial flow pattern and, on the opposite, hydrofoil A315 has an axial flow pattern. The "basic plane" models for each impeller are presented at Figure 2.

SHAFT

IMPELLER

- - → : turbulence flow rate q_e
← - - : turbulence flow rate q_e
→ : convective flow rate q_c
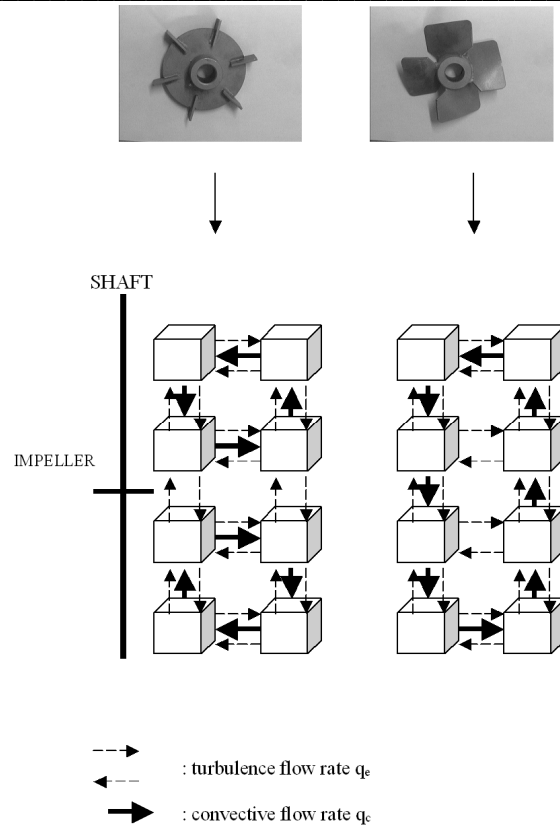
Figure 2: "Basic plane" compartment network for a radial impeller (RDT6 on the left) and an axial impeller (A315 on the right)

These basic structures can be combined to model a multi-staged vessel. In the case of a three-dimensional model, eight basic plane structures are arranged in series for an agitation stage, these planes being linked to each other by a tangential flow rate q_t (Figure 3).

SHAFT

- - →
← - - : turbulence flow rate q_e

→ : convective flow rate q_c

↗ : tangential flow rate q_t
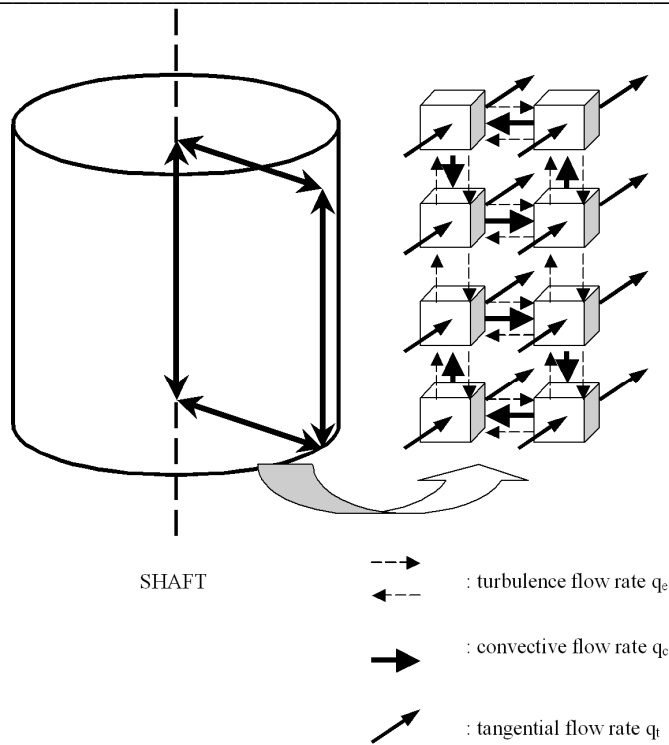
Figure 3: Arrangement scheme of "basic plane" structures to give a three-dimensional compartment model

The first step in this study was the estimation of the parameter q_e of the CM model. This allowed the determination of the ratio q_c/q_e, which would then be used for the qualitative analysis of the stochastic model. The translation from the CM model to the stochastic context is illustrated in Figure 4. This figure represents the global structure of the two models.

Compartment model	Corresponding stochastic model
- - → : turbulence flow rate q_e ← - -	⟲ : probability to stay in the actual state
→ : convective flow rate q_c	→ : probability to shift to another state
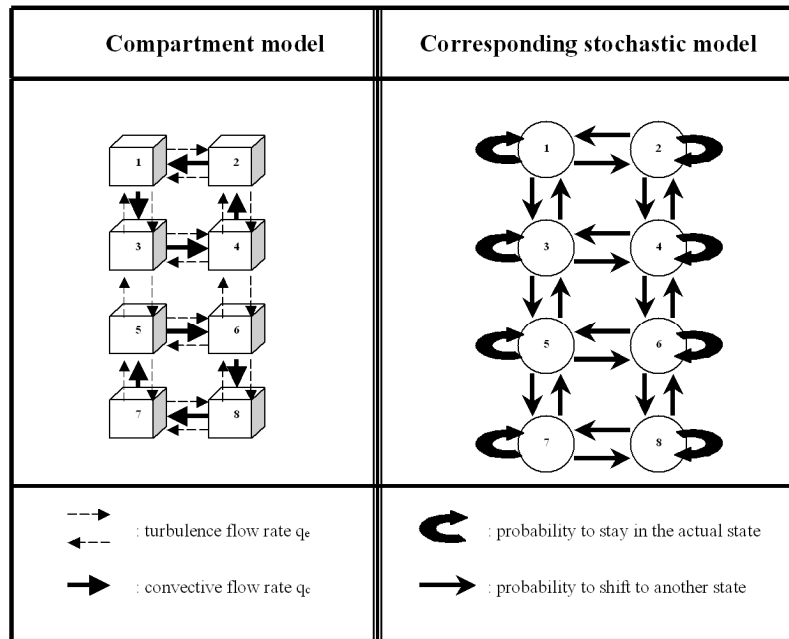
Figure 4: Comparison of the compartment model and stochastic approach

The ratio q_c/q_e coming from the CM model was used to calculate the probabilities of shifting from one state to another in the stochastic model. These probabilities were collected in the transition matrix T. An example of a transition matrix valid for a RDT6 system is given in Figure 5.

$$
\begin{array}{c c c c c c c c}
& S_1 & S_2 & S_3 & S_4 & S_5 & S_6 & S_7 & S_8
\end{array}
$$

$$
\begin{array}{c}
S_1 \\ S_2 \\ S_3 \\ S_4 \\ S_5 \\ S_6 \\ S_7 \\ S_8
\end{array}
\begin{bmatrix}
\frac{2q_e}{4q_e+q_c} & \frac{q_e}{4q_e+q_c} & \frac{q_e+q_c}{4q_e+q_c} & 0 & 0 & 0 & 0 & 0 \\[2mm]
\frac{q_e+q_c}{4q_e+q_c} & \frac{2q_e}{4q_e+q_c} & 0 & \frac{q_e}{4q_e+q_c} & 0 & 0 & 0 & 0 \\[2mm]
\frac{q_e}{6q_e+q_c} & 0 & \frac{3q_e}{6q_e+q_c} & \frac{q_e+q_c}{6q_e+q_c} & \frac{q_e}{6q_e+q_c} & 0 & 0 & 0 \\[2mm]
0 & \frac{q_e+q_c}{6q_e+q_c} & \frac{q_e}{6q_e+q_c} & \frac{3q_e}{6q_e+q_c} & 0 & \frac{q_e}{6q_e+q_c} & 0 & 0 \\[2mm]
0 & 0 & \frac{q_e}{6q_e+q_c} & 0 & \frac{3q_e}{6q_e+q_c} & \frac{q_e+q_c}{6q_e+q_c} & \frac{q_e}{6q_e+q_c} & 0 \\[2mm]
0 & 0 & 0 & \frac{q_e}{6q_e+q_c} & \frac{q_e}{6q_e+q_c} & \frac{3q_e}{6q_e+q_c} & 0 & \frac{q_e+q_c}{6q_e+q_c} \\[2mm]
0 & 0 & 0 & 0 & \frac{q_e+q_c}{4q_e+q_c} & 0 & \frac{2q_e}{4q_e+q_c} & \frac{q_e}{4q_e+q_c} \\[2mm]
0 & 0 & 0 & 0 & 0 & \frac{q_e}{4q_e+q_c} & \frac{q_e+q_c}{4q_e+q_c} & \frac{2q_e}{4q_e+q_c}
\end{bmatrix}
$$

Figure 5: Example of transition matrix corresponding to the stochastic model presented in Figure 4 (right hand side)

67

The ratio q_c/q_e only has an impact on the shape of the tracer curves and governs only the qualitative aspect of the results. The quantitative aspect is taken into account by fixing the time required to achieve a transition when running a simulation with the stochastic model. This aspect will be analysed in detail in the results and discussion section.

Parameter estimation procedure

For the two-dimensional compartment model, there are two adjustable parameters: q_e and q_c. The circulation flow rate q_c was calculated by the use of the following equation coming from dimensional analysis [3]:

$$q_c = \frac{N_{qc}.N.d^3}{n_{loop}} \qquad (4)$$

with n_{loop} being the number of circulation loops implemented by the model ($n_{loop} = 2$ for the RDT6 and $n_{loop} = 1$ for the A315 impeller). N_{qc} is a dimensionless circulation number that depends only on the impeller geometry in the turbulent flow regime ($N_{qc} = 1.51$ for RDT6; $N_{qc} = 1.3$ for A315).

The turbulence flow rate q_e was estimated by sensitivity analysis. For a calculated value of q_c, the value of q_e was modulated to match the measured mixing time. The maximum and the minimum values of q_e matching with the experimental mixing time were determined, the mean corresponding to the used value of q_e in the simulations.

For the three-dimensional versions (Figure 3), there was an additional parameter to determine: the tangential flow rate q_t. The determination of this parameter will be discussed in the following sections.

After parameter determination of the CM model, all the flow rates q_c, q_e and q_t were collected to calculate the transition matrix T of the corresponding stochastic models (q_c and q_e for the two-dimensional versions ; q_c, q_e and q_t for the three-dimensional versions).

_____

Results and discussion

Two-dimensional mixing time experiments

As previously discussed, the compartment model has two adjustable parameters. The circulation flow rate q_c was calculated with the dimensional equation (4). The turbulent flow rate was estimated by the procedure outlined in the Material and methods section. All the results concerning these two parameters are presented in Table 1.

Table 1: Estimation of the adjustable parameters of the compartment model for each impeller system investigated

	N (min^{-1})	Calculated q_c (m³/s)		Estimated q_e (m³/s)
		Lower stage	Upper stage	
RDT6	230	0.0028	-	0.0155
RDT6	270	0.0033	-	0.0205
RDT6	360	0.0045	-	0.0295
RDT6	450	0.0056	-	0.029
RDT6-RDT6	230	0.0028	0.0028	0.04
RDT6-RDT6	270	0.0033	0.0033	0.0475
RDT6-RDT6	360	0.0045	0.0045	0.0645
RDT6-RDT6	450	0.0056	0.0056	0.0725
RDT6-A315	230	0.0028	0.0049	0.084
RDT6-A315	270	0.0033	0.0058	0.123
RDT6-A315	360	0.0045	0.0078	0.122
RDT6-A315	450	0.0056	0.0097	0.158

Figure 6 shows a comparison between experimental results and a compartment model simulation for the mixing of tracer pulse poured at the top of the vessel.

_____
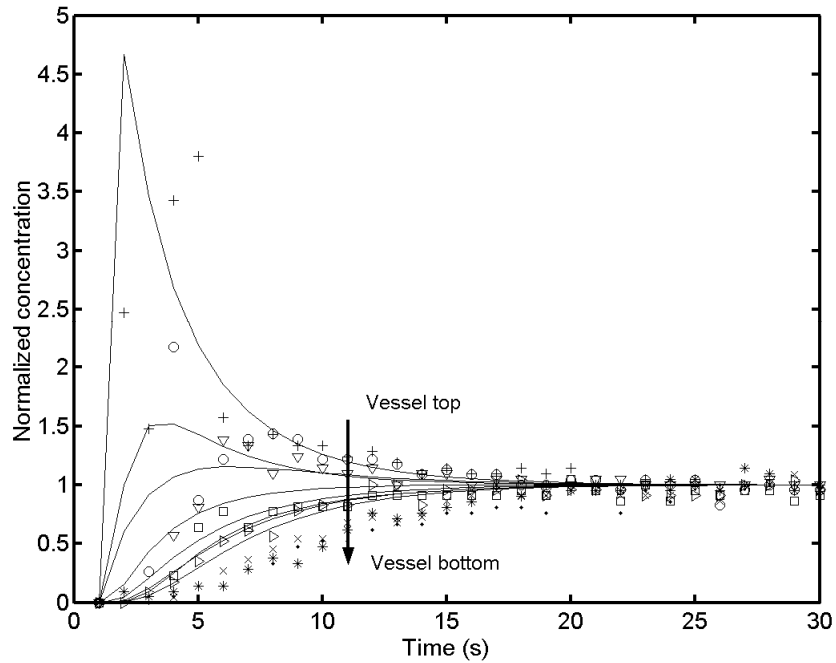
Figure 6: Comparison of experimental results and simulation results obtained with an RDT6-RDT6 compartment model (simulated values correspond to the continuous lines)

Adjustable parameters were calculated according to the method discussed in the Material and methods section. The mixing times given by the model matched the experimental ones exactly, but the shape of tracer curves recorded by the probes at different locations in a vertical plane of the vessel did not exactly match with the simulation results. Nevertheless, simulated tracer curves presented the same tendencies as the real ones (e.g., the tracer curves recorded near the pulse location exhibited a strong peak, which was not observed for the lower locations in the vessel).

There are two principal factors affecting the quality of the simulation. First, the number of compartments considered. If the number increases, the resolution of the model will be higher and tracer curves may be more differentiated. A high resolution can be obtained with models containing a large number of compartments with several parallel circulation loops. Such models are called network-of-zones (NOZ).

Secondly, the model is limited to two dimensions. Indeed, a three-dimensional model takes into account the tangential component of the mixing action. This aspect will be improved upon in the next section with the inclusion of a tangential flow rate.

At this level, the goal is to translate the CM structure from a determinist to a probabilistic context. To achieve this, the stochastic Markov chain theory was chosen, because its applicability in mixing processes (to date, especially in the case of particulate mixing processes) has been previously proved [13-15, 17, 19-22].

The first step is to take the same interconnected compartments network used in the CM. For each compartment (called a state, in the stochastic context) the probabilities of shifting to an adjacent compartment (state) or of staying within the initial compartment (state) were calculated. The flow rates were then translated into probabilities of shifting from one state to another, these probabilities depending on the flow structure (radial or axial) and the ratio of circulating flow on turbulence flow. All the probabilities were collected to construct a transition matrix (Figure 5), which governs the evolution of the system from a state $S_i(t)$ to a state $S_i(t+\Delta t)$ during a transition time Δt. The time taken to achieve a transition is not explicitly given by the model. This important aspect will be studied further in this section.

When having the stochastic model structure derived from CM, the adjustable parameters of the new model must be identified and the estimation method must be elaborated.

The first parameter to estimate is the ratio of the circulation rate on the turbulence rate. This parameter only has an impact on the qualitative results (on the shape of the tracer curves). The q_c/q_e ratio was calculated for each structure (RDT6, RDT6-RDT6 and RDT6-A315) (Table 2).

Table 2: Calculation of parameters necessary for the shift from a CM to a stochastic model (Two-dimensional case)

Impeller(s)	N (min^{-1})	q_c/q_e	k	$t_{m85\%}$ (s)	Δt (s)	t_c (s)
RDT6	230	0.18	32	5	0.15	1.72
RDT6	270	0.16	32	4	0.12	1.47
RDT6	360	0.15	32	3	0.09	1.1
RDT6	450	0.19	32	3	0.09	0.88
RDT6-RDT6	230	0.07	154	14	0.09	1.72
RDT6-RDT6	270	0.07	154	12	0.07	1.47
RDT6-RDT6	360	0.07	154	9	0.05	1.1
RDT6-RDT6	450	0.07	154	8	0.05	0.88
RDT6-A315	230	0.04	133	7	0.05	1.86
RDT6-A315	270	0.03	133	5	0.04	1.59
RDT6-A315	360	0.05	133	5	0.03	1.19
RDT6-A315	450	0.04	133	4	0.026	0.95

On observing the results, it can be seen that the q_c/q_e ratio is lower when the mixing system comprises an axial flow impeller. These results seem to be in discordance with the general literature covering mixing processes, which recognises axial impellers as high circulation and low turbulence inducing impellers. But the comparison of stirring systems must be performed when operating at the same volumetric power. In our case, the comparison was performed at the same stirrer speed and it was thus normal to obtain a lower value of q_c when operating with an axial flow impeller.

The second parameter to estimate is the effective duration of a transition Δt. This parameter is very important, since it governs the quantitative result of the simulation and thus the mixing time value. If we look at a simulation (Figure 7), it can be seen that a given number n of transitions are necessary before all the states of the models are visited by tracer particles. It thus seems interesting to determine this number n. This can be easily done by observing the course of a simulation. When running a simulation with a single-staged agitated vessel, 5 transitions are required before observing the first tracer molecules on the lower part of the vessel. When considering a two-staged stirred vessel, the number of transitions increases to 8 (the concentrations in the last states are very low and cannot be correctly viewed in Figure 7). We can see from Figure 7 that the tracer evolution for the RDT6-A315 system exhibits oscillations that are typical of axial flow impellers.
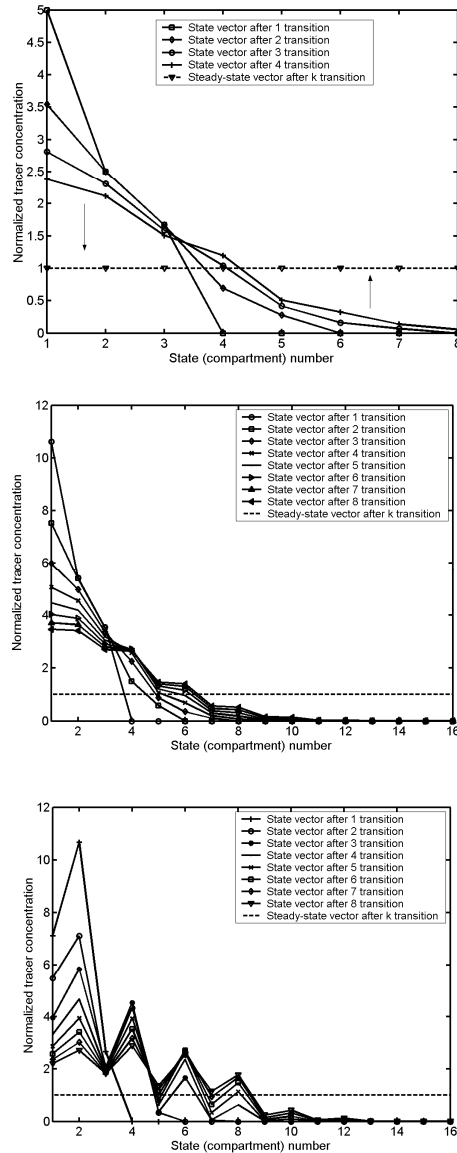
Figure 7: Repartition of tracer concentrations through the different states of the stochastic model during a simulation (consisting of a series of transitions from state to state). Three impeller systems are presented from top to bottom : RDT6 (A), RDT6-RDT6 (B), RDT6-A315 (C). The corresponding state number can be found for the RDT6 system in Figure 4.

It is important to observe that this number n does not depend on the operating conditions, but only on the model structure and the number of states. Thus, for a

given geometry and states network, n will be constant for every operating condition. This number n will be used further.

The time interval Δt of the stochastic model was determined from experimental data by using the following equation:

$$\Delta t = \frac{t_m}{k} \qquad (5)$$

Results of this analysis are presented in Table 2.

To give some physical significance to our model, Δt must be linked to a characteristic time of the mixing process that can be easily calculated by the operator. We chose here the circulation time, which is known to have a strong physical signification for the mixing process. Indeed, Figure 8 shows that, when increasing the mixing performances and thus when decreasing the circulation time, the parameter Δt drops down to a limiting value, which can be assimilated into the maximum homogenisation capability of the system. (Looking at Figure 2, it can be seen that the mixing time values are very low for these operating conditions.) These observations suggest a strong correlation between circulation time and Δt.
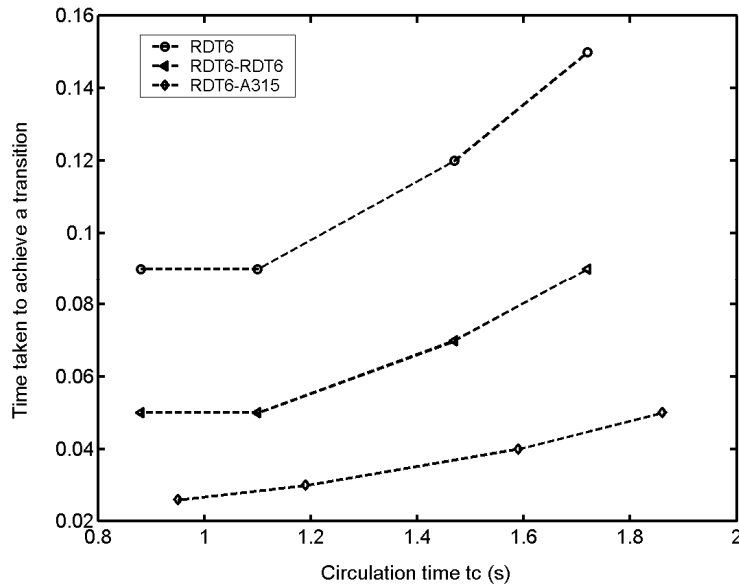
Figure 8: Evolution of Δt in function of circulation time

In order to extract a correlation from these data, the following equation was considered:

$$\Delta t = \frac{t_c}{n.c} \qquad (6)$$

with c being a correlating factor between t_c and Δt. The parameter n corresponds to the number of transitions before all the states (corresponding in practice to the flow regions) are visited by tracer particles. This number of transitions is indeed linked in the physical sense to the circulation time, the circulation process assuming transport of particles throughout the whole volume of the stirred vessel. In Figure 9, it appears that c is constant for a given impeller geometry and vessel size. Indeed, Δt must intuitively increase with scale-up and such behaviour can be denoted when comparing the RDT6 and RDT6-RDT6 systems.

Figure 9: Evolution of the correlation factor c involved in equation (6) with stirrer speeds for different mixing systems

Mean values of c for each stirrer system are compiled in Table 3.

_____

Table 3: Mean values of c (see equation (6))

	c	q_c/q_e
RDT6	2.28	0.17
RDT6-RDT6	2.49	0.07
RDT6-A315	4.78	0.04

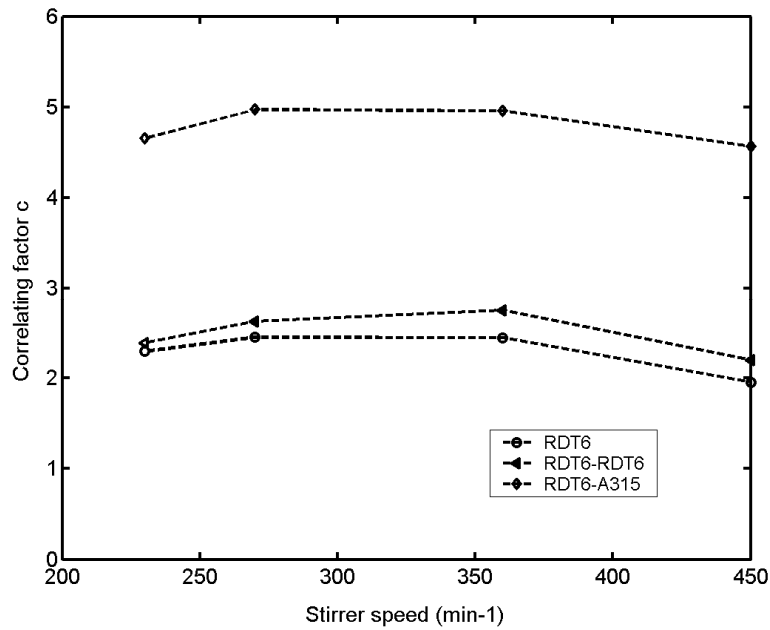At this stage of the study, it appeared that two parameters needed to be determined in order to run stochastic simulations in the case of mixing in a stirred vessel. The first parameter was the ratio q_c/q_e, which does not vary significantly for a given stochastic model structure and which only has an impact on the qualitative aspect of the simulation. The second was the time interval, which is the most important parameter. It has been proven that this parameter can be linked to the circulation time by a simple correlation (equation 6).

In the next section, knowledge gained from the two-dimensional model will be extended to a three-dimensional model.

Three-dimensional mixing time experiments

Two-dimensional results obtained in the previous section can be used to quantify the ratio of circulating flow on turbulence-induced flow in each plane of the 3D-version of the model. But in the 3D-model, a third kind of flow, named tangential flow, is necessary to make the connexion between adjacent planes. Tangential flow is responsible for the dispersal of tracer across the different planes of the vessel. Its determination can be made by matching simulations with experimental results. However, we showed, by using a sensitivity analysis, that a q_e/q_t ratio equal to one leads to better results. Indeed, we also modelled tangential flow by a backmixing flow. It is thus normal for tangential flows to have values equal to those of turbulence flows, because of the analogy between the two dispersive mechanisms.

Translating the model into a 3D version leads to the modification of some parameters previously defined for the two-dimensional model. The increase in the number of states in the model is traduced by an increase of the n and k parameters.

Indeed, the value of n for a single-staged vessel is 8, and 12 for a two-staged vessel. Values of k can be found in Table 4.

Table 4: Calculation of the parameters involved in stochastic models (Three-dimensional case)

Impeller(s)	N (min^{-1})	q_c/q_e	q_t/q_e	k	$t_{m85\%}$ (s)	Δt (s)
RDT6	230	0.18	1	80	5	0.062
RDT6	270	0.16	1	80	4	0.05
RDT6	360	0.15	1	80	3	0.037
RDT6	450	0.19	1	80	3	0.037
RDT6-RDT6	230	0.07	1	292	16	0.054
RDT6-RDT6	270	0.07	1	292	14	0.047
RDT6-RDT6	360	0.07	1	292	12	0.041
RDT6-RDT6	450	0.07	1	292	10	0.034
RDT6-A315	230	0.04	1	290	12	0.041
RDT6-A315	270	0.03	1	290	10	0.034
RDT6-A315	360	0.05	1	290	10	0.034
RDT6-A315	450	0.04	1	290	8	0.027

Concerning this table, the same methodology was used to determine the time interval Δt of a simulation in function of the mixing performance of the system (see equation (6) previously elaborated for the 2D models).

Figure 10 presents the evolution of the correlation factor c in function of stirrer speed for each impeller system tested.

_____
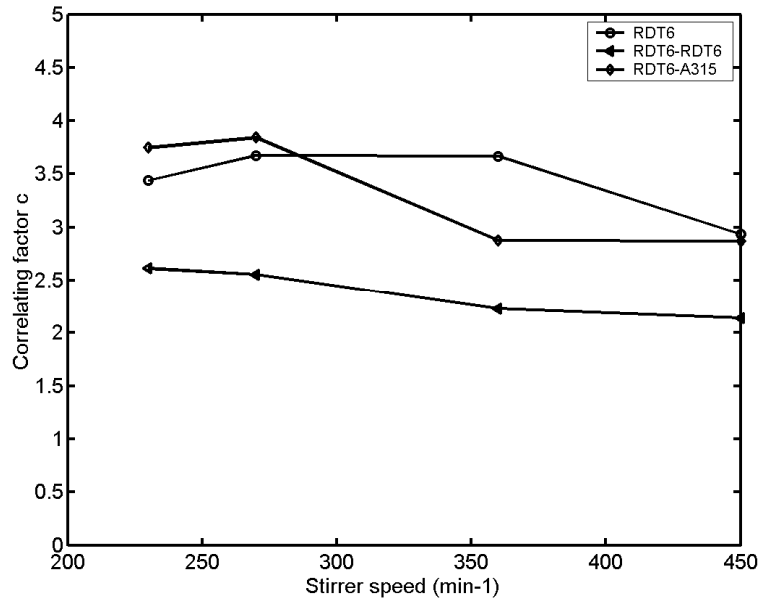
Figure 10: Evolution of the correlation factor c involved in equation (6) with stirrer speed for different mixing systems (Three-dimensional system)

As previously noted for the 2D case, values of c do not vary significantly for a given impeller system. Mean values of c are compiled in Table 5.

Table 5: Mean values of c for a 3D-model (see equation (6))

	c
RDT6	3.42
RDT6-RDT6	2.38
RDT6-A315	3.33

Equation (6) and the values of c reported in Table 5 were used to perform several simulations. Figure 11 shows a comparison of these simulations with experimental results. It can be seen that the proposed parameter evaluation methodology led to acceptable results.
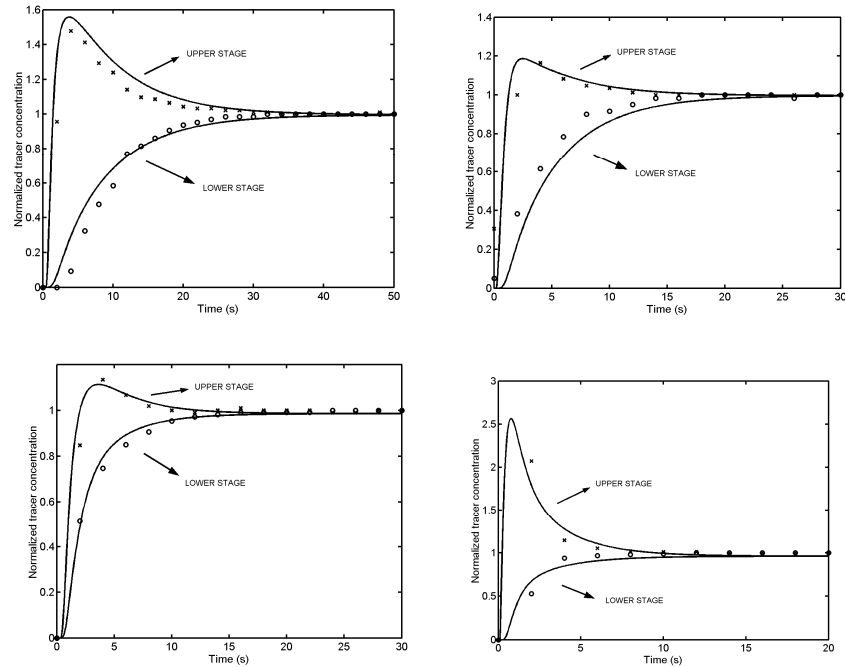
Figure 11: Comparison between experimental (dot) and simulated results (line) with three-dimensional stochastic models

Residence time distribution (RTD) experiments

In order to perform RTD simulations, the 3D-model must be adapted by adding an additional state, named the absorbing state. This state is responsible of the absorption of tracer molecules and represents the lower zone of the vessel, including the liquid evacuation hole. The transition matrix (Figure 5) must be adapted to contain the absorbing state and has the aspect shown in Figure 12 [19].

$$\begin{bmatrix} T_{batch} & B \\ 0 & 1 \end{bmatrix}$$

Figure 12: Transition matrix containing an absorbing state used to perform RTD simulations

79

In this matrix, T_{batch} is the transition matrix previously presented in Figure 5 ; B is a column vector containing zero elements and a single element containing q_{exit} ; 0 is a line vector containing zero elements and 1 is a unit element responsible for the absorbing process.

In this case, an additional parameter expressing the liquid flow rate leaving the system must be determined. This flow is experimentally known and its determination don't cause any difficulties.

At this stage, it is thus possible to perform simulations by entering the previously determined parameters of the model. In this section, we will perform simulations and compare the results with experimental data. Examples of the quality of the simulations can be viewed in Figure 13.
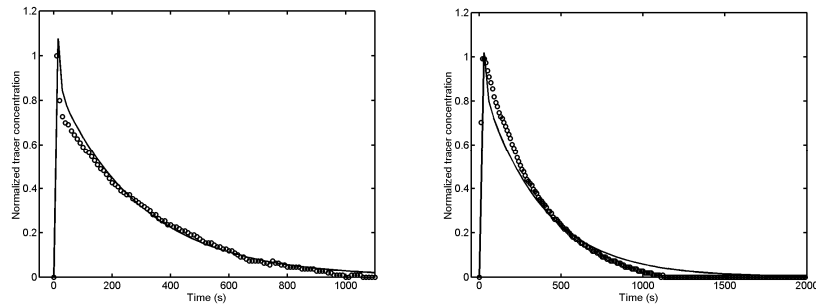
Figure 13: Comparison between experimental (dot) and simulated RTD results (line). On the right: RDT6-A315 system; on the left: RDT6-RDT6 system

These simulations were performed by using parameters (q_c, q_e, q_t and Δt) coming from three-dimensional mixing experiments (see Tables 4 and 5 in the previous section). The simulations improved the validity of these parameters for the mixing systems considered.

Stochastic simulation of particle circulation in a stirred vessel

Another interesting property of the stochastic model is that the transition matrix T can be directly used to perform single particle circulation simulations. Indeed, the T matrix contains all the transition probabilities from state to state and these probabilities can be used in conjunction with a random number generator to provide

the path taken by a particle in displacement inside the stirred vessel. In a bioprocess context, it is very important to know the passage frequency of the micro-organisms in some crucial flow regions of the bioreactor (for example, the substrate addition point in the case of a fed-batch culture, which can cause a stress due to the high concentration levels). In the case of a circulation process simulation, only the axial planes of the vessel are important. We can thus limit our observations by using only one of the basic planes of the three-dimensional model defined in Figure 3. An example of particle travel from state to state is given in Figure 14.
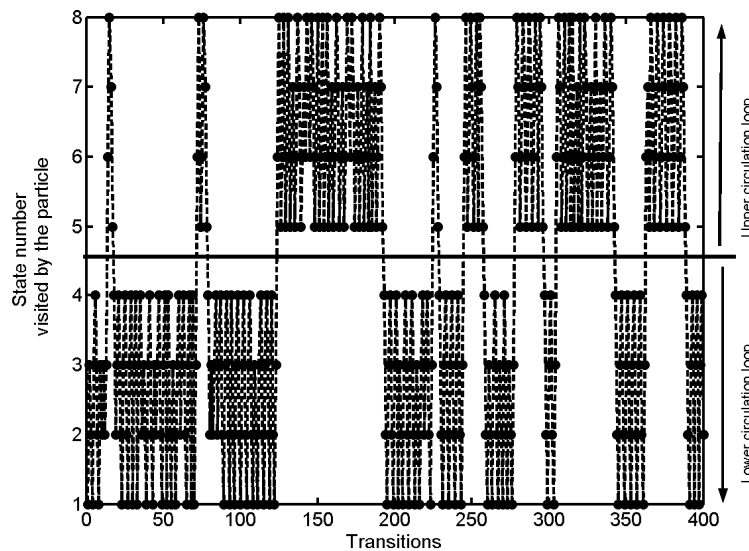
Figure 14: Stochastic simulation of a particle circulation inside a stirred vessel. The arrangement of states corresponds to the axial "basic plane" defined in Figure 3.

These results can be exploited to calculate the passage frequency of a particle inside a given state and, in this way, the circulation time in relation with this state. When simulation involves a lot of transitions, circulation time distribution can be established for a given state or a given set of states. Such an example is given in Figure 14 for 200,000 transitions, which correspond more or less to 2300 circulations through a particular state. The state chosen here corresponds to the flow region located at the top of the vessel, which, in case of a fed-batch bioprocess, is subject to substrate pulse addition. This in turn can affect cellular metabolism. An

important fact is that the circulation time distribution (CTD), represented in Figure 15, exhibits a log-normal shape, as described in the literature [16].
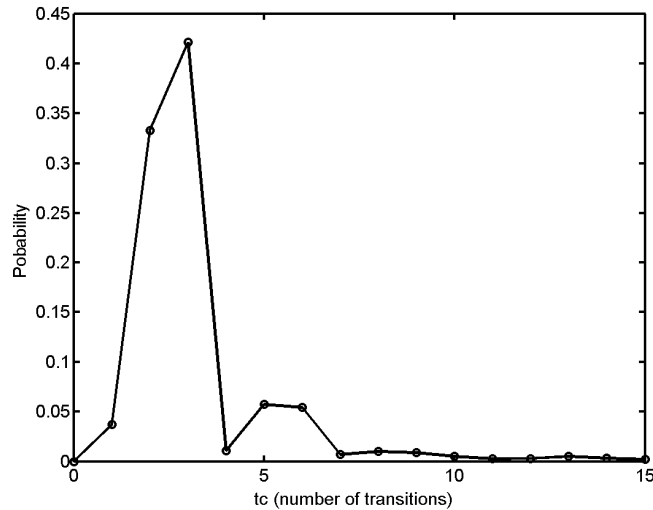
Figure 15: Circulation time distribution related to a given state of the stochastic model (circulation time t_c is not express here in seconds but in number of transitions)

The maximum of probability corresponds to 3 transitions before returning to the specified state and is in accordance with the basic plane structure of the model, which involves 4 states per circulation loop. This phenomenon can also be viewed in Figure 14, which highlights the presence of 2 circulation loops in the axial plane of the vessel. The variance comes from the fact that the particle can bypass the circulation loop constituted by a set of 4 states. The variance can be increased by considering several concentric circulation loops, but this requires a modification of the model structure. This important fact, as well as the extensive development of the circulation aspect, emerges from the objectives of this publication and would need a separate study.

Conclusion

A methodology has been presented here aimed at facilitating the calculation of the parameters of stochastic models. It involves the use of estimated flow rates coming

from compartment mixing model (CM) analysis. The ratio between these flow rates can be assumed to be constant for a given impeller system, which greatly facilitates the elaboration of the transition matrix. A second important parameter to determine is the time interval Δt, necessary to achieve a simulation step. This time step is not explicitly given by the model but, after appropriate analysis, it appears that a simple correlation could be used to make the connexion between a simulation step and a real time interval (Δt). The correlation (equation 6) contains an adjustable parameter, which depends only on the impeller geometry, in the range of operating conditions tested. Corresponding values of c can be found in Table 3 for two-dimensional models and in Table 5 for three-dimensional ones.

The stochastic model can be used for model mixing behaviour of different impeller systems in stirred vessels, resolution being equivalent with that obtained with classical CM. Indeed, simulation performances were similar for each kind of model investigated in this study. This equivalency allows the application of the stochastic model to the study of mixing in fluid systems. This approach is interesting because of the exclusive properties of the stochastic model (not found in the classical CM), which can be used to investigate special mixing behaviour in the process industry. The aim of our study was to combine a structured hydrodynamic model (such as CM or more recently the stochastic model) with microbial kinetics. In this area, the exposure of micro-organisms to gradients can be investigated by performing particle-tracking simulations. These simulations can be simply performed by using the transition matrix of the model, as shown in this study. A second advantage of the stochastic model in this area comes from the discrete evolution of the system during a simulation run. Indeed, this characteristic of the stochastic model allows the calculation of a given state by using equation (3) ($S_i = T^i . S_0$). This property can be exploited when dealing with complex models involving reactor hydrodynamics and reacting species (such as micro-organisms in the presence of a nutrient), which require a large amount of computational time and space [23].

Notation

CM : compartment model

_____

c : correlating factor for the determination of the transition time interval

d : impeller diameter (m)

D : stirred vessel diameter (m)

k : number of transitions that are necessary to reach homogeneity

n : number of transitions before all states are visited by tracer particles

n_{loop} : number of circulation loops in a two-dimensional CM

N : stirrer speed (s^{-1})

NOZ : network-of-zones

N_{qc} : circulation or flow number (dimensionless)

Q_c : circulation flow rate (m³/s)

q_c : circulation flow rate per loop in the CM (m³/s)

q_e : turbulent flow rate (m³/s)

q_t : tangential flow rate (m³/s)

q_{exit} : evacuation flow rate used in RTD experiments (m³/s)

RTD : residence time distribution

S : state vector

S_0 : initial state vector

S_i : state vector after i^{th} transition

T : transition matrix

t_c : circulation time (s)

t_m : mixing time (s)

References

1.   Vrabel P., van der Lans R.G.J.M., van der Schot F.N., Luyben K.Ch.A.M., Xu B., Enfors S.O., CMA : integration of fluid dynamics and microbial kinetics in modelling of large-scale fermentations, Chem. Eng. J. 84 (2001) 463-474.
2.   Vlaev D., Mann R., Lossev V., Vlaev S.D., Zahradnik J., Seichter P., Macro-mixing and Streptomyces fradiae : modelling oxygen and nutrient segregation in an industrial bioreactor, Trans IchemE 78 (2000) 354-362.
3.   Zahradnik J., Mann R., Fialova M., Vlaev D., Vlaev S.D., Lossev V., Seichter P., A network-of-zones analysis of mixing and mass transfer in three industrial bioreactors, Chem. Eng. Sci. 56 (2001) 485-492.

4. Cui Y.Q., van der Lans R.G.J.M., Noorman H.J., Luyben K.Ch.A.M., Compartment mixing model for stirred reactors with multiple impellers, Trans IchemE 74 (1996) 261-271.

5. Machon V., Jahoda M., Liquid homogenization in aerated multi-impeller stirred vessel, Chem. Eng. Technol. 23 (2000) 869-876.

6. Mayr B., Horvat P., Nagy E., Moser A., Mixing models applied to industrial batch reactor, Bioprocess Eng., 9 (1993) 1-12.

7. Mayr B., Nagy E., Horvat P., Moser A., Scale-up on basis of structured mixing models : a new concept, Biotechnol. Bioeng. 43 (1994) 195-206.

8. Vasconcelos J.M.T., Alves S.S., Nienow A.W., Bujalski W., Scale-up of mixing in gassed multi-turbine agitated vessels, Can. J. Chem. Eng. 76 (1998) 398-404.

9. Vasconcelos J.M.T., Alves S.S., Barata J. M., Mixing in gas-liquid contactors agitated by multiple turbines, Chem. Eng. Sci. 50 (1995) 2343-2354.

10. Vrabel P., van der Lans R.G.J.M., Luyben K.Ch.A.M., Boon L., Nienow A.N., Mixing in large-scale vessels stirred with multiple radial or radial and axial up-pumping impellers : modelling and measurements, Chem. Eng. Sci. 55 (2000) 5881-5896.

11. Mann R., Pillai S.K., El-Hamouz A.M., Ying P., Togatorop A., Edwards R.B., Computational fluid mixing for stirred vessels : progress from seeing to believing, Chem. Eng. J. 59 (1995) 39-50.

12. Mann R., Vlaev D., Lossev V., Vlaev S.D., Zahradnik J., Seichter P., A network-of-zones analysis of the fundamentals of gas-liquid mixing in an industrial stirred bioreactor, Récents progrès en génie des procédés 11(52) (1997) 223-230.

13. Pippel W., Philipp G., Utilization of Markov chains for simulation of dynamics of chemical systems, Chem. Eng. Sci. 32 (1977) 543-549.

14. Rubinovitch M., Mann U., Single-particle approach for analyzing flow systems. Part I : visits to flow regions, AIChE J. 29(4) (1983) 658-662.

15. Fan L.T., Fan L.S., Nassar R.F., A stochastic model of the unsteady state age distribution in a flow system, Chem. Eng. Sci. 34 (1979) 1172-1174.

16. Namdev P.K., Thompson B.G., Gray M.R., Effect of feed zone in fed-batch fermentations of Saccharomyces cerevisiae, Biotechnol. Bioeng. 40(2) (1992) 235-246.

17. Howes T., Brannock M., Corre G. Development of simplified flow models from CFD simulations, *Third international conference on CFD in the minerals and process industries* (2003) CSIRO, Melbourne, Australia.

18. Mayr B., Horvat P., Moser A., Engineering approach to mixing quantification in bioreactors, Bioprocess Eng. 8 (1992) 137-143.

19. Berthiaux H., Dodds J., Modeling classifier networks by Markov chains, Powder Technol. 105 (1999) 266-273.

20. Rubinovitch M., Mann U., A single particle approach for analysing flow systems. Part II : regional residence times and local flow rates, AIChE J. 29(4) (1983) 663-668.

21. Rubinovitch M., Mann U., A single particle approach for analysing flow systems. Part III : multiple fluids, AIChE J. 31(4) (1985) 615-620.

22. Szépvölgyi J., Diaz E., Gyenis J., New stochastic modelling of mixing in process operations, Chem. Eng. Process. 38 (1999) 1-9.
23. Delvigne F., El Mejdoub T., Destain J., Delroisse J.M., Vandenbol M., Haubruge E., Thonart P., Estimation of bioreactor efficiency through structured hydrodynamic modelling : case study of a Pichia pastoris fed-batch process, Appl. Biochem. Biotechnol. 121-124 (2005) 653-671.

CHAPITRE 4
Utilisation des modèles stochastiques pour le dimensionnement d'un réacteur *scale-down* représentatif

_____

Abstract

Scale-up is traduced in practice by an increase of the dimensions of the bioreactors, leading to a modification of the time scale and thus of the process dynamics. In the present work, a methodology to study the effect of scale-up on bioreactors hydrodynamics and to put in place scale-down reactors representative of the flow properties encountered in real scales bioreactors is detailed.

In order to simplify the analysis, we have proposed the use of a stochastic model which is directly affected by the time scale. Indeed, to run simulations with such models, we have to specify the time taken to achieve a transition Δt. Stochastic models are thus reliable to study scale-up effect on stirred reactors hydrodynamics. In addition, these models permit to have an insight on the internal dynamic of the process.

In the case of the circulation process, qualitative aspects have to be taken into account and induce a modification of the flow regions arrangement of the model. The stochastic analysis of large-scale bioreactors permits to propose a translating methodology into a scale-down context. Optimised scale-down reactors can be used further to carry out fermentation tests with the hydrodynamic conditions of the industrial scale. In a general rule, the performances of stochastic model allow to facilitate greatly the analysis of the scale-up effect and the hydrodynamic characteristics of both large-scale and scale-down reactors.

_____

Introduction

One of the most important problem arising when dealing with bioprocesses is the scale-up of the results at the industrial scale. One of the problems is caused by difficulties to represent hydrodynamic evolution of stirred reactors during scale-up. The aim of this study is to propose a methodology involving simple structured hydrodynamic models in order to resolve scale-up problems. Data obtained from the hydrodynamic analysis and modelisation of large-scale bioreactors will be used to elaborate a scale-down reactor having the capacity to reproduce the hydrodynamic encountered at the industrial scale. Such reactors have been widely described in the literature and different variants can be found : a small stirred bioreactor coupled with a pipe [1-6], two or more stirred bioreactor with recycle [7-11], a single stirred bioreactor with randomly fluctuating substrate addition [12-15], a single stirred reactor with physically separated internal compartments [16]. Among these, the system comprising a bioreactor coupled with a plug-flow section seems to be the more promising.

Material and methods

Mixing time experiments

Three different stirred vessels are used for mixing time experiments : a 30 litters Perspex vessel, a 500 litters bioreactor (Biolaffite-France) and a 2000 litters bioreactor (Biolaffite-France). Dimensions of these stirred reactors can be found in table 1.

Table 1 : dimensions of the stirred vessels investigated in this study

	D (m)	d (m)
Perspex vessel 30L	0.24	0.1
Bioreactor 500L	0.62	0.25
Bioreactor 2000L	1.02	0.4

Four different kinds of scale-down apparatus are studied. These apparatus comprise a 30 litters vessel (the same vessel as presented previously, with a working volume of 10 litters) assumed to be perfectly mixed combined to a plug flow section. A peristaltic pump ensures the liquid circulation between the mixed and the plug flow sections. The four scale-down systems differ by the design of the plug flow section. We have used : a silicone tubing (internal diameter : 8mm ; length : 7.5m) (System A), a glass bulb (internal diameter : 85 mm ; length : 0.25 m ; connexions of 8 mm diameter at each end) (System B), two glass bulbs in series (System C) and two glass bulbs in parallel (System D). These apparatus can be viewed schematically at figure 1.
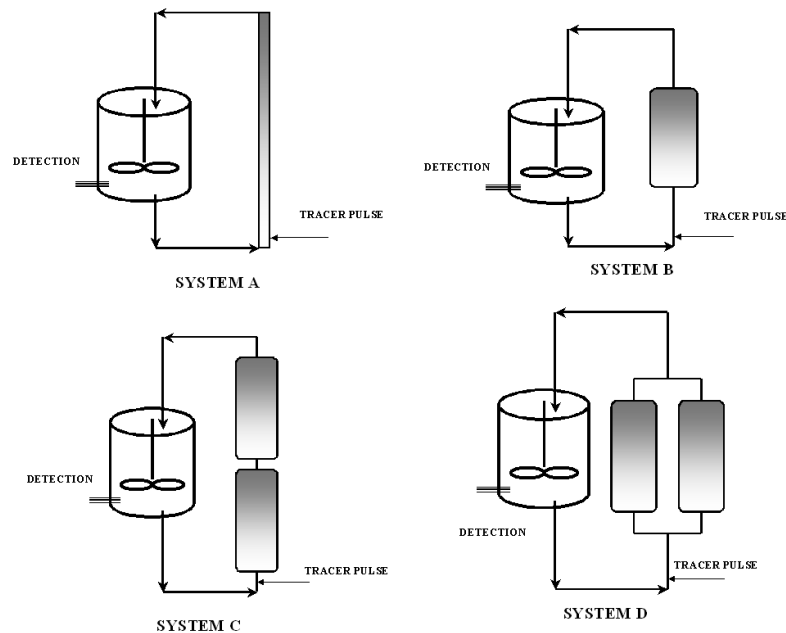
Figure 1 : schematic representation of the scale-down reactors investigated in this study. The mixed part correspond to a classical stirred vessel with a working volume of 10L

Homogenisation experiments have been performed on each bioreactor and scale-down reactor by using a tracer pulse injection method. The technique employed consists in recording the conductivity evolution after the injection of a saturated NaCl solution at the top of the vessel (2% of the total volume of the reactor). Mixing

time is calculated from tracer curves by the method of [17]. In the case of scale-down reactors, the technique is somewhat different and is explained at figure 1.

In addition, RTD experiments have been performed at the level of the mixing section of the scale-down reactors. Methodology is the same as presented above, the stirred vessel operating in the continuous mode (fresh water is continuously added and extracted from the stirred vessel).

Stochastic modelling of mixing curves

The stochastic model used here is in fact a Markov chain. This kind of model has been widely used in the area of particulate mixing [18, 19], but can also be applied in the field of fluid mixing [20, 21]. When performing stochastic simulations, a state vector containing the description of the state of the system at a given time interval is multiplied with a transition matrix (which contains the probabilities to shift from state to state) to give a new vector describing the state of the system at the next time interval. This new vector can be multiplied again by the transition matrix. This procedure is repeated to obtain the evolution of the state vector in function of time or transitions. The mathematical procedure can be written as :

For a first transition, when starting from an initial state S_0 : $S_1 = T . S_0$ $\qquad$ (1)

The following steps involve the multiplication of the new state vector S_1 with the same transition matrix until a state S_i is reached. In our case, the state S_i corresponds to the steady-state for which the system can be considered as homogenous. The mathematical procedure can be written as follow :

For the second transition : $(S_2 = T . S_1)$ or $(S_2 = T^2 . S_0)$ $\qquad$ (2)

For the ith transition : $(S_i = T . S_{i-1})$ or $(S_i = T^i . S_0)$ $\qquad$ (3)

With S being the state vector and T the transition matrix. In our case, the state vector contains the tracer concentrations for all states, a state corresponding to a region of the stirred vessel, and a transition corresponding to a time interval. The numerical implementation of a stochastic model is thus very simple because only involving matrix multiplication.

The model investigated contains 8 states per planes, the whole volume of the vessel being modelised by 8 planes. There is thus a total of 64 states per agitation stages,

these states being interconnected by probabilities which are function of circulation, turbulence and tangential flow rates physically encountered in stirred vessels (figure 3). The general structures of the models have been previously improved [22] (figure 3).

SHAFT

$\cdots\blacktriangleright$
$\blacktriangleleft\cdots$: turbulence flow rate q_e

$\longrightarrow$: convective flow rate q_c

$\nearrow$: tangential flow rate q_t
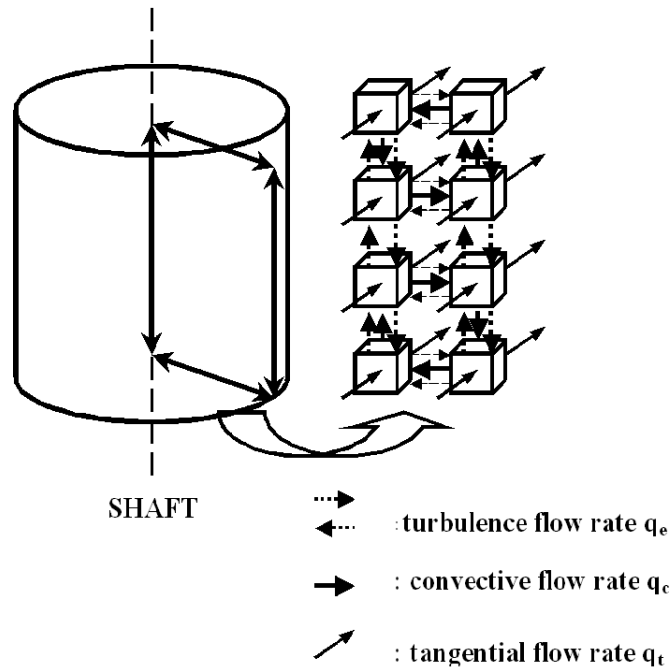
Figure 3 : physical structure of the model involved in this study. Each states are interconnected with each others by probabilities calculated on the basis of circulation, turbulence and tangential flow rates. The circulation flow rates orientations are valid only in the case of a radial impeller

Stochastic modelling of particle flow path

The circulation of a particle inside a stirred bioreactor is very easy to simulate by the aim of the transition matrix of a stochastic model. Nevertheless, the flow network must be modified in order to represent more precisely the circulation flow paths. Indeed, if the previous network structure is used (figure 3), the circulation process can't be efficiently represented because of the bi-directional nature of the turbulence flow rates. These flow rates contribute to assimilate the circulation process to a random walk. To avoid this effect, a diagonal flow rate structure (figure 2) can be

adopted [23]. This structure permits to represent more clearly the circulation process. In order to be in accordance with the previously presented mixing model, the probability to remain in the circulation loop is calculated in function of the circulation flow rate generated by the impeller. The probability to shift to an adjacent flow loop is extracted from the value of the turbulent flow rate (figure 3).
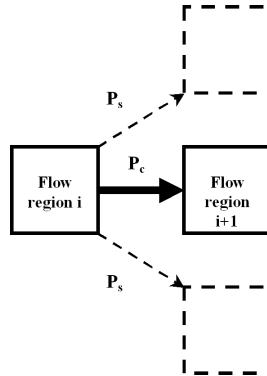
Figure 2 : diagonal flow structure proposed by [23] used to perform stochastic particle displacement simulation

Results and discussion

Preliminary comparison of stirred bioreactors and scale-down reactors : time constants analysis

The bioreactor hydrodynamics must be optimised in order to ensure a good homogenisation of the broth and minimise the appearance of concentration gradients. The parameter generally used to quantify the homogenisation process is the mixing time. This mixing time t_m has been measured for several bioreactor volumes under varying operating conditions (stirrer speed and impeller combinations). In order to allow comparison on a reliable basis, some results of mixing time are presented in function of the reactor volume at constant volumetric power consumption (figure 4) [24].
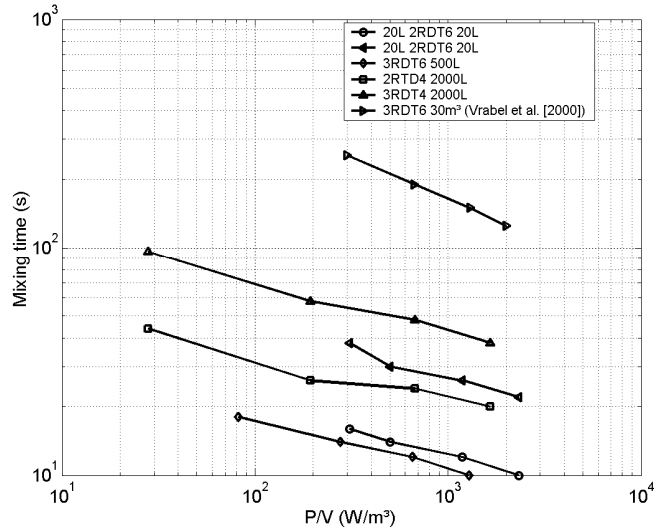
Figure 4 : evolution of mixing time in function of volumetric power consumption. Bioreactor 30 m³ results are extracted from the literature [24].

It can be seen that the increase of the volume of the reactor leads to the drop of the homogenisation efficiency (traduced by an increase of the mixing time). A particular attention must be paid on the fact that an important increase of mixing time is observed when passing from a two-staged to a three-staged mixing vessel. This can be attributed to the radial behaviour of the impellers used. It has been previously proven that these impeller configurations induce a strong compartmentalisation effect. Previous studies have shown that incorporation of an axial flow impeller permits to decrease drastically the mixing time of the whole system [24, 25].

One of the goal of this study is to make the link between scale-down and large-scale reactors. In other words, a relation between operating parameters of the two kinds of system must be highlighted. We can begin our comparison by determining the time constants related to the reactors hydrodynamics : the circulation time t_c and the mixing time t_m. From figure 5, it can be seen that mixing time curves representative to those encountered in large- scale bioreactors can be obtained by using scale-down reactors.

_____
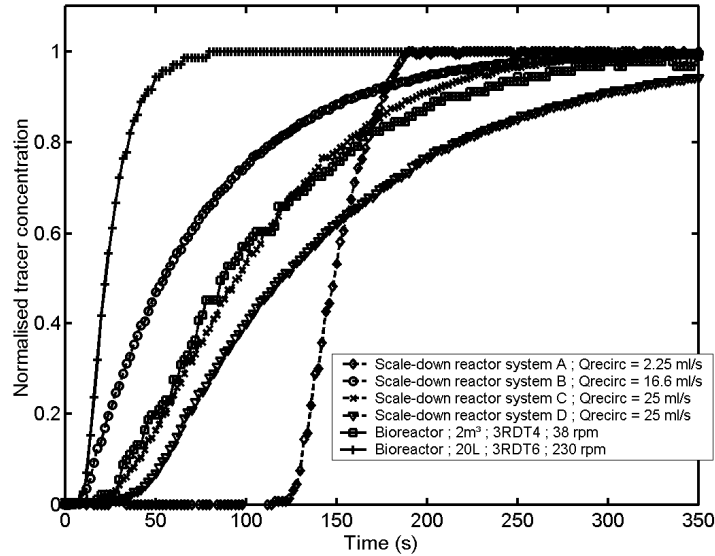
Figure 5 : tracer curves obtained for different reactor configurations

The adaptation of the shape of the mixing curves can be performed by varying the recirculation flow rate, as well as the volume and the diameter of the plug-flow section. The residence time in the plug-flow section of a scale-down reactor can be assimilated to the circulation time observed in the case of a large-scale reactor. Indeed, these characteristic times correspond both to the time between two consecutive passages of a particle at the level of the impeller plane.

In the case of stirred bioreactors, the circulation time value can be obtained by using the following correlation :

$$t_c = \frac{V_L}{Q_c} = \frac{V_L}{N_{qc}.N.d^3} \qquad (4)$$

By analogy to the t_c in real bioreactors, the circulation time in scale-down reactor can be considered to the mean time taken by a particle entering in the plug-flow section before going back to the mixed section. The values of $t_{c\ plug\text{-}flow}$ are first considered as equal to the theoretical retention time of the plug-flow section. We have thus :

$$t_{c_{plug-flow}} = t_{r_{plug-flow}} = \frac{V_{plug-flow}}{Q_{recirc}} \qquad (5)$$

All the results concerning time constants analysis for scale-down and real reactors are summarized respectively in table 2 and 3.

Table 2 : characteristic time constants determined for scale-down reactors

Scale-down reactor configuration	Recirculation flow rate Q_{recirc} (ml/s)	Plug flow part volume (ml)	Theoretical circulation time $t_{cplugflow}$ (s) in the plug flow section	Mixing time $t_{m85\%}$ (s)
A	2.25	380	168	170
A	3.9	380	96	130
A	8.33	380	45	56
A	16.66	380	23	32
B	8.33	1000	120	292
B	16.66	1000	60	134
B	25	1000	40	104
B	33.33	1000	30	70
C	16.66	2000	120	224
C	25	2000	80	170
C	33.33	2000	60	130
D	8.33	2000	240	534
D	16.66	2000	120	246
D	25	2000	80	176
D	33.33	2000	60	130

Table 3 : characteristic time constants determined for real bioreactors

Reactor	Working volume (L)	Impeller(s)	N (s^{-1})	t_c (s)	$t_{m85\%}$ (s)
Perspex vessel 30L	10	RDT6	3.83	1.72	5
	10	RDT6	4.5	1.47	4
	10	RDT6	6	1.1	3
	10	RDT6	7.5	0.88	3
Perspex vessel 30L	20	2 RDT6	3.83	1.72	16
	20	2 RDT6	4.5	1.47	14
	20	2 RDT6	6	1.1	12
	20	2 RDT6	7.5	0.88	10
Perspex vessel 30L	30	3 RDT6	3.83	1.72	38
	30	3 RDT6	4.5	1.47	30
	30	3 RDT6	6	1.1	26
	30	3 RDT6	7.5	0.88	22
Bioreactor 500L	350	2 RDT4	0.83	8.9	36
	350	2 RDT4	1.66	4.45	24
	350	2 RDT4	2.5	2.96	22
	350	2 RDT4	3.33	2.22	20
Bioreactor 2000L	1200	2 RDT4	0.63	13	60
	1200	2 RDT4	1.2	6.9	42
	1200	2 RDT4	1.81	4.56	26
	1200	2 RDT4	2.36	3.5	26
Bioreactor 2000L	1800	3 RDT4	0.63	13	188
	1800	3 RDT4	1.2	6.9	100
	1800	3 RDT4	1.81	4.56	52
	1800	3 RDT4	2.36	3.5	53

At this stage of the study it is important to know the circulation time $t_{c\,plug\text{-}flow}$ range which permits to match the mixing times encountered in large-scale bioreactors. Figure 6 presents the evolution of mixing time in function of circulation time for different bioreactors and scale-down reactor configurations.
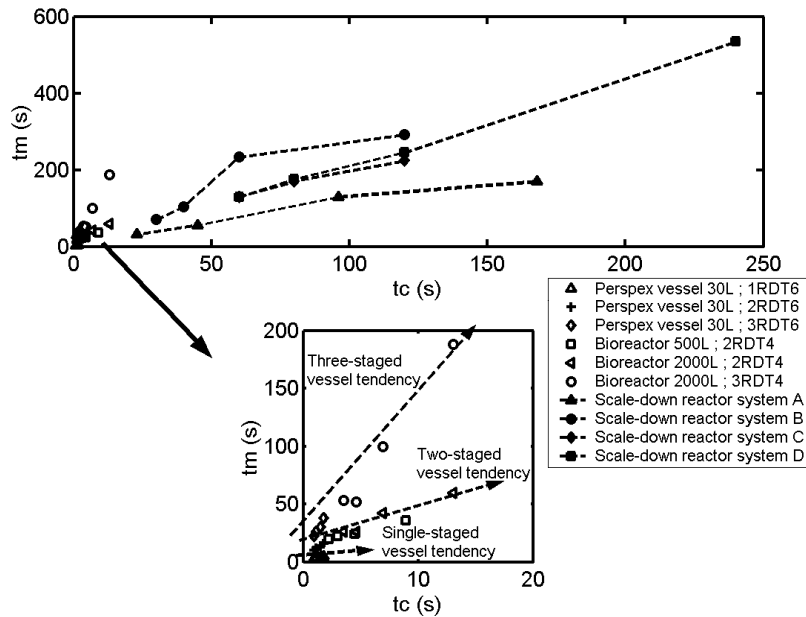
Figure 6 : mixing time – circulation time relationship for different reactor configurations

Some tendencies can be highlighted when considering mono and multi-agitated bioreactors. Indeed, three tendencies can be observed in function of the number of agitation stages in the case of large-scale bioreactors. This can be attributed to the fact that, when the number of agitation stages increases, the theoretical circulation time remains constant but not the mixing time. This effect is attenuated in the case of a combination comprising an axial flow impeller. These tendencies can be extrapolated by scale-down mixing time results, but comparison is difficult because of the few points matching with results obtained in the case of large-scale reactors. It comes from the fact that bioreactor scales considered in this study are relatively small compared to the sale-down results which are representative of bigger scales.

Time constants analysis is not sufficient to describe precisely the bioreactor hydrodynamics. In reality, there isn't a single value for t_c, but we can observe a circulation times distribution (CTD) for a given stirred bioreactor and for a given range of operating conditions. The same observation can be done for a scale-down reactor in which there is a retention time distribution depending of the geometry of the plug-flow element and of the recirculation flow rate. We need thus a tool to describe the circulation time distribution.

We have also shown that it is possible to obtain mixing time value in scale-down bioreactors similar to the one observed in large-scale reactors. However, the mixing time is only a parameter, and elaborating a scale-up strategy on the basis of this single parameter leads to wrong results. Indeed, mixing time don't predict the flow direction in bioreactors and the way in which microorganisms are exposed to gradient. To obtain a good representation of these phenomena, we need a hydrodynamic modelisation tool. We use here a stochastic model which presents the advantages to predict not only the way in which homogenisation is achieved, but also the circulation paths followed by particles inside the bioreactor. It has been previously proven that stochastic model has the same mixing simulation potentiality than the well-known compartment or network-of-zones models.

In the following sections hydrodynamics characteristics of scale-down reactors and large-scale stirred bioreactors will be compared on the basis of tracer mixing curves and particle circulation paths. Stochastic models will be used to facilitate these analysis.

Analysis of bioreactors hydrodynamics by stochastic modelling

1. Scale-up effect on the simulation time interval of stochastic models

Stochastic model has been previously improved to simulate mixing curves of stirred bioreactors under several operating conditions. The efficiency of this kind of model has been previously proven [22].

In this section, two goals have to be achieved. First, the quantification of the scale-up effect in stirred bioreactors by using stochastic models. Then, always in a

97

stochastic modelisation context, the comparison of the mixing process in large-scale bioreactors and in scale-down apparatus. In order to resolve the problem, we need to find a parameter of the model which is particularly affected by the scale-up procedure. Intuitively, the lone parameter affecting the time scale of the process is the time interval taken to achieve a stochastic model transition. There is also a space scale which is affected by scale-up, but this scale is explicitly included in the model by states or flow regions.

In order to simplify the approach, a previously presented methodology [22] will be used and it will be assumed that the ratio of circulation flow on turbulent flow will be constant for each simulations. This methodology permits to find the time taken to achieve a transition during a simulation with a stochastic model. The parameter Δt is thus calculated from mixing time experiments by the relation :

$$\Delta t = \frac{t_m}{k} \tag{6}$$

k being the number of transitions required before reaching homogeneity in the context of the stochastic model. The parameter k depends only on the number of states constituting the model (these state correspond in our case to the different flow regions by analogy to the well-known compartment models) and on the arrangement of these states (in other words, it depends on the nature of the flow loops generated by the impeller, these loops differing in function of the radial or axial behaviour of the impeller). The parameter k = 80 for a single-turbine system, k = 299 for a two-turbines system and k = 670 for a three-turbines system. This number of transitions needs to be related to an effective time in order to enhance the reality of the stochastic simulations. This can be achieved experimentally by using equation (6), and the following correlation can be written as :

$$\Delta t = \frac{t_c}{n.c} \tag{7}$$

n being the number of transitions before all states of the model are visited by ay least on tracer molecule. As in the case of k, this parameter depends only of the model structure : n = 8 for a single-turbine system, n = 12 for a two-turbines system and n = 16 for a three-turbines system. The parameter c is a correlating factor. The use of n

permits to give more significance to the correlating parameter c by deleting its dependence to the model flow regions structure. It has been previously noted that this parameter c is constant for a given impeller geometry [22]. As it will be seen further, this remark is only valid for a given scale. Indeed, the parameter c must intuitively vary when increasing the operating scale.
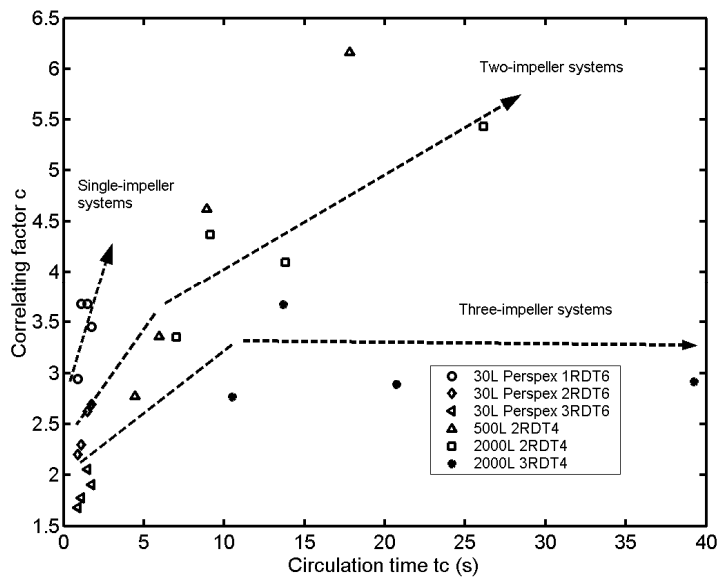

Figure 7 : evolution of the correlating factor c in function of circulation time for different bioreactors configurations. The correlating factor is used to translate the simulation transitions into a real time referential

The magnitude of this variation is represented at figure 7 in relation with some tracer experiments. A special attention must be paid to the evolution of the correlating factor c in function of the operating scale. At small scale (10 to 30 litters, mono or multi-staged vessel), the correlating factor c is almost constant in function of the circulation time (or more generally in function of the stirrer speed) and for a given impeller configuration. When increasing the scale, a significant variation of c is observed when increasing the stirrer speed. In fact, when considering small-scale reactor, circulation time doesn't vary on a great extent and c seems to be constant. But when increasing the reactor volume in order to induce a significant increase of the circulation time, differences at the level of c values appears. We assist at a

significant increase of the correlating factor, but not sufficient compared with the circulation time increase. As a result, the time interval Δt increased. It can be concluded that the scale-up induce, at the stochastic model level, an increase of the timescale, this effect being more pronounced for multi-impeller systems.

This effect can be partly explained by reasoning on a basic scale-up principle. Indeed, if it is assumed that the scale-up effect is primarily due to a timescale modification, some explanations can be given to our results. In larger vessels, fluid elements must circulate over longer distances. To ensure an homogenisation effect similar to those encountered at small scale, the fluid velocity must be greater. Unfortunately, the fluid velocity is directly proportional to the volumetric power which constrained the large vessel to run under greater values of P/V. Such required P/V are not technically achievable and this limitation is the basis of scale-up problems.

This is in accordance with the fact that the mixing process in stirred reactor is closely linked to the circulation time. According to the related literature, homogenisation of the system is achieved after a time interval equal to four or five times t_c [26]. The use of equation (7) to run simulation improves thus the physical significance of our stochastic model.

2. Analysis of circulation process in bioreactors

The circulation of a particle inside a stirred bioreactor is very easy to simulate by the aim of the transition matrix of a stochastic model. The problem which appears when using a structured model is that the spatial dimension is governed by the arrangement of the flow regions. To analyse the scale-up phenomena only the temporal dimension has been exploited, but this method induces some problems linked to the spatial aspect of the model. Indeed, when scaling-up, the spatial dimensions of the system increase, which is traduced at the level of the model by an increase of the flow regions volume. Nevertheless, in the case of the circulation process no qualitative differences have been observed, primarily because the flow regions number and arrangement are the same. If we take for example our basic three-dimensional flow regions network for simulating the circulation of a particle in

the reactor, problems can arise when proceeding to a scale-up analysis. The circulation phenomena is mainly limited to the axial planes which involves each 8 flow regions (figure 3). During a scale-up analysis, the volume of the flow regions must be increased, as well as the probability for the particle to remain inside a particular region. This phenomena leads to a CTD with a maximum probability observed for a t_c equal to zero (which corresponds to the retention of the particle inside the same flow region). In conclusion, the qualitative aspect play an important role in the case of circulation path simulation. This is traduced in practice by an increase of the number of circulation loops n_{loops} in the axial plane of the vessel (figure 8).

n_{loops} : 2
n_{visits} : 4

n_{loops} : 4
n_{visits} : 4, 12

n_{loops} : 6
n_{visits} : 4, 12, 20

D (m)
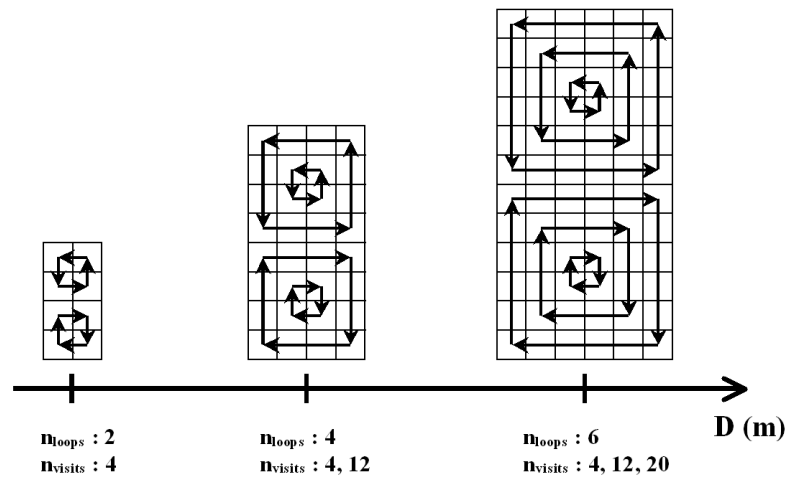
Figure 8 : expected evolution of the circulation model structure with scale-up

In function of the number of flow loops included in the model, particles are allowed to achieve different sequences of transitions. For example, in the case of the 72 flow regions model, particles can follow three kinds of circulation loops : circulation loop composed of 4 flow regions, 12 flow regions or 20 flow regions. These differences contribute to the probabilistic aspect of the circulation process. The quantitative aspect is anew governed by a simulation transition - Δt real time interval relationship which is very easy to establish by considering that the time taken by a particle to follow the longer circulation loop corresponds to the theoretical circulation time

expressed by equation (4). All the results concerning the Δt conversion obtained by using equation 8 have been compiled in table 5 :

$$\Delta t_{circ} = \frac{t_c}{s_{loop}}$$

(8)

Table 5 : stochastic model parameters for scale-down reactors (system B)

Qrecirc (ml/s)	Penter	Pstay	Pback	Δt (s)
8.33	0.15	0.75	0.1	3.65
16.66	0.31	0.59	0.1	1.675
25	0.5	0.4	0.1	1.3
33.33	0.69	0.21	0.1	0.875

The analysis has been focused on the model structure proposed by [23]. These authors have shown that a ratio of 0.85:0.15 between P_c (probability to remain in the main flow loop) and P_s (probability to shift to another flow loop) leads to results representative of large-scale vessels. To illustrate the principles presented at figure 8, simulations have been performed with three model structures comprising respectively 8, 32 and 72 flow regions, which correspond to 2, 4 and 6 circulation loops. To run simulations, P_c and P_s were maintained respectively at 0.85 and 0.15 for all the simulations. Simulation results are presented at figure 9 and have been compared with the theoretical log-normal distribution of the circulation times having the following form [27]:

$$f(t_c) = \frac{1}{\sqrt{2\pi}.\sigma.t_c} \cdot \exp\left[-\frac{1}{2}\left\{ \left(\frac{\ln t_c - m}{\sigma} \right) \right\}^2 \right]$$

(9)

For each simulation, 200,000 random transitions have been performed and these numbers of transitions have been converted into real time interval Δt_{circ} by using equation 8.

From figure 9, it can be seen that the scale-up induces an dispersion of the CTD. All the simulations show a log-normal behaviour in accordance with the literature [23, 27].
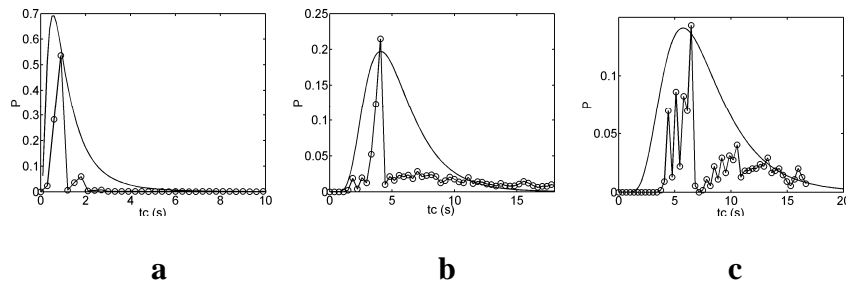
Figure 9 : circulation simulation according to the model structures presented at figure 8. From left to right : 8 states model (a), 32 states model (b) and 72 states model (c)

Hydrodynamic characterisation of scale-down reactors by stochastic modelling

Structured models allow to gain a more precise insight into the internal hydrodynamics of stirred bioreactors. In this section, stochastic modelling of scale-down reactor will be considered. Simulation mixing curves obtained by this approach will be used to make some comparisons with those obtained in the case of large-scale bioreactors.

In the case of a scale-down reactor, in the specified range of operating conditions, the homogenisation process is limited by the tracer retention inside the pipe section. Indeed, the tracer has been injected at the level of the plug-flow section and the operating conditions in the mixed part have been chosen to lead to a mixing time of 5 seconds. We'll thus focus our attention on the plug-flow part of the scale-down reactor.

Table 4 presents a comparison between the theoretical residence time of the plug-flow part (obtained by equation 5) and the minimum and the maximum experimental retention times.

Table 4 : characteristic circulation time relative to the scale-down reactors

System	Q_{recirc} (ml/s)	$V_{plug-flow}$ (ml)	Theoretical retention time (s)	Experimental minimum retention time (s)	Experimental maximum retention time (s)
A	2.25	370	164	124	170
A	3.9	370	95	78	130
A	8.3	370	45	38	56
A	16.6	370	22	22	32
B	8.3	1000	120	26	292
B	16.6	1000	60	8	134
B	25	1000	40	8	104
B	33	1000	30	8	70
C	16.6	2000	120	24	224
C	25	2000	80	10	170
C	33	2000	61	10	130
D	8.3	2000	241	80	534
D	16.6	2000	120	30	246
D	25	2000	80	20	176
D	33	2000	61	8	130

These experimental retention times have been measured from mixing time curves by recording the appearance of the first tracer molecules in the mixed part (minimum retention time) and by calculating the mixing time (maximum retention time). We can see that small diameter plug-flow part (system A) exhibits a strong plug-flow behaviour because the maximum and the minimum experimental retention time values are close to the theoretical retention time. This is not the case of the large diameter plug-flow parts (systems B, C and D) for which dispersion effect occurs. Two cases can be highlighted depending on the plug-flow part diameter :

- For small diameter, tracer dispersion is very low and the pulse is convoyed trough the plug-flow part. The system can thus be assimilated to a single circulation channel who behave like a perfect plug-flow.

- For bigger diameters, the dispersion effect is more intensive. Large diameter plug-flow part behave like a set of several flow channels which interacts with each other, the inter-channel exchanges being responsible of the tracer dispersion.

In order to perform stochastic simulations for the fluid mixing, we have considered in all cases the mixed section with the parameters previously determined in the case of the 30L perspex reactor with 10L of working volume (this reactor being effectively used in practice as the mixed part of the scale-down apparatus), which permits to stay within the same modelling referential. The model arrangement is presented at figure 10.
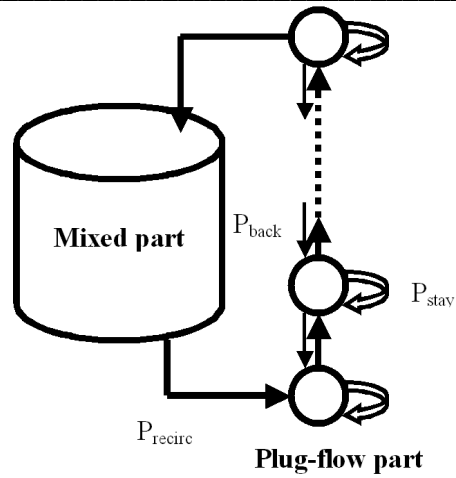
Figure 10 : scale-down stochastic model arrangement

The plug-flow section has been modelled by a set of states put in series. Transitions between the states of the plug-flow part are governed by P_{recirc}, the probability for a particle to be carried by the general circulation flow, P_{stay}, the probability to be retained at the level of a given state and by P_{back}, the probability of backmixing. Anew, the theoretical time of the model (expressed as a number of transitions) must be translated into real time interval Δt. The validity of this translation needs some verifications because we consider now a hybrid reactor. To do this, the RTD of the mixed part of the scale-down system has been measured in order to verify the time effectively spent by a particle in this section of the reactor. Experimental results have been compared with simulations performed with the model presented at figure 11.

_____
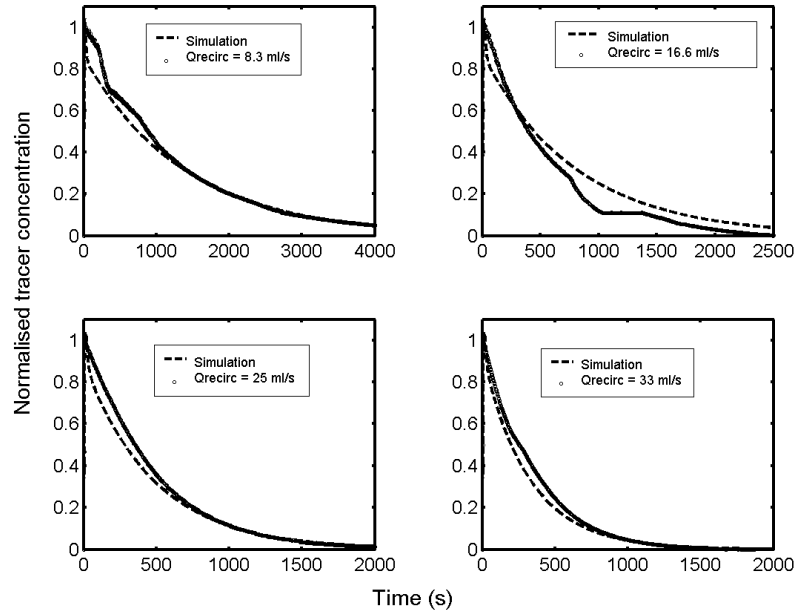
Figure 11 : comparison of RTD experiments and simulation

This comparison allows to fix the probability for a particle to enter in the plug-flow section P_{enter} when passing at the vicinity of the evacuation hole of the mixed section (this evacuation hole being comprised in a particular state of the model called an absorbing state [28]). This probability must, in principle, be proportional to the recirculation flow rate, and figure 12 shows that this tendency is respected by the model.

Figure 12 : linear relationship between the recirculation flow rate and the probability to enter in the plug-flow section of the scale-down reactor

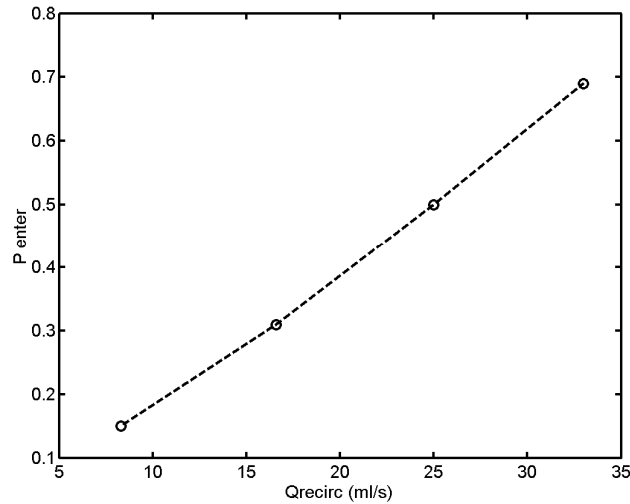In a second step, the plug-flow section internal hydrodynamic parameters must be determined, and more precisely the probabilities P_{stay} and P_{back}. This determination has been performed on the basis of the mixing time experiments performed on the whole scale-down system. From sensitivity analysis, it has been determined that P_{back} has only a limited impact on simulations results and our attention has been especially given to the P_{stay} parameter. The basic structure of he model comprises 9 states in series for the plug-flow section. This structure is efficient to represent fluid mixing in systems B, C and D, but not in the case of system A. In this case, the number of states must be increased to 50, which shows anew the strong plug-flow behavior of system A. The whole analysis is not shown here, but the most important results concerning system B, and notably the Δt parameter, are presented at table 5. We can see that Δt values are representative of those calculated in the case of large-scale bioreactors. In general, Δt values are more elevated because of the most important mixing times encountered in these scale-down systems. Example of mixing simulation efficiency will be shown in the next section.

Table 4 can also be used to establish the CTD of scale-down reactors. Indeed, the circulation loop being physically delimited by a pipe section, the residence time

inside the plug-flow part of a scale-down reactor can be assimilated to a circulation time. It comes from this fact that three characteristic values of circulation time can be obtained from table 4. The same model structure than the one presented at figure 10 can be used in a circulation simulation context.

Comparison of real bioreactors and scale-down reactors

The scale-down reactor must reproduce as precisely as possible the large-scale bioreactor hydrodynamics. Several criteria can be used in order to establish the hydrodynamic similarities between scale-down and real reactors. The first category of criteria contains the characteristic time constants t_m and t_c. These criteria permit to determine roughly if the chosen scale-down reactor is representative of a given large-scale bioreactor. Performing a selection on the basis of these simple criteria can induce important losses of representativeness for a scale-down reactor. It is preferable to use a second category of criteria coming from structured stochastic models analysis (compartment models can be used, but their potentialities are more limited than those coming from stochastic models). An important factor to take into account when dealing with bioprocesses is the environment experienced by microorganisms travelling in the bioreactor. In the case of a fed-batch culture, substrate is fed in the vessel and continuously absorbed by microbes. We assist thus at a very complex dynamic system. In order to simplify the methodology, we'll perform a mixing simulation and choose a given inhomogeneity degree. We'll concentrate our attention on the concentration field at this time, this field being considered as a structured criteria. The parameter Δt must be determined in order to present the results in a real temporal referential. After this step, a circulation simulation can be performed with the same model structure than the one used for mixing simulation. It is the second structured criteria. By superimposing the two structured criteria, i.e. the concentration field at a given inhomogeneity degree and the stochastic displacement inside the bioreactor, a representative view of the concentrations encountered by a micro-organism can be obtained.

In order to prove the powerfulness of such structured criteria, figure 13 shows a comparison between a 2m³ bioreactor and a scale-down reactor (system B). To

achieve these simulations, 20,000 transitions have been performed, which correspond approximatively to 18 hours in a real time referential. In the case of a 2m³ bioreactor, the three-dimensional model structure have been used to match the CTD presented at figure 9. Operating conditions have been chosen to lead to a t_m = 188 s and a t_c = 13 s in the case of the 2m³ bioreactors and to a t_m = 134 s and a t_c = 60 s in the case of the scale-down reactor. Circulation time values are significantly different, but t_c is not a structured criteria and it has been shown that it can deviate from its theoretical value (table 4).
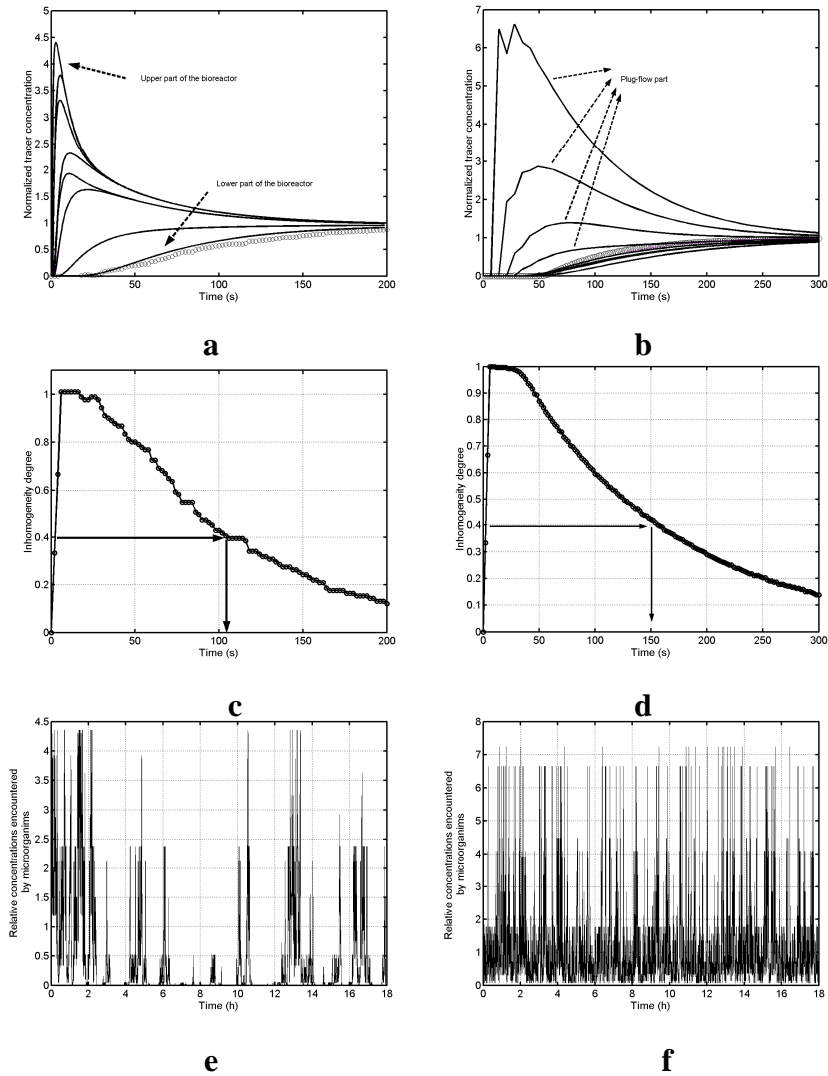
Figure 13 : stochastic structured characterisation of reactors. At the right side : scale-down reactor system B. At the left side : 2m³ bioreactors equipped with three RDT4 impellers. From top to bottom : stochastic mixing simulation (a and b) ; calculation of the inhomogeneity degree and selection of the concentration field at an inhomogeneity degree of 0.4 (c and d) ; superimposition of the concentration field with the stochastic circulation of a micro-organism (e and f)

Figure 13E and F show significant differences at the level of the environment expected by micro-organisms travelling in the bioreactor and in the scale-down

reactor. Indeed, in the case of the scale-down reactor, the microorganism tends to be more frequently submitted to concentration peaks. Figures 14 A and 14C validate this fact by showing that the probability for a microorganism to be submitted to high concentration is more elevated in the case of the scale-down reactor.
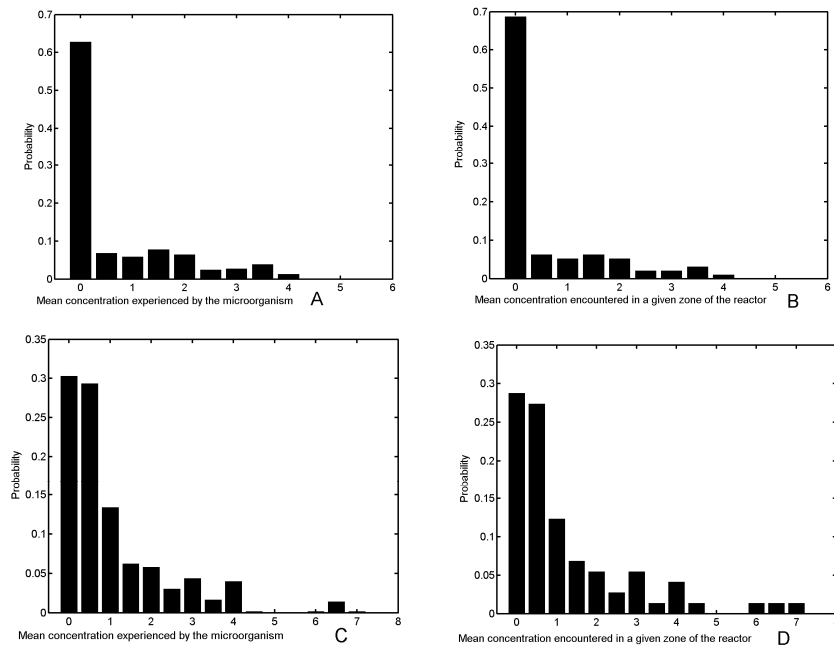

Figure 14 : comparison of : the probability distribution of the relative concentration experienced by a microorganism during a sojourn time of 18 h in a 2m³ stirred bioreactor equipped with three RDT4 impellers (A) ; the probability distribution of the relative concentration that can be experienced in a given zone of the 2m³ stirred bioreactor at an inhomogeneity degree of 0.4 (B) ; the probability distribution of the relative concentration experienced by a microorganism during a sojourn time of 18 h in a scale-down reactor system B (C) ; the probability distribution of the relative concentration that can be experienced in a given zone of the scale-down reactor system B at an inhomogeneity degree of 0.4 (D)

This can be explained partly by the fact that the bioreactor comprises three agitation stages, and circulation simulations have shown in this case that micro-organisms tend to stay at the level of an given impeller stage in which the environment is rather homogenous. This is not the case of the scale-down reactor which contains only one agitation stage. In addition, micro-organisms entering in the plug-flow section is submitted to important concentration fluctuations induced by the poor mixing

111

performances. This suggests that, by reducing the recirculation flow rate between the mixed section and the plug-flow section of the reactor, it is possible to reproduce an environment matching the one encountered in large-scale reactor. Figure 14 permits to validate the simulations involving the environment experienced by the microorganisms by comparing the distribution relative to the time probability for a microorganism to be submitted to a given relative concentration in the reactor, and the distribution relative to the spatial probability to encounter such relative concentration (calculated according to the respective zones included in the model structure). In the case of the large scale reactor the two probability distributions are in good accordance (figures 14A and 14B). Some differences can be observed in the case of the scale-down reactor in the sense that the spatial probability distribution (figure 14D) shows a higher probability to be submitted to high relative concentrations than the time probability (figure 14C). This fact can be attributed to the physical separation of the scale-down reactor, the higher concentrations being encountered at the level of the plug-flow section. In general, the two kinds of frequency distribution are in good accordance, suggesting that the superimposition of the circulation process is not necessary and that the gradient field inside the reactor is sufficient to characterise the microorganism exposure. However, only one microorganism has been considered when running simulation. In perspective, it would be interesting to consider the circulation of a population comprising several microbial cells in a continuously changing environment, such as the one encountered in fed-batch processes.

In addition, figure 14 validate anew the fact that the environment experienced in the scale-down reactor is rather different that the one encountered in large-scale reactor. These distribution can be used as a tool to estimate the environmental heterogeneity that can be encountered by a microorganism in a given reactor, and thus as a tool to design representative scale-down reactors.

The methodology presented above allows a radical simplification of the study of the microbial stress induced by gradient formation in bioreactors. Nevertheless, an additional validation step seems to be required for simulating circulation in stirred bioreactors. Indeed, the results presented in this study have been validated by the use

of data coming from the literature. Modern techniques of particles tracking can give more insights about the circulation process, but were not at our disposal.

Conclusion

Scale-up has a great impact on mixing efficiency and circulation characteristics of stirred bioreactors and can be studied by the use of stochastic models. The use of such model requires the knowledge of the model transition-Δt relationship. This relationship can be directly used in a scale-up context because the increase of reactor volume is traduced in practice by an increase of the hydrodynamic characteristic time constants (e.g., mixing and circulation times). Nevertheless, when scaling-up a bioreactor, the spatial dimension is also involved. This dimension is included in the model as a rigid network of flow regions called states. It becomes problematic when dealing with circulation problem for which the spatial dimensions are very important because it affects the shape of the circulation times distribution. In this case, the network structure of the stochastic model must be adapted. A procedure has been proposed to perform such modification in accordance with the scale-up rules and the literature.

By using stochastic models, we are able to propose a simple procedure to translate the hydrodynamic characteristics of a big scale bioreactor at the level of a scale-down reactor comprising a perfectly mixed part and a plug-flow part. This procedure involves two steps, the first one leading to the determination of a concentration field at a given inhomogeneity degree, and the second one involving the use of structured parameters coming from stochastic simulations. Each step leads to the calculus of a structured criteria which is represent efficiently the mixing and the circulation capacities of the system. By superimposing the two structured criteria, the concentrations fluctuations encountered by a micro-organism during his sojourn in the bioreactor can be obtained.

In order to validate an efficient scale-down reactor configuration it seems interesting to test each of the configurations proposed in this paper in the case of a given bioprocess. By this way, the impact of the reactor hydrodynamics on microbial physiology can be recorded and facilitate the selection of an efficient apparatus.

113

_____

NOTATIONS

CTD : circulation time distribution

d : impeller diameter (m)

D : stirred vessel diameter (m)

m : mean of the lognormal distribution

N : stirrer speed (s^{-1})

n_{loops} : number of circulation loops

N_{qc} : circulation number (adimensional)

N_p : power number (adimensional)

P_{back} : probability to assist to backmixing in the case of a scale-down model

P_c : probability to stay in the main flow loop in the case of a bioreactor circulation model

P_{enter} : probability to enter in the plug-flow section of a scale-down apparatus

P_s : probability to shift to another flow loop in the case of a bioreactor circulation model

P_{stay} : probability to assist to retention in the case of a scale-down model

Q_{recirc} : recirculation flow rate in the scale-down reactor (m^3/s)

rpm : rounds per minute

RTD : retention time distribution

RDT6 : rushton disk turbine with 6 blades

RDT4 : rushton disk turbine with 4 blades

s_{loop} : number of states comprised in the longer circulation loop of a stochastic model

T : transtion matrix

t_c : circulation time (s)

$t_{c\ plug-flow}$: circulation time in the plug-flow section of a scale-down reactor (s)

t_m : mixing time (s)

$t_{r\ plug-flow}$: theoretical retention time in the plug-flow part of a scale-down apparatus (s)

V_L : stirred reactor effective volume (m^3)

ρ : agitated fluid density (kg/m^3)

σ : standard deviation of the lognormal distribution

Δt : real time interval when performing mixing simulation with a stochastic model (s)

Δt_{circ} : real time interval when performing circulation simulation with a stochastic model (s)

References

1. Namdev P.K., Thompson B.G., Gray M.R., *Effect of feed zone in fed-batch fermentations of Saccharomyces cerevisiae,* Biotechnology and bioengineering **40**(2) (1992) 235-246.

2. Fowler J.D., Dunlop E.H., *Effects of reactant heterogeneity and mixing on catabolite repression in cultures of Saccharomyces cerevisiae.* Biotechnology and bioengineering **33** (1989) 1039-1046.

3. Neubauer P., Häggström L., Enfors S.O., *Influence of substrate oscillations on acetate formation and growth yield in Escherichia coli glucose limited fed-batch cultivations.* Biotechnology and bioengineering **47** (1995) 139-146.

4. Enfors S.O., Jahic M., Rozkov A., Xu B., Hecker M., Jürgen B., Krüger E., Schweder T., Hamer G., O'Beirne D., Noisommit-Rizzi N., Reuss M., Boone L., Hewitt C., McFarlane C., Nienow A., Kovacs T., Trägardh C., Fuchs L., Revstedt J., Friberg P.C., Hjertager B., Blomsten G., Skogman H., Hjort S., Hoeks F., Lin H.Y., Neubauer P., van der Lans R., Luyben K., Vrabel P., Manelius A., *Physiological responses to mixing in large scale bioreactors.* Journal of biotechnology **85** (2001) 175-185.

5. Amanullah A., Mac Farlane.C.M., Emery A.N., Nienow A.W., *Scale-down model to simulate spatial pH variations in large-scale bioreactors.* Biotechnology and bioengineering **73**(5) (2001) 390-399.

6. Hewitt C.J., Nebe-Von Caron G., Axelsson B., Mc Farlane C.M., Nienow A.W., *Studies related to the scale-up of high-cell-density E. coli fed-batch fermentations using multiparameter flow cytometry : effect of a changing microenvironment with respect to glucose and dissolved oxygen concentration.* Biotechnology and bioengineering **70**(4) (2000) 381-390.

7. Lovitt R.W., Wimpenny J.W.T., *The gradostat : a bidirectional compound chemostat and its application in microbiological research.* Journal of general microbiology 127 (1981) 261-268.

8. Tanner R.D., Dunn I.J., Bourne J.R., Klu M.K., *The effect of imperfect mixing on an idealized kinetic fermentation model.* Chemical engineering science **40**(7) (1985) 1213-1219.

9. Oosterhuis N.M.G., Kossen N.W.F., Olivier A.P.C., Schenk E.S., *Scale-down and optimization studies of the gluconic acid fermentation by Gluconobacter oxydans.* Biotechnology and bioengineering **27** (1985) 711-720.

10. Sweere A.P.J., Janse L., Luyben K.C.A.M., Kossen N.W.F., *Experimental simulation of oxygen profiles and their influence on baker's yeast production. Part 2 : two-fermentor system.* Biotechnology and bioengineering **31** (1988) 579-586.

11. Oosterhuis N.M.G., Groesbeek N.M., Olivier A.P.C., Kossen N.W.F., *Scale-down aspects of the gluconic acid fermentation.* Biotechnology letters **5**(3) (1983) 141-146.

12. Namdev P.K., Yegneswaran P.K., Thompson B.G., Gray M.R., *Experimental simulation of large-scale bioreactor environments using a monte carlo method.* Canadian journal of chemical engineering **69** (1991) 513-519.

13. Sweere A.P.J., Mesters J.R., Janse L., Luyben K.C.A.M., Kossen N.W.F., *Experimental simulation of oxygen profiles and their influence on Baker's yeast production. Part I : one-fermentor system.* Biotechnology and bioengineering **31** (1988) 567-578.

14. Thompson B.G., *Effect of temporary localized operating conditions on fermentations of Saccharomyces cerevisiae.* Biotechnology and bioengineering **29** (1987) 786-788.

15. Lin H.K., Neubaueur P., *Influence of controlled glucose oscillations on a fed-batch process of recombinant Escherichia coli.* Journal of biotechnology **79** (2000) 27-37.

16. Schilling B.M., PfefferleW., Bachmann B., Leuchtenberger W., Deckwer W.D., *A special reactor design for investigations of mixing time effects in a scaled-down industrial L-lysine fed-batch fermentation process.* Biotechnology and bioengineering, **64**(5) (1999) 599-606.

17. Mayr B., Horvat P., Moser A., *Engineering approach to mixing quantification in bioreactors.* Bioprocess engineering **8** (1992) 137-143.

18. Berthiaux H., *Analysis of grinding processes by Markov chains.* Chemical engineering science **55** (2000) 4117-4127.

19. Berthiaux H., Dodds J., *Modeling classifier networks by Markov chains.* Powder technology **105** (1999) 266-273.

20. Fan L.T., Fan L.S., Nassar R.F., *A stochastic model of the unsteady state age distribution in a flow system.* Chemical engineering science **34** (1979) 1172-1174.

21. Rubinovitch M., Mann U., *Single-particle approach for analyzing flow systems. Part I : visits to flow regions.* AIChE journal **29**(4) (1983) 658-662.

22. Delvigne F., Destain J., Thonart P., *Structured mixing model for stirred bioreactor : extension to the stochastic approach.* Submitted for publication in Chemical engineering journal (2005).

23. Mann R., Mavros P.P., Middleton J.C.,, *A structured stochastic flow model for interpreting flow-follower data from a stirred vessel.* Trans IChemE **59** (1981) 271-278.

24. Vrabel P., van der Lans R.G.J.M., Luyben K.Ch.A.M., Boon L., Nienow A.N., *Mixing in large-scale vessels stirred with multiple radial or radial and axial up-pumping impellers : modelling and measurements.* Chemical engineering science **55** (2000) 5881-5896.

25. Delvigne F., El Mejdoub M.T., Destain J., Delroisse J.M., Vandenbol M., Haubruge E., Thonart P., *Estimation of bioreactor efficiency through structured hydrodynamic modelling : case study of a Pichia pastoris fed-batch process.* Applied biochemistry and biotechnology (2004), in press

26. Nienow A.W., *Hydrodynamics of stirred bioreactors.* Applied mechanics review, **51**(1) (1998) 3-32.

27. Bajpai R.K., Reuss M., *Coupling of mixing and microbial kinetics for evaluating the performance of bioreactor.* Canadian journal of chemical engineering **60** (1982) 384-392.

28. Bittorf K.J., Kresta S.M., *Active volume of mean circulation for stirred tank agitated with axial impellers.* Chemical engineering science **55** (2000) 1325-1335.

CHAPITRE 5
Impact des performances d'homogénéisation du bio-réacteur sur la cinétique microbienne : cas de *Escherichia coli*

Abstract

A micro-organism circulating in a bioreactor can be submitted to hydrodynamic conditions inducing a significant effect on its physiology. The mixing time exhibited by the stirred bioreactor and the circulation of micro-organisms are both involved in this reacting system. The mixing component determinates the intensity of the concentration gradient and the circulation component determinates the way by which the micro-organism is exposed to this gradient. These two components linked to the experimental evaluation of microbial physiology can be analysed by a structured stochastic model in the case of a partitioned or "scale-down" reactor. A stochastic model indeed enables to simulate the mixing process as well as the circulation of microorganisms in scale-down reactors. The superimposition of mixing and circulation processes determines the concentration profile experienced by a microorganism in the reactor. In the present case, the glucose concentration experienced by *Escherichia coli* has been modelled during a fed-batch culture. In this context, the use of a stochastic hydrodynamic model has permitted to point out an interesting feed pulse retardant effect in the SDRs. Nevertheless, the metabolic response of *E. coli* is not easy to interpret because of the possible simultaneous developments of overflow metabolism and mixed acid fermentation induced by the strong glucose concentration in the reactor.

_____

Introduction

The hydrodynamic behaviour of a stirred bioreactor can be schematised by an impeller zone surrounded by a bulk zone in which the mixing intensity is less pronounced. These two zones are interconnected by circulation flow loops induced by the impeller pumping and circulating capacity. In the impeller region, turbulence forces are intensive and ensure a homogeneity degree of the broth close to the perfect homogeneity. This is not the case of the bulk region in which turbulence intensity is less intensive. This conceptualisation has led to the design of the scale-down reactor (SDR) which generally comprises a small stirred bioreactor connected to a pipe section mimicking the circulation flow loops. This kind of SDR has been previously recognized to generate hydrodynamic behaviour close to the one encountered in large-scale stirred bioreactors and thus inducing a representative impact on micro-organisms physiology [1-6].

In the case of a process improvement perspective, it is interesting to determine the micro-organisms/bioreactor hydrodynamic interactions. In order to achieve this, we propose a numerical model considering the progression of micro-organisms in the bioreactor and able to determinate its exposure to concentration fluctuations. In function of the intensity and the frequency of these fluctuations, physiological stress response will be more or less pronounced, depending on the micro-organism considered. It is very important since some micro-organisms exhibit rapid physiological responses when exposed to concentration gradients (production of acetate in the case of *E. coli*, production of ethanol in the case of *S. cerevisiae*,…). The circulation process must then be analysed in parallel with the mixing phenomena to study the bioreactor hydrodynamic performances.

The methodology adopted to determine the hydrodynamic effects on microbial growth and physiology is defined in the context of a fed-batch cultivation of *E. coli*. This bacteria has been cultivated in a small-scale stirred bioreactor and in a partitioned reactor composed of a mixed section and a plug-flow section. This kind of partitioned bioreactor design is inspired from the SDR concept in order to facilitate the hydrodynamic analysis.

At first, the intensity of overflow metabolism and other microbial growth associated parameters have been examined. Then, the hydrodynamic behaviour of classical and scale down reactors have been determined by the aim of a stochastic model.

Material and methods

Fermentation runs

Fermentation tests have been carried out with a constant feed flow rate of 1.5 ml/min (Glucose concentration of the feed : 370 g/l) started after 5h of culture, without substrate inlet regulating system. It permits to study the direct impact of bioreactor performances and to avoid interactions with the regulating system.

Cultures were performed in a stirred bioreactor (impeller diameter d = 0.1 m ; vessel diameter D = 0.22 m) (Biolaffite-France) with a working volume corresponding to 12 litters. In the case of experiments performed in the context of a partitioned reactor (or scale-down reactor SDR), the above stirred vessel was connected to a silicone tubing (diameter : 8 mm ; length : 7.5 m). This tube acts as a plug-flow section to promote gradient formation inside the bioreactor. Fed addition of glucose is carried out at the entry of the plug-flow section while a peristaltic pump ensures broth circulation between the vessel and the pipe section.

Dissolved oxygen tension is measured by a polarographic probe (Ingold). Oxygen and carbon dioxide percentage in the outlet gas event are measured by paramagnetic and infrared analysers (Servomex). *Escherichia coli* ATCC 10536 is growing on rich medium (20 g/l glucose ; 10 g/l casein pepton ; 10 g/l yeast extract). Microbial growth is observed by optical density measurement (wavelength : 600 nm) and correlated with cell dry weight (drying at 105°C during 24 h after filtration on 0.45 µm filter). Glucose is enzymatically analysed by successive reactions based on glucose oxidase (YSI 2700, Yellow Springs Instruments). Acetate is analysed by UV spectrophotometry (wavelength 375 nm) after being submitted to a set of enzymatic reactions (Boeringher Manheim kit n° 10148261035)

_____

Tracer tests

Homogenisation experiments are performed on classical bioreactor and SDR by a tracer pulse injection method. The technique employed consists to record the conductivity equilibration after injection of a saturated NaCl solution at the top of the vessel (2% of the total volume of the reactor). The conductivity is measured by the use of a Conducell 4-U series probe (Hamilton) placed at the level of the stirred vessel part of the SDR and the signal is recorded by a Daqstation DX-100 (Yokogawa). Mixing time is calculated from tracer curves by the method of Mayr *et al.* [7]. In the case of SDR, pulse is injected at the inlet of the plug-flow section.

Stochastic models

In order to facilitate the results analysis, a structured hydrodynamic model has been used instead of the classical compartment model. Indeed, probabilistic models presents some advantages that cannot be found with deterministic ones. Among these, we can highlight three distinct characteristics which are used in this study :

- mathematical implementation simpler than in the case of deterministic models ;
- discrete behaviour of the equations system, which permits to study the pulse effect without inducing divergence from the mathematical solution ;
- probabilistic nature of the model which permits to study both mixing and circulation phenomena inside the reactors.

In this stochastic model, the scale-down reactor is virtually divided in several states. Each state is interconnected with each others. All are linked by probabilities which are governed by the flow behaviour exerted by the impeller for the mixed section of the reactor, and by the recirculating pump for the plug-flow section. The resulting probabilities network is collected into a transition matrix T, and the concentration field at a simulation step i is described by a state vector S_i. The methodology concerning the transition matrix construction has been described in a previous publication [8]. Simulation of the concentration dynamic inside the scale-down reactor can be achieved by the following implementation :

$$S_i = T \cdot S_{i-1} \qquad (1)$$

This equation can be used to simulate the tracer mixing after a punctual injection inside the apparatus. When considering the mixing phenomena in the case of a frequently repeated pulse addition, as in the case of a fed-batch reactor, the following equation has to be used to describe the evolution of the state vector :

$$S_i = T \cdot S_{i-1} + S_{pulse} \qquad (2)$$

With :

$$S_{pulse} = \begin{bmatrix} C_{pulse} & 0 & 0.. & 0 & C_{pulse} & 0... \\ 0 & 0 & 0 & & & . \\ . & & . & . & & . \\ . & & . & . & & . \\ . & & . & . & & . \\ . & & . & . & & . \\ 0 & 0 & 0. & . & . & ..0 \end{bmatrix} \qquad (3)$$

In the first row, the number of zero elements between two pulses (C_{pulse} being the concentration of the tracer pulse) depends on the feed pump activation frequency. The number of elements in a column corresponds to the number of states in the model. In this matrix, it is to be considered that the pulse is added at the level of the first state of the model (first element in a column). The number of elements in a row corresponds to the number of simulation steps performed.

In order to modelise the SDR described in this study, the model structure presented at figure 1 has been adopted. The relative number of states in the mixed section and in the plug-flow section of the scale-down apparatus must be chosen in function of the mixing time in the mixed section of the SDR comparatively to the retention time in the plug-flow section. Indeed, mixing time is very low in the stirred vessel (approximatively 5 s) and the limiting element is thus the plug-flow section (which exhibits theoretical residence times varying from 78 to 124 s in the range of our operating conditions). This section has been modelised by a set of 50 states placed in series, by comparison with the mixed section which has been modelised by 8 vertical planes in series comprising each 8 states (figure 1).
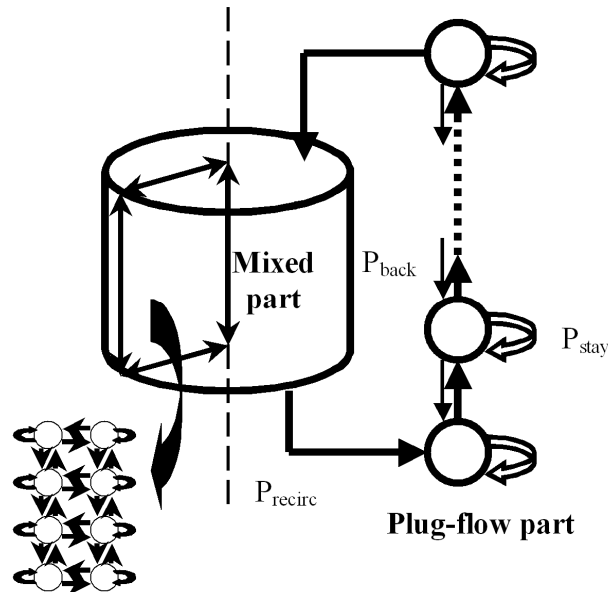
Figure 1 : representation of the stochastic model in the case of a SDR. The plug-fow part comprises a set of states placed in series. Mixed part is constituted from 8 states per axial plane, for a total of 8 planes (64 states, not shown here for reason of clarity). The transitions from states to states in a plane are arranged in accordance with the global hydrodynamic generated by the impeller (in our case, the impeller promotes a radial flow)

In figure 1, P_{recirc} corresponds to the probability to be recirculated inside the plug-flow part ; P_{stay} corresponds to the probability to stay in the actual state during a simulation step ; P_{back} corresponds to the probability to be backmixed when circulating along the plug-flow part.

Results and discussion

Scale-down fermentation tests

Three fermentation runs have been performed. A SDR has been used for the two first tests, by varying the recirculation flow rate between the plug-flow and the mixed section, and the last one without the plug-flow section as a reference

fermentation. We can see from figure 2B that a glucose gradient appears between the two parts of the SDR, and is more pronounced for the lower recirculation flow rate.
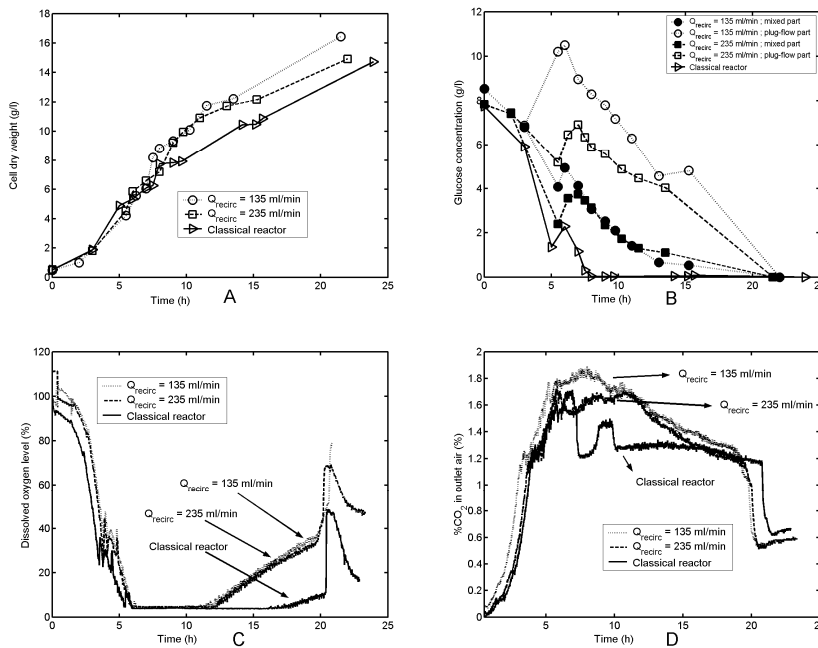

Figure 2 : results of the three fermentations tests. A : evolution of the cell dry weight during the cultures ; B : evolution of the glucose concentration ; C : evolution of the dissolved oxygen level in the mixed part ; D : evolution of the percentage of CO_2 in the outlet air

The lower biomass yield has been noted for the classical stirred fermentor without plug-flow part (Y_{xs} = 0.22 by comparison with Y_{xs} = 0.26 and 0.24 in the case of SDR with recirculation flow rate of respectively 235 and 135 ml/min). In addition, figure 3 shows that more acetate is produced in the case of the classical bioreactor than for the SDRs.
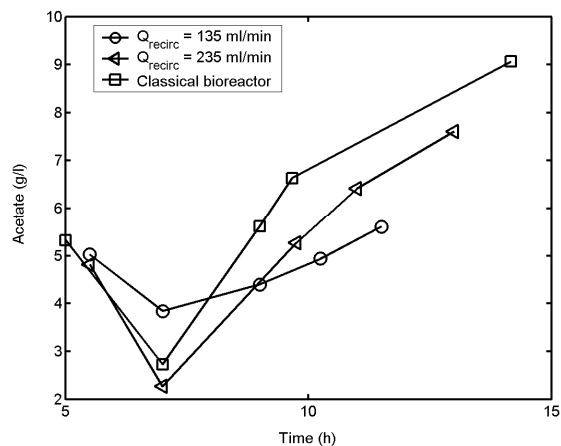
Figure 3 : acetate evolution in SDR and classical reactor

Due to the high glucose concentrations resulting from the constant feed flow rate imposed to the system, two kinds of metabolism can be induced. At first, the overflow metabolism resulting from the passage of microorganisms in high glucose concentration zones leading to the formation of acetate. Then, the mixed acid fermentation which results from the passage of microorganisms in oxygen depleted zones inducing the transformation of glucose into acetate and other by-products [9]. One of the possible explanation for the lower acetate production in SDR is the physical retention of glucose pulses into the plug-flow section. In this case, the volume of broth submitted to strong glucose concentrations is more restricted. From this point of view, it is thus interesting to analyse more precisely the SDR hydrodynamics. To achieve this, the structured stochastic model previously presented has been used. However, the influence of the mixed acid fermentation must also be kept in mind. Indeed, figure 2C reveals that there is a possible oxygen depletion which occurs during the culture. Considering this phenomena, it is difficult to attribute the entire acetate formation to the overflow metabolism. Indeed, the higher acetate concentration observed in the case of the classical bioreactor could be attributed to the mixed acid fermentation. However, the aeration conditions were the same for all the fermentation experiments (dissolved oxygen level was maintained above 30% by varying stirrer speed) which could suggest that there is another impact of the glucose pulse retention at the level of the SDR. Indeed, the

glucose pulse retention inside the plug-flow section of a SDR can limit the amount of glucose entering the mixed section and thus the oxygen depletion in this part of the reactor. However, additional experiments are required to validate this assumption. In the next section, the glucose pulse retention phenomena will be analysed by the use of a structured stochastic model.

Tracer experiments and modelisation of mixing and circulation

The plug-flow section considered consists in a small diameter silicone pipe. Tracer tests reveals that this kind of apparatus generates a near plug-flow hydrodynamic. In other words, the pulse of glucose generated by the feed pump is transported through the pipe length without strong dispersing effect. This kind of plug-flow section acts thus as a pulse retardant. In the previous section, we have postulated that scale-down hydrodynamic has a significant impact on cell physiology. This impact should have to be explained by the pulse retardant effect and this assumption will be discussed in this section. The stochastic models have been used first to model mixing curves obtained by tracer experiments. It has permitted to determine the adjustable parameters of the model. Probabilities to shift from one state to another in the mixed section have been determined according to circulation, turbulence and tangential flow rate knowledges [8]. The probability for a particle to enter the plug-flow section has been directly determined from tracer curves (figure 4).
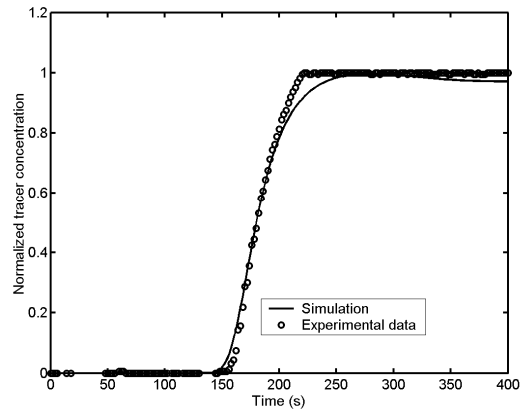
126

Figure 4 : characteristic tracer curve obtained for a SDR (injection at the beginning of the plug-flow section at time t = 0) : comparison of experimental and simulated results

Inside the plug-flow section, the backmixing probability has been minimised because of the nearly perfect plug-flow observed. The last step consists to convert simulation transition into real time interval. From mixing time experiments, it has been determined that a transition corresponds approximatively to 0.43 s for the recirculation flow rates investigated in this study (135 ml/s and 235 ml/s).

On the other hand, the stochastic model has been used to simulate pulse addition of substrate during a fed-batch culture of *E. coli* in SDR. As said previously, one of the interests of the stochastic models lies in their discrete nature. This permits to compute a repeated pulse perturbation without inducing resolution divergence. In order to facilitate the comparison with fermentation tests, a consumption term has been added to the equations system. We can see from figure 5 that the pulsations induced at the inlet of the plug-flow section decrease when going through the plug-flow section. The residence time of this section induces a lag effect in the appearance of glucose at the level of the mixed section. This is clearly shown by the simulation provided at figure 5, in which we can observe a concentration difference between the plug-flow and the mixed section.
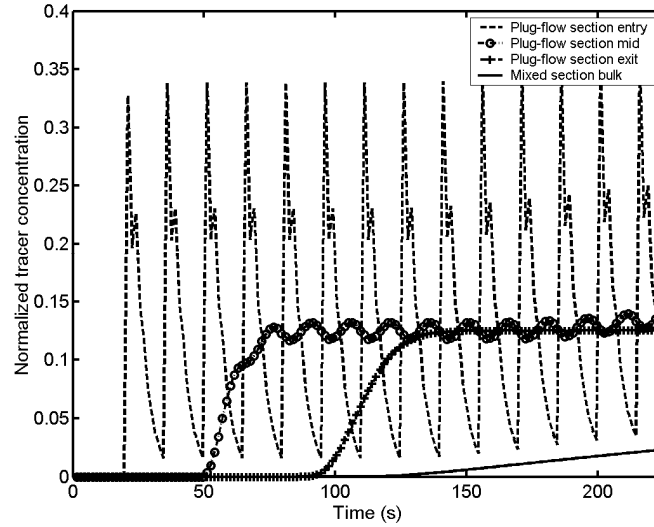
Figure 5 : pulse mixing simulation with the stochastic model relative to the SDR

These retention and lag effects could induce a limitation at the level of the acetate overflow metabolism. This assumption cannot be validated in this study due to the possible intervention of the mixed acid metabolism. The following step is to determine the exposure of *E. coli* to concentration gradients. This can be achieved by superimposing the gradient field to a typical circulation path followed by a microorganism.

The circulation process is more difficult to analyse since experimental methods are not available. Nevertheless, circulation in the plug-flow section is very easy to simulate because it physically corresponds to its residence time. Circulation time in the mixed section can be calculated with the following equation :

$$t_c = \frac{V_L}{Q_c} = \frac{V_L}{N_{qc}.N.d^3} \qquad (4)$$

With V_L being the liquid volume in the stirred vessel (m³), Q_c the circulation flow rate (m³/s), N_{qc} the flow number (adimensionnal and equal to 1.61 in the case of a rushton impeller in the turbulent flow regime), N the stirrer speed (s⁻¹) and d the impeller diameter (m). Circulation times calculation or experimental determination are collected in table 1. These values constitute the basis for circulation simulations

by the aim of the stochastic model. The path followed by a micro-organism in the SDR is simulated by using the same transition matrix T used to perform mixing simulation.

Table 1 : characteristic circulation times obtained in SDR

	135 ml/min	235 ml/min
Theoretical circulation time in the mixed section (s)	1.03	1.03
Theoretical retention time in the plug-flow section (s)	164	95
Experimental minimum retention time in the plug-flow section (s)	124	78
Experimental maximum retention time in the plug-flow section (s)	170	130

In the present case, the transition matrix is not used for simulating the dispersion of a tracer pulse comprising several particles (tracer molecules), but to simulate the path of a single particle (micro-organism). On the contrary of mixing modelling, circulation process in stirred vessel is thus mainly influenced by circulation (which governs the mean of the circulation time distribution) and not by turbulence (which governs the variance of the circulation time distribution). Proportion between circulation probabilities and turbulence/tangential flow probabilities has consequently to be rearranged, and a ratio of 80% has been chosen referring to [10]. This value permits to match the representative circulation time distribution [11]. The probability for a micro-organism to enter the plug-flow section has been determined by residence time experiments on the stirred vessel for the two recirculation flow rates investigated.

The simulated circulation path is superimposed to the gradient filed in order to obtain the concentrations experienced by micro-organisms. Nevertheless, the resulting simulations do not reflect perfectly the reality, but reasonably permit to compare SDR and classical bioreactor on the basis of mixing and circulation performances. In order to enhance the quality of the simulations, a microbial kinetic model has been added to the bioreactor hydrodynamic model .

It can be seen from figure 6 that micro-organisms are submitted to higher and more frequent concentration pulses than in the SDR. This phenomena can be explained by the retention of the pulses into the plug-flow part of the SDR. In this systems, concentration gradients are retained in the pipe section which could minimize the overflow metabolism in the whole apparatus. Nevertheless, it is not easy to interpret this effect from a physiological point of view, considering the possible simultaneous development of a mixed acid metabolism.
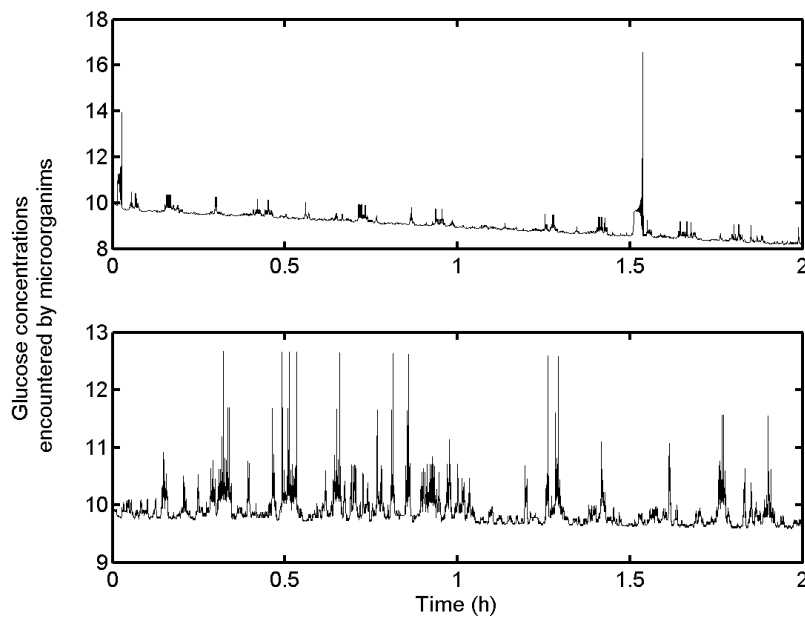
Figure 6 : superimposition of concentration field obtained by mixing stochastic model and micro-organism stochastic circulation. This methodology permits to obtain characteristic glucose concentrations (in g/l) encountered by micro-organisms in different systems : SDR (top) and classical small-scale bioreactor (bottom)

Conclusion

Fermentation tests have been carried out without fed-batch regulation at constant feed rate. This strategy leads to the appearance of high glucose concentrations inside the reactor and acetate overflow metabolism, as well as mixed acid fermentation, can be induced. In this context, an interesting effect results from by the geometry of

the SDR. Indeed, the near perfectly plug-flow generated inside the pipe section of the SDR induces a lag in the appearance of the glucose pulse in the mixed section (which represents the major volume of the SDR). This effect could be traduced at the level of the micro-organism by a limitation of the overflow metabolism, but the results are difficult to interpret considering the possible simultaneous production of acetate by the mixed acid fermentation pathway.

Nevertheless, the partitioned reactor has shown clearly an impact of hydrodynamics on microbial physiology in the case of a fed-batch of *E. coli*. A direct application of the stochastic methodology presented here is the study of the scale-down effect in the perspective of the elaboration of large-scale processes. This effect have been previously observed in scale down reactors. We have shown that these SDR can be optimised by modifying the recirculation rate between mixed and plug-flow sections, as well as the diameter of the plug-flow section, in order to match the hydrodynamic of large-scale bioreactors. In this perspective, this show the interest of using stochastic hydrodynamic model.

References

1. Enfors S.O., Jahic M., Rozkov A., Xu B., Hecker M., Jürgen B., Krüger E., Schweder T., Hamer G., O'Beirne D., Noisommit-Rizzi N., Reuss M., Boone L., Hewitt C., McFarlane C., Nienow A., Kovacs T., Trägardh C., Fuchs L., Revstedt J., Friberg P.C., Hjertager B., Blomsten G., Skogman H., Hjort S., Hoeks F., Lin H.Y., Neubauer P., van der Lans R., Luyben K., Vrabel P., Manelius A. (2001) *Physiological responses to mixing in large scale bioreactors.* Journal of biotechnology **85**: 175-185.
2. Neubauer P., Häggström L., Enfors S.O. (1995) *Influence of substrate oscillations on acetate formation and growth yield in Escherichia coli glucose limited fed-batch cultivations.* Biotechnology and bioengineering **47**: 139-146.
3. Namdev P.K., Thompson B.G., Gray M.R. (1992) *Effect of feed zone in fed-batch fermentations of Saccharomyces cerevisiae.* Biotechnology and bioengineering **40**(2): 235-246.
4. Fowler J.D., Dunlop E.H. (1989) *Effects of reactant heterogeneity and mixing on catabolite repression in cultures of Saccharomyces cerevisiae.* Biotechnology and bioengineering **33**: 1039-1046.
5. Amanullah A., MacFarlane C.M., Emery A.N., Nienow A.W. (2001) *Scale-down model to simulate spatial pH variations in large-scale bioreactors.* Biotechnology and bioengineering **73**(5): 390-399.

6. Hewitt C.J., Nebe-Von CaronG., Axelsson B., Mc Farlane C.M., Nienow A.W. (2000) *Studies related to the scale-up of high-cell-density E. coli fed-batch fermentations using multiparameter flow cytometry : effect of a changing microenvironment with respect to glucose and dissolved oxygen concentration.* Biotechnology and bioengineering **70**(4): 381-390.

7. Mayr B., Horvat P., Moser A. (1992) *Engineering approach to mixing quantification in bioreactors.* Bioprocess engineering **8**: 137-143.

8. Delvigne F., Destain J., Thonart P. (2005) *Structured mixing model for stirred bioreactor : an extension to the stochastic approach.* Chemical engineering journal, In Press

9. Xu B., Jahic M., Blomsten G., Enfors S.O. (1999) *Glucose overflow metabolism and mixed-acid fermentation in aerobic large-scale fed-batch processes with Escherichia coli.* Applied microbiology and biotechnology **51**: 564-571.

10. Mann R., Mavros P.P., Middleton J.C. (1981) *A structured stochastic flow model for interpreting flow-follower data from a stirred vessel.* Trans IChemE **59** 271-278.

11. Davidson K.M., Sushil S., Eggleton C.D., Marten M.R. (2003) *Using computational fluid dynamics software to estimate circulation time distribution in bioreactors.* Biotechnology progress **19**:1480-1486.

CHAPITRE 6
Impact des performances d'homogénéisation du bio-réacteur sur la cinétique microbienne : cas de *Saccharomyces cerevisiae*

Abstract

The mechanisms of interaction between microorganisms and their environment in stirred bioreactor can be modelled by a stochastic approach. The procedure comprises two sub-models : a classical stochastic model for the microbial cell circulation and a Markov chain model for the concentration gradient calculus. The advantage lies on the fact that the core of each sub-model, i.e. the transition matrix (which contains the probabilities to shift from a perfectly mixed compartment to another in the bioreactor representation), is identical for the two cases. That means that both particle circulation and fluid mixing process can be analysed by use of the same modelling basis. This assumption has been validated by performing inert tracer (NaCl) and stained yeast cells dispersion experiments that have shown good agreement with simulation results. The stochastic model has been used to define a characteristic concentration profile experienced by the microorganisms during a fermentation test performed in a scale-down reactor. The concentration profiles obtained by this way can explain the scale-down effect in the case of a *Saccharomyces cerevisiae* fed-batch process. The simulation results are analysed in order to give some explanations about the effect of the substrate fluctuation dynamics on *S. cerevisiae*.

_____

Introduction

In stirred bioreactors, microorganisms are submitted to concentration fluctuations (substrate, oxygen, pH,…) with an intensity and a frequency depending on the operating scale. In a scale-up procedure, it is thus important to characterize the concentration gradient, as well as the way in which microorganisms are exposed to these gradients. We propose two modelling approaches based on the compartment principle. This kind of model is generally expressed by a set of ordinary differential equations [1]. The originality here lies in the stochastic expression of these models, this approach providing new potentialities. Indeed, by using this model, fluid mixing and particle circulation can be simulated with the same model structure. In this study, the descriptive analysis of a fed-batch culture of *Saccharomyces cerevisiae* (microbial growth and glucose consumption) performed in a small-scale stirred bioreactor (20 l) and in a scale-down reactor comprising a mixed part and a non-mixed part will be followed by two structured hydrodynamic modelisation procedures in order to give more insight about the mixing impact on *S. cerevisiae* productivity. In particular, the study will be focused on the microorganism - fluid mixing interactions. The scale-down reactor (SDR) used in this study permits to obtain at a small scale the environment heterogeneity encountered in large-scale bioreactors. This kind of system has been previously used in several applications [2-7]

The originality here lies on the fact that the microorganism-environment interactions will be entirely modelled by a stochastic approach. The concentration gradient developed when running in fed-batch mode will be represented by a Markov chain which is a special kind of stochastic model. The Markov chain has been previously developed in the case of a stirred bioreactor and has shown a lot of potentialities compared with classical deterministic compartment models [8]. The microorganism circulation paths inside the bioreactor are modelled by a stochastic model involving the same transition matrix as for the Markov chain. The superimposition of the gradient field and the microorganism circulation paths leads to the concentration profiles experienced by the microbial cells. These concentration profiles are

discussed in function of the biomass yield and the operating conditions of the fermentation tests performed in scale-down reactor.

Material and methods

1. Cultures in stirred bioreactor and in scale-down reactor (SDR)

Saccharomyces cerevisiae (MUCL 43341 ; misapplied name : *boulardii*) strain is stored at –80°C. Cultures are performed in 20l stirred bioreactors (D = 0.22 m) (Biolaffite-France) equipped with a RDT6 rushton turbine (d = 0.1 m). The regulation of the culture parameters (pH, temperature,…) is ensured by a direct control system (ABB). Dissolved oxygen level is maintained above 30% of saturation by modulating the stirrer speed. For the scale-down tests, the previously described stirred vessel has been connected to a glass bulb of 1 litter (diameter : 0.085 m ; length : 0.25 m). During fermentation runs, the broth has been continuously recirculated between the stirred vessel (mixed part) and the glass bulb (non-mixed part) by a peristaltic pump (Watson Marlow 323S/D). In the case of the scale-down reactor (SDR) experiments, glucose addition is performed at the level of the non-mixed part. In the case of the classical bioreactor experiments, glucose is fed by the top of the stirred vessel. Glucose addition is controlled by an exponential feeding algorithm according to the equation $F = F_0 . \exp(\mu.t)$. With F being the feed flow rate (m³/s), F_0 the initial feed flow rate (m³/s), μ the microorganism growth rate (h^{-1}) and t the culture time (h). The two parameters $\mu = 0.005$ min^{-1} and $F_0 = 0.086$ ml/min are calculated from growth data of *Saccharomyces cerevisiae* in a batch bioreactor.

2. Tracer tests : inert tracer and biological tracer

Two kinds of experiment have been performed using the SDR : tracer experiments in classical mode and in "open system" mode, that is with the SDR reactor running in continuous mode. Liquid is injected at the top of the mixed section and is extracted at the outlet of the non-mixed section at a given flow rate. Tracer tests are

performed by injecting a short pulse (injection time < 3 s) at the top part of the mixed section.

Two kinds of tracers have been used : an inert tracer (saturated NaCl solution) and a biological tracer (suspension of microbial cells). Biological tracer experiments are performed by injecting a pulse of a solution containing stained cells in the bioreactor. The cells are stained with a fluorescent dye (Vybrant CFDA SE cell tracer kit V-12883) which facilitates the detection by epifluorescent microscopy. The staining protocol consists to perform a preculture in a 500 ml Erlenmeyer flask in order to obtain the required amount of biomass for further staining. An aliquot of the preculture is centrifuged (5 minutes at 4000 rpm). The precipitate is washed with 10 ml of sterile PBS buffer (NaCl 8 g/l ; KCl 0.2 g/l ; K_2HPO_4 1.44 g/l ; KH_2PO_4 0.24 g/l ; adjusted to pH 7.5 with K_2HPO_4 and KH_2PO_4). Three successive centrifugation/washing sequences are performed. After this, microbial cells are stained by addition of 1mM of CFDA SE (carboxyfluorescein diacetate succinimidyl ester), followed by an incubation during 3 hours at 30°C. After incubation, the solution is centrifuged and the precipitate is washed with PBS buffer. When performing a biological tracer test, 5 ml of the stained cells suspension (2.10^8 cells/ml) are poured at the level of the non-mixed part of the SDR, whereas samplings are taken at the level of the mixed part. Cells are directly counted by fluorescent microscopy. For each sample, three aliquots of 10 µl each are placed on a microscopic plate for further counting. For each aliquot, three counts are performed for three widths of the microscopic plate. Mean and standard deviation are calculated for each sample.

3. Mathematical models

The structured or compartment models can be divided in two categories : stochastic or deterministic. Stochastic models have a discrete nature and are generally used when considering small populations where heterogeneities and fluctuations are important. Up to now, they have been especially used to simulate particulate mixing processes [9]. Here, these stochastic models are employed to simulate microbial cells circulation in bioreactors and, in a second time, are adapted to simulate fluid

mixing. Deterministic compartment models are used to represent fluid mixing and are mathematically expressed by continuous ordinary differential equations. In this study, deterministic model will be used to simulate the mixing of a salt tracer pulse and as a reference for comparison with the performances of stochastic models for fluid mixing. The goal here is to find a stochastic model which can be used both in the case of particle flow and fluid mixing, in order to simulate concentration profiles experienced by microorganisms travelling in bioreactors. It implies that the relation between microbial cells circulation and fluid mixing in bioreactor is to be carefully examined.

Model 1 : stochastic and deterministic expression from a simplified structure

A simplified model structure is used at first :

- To validate the equivalency assumption for the fluid mixing and microorganisms circulation processes in bioreactors.
- To validate the assumption that the biomass yield loss in SDR can be attributed to the passage of microorganisms at the level of the non-mixed part of the reactor.

Figure 1 presents the simplified model structures.

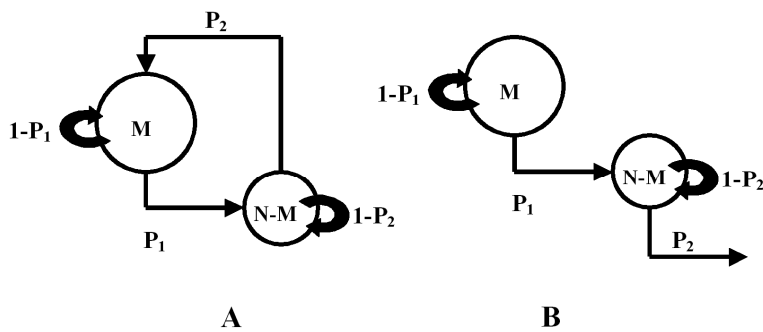**A**   **B**

Figure 1 : simplified structures for the SDR model (M : mixed section ; N-M : non-mixed section) with the corresponding transition probabilities. A : classical SDR (closed system) ; B : open system. P : probability to shift from a compartment to another ; 1-P : probability to remain in the actual compartment.

137

The non-mixed part of the SDR has been represented by a single compartment. This approach can be validated by the high dispersing effect of the reactor which strongly perturbs the plug-flow inside this part of the reactor. The tracer experiments relative to the "closed" SDR have been first considered. The probabilities between the two compartments have been calculated from the real flow rate by the equation P = Q/V (where Q represents the flow rate in m³/s and V the compartment volume in m³). This simplified model will be used in its stochastic form to express particles dispersion in the SDR. This is numerically done by comparing random numbers and the respective transition probabilities that allow displacement from one compartment to another. A deterministic expression with the same model structure has also been used to characterize fluid mixing in the SDR. The deterministic compartment model has been widely used in the area of fluid mixing in stirred bioreactors [1, 10-13]. Its principle is based on the tank-in-series concept, each compartment being assumed to be perfectly mixed. The mathematical expression of the model involves a set of ordinary differential equations representing the mass balance for each compartment considered. The deterministic compartment model will be used in this study as a reference for the stochastic expression of the simplified model structure. The same model structure (i.e., the same well-mixed compartments arrangement) presented in figure 1 and 2 can be used, but the mathematical expression is fundamentally different. Indeed, in the case of a deterministic formulation, the probabilities are replaced by flow rates between compartments. The mathematical expression of the model comprises a set of ordinary differential equations (ODEs) for the mass balance for each compartment. For example, in the case of the model presented at figure 1A, the mathematical expression is :

$$\frac{dC_M}{dt} = Q_{IN} \cdot C_{NM} - Q_{OUT} \cdot C_M \qquad (1)$$

$$\frac{dC_{NM}}{dt} = Q_{IN} \cdot C_M - Q_{OUT} \cdot C_{NM} \qquad (2)$$

C_M being the tracer concentration in the mixed compartment ; C_{NM} the tracer concentration in the non-mixed compartment ; Q_{in} the flow rate (m³/s) entering in

138

the compartment ; Q_{out} the flow rate (m³/s) from the compartment. The set of ODEs is numerically resolved by a Runge-Kutta algorithm.

Model 2 : complex structure allowing a better resolution on the hydrodynamic mechanisms in SDR

The second model structure used in this study is more elaborated and allows a higher resolution at the level of the concentration gradient and the microorganism circulation path. The expression of this model is stochastic, but the algorithm differs according to whether this is fluid mixing or particle circulation that must be simulated. These procedures will be further described in details. The structure of the model is presented at figure 2.
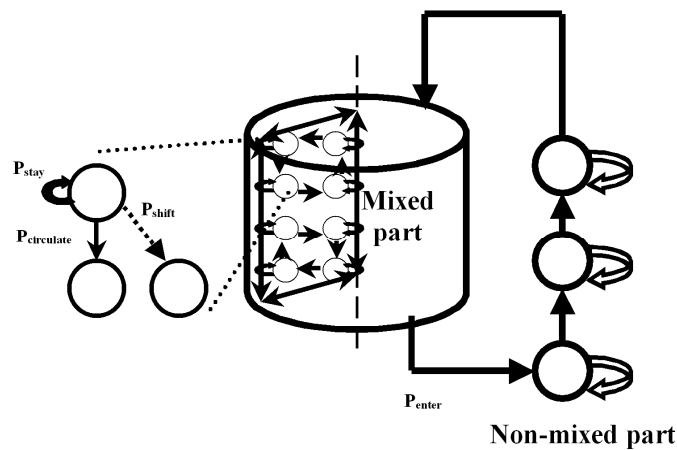

Figure 2 : complex three-dimensional model structure : P_{stay} : probability to stay in the actual compartment ; $P_{circulate}$: probability to be convoyed by the impeller circulation flow ; P_{shift} : probability to shift from the circulation loop ; P_{enter} : probability to enter in the non-mixed part.

The stirred vessel constituting the mixed part of the SDR has been modelled by using eight vertical planes, each of them comprising eight compartments. The interconnections between compartments are in accordance with the radial flow developed by the rushton turbine used for the experiments.

Two possibilities can be envisaged. Firstly, the direct translation of the equivalent deterministic compartment model in a probabilistic context. In this case, the

transition probabilities are calculated from the ratio of flow rates allocated to a given compartment. This approach has been tested in a previous study that has shown the great potentialities of Markov chain models in the case of fluid mixing [8]. Secondly, and it is this option that has been chosen, we can completely adapt the model structure by considering four kinds of probabilities : the probability to reamin in a given circulation flow loop, the probability to remain in the same compartment, the probability to shift to another plane, and the probability to switch from the main flow loop (this method has been proposed by [14]). The circulation probability can be estimated from dimensionless correlation by the circulation flow rate (m³/s) :

$$Q_c = N_{qc}.N.d^3 \qquad (3)$$

With N_{qc} being the dimensionless circulation number having a constant value of 1.51 in the turbulent flow regime for a rushton impeller with 6 blades ; N being the impeller speed (s^{-1}) ; d being the impeller diameter (m).
and :

$$P_{circulation} = \frac{Q_c}{V_{compartment}} \cdot \Delta t \qquad (4)$$

With $V_{compartment}$ being the respective volume occupied by a compartment in the model (m³) and Δt being the time step chosen to run simulation (in our case $\Delta t = 1s$). Two components are involved in the fluid mixing process in stirred vessel : a circulation component and a turbulence component. The circulation component has been described by a probability expressed in equation 4. For each compartment of the model, a particle or a fluid element has a probability to follow the global circulation pattern induced by the impeller, but can also switch from this flow pattern under the influence of the turbulence forces. This is expressed by the following equation :

$$P_{switch} = P_{tangential} = P_{stay} = \left(1 - P_{circulation}\right)/3 \qquad (5)$$

With P_{stay} being the probability to stay in the actual compartment ; $P_{tangential}$ being the probability to shift to another plane ; P_{switch} being the probability to shift from the main circulation flow loop. The assumption has been made that all these

probabilities have an equal value. This assumption can be accepted since it allows to match the experimental tracer curves (as it will be shown in figure 6B).

In our model, particles are allowed to switch diagonally from the flow loop in the same plane, or to switch perpendicularly from the actual plane to the adjacent planes. All the calculated transition probabilities are stored in a transition matrix T that will be used to run simulations. The stochastic simulation procedure is the same as the one described for the simplified model and consists to generate a random number that governs the displacement of a particle according to the respective probability of the transition matrix T.

The second step, after simulating particles circulation, is to describe the concentration gradient inside the reactor. This can be achieved by considering a large amount of particles, but this method is fastidious because of the important computational time required. It has also been previously shown that it is possible to use a Markov chain stochastic model to obtain the value of the concentration gradient. This approach has been previously used to model fluid mixing in stirred bioreactors [8]. In this case, the transition matrix previously presented for the non-Markovian model is multiplied by a state vector representing the concentration in each compartment. This multiplication leads to the state vector of the system at the following time increment. The evolution of the concentration gradient in the modelled bioreactor can be expressed by this way by performing a cascade of state vector – transition matrix multiplications. The advantage of this method lies on the fact that the same transition matrix than those used for particle circulation can be used.

The Markov chain stochastic model consists of an initial state vector S_0, which is multiplied with a transition matrix T to give a new state, S_1. This can be written as :

For the first transition: $S_1 = T \cdot S_0$ (6)

The next step involves the multiplication of the new state vector S_1 with the same transition matrix T until a steady-state is reached:

For the second transition: $(S_2 = T \cdot S_1)$ or $(S_2 = T^2 \cdot S_0)$ (7)

For the ith transition: $(S_i = T \cdot S_{i-1})$ or $(S_i = T^i \cdot S_0)$ (8)

In our case, the state vector contains the tracer concentration values for all compartments.

Results and discussion

1. SDR experiments

Fed-batch cultures of *S. cerevisiae* have been performed in different bioreactor configurations. For each culture, the biomass yield has been calculated (table 1) and the growth curves are plotted in figure 3.

Table 1 : biomass yield coefficients obtained for fed-batch cultures of *S. cerevisiae* and for different bioreactor configurations

Reactor	Biomass yield Y_{xs}
Classical bioreactor	0.48
Reference SDR (glucose fed at the level of the mixed part)	0.47
SDR recirculation flow rate Q = 18 l/h	0.36
SDR recirculation flow rate Q = 39 l/h	0.45

The analysis of the results presented in table 1 reveals a clear impact of the exposure of microorganisms to glucose concentration fluctuations. Indeed, the yield coefficient Y_{xs} has a value of 0.48 in the case of the classical bioreactor (stirred bioreactor without the non-mixed part). This value drop to 0.36 in the case of the SDR with recirculation flow rate of 18 l/h, and to 0.45 when the flow rate is increased to 39 l/h. This drop can be attributed to the passage of microorganisms trough the non-mixed part where the pH, the temperature and the dissolved oxygen concentration can be heterogeneous and where yeast cells are exposed to flocculation.
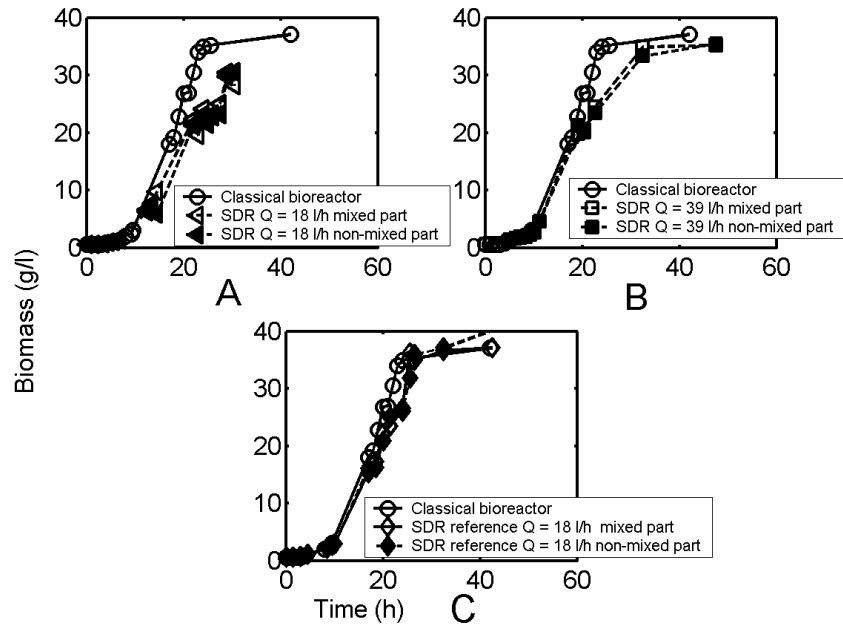
Figure 3 : comparison of microbial kinetic in a classical stirred bioreactor and in a scale-down reactor (SDR). The SDR tests have been performed by varying the recirculation flow rate (A : Q = 18l/h ; B : Q = 39 l/h) or the glucose feed location (C : SDR with Q = 18 l/h but with a glucose feed point located in the mixed part of the reactor instead of the non-mixed as for experiments A and B). For all the experiments, the growth curve is compared to an "ideal" growth curve obtained in a classical stirred bioreactor

This effect has been tested by performing a SDR test in which glucose was injected at the level of the mixed part. The results can be viewed at figure 1 (lower part) and it can be concluded that this effect is very slight (Y_{xs} equal to 0.47 comparatively to 0.48 in the case of the classical bioreactor).

Differences between the growth curves obtained in classical and in scale-down reactors appear after approximately 20 hours of cultures (figure 1). This lapse of time includes the batch phase (4 hours) and the 15 first hours of the fed-batch phase for which the glucose pulses are very spaced according to the exponential regulation of the feed flow rate. After 15 hours, the pulse frequency becomes significative by comparison with the mixing time of the SDR reactor.

From the results showed at figure 1, we can make the assumption that the loss of productivity can be attributed to the exposure of microorganisms to a fluctuating

environment, and more precisely to fluctuating glucose concentrations. The scale-down effect can be attributed to the liquid recirculation flow rate between the mixed and the non-mixed section of the SDR. It also depends on the non-mixed section configuration and notably of the diameter of the non-mixed section. Other authors have recorded productivity losses in function of the recirculation flow rate and the non-mixed section configuration [5, 6]. This assumption will be tested in the following sections by the use of a structured modelling strategy.

2. First modelling approach (model 1) : circulation of a set of microorganisms inside the bioreactors

This first modelling approach is coarse and is based on the basic assumption that the loss of productivity in SDR can be attributed to the passage of microorganisms through the non-mixed part. The explanations relative to this model can be found in the material and methods section (model 1).

When simulating the mixing of a small amount of particles, the results are greatly influenced by the probability effect. In order to study the impact of this effect, several simulations have been performed by varying the number of particles (figure 3).
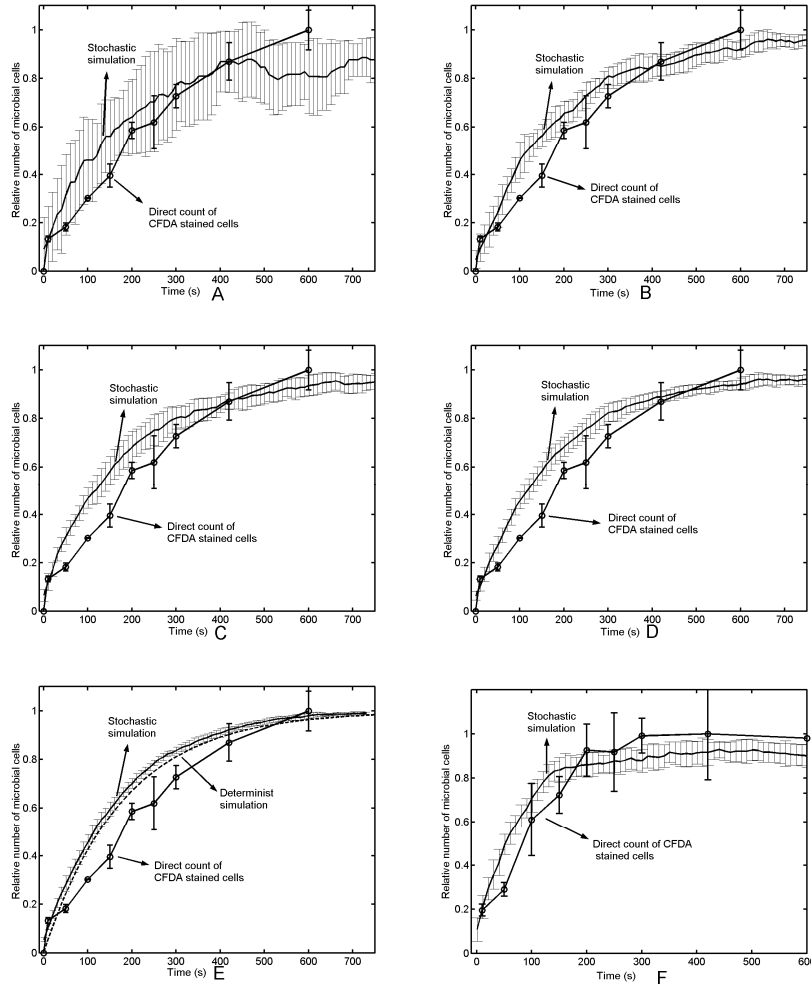
Figure 4 : stochastic simulations performed with 10 (A), 50 (B), 100 (C), 200 (D) and 500 (E) particles with a recirculation flow rate of 18 l/h, or with 50 particles with a recirculation flow rate of 39 l/h (F). The particles are starting from the non-mixed part of the SDR (compartment NM at figure 1) and the relative number evolution is recorded at the level of the mixed part (compartment M in figure 1). For each conditions, 10 simulations have been performed and the mean as well as the standard deviation are represented on the graphs. Comparison with experimental yeast cells tracer test is shown. In the case of simulation E, comparison with the equivalent deterministic compartment model has been done.

Figure 4A shows that when operating with only 10 particles, variation from a simulation to another is important (represented by the standard deviation). But the standard deviation rapidly drops   when the number of particles involved in the

simulation reached 50 (figure 4B). For the cell tracking experiments, the microscopic direct counting technique is involving a maximum of about 100 stained yeast cells per microscopic plate. Thus, simulations with 50 or 100 particles can be used to match the experimental results (Figures 4B and 4C show a good correspondance between simulated and experimental values). But this number of cells doesn't include the entire microbial population in the bioreactor. In reality, the microbial population is important and its repartition in the bioreactor can be represented by a deterministic model or by a stochastic model involving an important number of particles (figure 4E). This fact highlights the relation existing between stochastic and deterministic or discrete and continuous formulation of the models.

The parameters considered for the previous tracer experiments can be used to perform simulations when the system is running in continuous ("open system") mode (figure 5). The model structure corresponding to this operating mode can be found in figure 1B.
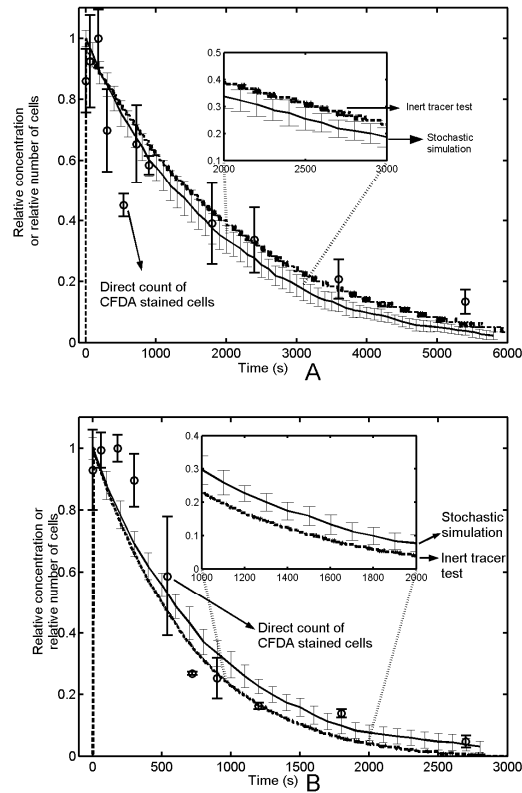
Figure 5 : stochastic simulations performed in the "open system" with a recirculating and exit flow rate of 18 l/h (A) and 39 l/h (B). Simulations represent the tracer concentration evolution at the level of the mixed part of the SDR (compartment M in figure 1). For each condition, 10 simulations are performed and the mean as well as the standard deviation are represented on the graphs. Comparison with experimental yeast cells tracer test, as well as with inert tracer tests (NaCl) is given.

The results showed at figure 5 highlight other important phenomena such as the time required for a microbial population to leave the mixed or the non-mixed section of the SDR. From a methodological point of view, the inert tracer is used to validate the fluid mixing - deterministic models and the cells suspension is used to implement the particle circulation – stochastic models, but from the obtained results (figure 5), it can be seen that the two kinds of experiments can be explained both in a deterministic or stochastic context. This is quite important, since a single model

147

can be used to simulate fluid mixing and particles circulation. Some precautions must however be taken, concerning for example the importance of microbial population investigated. Indeed, for a reduced population, the probabilistic aspect has an important role (see figure 4) and the stochastic model must be used. On the contrary, for an important population (such as the number of NaCl molecules in an inert tracer pulse), only will prevail the general trend, and the deterministic model is recommended. But, in this case, a previous study has shown that the transition matrix can be used in a Markov chain context and gives results similar to those obtained with a determinist model [8]. In the following section, only the stochastic basis will be used to elaborate the fluid mixing and circulation models, the fluid mixing being simulated with a Markov chain stochastic model and the particle circulation with a stochastic non-Markov model.

At this level, we can thus estimate the transition probabilities between the two parts of the SDR and determinate the repartition of a microbial population in this reactor. But these probabilities doesn't explain the fluid dynamic effect on microbial growth and it is necessary to refine the model. Indeed, the concentration gradient will be influenced by the recirculation flow rate and by the pulse frequency of the feed pump. A more elaborated model is thus needed to represent precisely the evolution of the concentration field at some points of the reactor.

Another important conclusion is that the yeast cells appear to behave like the inert tracer and consequently must be considered as following the global flow inside the reactor. It is very important in the case of the microbial cell circulation model elaboration. Indeed, we can conclude in our case that the same model structure can be used to model the fluid mixing process and cells circulation, and this property will be exploited in the next section.

3. Second modelling approach (model 2) : superimposition of microorganisms circulation on the concentration gradient inside bioreactors

A more elaborated modelling approach can lead to the visualisation of the concentration gradient establishment and to a higher resolution on the path taken by

the microorganism during his circulation in the reactor. The idea here is to superimpose the microorganism circulation path to the gradient field, in order to obtain a characteristic concentration profile experienced by the circulating microorganisms. If increasing the number of compartments, we approach the structure of a more elaborated compartment model generally called network-of-zones. This kind of model has been used to represent fluid mixing in bioreactors [1, 15] and we will extent its use in a stochastic context. Figure 2 shows the complex network of compartments used here in the case of the SDR (constituted by a mixed part and a non mixed part).

Figure 6A shows a simulation performed with 3500 particles (50 microbial cells per compartment), which roughly correspond to the number of microorganisms detected during the CFDA stained cells experiments. By running simulations with this model, we observe a probabilistic fluctuation more pronounced than the one which occurs in the case of the simplified stochastic flow models used in the previous section. This can be explained by the increasing number of compartments which leads to a multiplication of the possible trajectories that can be taken by the flowing particles. It should also be noted that the number of cells at the equilibrium is higher for the compartments located in the non-mixed section of the reactor. This is simply due to the fact that the volume of these compartments is more important than the one of those located in the mixed section.
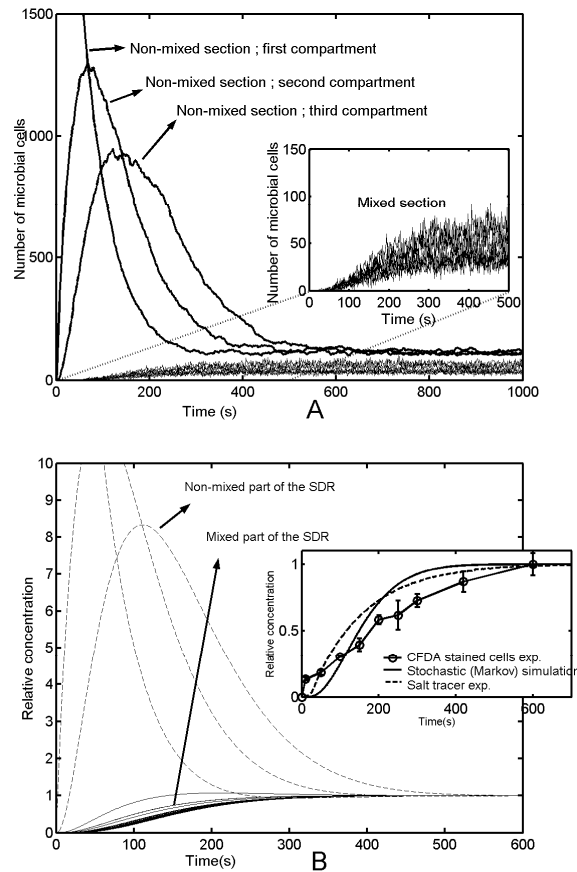
Figure 6 : A : random number stochastic simulation of microbial cells dispersion in SDR (three-dimensional model with a recirculation flow rate : 18l/h). Microbial cells (quantity : 3500) were initially located at the level of the first compartment of the non-mixed section ; B : Markov chain simulation of tracer dispersion in SDR reactor (three-dimensional model with a recirculation flow rate of 18 l/h). The pulse injection of tracer was performed at the level of the first compartment of the non-mixed part of the SDR.

The Markov chain procedure (described in the material and methods section) can be used to perform a fluid mixing simulation with the same model structure and with the same transition matrix. Figure 6B shows the results of the simulation. We can see that there is a good agreement between the stochastic random number (figure 6A) and the Markov simulation results (figure 6B), this observation validating the fact that the same transition matrix can be used to simulate fluid mixing and particle

150

circulation. As shown before [8], the Markov chain model exhibits the same potentialities than the deterministic compartment models and can be used to calculate the concentration field inside the reactor. This fact is anew reinforced by the logical evolution of the simulated tracer curves obtained in this study (figure 6B). Indeed, concentration variations are very pronounced in the compartments located at the level of the non-mixed whereas those located in the mixed part exhibit tracer curves which are very close to each others due to the high homogenisation efficiency in this part of the reactor. From these results, we can say that the model structure is sufficiently elaborate to obtain a good resolution, both for the fluid mixing and the cell circulation simulations. This is important for the circulation simulation for which the model structure has an impact on the variance of the circulation time distribution.

In order to obtain a good representation of the concentration field evolution during the bioprocess, the pulse effect of the feed pump too must be taken into account. In our case, the pulse frequency is time varying because of the exponential increase of the feed flow rate during the culture. This pulse frequency can be included in the stochastic model by the use of the following matrix :

$$S_{pulse} = \begin{bmatrix} C_{pulse} & 0 & 0.. & 0 & C_{pulse} & 0... \\ 0 & 0 & 0 & & & . \\ . & . & . & & & . \\ . & . & . & & & . \\ . & . & . & & & . \\ . & . & . & & & . \\ 0 & 0 & 0. & . & . & ...0 \end{bmatrix} \qquad (9)$$

In the first row, the number of zero elements between two pulses (C_{pulse} being the concentration of the tracer pulse) depends of the feed pump activation frequency. The number of elements in a column corresponds to the number of compartments in the model. In the case of this matrix, the pulse is added at the level of the first state of the model (first element in a column). The number of elements in a row corresponds to the number of simulation steps performed.

The matrix S_{pulse} is included in the standard Markov chain procedure (see equation 8) to describe the evolution of the state vector :

$$S_i = T \cdot S_{i-1} + S_{pulse} \qquad (10)$$

The strategy adopted here consists in superimposing the gradient field obtained with the Markov chain model with the microorganisms circulation process obtained with the classical stochastic model (i.e., with random number generator), in order to obtain the concentration profile experienced by a population comprising a given number of microorganisms.

The first step consists in calculating the evolution of the glucose concentration in each compartment of the model. The problem here comes from the reactive behaviour of the investigated system. Indeed, a substrate consumption component exerted by yeast cells modifies the glucose gradient field appearance in the bioreactor. Figure 7 shows that glucose concentration at the outlet of the non-mixed section is the same as the one observed in the bulk of the mixed section of the SDR.
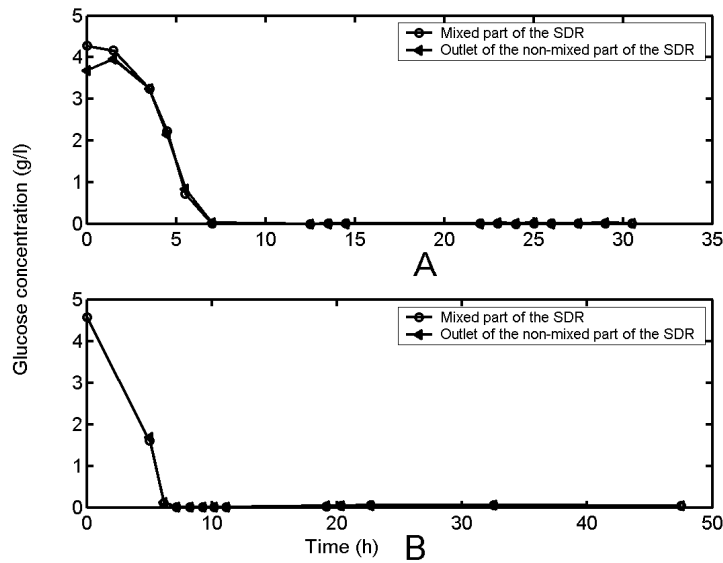
Figure 7 : evolution of glucose concentration during SDR experiments (A : Q_{recirc} = 18 l/h ; B : Q_{recirc} = 39 l/h)

Due to the large sample interval between glucose concentration determination experiments, the oscillatory effect induced by the pulse addition of glucose could be not visible. But, in general, there are no significant glucose concentration differences between the two parts of the SDR. As shown in this study and in others, during a

fed-batch culture, the average glucose concentration in the bioreactor is low, the cell density is high and the glucose pulses are located in the immediate vicinity of the feed addition point. The concentration profiles in the different compartments of the model will consequently be expressed in terms of relative differences. In others words, the situation in a compartment for a given time interval will be calculated as the difference beteween the relative concentration in this compartment and the one in the compartment exhibiting the smallest relative concentration. This approach permits to calculate a representative normalised concentration field in accordance with the mixing performances of the system. In order to compare the different SDR tests on the basis of the mixing performance, Markov chain simulations have been performed according to the feed pump pulse profile. The pulse frequency matrix S_{pulse} (equation 10) has been extracted from the experimental feed profile recorded by the bioreactor control unit. The feed profile was performed according to an exponential regulation (described in the material and methods section). Simulations obtained by this way in the case of a SDR operating at a recirculating flow rate of 39 l/h are shown at figure 8.
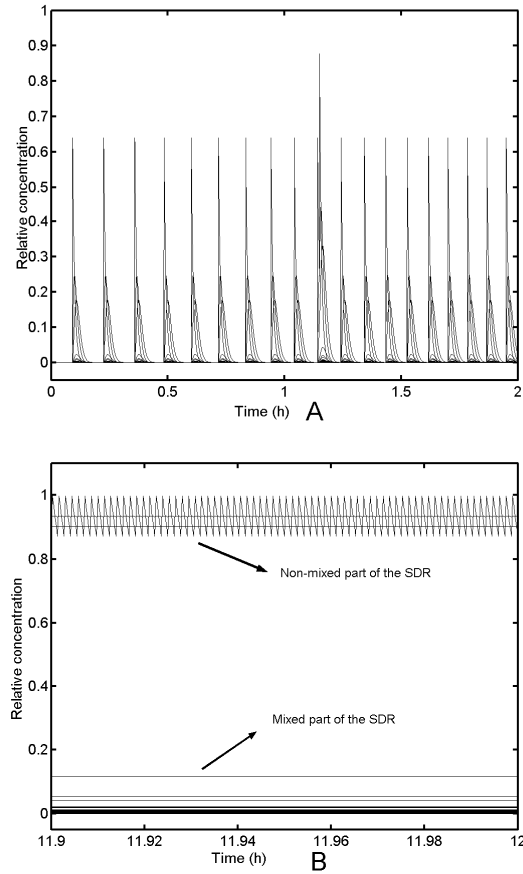
Figure 8 : Markov chain simulation of tracer dispersion in SDR (Q_{recirc} = 39 l/h) according to the pulse profile of the feed pump employed during fed-batch test. The system is assumed to be non-reacting (no substrate consumption by the microorganisms). A : concentration gradient in the case of an exponential feeding strategy with a time between two pulses always superior to 30 seconds. B : concentration gradient in the case of a constant feeding strategy with a time interval between two pulses equal to 5 seconds (corresponding in practice to the end of the fed-batch culture). For the sake of simplicity, results are expressed in relative concentration in non-reacting system (no consumption of the tracer), each pulse having a unitary intensity.

On the basis of the intermittent behaviour of the feed pump, two limiting cases can be highlighted : the first one when the mixing time of the SDR is inferior to the time interval between two pulses (T) ; the second one arising when the mixing time of the SDR is superior to T. Gradient appearance and persistence arises when the

154

characteristic mixing time of the bioreactor is larger than T. This phenomenom is showed at figure 10, in which the impact of the increase of the pulse frequency on the concentration gradient is clearly marked. This impact is traduced by an increasing difference of concentration between the mixed and the non-mixed section of the SDR. The gradient is expanded to the mixed section of the SDR when the mixing time related to this section of the reactor is larger than the characteristic time of the feed pump (figure 8B). These observations highlights the fact that our model is in accordance with the conclusions of a classical regime analysis of the process [16]. From these observations, we can conclude than when performing a SDR experiment at a lower recirculation flow rate, the concentration gradient appears earlier and tends to be more pronounced. This is a possible explanation for the Y_{xs} drop noted between the two SDR experiments presented in this study (figure 3).

A second explanation, that has been related in the literature [17], involves the impact of the pulse addition of glucose on the metabolic oscillations inside microbial cells. It is clear that, from the above mentioned observations, a yeast cell in displacement in the SDR is submitted to a fluctuating extracellular environment, in terms of glucose concentrations. Several reports show that these environmental fluctuations induce a metabolic response. [17] have shown that, in the case of the baker's yeast, glucose pulses induce an oscillatory response at the level of the intracellular dynamics. Yeast cells submitted at a given frequency to this stimulus show to be able to withstand these perturbations. In other words, yeast cells are trained to be exposed further to environmental changes. This training mechanism could also explain the scale-down effect recorded during our SDR experiments.

At the level of the bioreactor, the exposure of microbial cells to a pulsing environment is difficult to represent because of the strong probabilistic nature of the system. However, this can be achieved by using our stochastic model methodology. The gradient field calculated by the Markov chain model is superimposed to the circulation of yeasts cells in the bioreactor in order to obtain the concentration profiles experienced by microorganisms. To achieve this, we'll focus our attention on the constant flow rate period of the fed-batch culture, where glucose fluctuations are the most intensive. On the other hand, the size of the microbial population to be

155

considered in the stochastic circulation model must be determined in order to obtain a representative simulation. Several approaches can be considered :

- Firstly, simply by considering a single microbial cell. This approach was adopted in a previous work in the case of real large-scale bioreactors [18]. An example of a simulation performed in the case of a SDR is shown at figure 9. It can be seen that microbial cell is submitted to rapid concentration fluctuations, especially when entering in the non-mixed part of the SDR. It can be deduced that the scale-down effect is due to the passage of microorganisms trough the non-mixed part of the SDR because of the larger concentration fluctuations encountered in this part of the reactor compared to those encountered at the level of the mixed part.
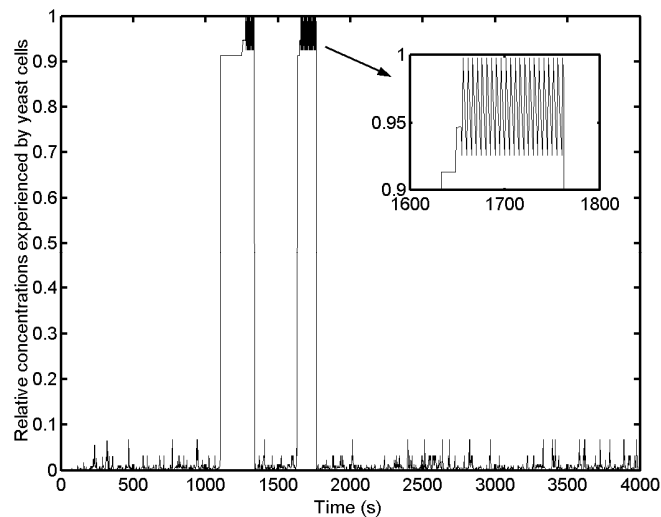

Figure 9 : simulation of the relative concentration profile experienced by a yeast cell in displacement inside the SDR.

- Secondly, by considering a microbial population of n microorganisms. In this case, concentration profile is calculated as the mean of all the glucose concentration profiles experienced by the microbial population on the time interval considered.

156

The use of the second strategy would allow us to follow the history of a microbial population inside the bioreactor. The difficulty about the simulation results analysis come from the fact that each microbial cell involved in the model (3500 cells in this case) has its own history. In order to overcome the complexity of this analysis, frequency distributions of the mean relative concentration experienced by microorganisms have to be considered. These distributions have been calculated from the superimposition of the relative gradient field simulation with the circulation simulation of a population of 3500 microbial cells. Four cases have been considered : scale-down tests performed with a recirculation flow rate of 18 or 39 l/h, by considering the microbial cells starting either from the mixed or the non-mixed part of the reactor (figure 10).
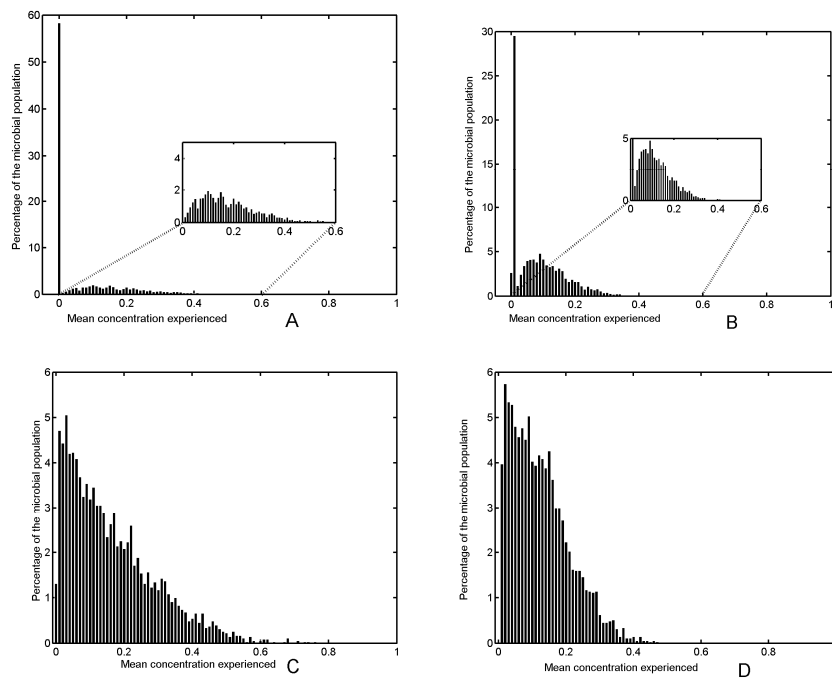
Figure 10 : frequency distributions of the mean relative concentration experienced by microorganisms circulating inside SDR. A : Q_{recirc} = 18 l/h, 3500 microbial cells starting from the mixed part of the reactor ; B : Q_{recirc} = 39 l/h, 3500 microbial cells starting from the mixed part of the reactor ; C : Q_{recirc} = 18 l/h, 3500 microbial cells starting from the non-mixed part of the reactor ; D : Q_{recirc} = 39 l/h, 3500 microbial cells starting from the non-mixed part of the reactor

Figure 10 shows that there are significant differences according to the initial location of the microbial population in the SDR. When the microorganisms are initially located at the level of the mixed part of the reactor, there is a major fraction of the microbial population experienced very low substrate concentration : about 60% of the microbial population experiencing a mean relative concentration centred on 0 for a Q_{recirc} of 18 l/h and about 30% when the Q_{recirc} reach 39 l/h. This is a logical result since when the recirculation flow rate Q_{recirc} is doubled, the microbial fraction that experiences small concentration variation centred on 0 drop from 60 to 30%. Indeed, in the stochastic model, the probability for a microorganism to enter in the non-mixed part of the SDR, where concentration fluctuations are very high, is multiplied by two. However, this phenomena is at the opposite of the fermentation tests results in SDR. Indeed, for these fermentation tests, the biomass yield increase when the recirculation flow rate increase. The frequency distributions 10A and 10B must not be analysed at the level of the fraction of the microbial population subjected to very low relative concentration centred on 0, but at the level of their dispersion. Indeed, we can see that the frequency distribution is more dispersed in the case 10A than in the case 10B, suggesting that the increase of the recirculation flow rate diminish the intensity of the relative concentration experienced by the microorganisms. This fact is in good accordance with the fermentation tests performed in the respective SDR. The same dispersion phenomena can be viewed more easily at the level of figures 10C and 10D. Indeed, it can be seen that when passing from a recirculation flow rate of 18 l/h to 39 l/h, there is a shift of the distribution to the left, which means that the microbial cells are exposed to less pronounced environment fluctuations. A percentage of about 7% of the microbial population is exposed to a relative mean concentration higher than 0.4 when operating with a recirculation flow rate of 18 l/h, whereas less than 0.8% are exposed to such elevated concentration when the recirculation flow rate is increased to 39 l/h. These results permit to explain the scale-down effect induced by increasing the recirculation flow rate between the two parts of the SDR. There is a strong probabilistic aspect involved in this effect which can be represented by stochastic models. Intuitively, by increasing the simulation time, the entire microbial population would have the time to visit the entire volume of the SDR, and thus to be exposed to the high fluctuating environment of the non-

158

mixed part of the reactor. The resulting simulations will be thus expressed by identical frequency distribution whatever the initial position of the microbial population in the reactor. These considerations will be taken into account in a further study.

Conclusion

Our contribution has consisted in the elaboration a stochastic structured model permitting to describe both the fluid mixing and the microbial cell circulation in stirred bioreactors and to use it in order to provide valuable insight about what happens to the microbial cells during a fed-batch process performed in a SDR. The following conclusions can be made :

- This study highlights the impact of the probabilistic aspect of both fluid mixing and particle circulation in stirred vessel. The probabilistic nature of such phenomena has a direct impact in the case of a bioprocess in the sense that it will not only affects the environment heterogeneity in a bioreactor, but also the way in which microbial cells are exposed to these environment fluctuations. The bioreactor mixing and circulation probabilistic components can be efficiently studied by stochastic models.

- The analysis puts in evidence a strong relation existing between microorganisms circulation and fluid mixing. This property has been tested by carrying out inert tracer and stained cells retention time experiments. The comparison of the two kinds of tracer experiment has shown strong similarities, which implies that yeast cells are submitted to fluid dynamics constraints similar to those of the classical inert tracer. Because of the above mentioned observations, the transition matrix of the stochastic model exposed in this study can be used both for the microbial cell circulation and the fluid mixing simulations.

The use of the stochastic model has permitted to describe the concentration fluctuations experienced by the microbial cells during the culture. From these observations, some assumptions can be advanced to explain the scale-down effect :

- The increase of the recirculation flow rate between the mixed and the non-mixed parts of the SDR can enhance the frequency at which yeast cells are exposed to glucose fluctuations. This phenomena can induce the adaptation phenomena reported by [17]. A similar adaptation phenomena has also been noted in the case of *E. coli* [19] which is also a gradient sensitive microorganism [6].

- The superposition of the circulation of 3500 microbial cells on the gradient field simulations has shown that the cells are submitted to higher mean relative concentrations in the case of a lower recirculation flow rate (results are presented in the form of frequency histograms at figure 10). These simulation results are in accordance with the real scale-down fermentation tests.

Nevertheless, several issues are required before being able to fully explain the yeast cells metabolism - fluid mixing interaction mechanisms. Some other components of the problematic have been described in the literature and the following considerations involve some of them :

- Our work is limited to the study of bioprocess in scale-down reactors which are easy to modelise from a fluid dynamic point of view. In large-scale bioreactors, circulation is more difficult to represent and experimental data are hard to be found. Nevertheless, some circulation time distributions are available in the literature and can be helpful for the stochastic modelisation of microbial cells circulation in large-scale bioreactors. The second difficulty come from the determination of the effective volume of the feed zone. This determination is easy in the case of a SDR because of the physical retention of the feed in the PFR section. In the case of a large-scale bioreactor, the volume of the feed zone depends on the fluid mechanics and of the feeding strategy. Some data are available in the literature, but are limited [5].

- In the perspective of a microorganism-fluid mixing interaction modelisation, the inclusion of a sufficiently realistic microbial kinetic model is the key factor. To go further, it can be said that

the importance of this model exceeds the hydrodynamic part of the problem. This fact has been highlighted by several authors and some observations made in this study show the same way. [20] have coupled a deterministic compartment model with a Monod kinetic to determine concentration gradient appearance in a stirred vessel. The same methodology was adopted by [21] but involving a structured metabolic model. This last approach has led to more reliable results about the impact of the bioreactor heterogeneity on bioprocesses. In the case of *Saccharomyces cerevisiae*, it is known that several glucose transporters are involved in function of the extracellular glucose concentrations [17]. This phenomena induces some variations concerning the affinity constant of the microorganism for the substrate which can't be taken into account by a simple Monod kinetic model.

-   The characterisation of the glucose gradient concentration and its perception by the microorganism is an efficient structured attempt to study the scale-down effect on microbial growth. But there are many other factors which also are playing a role in this effect. Among these, shear stress and dissolved oxygen gradient influence strongly the microbial process. It is possible to characterize these respective components by the use of the stochastic models presented in this study (e.g., shear stress can be characterised by calculating the passage frequency of microorganisms at the level of the compartments close to the impeller, and the dissolved oxygen gradient field can be calculated by adding to our model the computational method proposed by [22]).

Acknowledgement

_____

References

1. Mann R., Pillai S.K., El-Hamouz A.M., Ying P., Togatorop A., Edwards R.B., *Computational fluid mixing for stirred vessels : progress from seeing to believing.* Chemical engineering journal, 1995, **59**, 39-50.
2. Amanullah A., MacFarlane C.M., Emery A.N., Nienow A.W., *Scale-down model to simulate spatial pH variations in large-scale bioreactors.* Biotechnology and bioengineering, 2001. **73**(5), 390-399.
3. Enfors S.O., Jahic M., Rozkov A., Xu B., Hecker M., Jürgen B., Krüger E., Schweder T., Hamer G., O'Beirne D., Noisommit-Rizzi N., Reuss M., Boone L., Hewitt C., McFarlane C., Nienow A., Kovacs T., Trägardh C., Fuchs L., Revstedt J., Friberg P.C., Hjertager B., Blomsten G., Skogman H., Hjort S., Hoeks F., Lin H.Y., Neubauer P., van der Lans R., Luyben K., Vrabel P., Manelius A., *Physiological responses to mixing in large scale bioreactors.* Journal of biotechnology, 2001. **85**, 175-185.
4. Fowler J.D., Dunlop E.H., *Effects of reactant heterogeneity and mixing on catabolite repression in cultures of Saccharomyces cerevisiae.* Biotechnology and bioengineering, 1989. **33**, 1039-1046.
5. Namdev P.K., Thompson B.G., Gray M.R., *Effect of feed zone in fed-batch fermentations of Saccharomyces cerevisiae.* Biotechnology and bioengineering, 1992. **40**(2), 235-246.
6. Neubauer P., Häggström L., Enfors S.O., *Influence of substrate oscillations on acetate formation and growth yield in Escherichia coli glucose limited fed-batch cultivations.* Biotechnology and bioengineering, 1995. **47**, 139-146.
7. Onyeaka H., Nienow A.W., Hewitt C.J.,, *Further studies related to the scale-up of high-cell density Escherichia coli fed-batch fermentations : the additional effect of a changing microenvironment when using aqueous ammonia to control pH.* Biotechnology and bioengineering, 2003. **84**(4), 474-484.
8. Delvigne F., Destain J., Thonart P., *Structured mixing model for stirred bioreactor : an extension to the stochastic approach.* Chemical engineering journal, 2005, **in press**.
9. Berthiaux H., *Analysis of grinding processes by Markov chains.* Chemical engineering science, 2000. **55**, 4117-4127.
10. Mayr B., Horvat P., Nagy E., Moser A., *Mixing models applied to industrial batch reactor.* Bioprocess engineering, 1993. **9**, 1-12.
11. Mayr B., Nagy E., Horvat P., Moser A., *Scale-up on basis of structured mixing models : a new concept.* Biotechnology and bioengineering, 1994. **43**, 195-206.
12. Vasconcelos J.M.T., Alves S.S., Barata J. M., *Mixing in gas-liquid contactors agitated by multiple turbines.* Chemical engineering science, 1995. **50**(14), 2343-2354.
13. Machon V., Jahic M., *Liquid homogenization in aerated multi-impeller stirred vessel.* Chem. eng. technol., 2000. **23**, 869-876.

14. Mann R., Mavros P.P., Middleton J.C.,, *A structured stochastic flow model for interpreting flow-follower data from a stirred vessel.* Trans IChemE, 1981. **59**, 271-278.

15. Zahradnik J., Mann R., Fialova M., Vlaev D., Vlaev S.D., Lossev V., Seichter P., *A network-of-zones analysis of mixing and mass transfer in three industrial bioreactors.* Chemical engineering science, 2001. **56**, 485-492.

16. Sweere A.P.J., Luyben K.C.A.M., Kossen N.W.F., *Regime analysis and scale-down : tools to investigate the performance of bioreactors.* Enzyme and microbial technology, 1987. **9**, 386-398.

17. Reijenga K.A., Bakker B.M., van der Weijden C.C., Westerhoff H.V., *Training of yeast cell dynamics.* FEBS journal, 2005. **272**, 1616-1624.

18. Vlaev D., Mann R., Lossev V., Vlaev S.D., Zahradnik J., Seichter P., *Macro-mixing and Streptomyces fradiae : modelling oxygen and nutrient segregation in an industrial bioreactor.* Trans IChemE, 2000. **78**, 354-362.

19. Ferenci T., *Growth of bacterial cultures' 50 years on : towards and uncertainty principle instead of constants in bacterial growth kinetics.* Res. microbiol., 1999. **150**, 431-438.

20. Delvigne F., El Mejdoub T., Destain J., Delroisse J.M., Vandenbol M., Haubruge E., Thonart P., *Estimation of bioreactor efficiency through structured hydrodynamic modelling : case study of a Pichia pastoris fed-batch process.* Applied biochemistry and biotechnology, 2005. **121-124**, 653-671.

21. Vrabel P., van der Lans R.G.J.M., van der Schot F.N., Luyben K.Ch.A.M., Xu B., Enfors S.O., *CMA : integration of fluid dynamics and microbial kinetics in modelling of large-scale fermentations.* Chemical engineering journal, 2001. **84**, 463-474.

22. Mann R., Vlaev D., Lossev V., Vlaev S.D., Zahradnik J., Seichter P., *A network-of-zones analysis of the fundamentals of gas-liquid mixing in an industrial stirred bioreactor.* Récents progrès en génie des procédés, 1997. **11**(52), 223-230.

CHAPITRE 7
Etude de l'impact du bio-réacteur sur une population microbienne de taille limitée

Abstract

A methodology based on stochastic modelling is presented to describe the influence of the bioreactor heterogeneity on the microorganisms growth and physiology. The stochastic model is composed of two sub-models : a microorganism circulation sub-model and a fluid mixing sub-model used for the characterisation of the concentration gradient. The first one is expressed by a classical stochastic model (with random number generation), whereas the second one is expressed by a stochastic Markov chain. Their superimposition permits to obtain the concentration profiles experienced by the microorganisms in the bioreactor. The simulation results are expressed in the form of frequency distributions. At first, the study has been focalised on the design of scale-down reactors (SDR). This kind of reactor has been reported to be an efficient tool to study at a small-scale the hydrodynamic behaviour encountered in large-scale reactor [1]. Several parameters affecting the shape of the frequency distributions have been tested. Among these, it appears that the perturbation frequency, the exposure time and the design of the non-mixed part of the SDR have a significant influence on the shape of the distributions. The respective influence of all these parameters must be taken into account in order to obtain representative results. As a general trend, the increase of the recirculation flow rate between the mixed and the non-mixed part of the SDR induce a shift of the frequency distribution for the lower relative concentrations, which suggests an attenuation of the scale-down effect. This has been validated by using the SDR in the case of the cultivation of *Saccharomyces cerevisiae*. However, the influence of the non-mixed part of the SDR is not quite well understood if only taking account of the frequency distribution analysis, and supplementary experiments are required to elucidate the underlying mechanism.

The aspect of the frequency distributions suggests that both the design and the operating conditions of a scale-down reactor need to be adjusted in order to match the behaviour of a given large-scale reactor. Examples of frequency distributions obtained in the case of large-scale reactors are given.

_____

Introduction

Structured compartment models have been widely used to describe the hydrodynamics of stirred bioreactors [2-5]. They are generally mathematically expressed by a set of ordinary differential equations. Recently, stochastic models, already well described for particulate mixing applications [6, 7], have been developed in the case of fluid mixing in stirred bioreactors [8]. This kind of model has shown good results if compared with the classical deterministic compartment models. The main advantage lies on the fact that the stochastic models can be used both for fluid mixing and particle circulation simulation. The superimposition of the two mechanisms (i.e. fluid mixing and particle circulation) permits to obtain the concentration profiles experienced by microorganisms inside bioreactors. These profiles can be used to elucidate some fluid mechanics impacts on the microbial physiology. Indeed, the reactor heterogeneities do have a significant influence on the microorganisms physiology. This physiological change depends on the kind of microorganism considered, for example :

- In the case of *Escherichia coli*, spatial heterogeneities of glucose induce an overflow metabolism which leads to the formation of acetate [1, 9]. On the other hand, the passage of *E. coli* in oxygen depleted zones induces a mixed acid fermentation metabolism [9].

- In the case of *Saccharomyces cerevisiae*, spatial heterogeneities of glucose also induces an overflow metabolism traduced by the formation of ethanol [10-12].

When scaling-up a bioreactor, the homogenisation efficiency drops, which leads to the appearance of concentration gradient. In addition, the way in which microorganisms are exposed to this gradient evolves, on account of to the multiplication of the possible circulation paths while increasing the reactor volume. This phenomena can be represented by an increase of the variance of the corresponding circulation time distribution. In this way, the use of a model allowing the description of the extracellular substrate concentrations experienced by the microorganisms seems to be an efficient tool to elucidate the bioreactor effect on its biotic phase (constituted by the whole microbial population in the reactor).

Firstly, stochastic models as presented in this study will be used to characterise the mixing and circulation behaviours in scale-down reactors (SDR). This kind of reactor generally comprises a mixed part connected to a non-mixed part [1]. The recirculation of the liquid through the non-mixed loop of the reactor leads to the formation of concentration gradient. SDR is an efficient tool to study at small scale the fluid dynamic characteristics encountered in large-scale reactors. Secondly, the stochastic modelling methodology will be used in the case of large-scale reactors.

Material and methods

1. Scale-down reactor configuration

The scale-down reactor (SDR) comprises a mixed part and a non-mixed one. The mixed part consists of a 20l stirred bioreactor (D = 0.22 m ; working volume : 10 litters) equipped with a rushton disk turbine with 6 blades (d = 0.1 m).

The design of the non-mixed part can be adapted. In this study, two configurations have been tested :

- Configuration A (SDR type A) : the non-mixed part consists of a glass bulb (internal diameter : 85 mm ; length : 0.25 m ; connexions of 8 mm diameter at each end).
- Configuration B (SDR type B) : the non-mixed part consists of a silicone tubing (internal diameter : 8mm ; length : 7.5m).

The liquid flow between the two parts of the SDR is ensured by a peristaltic pump (Watson Marlow 323 SD).

2. Large-scale bioreactors configurations

Two kinds of large-scale reactors have been investigated :

- A 2 m³ stirred bioreactor (D : 1 m ; working volume : 1800 l ; three agitation stages ; rushton disk turbine with 4 blades ; d : 0.45 m)
- A 9m³ bubble column bioreactor (D : 2 m ; working volume : 9000 l)

---

3. Inert tracer test

Mixing experiments have been performed both in scale-down reactor and in large-scale reactors by a tracer pulse injection method. The technique consists in measuring the conductivity (Hamilton Conducell probe ; Daqstation Yokogawa recorder) evolution after the injection of a NaCl solution (the tracer solution volume corresponds to 1% of the working volume of the reactor). In the case of SDR, injection has been performed at the level of the inlet of the non-mixed part and conductivity has been measured in the mixed part. In the case of the large-scale reactors, injection has been performed at the top of the vessel, and conductivity has been measured in the lower part of the vessel.

4. Biological tracer tests

Biological tracer experiments are performed in SDR type A by injecting a pulse of a solution containing stained cells in the bioreactor. The cells are stained with a fluorescent dye (Vybrant CFDA SE cell tracer kit V-12883) which permits to facilitate the detection by epifluorescent microscopy. The staining protocol consists in performing a preculture in a 500 ml Erlenmeyer flask, in order to obtain the required amount of biomass for further staining. An aliquot of the preculture is centrifuged (5 minutes at 4000 rpm). The precipitate is washed with 10 ml of sterile PBS buffer (NaCl 8 g/l ; KCl 0.2 g/l ; K_2HPO_4 1.44 g/l ; KH_2PO_4 0.24 g/l ; adjusted to pH 7.5 with K_2HPO_4 and KH_2PO_4). Three successive centrifugation/washing sequences are performed. After this step, microbial cells are stained by adding 1mM of CFDA SE (carboxyfluorescein diacetate succinimidyl ester) followed by an incubation for 3 hours at 30°C. After the incubation, the solution is centrifuged and the precipitate is washed with PBS buffer. When performing a biological tracer test, 5 ml of the stained cells suspension (2.10^8 cells/ml) are poured at the level of the non-mixed part of the SDR, and samplings are taken in of the mixed part. Cells are directly counted by fluorescent microscopy. For each sample, three aliquots of 10 µl each are placed on a microscopic plate for further counting. For each aliquot, three

counts are performed, for three widths of the microscopic plate. Mean and standard deviation are calculated for each sample.

5.   Scale-down fermentation experiments

Saccharomyces cerevisiae (MUCL 43341) strain is stored at –80°C. Cultures are performed in a scale-down reactor including a 20l stirred vessel (D = 0.22 m) (Biolaffite-France) equipped with a RDT6 rushton turbine (d = 0.1 m) connected to a non-mixed part. The two non-mixed part design investigated in this study have been previously described in this material and methods section. Components of the culture media are : glucose 5 g/l ; yeast extract 10 g/l ; casein pepton 10 g/l. During the process, the broth is continuously recirculated between the stirred vessel (mixed part) and the non-mixed part by a peristaltic pump (Watson Marlow 323S/D). The regulation of the culture parameters (pH, temperature,…) is ensured by a direct control system (ABB). Dissolved oxygen is maintained above 30% of saturation level by modulating the stirrer speed. Glucose addition is performed in the inlet of the non-mixed part and is controlled by an exponential feeding algorithm according to the equation $F = F_0 . \exp(\mu.t)$. With F being the feed flow rate (m³/s), F_0 the initial feed flow rate (m³/s), μ the microorganism growth rate (h^{-1}) and t the culture time (h). The two parameters $\mu = 0.005$ min^{-1} and $F_0 = 0.086$ ml/min were calculated from growth data of *Saccharomyces cerevisiae* in a batch bioreactor.

6.   Stochastic modelling principles and distribution frequency calculation

The modelling strategy exposed is entirely based on stochastic processes. In fact, two sub-models are required : a first sub-model for the microbial cells circulation inside the bioreactor, and a second one for the simulation of the gradient concentration. The advantage of the stochastic formulation lies in the fact that the two sub-models have the same structure based on the compartmentalization of the bioreactor. The principle is based on the tank-in-series concept and each compartment, representing a given zone in the bioreactor, is assumed to be perfectly mixed. In stochastic modelling, the displacements from one compartment to another

are governed by probabilities. Figure 1 presents the model structure used in the case of the SDR. The stirred vessel constituting the mixed part of the SDR has been modelled by eight vertical planes comprising each eight compartments. The compartments interconnections are in accordance with the radial flow developed by the rushton turbine used for the experiments.
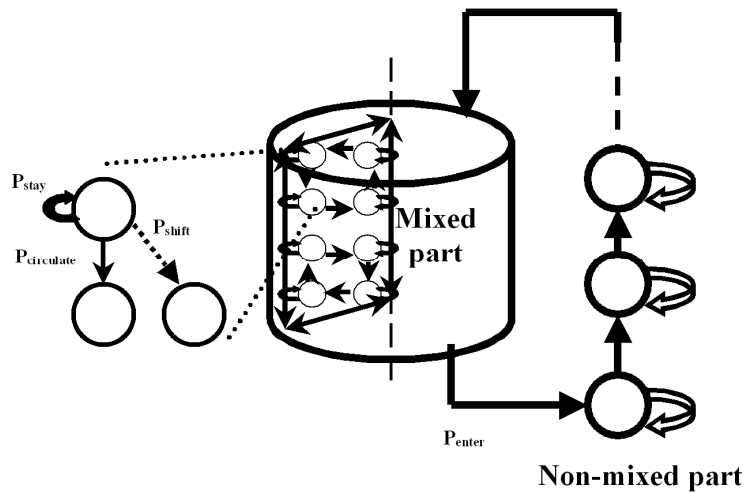

Figure 1 : structure of the compartment model used to run stochastic simulations. In the case of the SDR type A, the non-mixed part comprises 3 compartments (with the volume of each compartment being 0.33 l), whereas in the case of SDR type B, there are 15 compartments (the volume of each compartment being equal to 0.03 l).

The first sub-model describes the displacement of microorganisms inside the bioreactor. In this model, the displacement of a particle (e.g., a microbial cell or a tracer molecule) is calculated by comparison between a random number and the value of the transition probabilities. Four kinds of probabilities are to be considered to describe the displacement of particles in the mixed part of the SDR : the probability to stay in a given circulation flow loop, the probability to stay in the same compartment, the probability to shift to another plane, and the probability to switch from the main flow loop (this method has been proposed by [13]). The circulation probability can be estimated from dimensionless correlation with the circulation flow rate, and is written as :

169

$$Q_c = N_{qc}.N.d^3 \qquad (1)$$

N_{qc} being a dimensionless number having a constant value in the turbulent flow regime and N being the impeller rotational speed (s^{-1}),
and :

$$P_{circulation} = \frac{Q_c}{V_{compartment}} \cdot \Delta t \qquad (2)$$

Δt being the time interval between two transitions and $V_{compartment}$ the volume of a compartment in the model.

The switching probability express the level of turbulent mixing is written as :

$$P_{switch} = P_{tangential} = P_{stay} = \left(1 - P_{circulation}\right)/3 \qquad (3)$$

With P_{stay} being the probability to stay in the actual compartment ; $P_{tangential}$ being the probability to shift to another plane ; P_{switch} being the probability to shift from the main circulation flow loop.

In the case of a SDR, we also must express the probability for a particle to enter in the non-mixed part, which can be written as :

$$P_{enter} = \frac{Q_{recirc}}{V_{compartment}} \cdot \Delta t \qquad (4)$$

Q_{recirc} being the recirculation flow rate between the two parts of the SDR. The probabilities inside the non-mixed part are determined according to the recirculation flow rate and the respective compartment volume. All the transition probabilities to pass from a compartment to another are collected in a transition matrix for computational ease.

The second sub-model is also based on the same transition matrix as the one used for the previous sub-model, but the dispersion of tracer molecules is here described by a Markov process. The Markov chain stochastic model consists of an initial state vector S_0, which is multiplied with a transition matrix T to give a new state, S_1. This procedure can be written as:

For the first transition: $S_1 = T \cdot S_0$ \qquad (5)

The next stage involves the multiplication of the new state vector S_1 with the same transition matrix T until a steady-state is reached:

The second transition can be written as : $(S_2 = T \cdot S_1)$ or $(S_2 = T^2 \cdot S_0)$, (6)

And the ith transition: $(S_i = T \cdot S_{i-1})$ or $(S_i = T^i \cdot S_0)$ (7)

In our case, the state vector represents the tracer concentration values for all compartments. In order to obtain a valuable insight into the concentration field evolution during the bioprocess, the pulse effect of the feed pump must be taken into account. In our case, the pulse frequency is time varying because of the exponential increase of the feed flow rate during the culture. This pulse frequency can be included in the stochastic model by the use of the following matrix :

$$
S_{pulse} = \begin{bmatrix}
C_{pulse} & 0 & 0.. & 0 & C_{pulse} & 0... \\
0 & 0 & 0 & & & . \\
. & . & . & & & . \\
. & . & . & & & . \\
. & . & . & & & . \\
. & . & . & & & . \\
0 & 0 & 0.. & . & . & ..0
\end{bmatrix}
\tag{8}
$$

In the first row, the number of zero elements between two pulses (C_{pulse} being the concentration of the tracer pulse) depends of the feed pump activation frequency. The number of elements in a column corresponds to the number of compartments in the model. In the case of this matrix, the pulse is added at the level of the first state of the model (first element in a column). The number of elements in a row corresponds to the number of simulation steps performed.

The matrix S_{pulse} is used as follow to describe the evolution of the state vector :

$$S_i = T \cdot S_{i-1} + S_{pulse} \tag{9}$$

The strategy adopted here is to superimpose the gradient field obtained with the Markov chain model on the microorganisms circulation process obtained with the classical stochastic model, in order to obtain the concentration profile experienced by a population comprising a given number of microorganisms.

The superimposition results are expressed in terms of frequency distribution of the mean relative concentrations experienced by the microorganisms. The frequency

distributions calculated here are used to characterize the environment heterogeneity experienced by a microbial population of n cells on a time interval t for a given set of operating conditions and bioreactor configurations.

Results and discussion

    1.   Validation of the fluid mixing (Markov chain) and of the circulation (random number) models

Concentration gradient inside SDR is modelled by a stochastic Markov chain procedure. The non-mixed part of the SDR type A has simply been modelled by three compartments in series. This is justified by the strong dispersing effect that perturbs the establishment of a nearly plug-flow in this part of the reactor. Comparison between the experimental inert tracer test and the simulation results is shown at figure 2A.

In the case of the SDR type B, due to the strong plug-flow exhibited by the non-mixed part, the number of compartments in this section of the reactor has been increased. Different numbers of compartments have been used to modelize this part of the SDR. The best results are been obtained with 15 compartments in series. Comparison between the simulation and the experimental tracer test is shown at figure 2B. The results show that there is a good agreement between the Markov chain simulations and the experimental results.
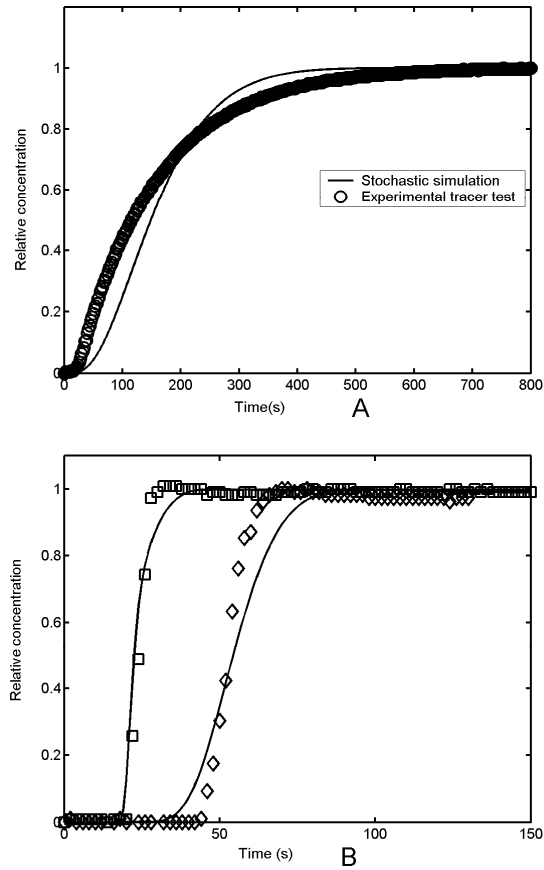
_____

Figure 2 : comparison of experimental tracer curve and stochastic (Markov chain) simulations results. A : SDR type A (Q_{recirc} = 18 l/h) ; B : SDR type B ($\square$: Q_{recirc} = 39 l/h ; $\lozenge$: Q_{recirc} = 18 l/h)

Figure 2 reveals fundamental differences between the hydrodynamics developed by the SDR type A and type B. This suggests that the scale-down effect will also be different. This important point will be analysed by using the stochastic modelling methodology presented in this study.

In order to follow the dispersion of a microbial population inside a bioreactor and thus to validate the circulation stochastic model, biological tracer tests are performed on the SDR type A, to validate the simulation results obtained by the stochastic non-Markov model (figure 3).
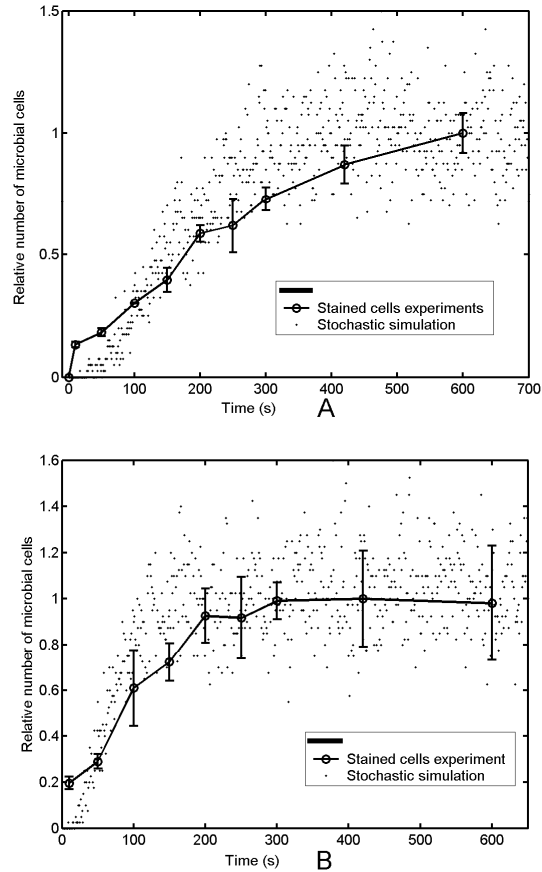
Figure 3 : comparison of biological tracer tests with stochastic non-Markov microbial cells dispersion simulations in SDR. A : SDR type A Q_{recirc} = 18 l/h ; B : SDR type A Q_{recirc} = 39 l/h

Figure 3 shows that both the experimental and simulation results show strong variations. Variations are more pronounced for the simulation results than for the experimental ones. Two explanations are possible. Firstly, the number of microbial cells used to perform simulations is not high enough and the stochasticity impact is thus very important. In order to decrease the fluctuations, the number of microbial cells used to run simulations must be increased, but in this case the computational time is increased too. Secondly, only three repetitions per sample have been performed during the biological tracer tests. Increasing the number of repetitions can increase the standard deviation on each sample.

174

However, the same general trend is observed for the experimental results as well as for the simulation ones. We can thus assume that the model is reliable enough to perform our microbial cells dispersion simulations.

2. Characterization of the concentration profiles experienced by the microbial cells

In the following sections, the stochastic bioreactor modelling methodology will be improved, mainly in taking account of the influence of several parameters on the final concentration frequency distributions.

### Effect of the glucose pulses frequency

During a fed-batch culture under exponential regulation of the substrate addition into the reactor, the pulse frequency of the feed pump is exponentially increasing until reaching a constant level at the end of the culture, to prevent glucose overflow. In the earlier stage of the exponential feed profile, glucose pulses are very spaced and the transient mixing behaviour of the system is sufficient to reach an acceptable degree of homogeneity during the time interval separating two successive pulses. In the final stage of the exponential feed profile, pulses are less and less spaced and a stable concentration gradient thus appears.

The frequency distribution is calculated from simulations performed in a scale-down system A, with a recirculation flow rate of 39 l/h, these simulations involving 3500 microbial cells starting from the non-mixed part (figure 4). These simulations show that the pulse profile of the feed pump greatly influences the frequency distribution of the mean concentration experienced by the microorganisms in the bioreactor :

- For a time interval between two pulses (T_{pulse}) smaller than the global mixing time of the system (figure 4A), the mean concentrations experienced by the microorganisms are very low. About 60% of the microbial population is exposed to a mean relative concentration centred on

a relative intensity of 0. This is due to the fact that, between two pulses, the concentration gradient at the level of the mixed part of the SDR disappears.

- For T_{pulse} approximatively equal to the mixing time of the scale-down reactor, figure 4B shows that a concentration gradient is maintained. This concentration gradient persistence leads to the increase of the mean concentration experienced by the microorganisms, as well as an increase of the variance of the frequency distribution.

- For T_{pulse} is inferior to the mixing time of the SDR (figure 4C), these observations are maintained, with anew increase both of the mean relative concentration experienced and of the variance of the frequency distribution.

- For T_{pulse} smaller than the mixing time related to the mixed part of the SDR (figure 4D), there is also establishment of a gradient in this part of the reactor.
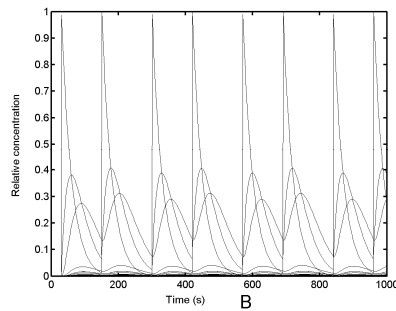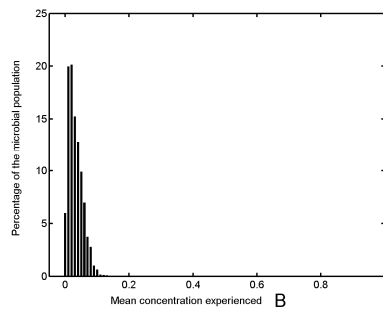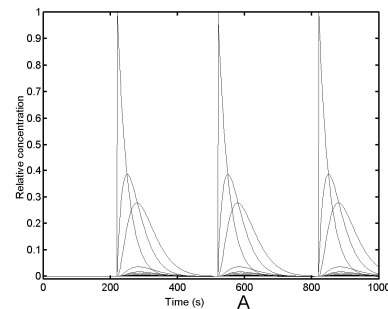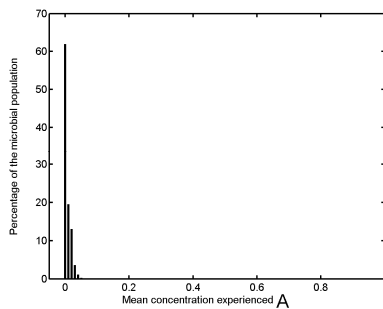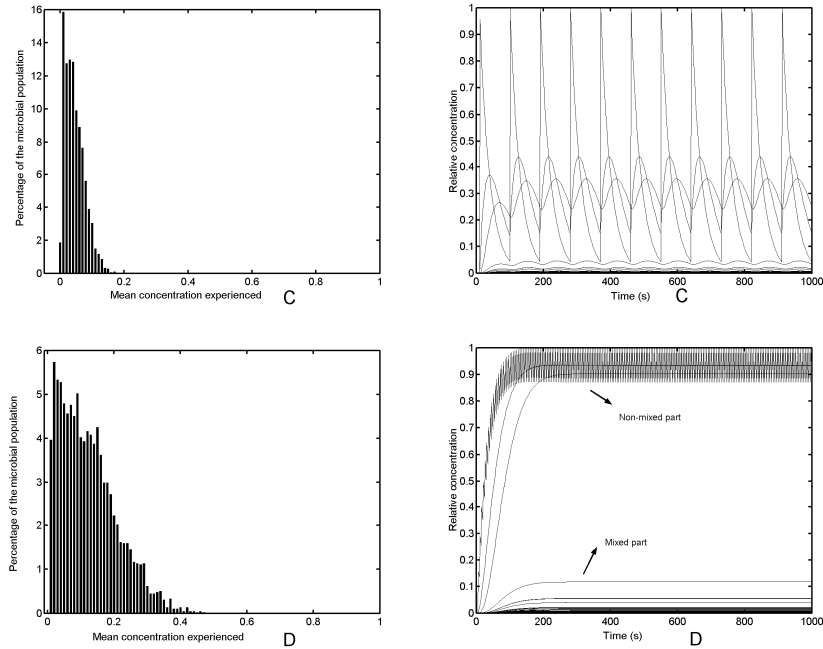
Figure 4 : evolution of the distribution frequency in function of the evolution of the feed pump frequency during a fed-batch culture in a SDR type A working at Q_{recirc} = 39l/h with the tracked microbial population starting from the non-mixed part of the reactor. A : moderate pulse frequency corresponding to the earlier stage of a fed-batch culture ; B : pulse frequency approaching the mixing time of the reactor ; C : pulse frequency inferior to the mixing time of the reactor ; D : constant pulse frequency of 5 s. For each distribution, the relative concentration profile is presented at the right side.

Figure 4 clearly shows the critical phase of the fed-batch culture, corresponding to the case 4D, displaying the most dispersed frequency distribution. For the next calculations, this stage of the fed-batch culture that will consequently be used.

Effect of the initial position of the tracked microbial population and of the exposure time

By considering the initial position of the microorganisms in the SDR, two kinds of simulation can be run. Firstly, a simulation involving an initial position located at the level of the mixed part of the SDR, and secondly a simulation involving an initial position located at the level of the non-mixed part of the SDR. Since the feed

addition is performed at the level of the non-mixed part inlet, differences can occur when comparing the respective frequency distributions. Indeed, if compared with figure 4D, which shows the frequency distribution obtained under the same operating conditions but with population starting from the non-mixed part, figure 5 shows that about 30% of the microbial population are submitted to very low extracellular concentration.
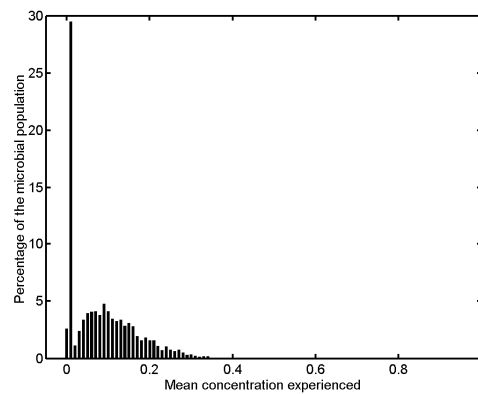
Figure 5 : distribution frequency obtained with a SDR type A (Q_{recirc} = 39 l/h) with a microbial population starting from the mixed part of the reactor

When performing a simulation with an initial position corresponding to the non-mixed part, each microorganism is exposed at least one time to high extracellular concentration fluctuations. This is not the case of those starting form the mixed part of the SDR, for which the shape of the frequency distribution is greatly influenced by the probability to enter in the non-mixed section. In this context, it is interesting to analyse the influence of the simulation time.
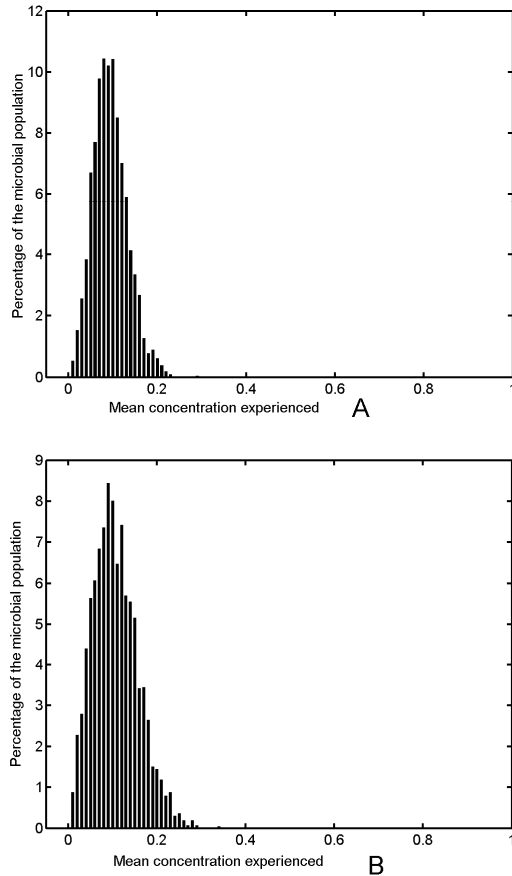
Figure 6 : frequency distributions obtained A : for a microbial population starting from the mixed part of the SDR and with an exposure time of 5000 s ; B : for a microbial population starting from the non-mixed part of the SDR and with an exposure time of 3000 s (for the two experiments : SDR type A ; 39 l/h ; 3500 microbial cells involved)

Figure 6 shows that when increasing the simulation time, the shapes of the frequency distributions are very similar for the two initial positions. This fact suggests that, for a sufficiently long simulation time, the initial position of the tracked microbial population can be assumed to have no influence on the shape of the frequency distribution.

Effect of the microbial population size

It is also important to determine if the amount of microbial cells considered in the simulations is sufficient to give a valuable insight into the behaviour of the whole population. Figure 7 shows the frequency distribution corresponding to population sizes of respectively 1000 and 10,000 microbial cells.
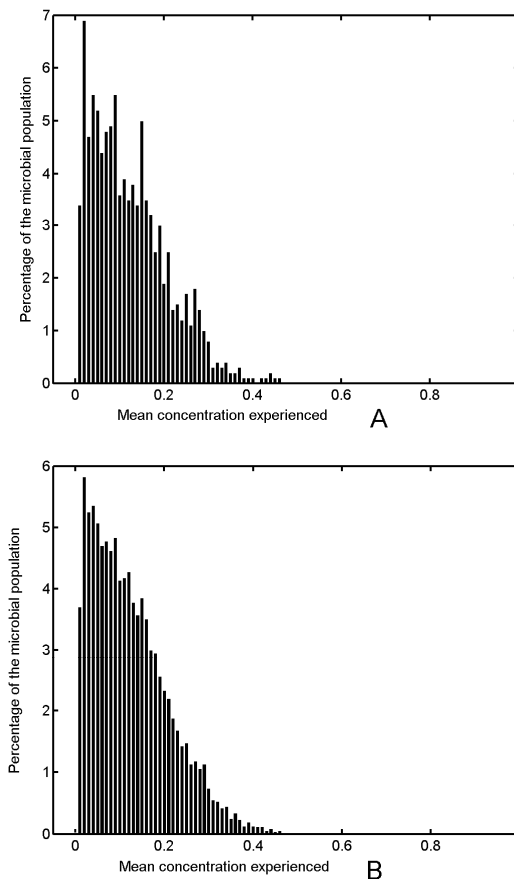
Figure 7 : distribution frequency obtained with a SDR type A (Q_{recirc} = 39 l/h), for an exposure time of 1000 seconds to a glucose pulse profile (T_{pulse} = 5 s). The microbial population comprises respectively 1000 cells (A) and 10,000 cells (B)

When considering a population of 1000 microbial cells (figure 7A), the corresponding distribution frequency displays slight differences compared with the one involving a larger amount of cells (figure 7B and figure 4D). However, in the

180

case of a population of 10,000 cells (figure 7B), no significant difference appears, compared with the results obtained for a limited population of 3500 microbial cells (figure 4D). Considering the large computational time required for microbial population comprising a large number of cells, only 3500 cells will be taken in account for the next simulations.

3. Application to the analysis of fermentation tests carried out in SDR

In order to improve the modelling methodology involved in this study, some fermentation tests were carried out in SDR, for different operating conditions and for different non-mixed part geometry. The results are presented at figure 8 and show a better biomass yield in the case of a classical stirred bioreactor than for the SDRs.
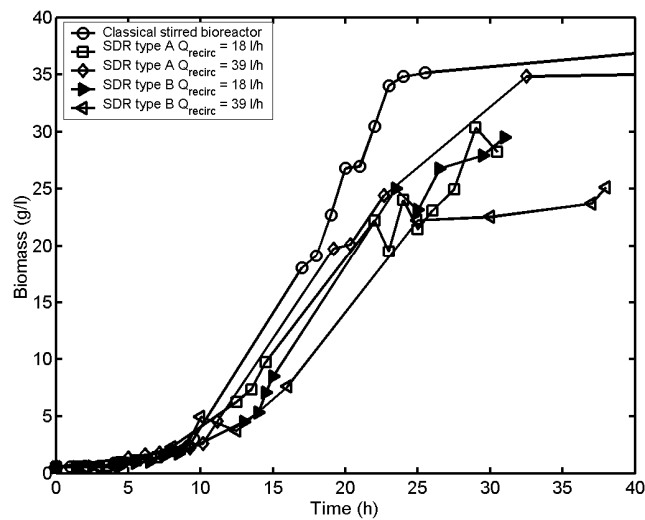
Figure 8 : microbial growth curves obtained from classical and scale-down stirred bioreactors

For each fermentation test, a stochastic simulation is performed in order to calculate the corresponding relative concentration frequency distribution. The simulations are performed by considering 3500 microorganisms, for a time interval of 5000 s. The

initial location of the microbial population in the model is the mixed part of the reactor, but a previous analysis has shown that this parameter has no impact if the exposure time is sufficiently long.
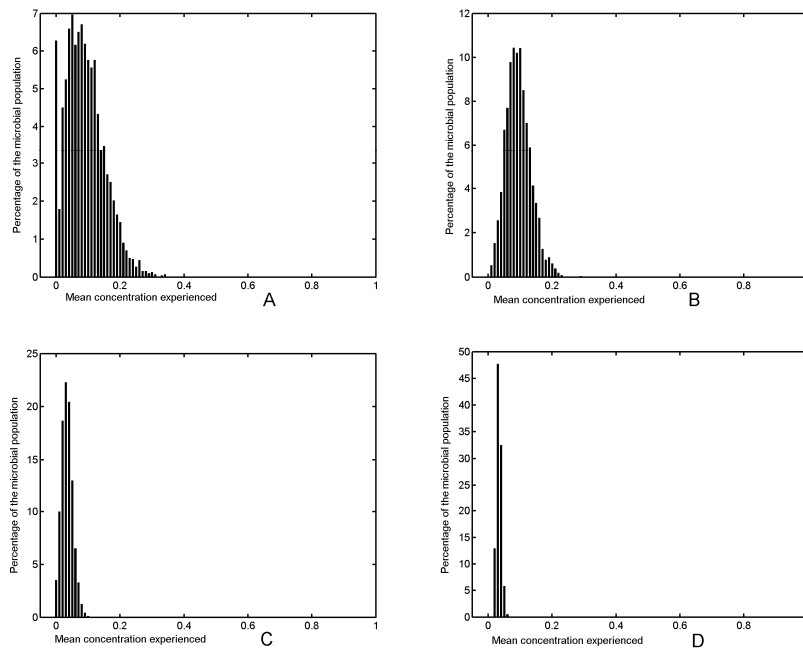
Figure 9 : frequency distributions obtained in the case of : A : a SDR type A Q_{recirc} = 18 l/h ; B : a SDR type A Q_{recirc} = 39 l/h ; C : a SDR type B Q_{recirc} = 18 l/h ; D : a SDR type B Q_{recirc} = 39 l/h. All the simulations involve a population of 3500 microorganisms for 5000 seconds

In the case of the SDR type A, figure 8 reveals a clear impact of the recirculation flow rate between the mixed and the non-mixed part of the reactor. Increasing the recirculation flow rate induces an increase of the biomass yield. The frequency distributions presented at figure 9 validate this observation. Indeed, it is to be noted that, when increasing the recirculation flow rate, there is a shift of the distribution to the left, which means that the microorganisms are exposed to less elevated extracellular substrate concentrations. This is also true in the case of the SDR type B (Figures 9C and 9B). Nevertheless, the biomass yield is very low for the two recirculation flow rates investigated in the case of the SDR type B (figure 8). On the other hand, analysis of the respective frequency distributions reveals better hydrodynamic conditions than for the SDR type A, but this fact is not confirmed by

fermentation experiments. Figure 10 shows that the exposure mechanisms in the SDR type A and for the type B are quite different. In the case of the SDR type B, microorganisms are subjected to large extracellular substrate relative concentration exceeding unity, whereas in the case of the SDR type A these fluctuations are less intensive but more extended on time. These differences can be attributed to the respective design of the non-mixed part of each SDR.

The impact of such fluctuations on the physiology and growth of *S. cerevisiae* is not actually well understood, but an hypothetical mechanism can be proposed. Indeed, a previous study as proven the capability of *S. cerevisiae* to adapt its glucose metabolism when submitted to repeated glucose pulses [14]. The authors highlight the fact that the time scale involved at the level of the microorganism exposure frequency to extracellular glucose fluctuations might have drastic implications for the metabolic performance of the cells and for their gene expression patterns. Figure 10 shows that two distinct exposure mechanisms are observed in function of the kind of SDR used. For the SDR type A, a microorganism entering in the non-mixed part is submitted to a fluctuating extracellular environment maintained for a relatively long time, whereas in the case of the SDR type B, these fluctuations are not maintained for a long time but are more frequent and more intensive. It can be assumed, on the basis of the previously described work [14], that microbial cells travelling in SDR type A are more adapted to a fluctuating extracellular environment than in the case of the SDR type B.

The connection of the stochastic hydrodynamic model presented in this study with a microbial kinetic model would be helpful to investigate the impact of the extracellular environment on the microorganisms physiology.
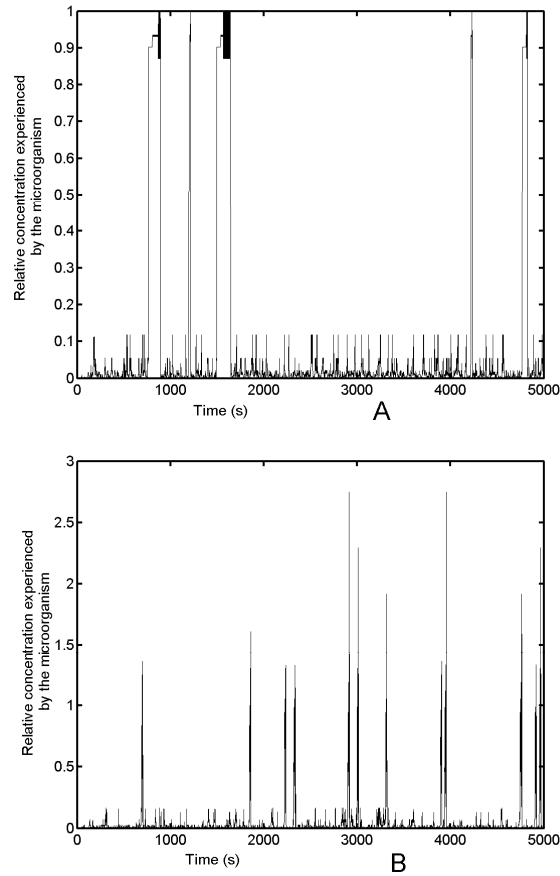
Figure 10 : sample path of the stochastic displacement of a microorganism in : A : a SDR type A ; B : a SDR type B ($Q_{recirc} = 39l/h$)

4. Are the SDR frequency distributions representative of those calculated for the large-scale reactors ?

All the previous frequency distributions are valid in the case of a SDR. But, are these distributions representative of a large-scale stirred bioreactor ? The following simulations have been performed on the basis of mixing time experiments in 2m³ three-staged bioreactor. This reactor has been modelled on the same basis than the SDR but without non-mixed part. The 2m³ reactor comprises three agitation stages and the compartment arrangement for one agitation stage corresponds to the one of

184

the mixed part of the SDR (figure 1). The volume of each compartment too has been modified to give a global volume of 1800 litters (which corresponds to the working volume of the 2m³ reactor). The transitions between the agitation stages have been assumed to correspond to switching probabilities (equation 3). In the case of a 9m³ bubble column (D = 2m), we assumed an axial liquid circulation flow pattern. Due to the height to diameter ration (1.5:1) of this apparatus, the compartments network of figure 1 has been modified in eight planes comprising each 12 compartments. In addition, the circulation transition probabilities orientation have been modified to be in accordance with an axial flow pattern. Liquid mixing in bubble columns is induced by the rise of bubbles through the liquid phase. The circulation flow rate can thus be calculated in function of the air flow rate. In this study, a correlation previously used by Zahradnik *et al.* [4] for a determinist compartments network has been selected :

$$Q_c = \left[\frac{D.u_g.(\rho_l - \rho_g)}{2.5\rho_l} \right]^{1/3} \qquad (10)$$

With D being the reactor diameter (m), u_g the gas superficial velocity (m/s), ρ_l the liquid density (kg/m³), ρ_g the gas density (kg/m³). In our case, the air is dispersed by a multi-pipe sparger (holes diameter : 3 mm) placed to cover the entire section of the reactor.

For all the large-scale simulations, the concentration gradient sub-model has been validated by inert tracer tests. In the case of the microorganisms circulation sub-model, the assumption has been made that fluid mixing – particle circulation equivalency applies too in the case of large-scale reactors (the realization of the biological tracer tests being hard to be realized on this kind of apparatus).
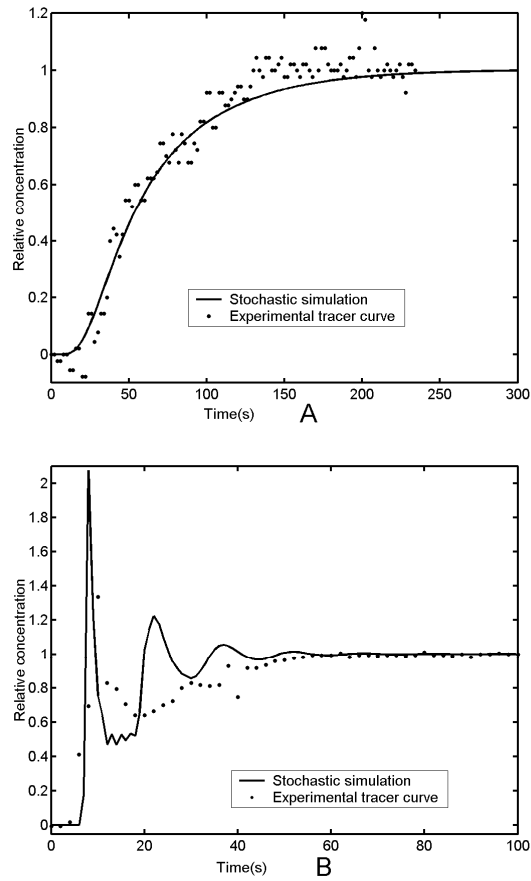
Figure 11 : simulated and experimental tracer curve for large-scale bioreactors (probe located at the bottom part of the reactor in each case). A : 2m³ three-staged (RDT6) stirred bioreactor operating at 38 rpm ; B : 9m³ bubble column operating at an air flow rate of 66 m³/h

_____
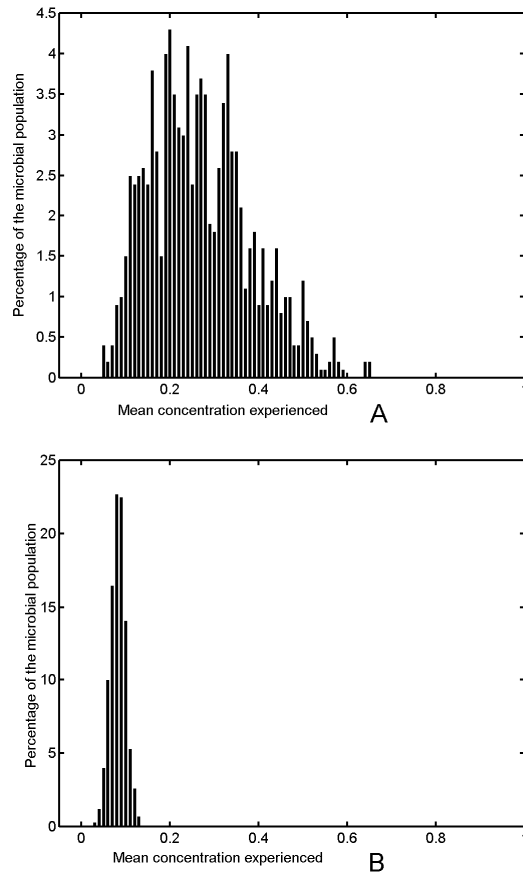
Figure 12 : distribution frequency obtained in the case of large-scale bioreactors. A : 2m³ three-staged (RDT6) stirred bioreactor operating at 38 rpm ; B : 9m³ bubble column operating at an air flow rate of 66 m³/h

On the basis of the homogenisation efficiency, figures 11B and 12B show that the bubble column reactor is better. But this comparison has not been performed at the same power input. Indeed, the stirred bioreactor operate at very low stirrer speed (38 rpm) which explains the poor mixing efficiency.

Figure 12 shows strong differences in terms of behavior between the 2m³ stirred bioreactor and the 9m³ bubble column hydrodynamic behaviour. Indeed, the frequency distribution shows a more dispersed behaviour in the case of the stirred bioreactor. This can be explained by the flow compartmentalisation induced by the three radial impellers delimiting three distinct agitation stages. It is interesting to

note that the frequency distribution presents some similarities with those of the SDR type A. In the case of the bubble column, the distribution is mainly centred on the mean. This is due to the strong circulation induced by the ascending bubbles in the whole volume of the reactor. On the opposite of the stirred bioreactor, it can be said that the behaviour of the bubble column can be approached by the SDR type B. These observations point out the fact that the non-mixed part design of SDR can be arranged in such fashion to reproduce efficiently the extracellular environment experienced by the microorganisms in displacement in a given large scale reactor.

In this section, simulation results relative to large-scale reactors have been presented. However, in large-scale reactors, the possible paths that can be taken by the circulating microorganisms are numerous. A more refined model structure (obtained by increasing the number of compartments and by considering concentric flow loops [15]) would lead to better results, in the sense that the circulation time distribution is affected by the number of compartments of the stochastic model.

Conclusions

A stochastic structured model has been elaborated in order to analyse both fluid mixing and microorganisms displacement dynamics in bioreactors. The superimposition of the concentration gradient on the microorganisms circulation paths has allowed to obtain the characteristic concentration profiles encountered in the bioreactor. The results are presented on the form of frequency distribution of the mean relative concentration experienced by microorganisms. It has been shown that these distributions reflect the mixing and circulation efficiency of a bioreactor, in connection with the microorganism exposure to gradient stress.

Several parameters being able to have an impact on the distributions have been tested. It has to be noted that the pulse frequency of the feed pump in a fed-batch context, the exposure time and the initial location of the microorganisms in the reactor have a significant influence on the shape of the distributions. For a sufficient exposure time (5000 s), simulations have shown that the initial location of the tracked population has no impact on the results. The design of the non-mixed part of the SDR too has a great impact on the frequency. Indeed, the frequency distributions

analysis provides valuable insights into the biomass yield differences obtained if increasing or decreasing the recirculation flow rate in the case of the fermentation tests performed in SDR, but cannot provides any explanation about the differences observed between the SDR type A and the SDR type B. This suggests that two distinct mechanisms for the microorganisms exposure to gradient stress have to be considered, the hydrodynamics generated by the SDR type A allowing the adaptation of microbial cells to a fluctuating extracellular environment.

The analysis of the distributions reveals that several microbial sub-populations can be delimited, differing by the extracellular substrate concentrations experienced. In the perspective to elucidate the stress mechanisms induced by the bioreactor hydrodynamic performances, it should be interesting to delimitate clearly these different sub-populations, by considering for example transition values of mean relative concentration experienced. This is not an easy task since each microbial strain has its own sensibility to concentration gradient. To be able to study these transitions between sub-populations, the elaboration of a microbial growth model taking into account the respective flow history of each cell, can be an efficient method. In this context, the stochastic methodology presented in this study could constitute the first step in the elaboration of a reliable microbial kinetic model. Nevertheless, there is a lack about the size of the observed microbial population. In our simulations, this size was not exceeding 10,000 microbial cells, whereas about 10^8-10^9 microbial cells per ml of broth have in fact to be considered. This fact could disturb the representativeness of the frequency distributions, but considering such a large microbial population is not quite possible due to the excessive computational time this would take.

In another perspective, other sources of heterogeneities can be studied by the methodology presented in this paper. For example, the oxygen gradient impact on the microbial population growth can be studied by this way [16].

Nomenclature

d : impeller diameter (m)

D : vessel diameter (m)

N : stirred speed (s^{-1})

N_{qc} : circulation flow number (dimensionless)

P : probability to achieve a given displacement in the stochastic model

Q_c : circulation flow rate (m³/s)

S : state vector of a Markov chain stochastic model

S_0 : initial state vector

S_{pulse} : matrix expressing the fed-batch pump pulses frequency

SDR : scale-down reactor

T : transition matrix of the stochastic model

u_g : gas superficial velocity (m/s)

ρ_g : density of the gas phase (kg/m³)

ρ_l : density of the liquid phase (kg/m³)

Acknowledgements

References

1.   Neubauer P., Horvat L., Enfors S.O., *Influence of substrate oscillations on acetate formation and growth yield in Escherichia coli glucose limited fed-batch cultivations.* Biotechnology and bioengineering, 1995. **47**: p. 139-146.
2.   Mayr B., Nagy E., Horvat P., Moser A., *Scale-up on basis of structured mixing models : a new concept.* Biotechnology and bioengineering, 1994. **43**: p. 195-206.
3.   Mayr B., Nagy E., Horvat P., Moser A., *Modelling of mixing and simulation of its effect on glutamic acid fermentation.* Chem. Biochem. Eng. Q., 1993. **7**(1): p. 31-42.
4.   Zahradnik J., Mann R., Fialova M., Vlaev D., Vlaev S.D., Lossev V., Seichter P., *A network-of-zones analysis of mixing and mass transfer in three industrial bioreactors.* Chemical engineering science, 2001. **56**: p. 485-492.
5.   Vlaev D., Mann R., Lossev V., Vlaev S.D., Zahradnik J., Seichter P., *Macro-mixing and Streptomyces fradiae : modelling oxygen and nutrient*

segregation in an industrial bioreactor. Trans IChemE, 2000. **78**: p. 354-362.

6. Berthiaux H., Dodds J., *Modeling classifier networks by Markov chains.* Powder technology, 1999. **105**: p. 266-273.

7. Berthiaux H., *Analysis of grinding processes by Markov chains.* Chemical engineering science, 2000. **55**: p. 4117-4127.

8. Delvigne F., Destain J., Thonart P., *Structured mixing model for stirred bioreactor : an extension to the stochastic approach.* Chemical engineering journal, 2005. **in press**.

9. Xu B., Jahic M., Blomsten G., Enfors S.O., *Glucose overflow metabolism and mixed-acid fermentation in aerobic large-scale fed-batch processes with Escherichia coli.* Applied microbiology and biotechnology, 1999. **51**: p. 564-571.

10. Namdev P.K., Thompson B.G., Gray M.R., *Effect of feed zone in fed-batch fermentations of Saccharomyces cerevisiae.* Biotechnology and bioengineering, 1992. **40**(2): p. 235-246.

11. George S., Larsson G., Olsson K., Enfors S.O., *Comparison of the Baker's yeast performance in laboratory and production scale.* Bioprocess engineering, 1998. **18**: p. 135-142.

12. Fowler J.D., Dunlop E.H., *Effects of reactant heterogeneity and mixing on catabolite repression in cultures of Saccharomyces cerevisiae.* Biotechnology and bioengineering, 1989. **33**: p. 1039-1046.

13. Mann R., Mavros P.P., Middleton J.C.,, *A structured stochastic flow model for interpreting flow-follower data from a stirred vessel.* Trans IChemE, 1981. **59**: p. 271-278.

14. Reijenga K.A., Bakker B.M., van der Weijden C.C., Westerhoff H.V., *Training of yeast cell dynamics.* FEBS journal, 2005. **272**: p. 1616-1624.

15. Mann R., Pillai S.K., El-Hamouz A.M., Ying P., Togatorop A., Edwards R.B., *Computational fluid mixing for stirred vessels : progress from seeing to believing.* Chemical engineering journal, 1995. **59**: p. 39-50.

16. Mann R., Vlaev D., Lossev V., Vlaev S.D., Zahradnik J., Seichter P., *A network-of-zones analysis of the fundamentals of gas-liquid mixing in an industrial stirred bioreactor.* Récents progrès en génie des procédés, 1997. **11**(52): p. 223-230.

CHAPITRE 8
Vers un modèle de cinétique microbienne prenant en compte les contraintes liées aux bio réacteurs et à leur extrapolation

_____

Abstract

A stochastic microbial growth model has been elaborated in the case of the culture of *E. coli* in fed-batch reactor and scale-down reactor (SDR). This model is based on the stochastic determination of the generation time of the microbial cells. The determination of generation time is determined by choosing the appropriate value on a lognormal distribution. The appropriateness of such distribution is discussed and permits to obtain growth curves which show good agreement compared with the experimental results. The mean and the standard deviation of the lognormal distribution can be considered to be constant during the batch phase of the culture, but vary when the fed-batch mode is started. It has been shown that the parameters related to the lognormal distribution are submitted to an exponential evolution. The aim of this study is to explore the bioreactor hydrodynamic effect on microbial growth. Thus, in a second time, the stochastic growth model has been reinforced by data coming from previous stochastic bioreactor mixing model [1]. The connexion of these hydrodynamic data with the actual stochastic growth model has allowed us to explain the scale-down effect associated with the glucose concentration fluctuations. It is important to point out that the scale-down effect is induced differently according to the feeding strategy involved in the fed-batch experiments.

Abbreviations :

MCPM : multiple change point model

SCPM : single change point model

SDR : scale-down reactor

1. __Introduction__

Microorganisms growing in industrial stirred bioreactors are submitted to heterogeneities which can affect their physiology. In a previous study [1], the substrate concentration profiles experienced by a microbial population have been modelled in the case of a fed-batch stirred bioreactors. This approach has been recognised as an efficient tool to characterize the gradient stress experienced by

microorganisms, but some underlying mechanisms inducing these stresses need to be investigated. In front of this, it would be interesting to model the growth of a microbial population evolving in a bioreactor by taking into account the perturbations induced by the mixing imperfections of these systems. Indeed, the knowledge of the impact of the non-ideal bioreactor hydrodynamic behaviour on microbial physiology is important to perform an efficient scale-up operation. The previous studies performed in this subject area have shown the stochastic behaviour of the microorganism exposition to environmental fluctuations in bioreactor [2, 3]. It is thus reasonable to suppose that the growth of a limited microbial population (comprising initially 30,000 individuals in our case) in relation with the bioreactor performances can be expressed by a stochastic model. We'll thus express the fate of a given microbial population in function of the bioreactor performances. Microbial cells are able to divide after a given period of time called generation time. In our case, this generation time will be extracted from a probability distribution, the respective probabilities being conditioned by the environment inside the bioreactor (in other words, longer generation times have more chance to occur if the bioreactor induces unfavourable environmental conditions for microbial growth). In a stochastic context, the model developed here can be assimilated to a branching process [4], each cell of the initial population having the capability to give birth to a series of daughter cells [5]. The determination of the generation time probability distribution is the key factor for a reliable model and a special attention must be attached to this point. Referring to the literature [6, 7], a log-normal shape will be adopted for the generation time probability distributions. The log-normal distribution has been reported to be ubiquitous in life science and notably in the area of cellular dynamics [8]. Indeed, the distribution of fluorescent proteins in bacterial cells (and notably in different *E. coli* strains) has been studied and has shown that the protein abundances obey to a log-normal law rather than a normal one. This fact was also pointed out in the case of several prokaryotic and eukaryotic microorganisms [9]. In a review about the application of log-normal law in science, it has been highlighted that the exponential growth can be supported by a log-normal distribution. In a more general context, the literature highlights the importance of this distribution in life science : medicine, environment, ecology, plant

physiology,… In the area of microbiology, the log-normal distribution permits to represent the bacterial population sizes at a given time [10], and notably in the case of *E. coli* [11]. Indeed, the cell lengths repartition for *E. coli* at a given culture time is log-normally distributed [12]. It is important to point out that the *E. coli* cells extent only in length and not in width, the division being induced by the constriction of the mother cell [13]. This fact highlights the relationship existing between cell length and the generation time in the case of *E. coli*. This property will be used further for the validation of the stochastic microbial growth model. The context of this study is the fed-batch culture of *E. coli* in small-scale and scale-down reactors. The scale-down reactor will be used here in order to obtain microbial kinetic data when bioreactor mixing imperfections occur [14, 15]. In addition, the environmental conditions developed in such reactors have been previously characterized by using a stochastic hydrodynamic model and the resulting data will be used in the present work.

2. <u>Material and methods</u>

Culture of E. coli in small-scale stirred bioreactor and in scale-down reactors (SDR)

Escherichia coli (ATCC 10536) strain is stored at –80°C. Fermentation medium is composed of glucose (10 g/l), casein pepton (10 g/l) and yeast extract (10 g/l). Cultures are performed in 20l stirred bioreactors (D = 0.22 m) (Biolaffite-France) equipped with a RDT6 rushton turbine (d = 0.1 m). The growth of *E. coli* inside the bioreactor is followed by optical density measurement (wavelength : 600 nm). A direct control system (ABB) ensure a constant temperature of 37°C and a pH of 7. Dissolved oxygen level is maintained above 30% of saturation by modulating the stirrer speed. For the scale-down tests, the previously described stirred vessel has been connected to a glass bulb of 1 liter (diameter : 0.085 m ; length : 0.25 m). During fermentation runs, the broth is continuously recirculated between the stirred vessel (mixed part) and the glass bulb (non-mixed part) by a peristaltic pump (Watson Marlow 323S/D). In the case of the scale-down reactor (SDR) experiments,

glucose addition is performed at the level of the non-mixed part. In the case of the classical bioreactor experiments, glucose is fed by the top of the stirred vessel. Glucose addition is controlled by an exponential feeding algorithm according to the equation :

$$F = F_0 \, \exp(\mu.t) \qquad (1)$$

With F being the feed flow rate (m³/s), F_0 the initial feed flow rate (m³/s), μ the microorganism growth rate (h^{-1}) and t the culture time (h). Two feeding strategies have been investigated :

- Feeding strategy 1 : for the first set of fermentation tests, the two parameters used for the exponential feeding algorithm are $\mu = 0.36$ h^{-1} and $F_0 = 0.012$ L/h, the exponential feed rate regulation being started after 2 hours of culture followed by a constant feed rate of 0.15 L/h after 10 hours of culture. This feed profile induces a strong accumulation of glucose during the course of the culture, the maximum growth rate of our strain being on the order of 0.3 h^{-1}. It is important to point out that, for the SDR experiments, the glucose level is only measured at the level of the mixed part. According to the arrangement of the SDR, it is reasonable to assume that stronger glucose concentrations are encountered in the nonmixed part of the system.

- Feeding strategy 2 : in this case, the parameters of the feed equation, i.e. $\mu = 0.24$ h^{-1} and $F_0 = 0.012$ L/h have been calculated to limit the accumulation of glucose inside the bioreactor. The exponential feed rate regulation is started after 2 hours of culture followed by a constant feed rate of 0.15 L/h after 13 hours of culture.

Microbial growth stochastic model : branching process

Each cell is individually characterised by a generation time stochastically extracted from a given probability distribution. This probability distribution is the core of the model and its impact on the simulations will be observed in the results and discussion section. It will be shown that the shape of the distribution is continuously modified during the course of the culture. The simulation is started with 30,000

microbial cells for which the generation time is determined from the above mentioned probability distribution. Two parameters are used to describe the shape of the distribution : μ and σ [10], μ being the mean of the distribution and σ its standard deviation.

Indeed, it is assumed that each cell will evolve differently inside the bioreactor, leading to a given value of generation time (the best conditions leading to a decrease of the generation time). The simulation is discrete in time and each time increment is progressively withdrawn from the respective generation time of individual cells. Once a cell reaches its generation time, division occurs and two new generation times are extracted from the distribution (one for the mother cell and another for the daughter cell). The development pattern of the microbial population with the mother cells and the daughter cells follows a branching process [4]. This simulation procedure is schematised at figure 1.
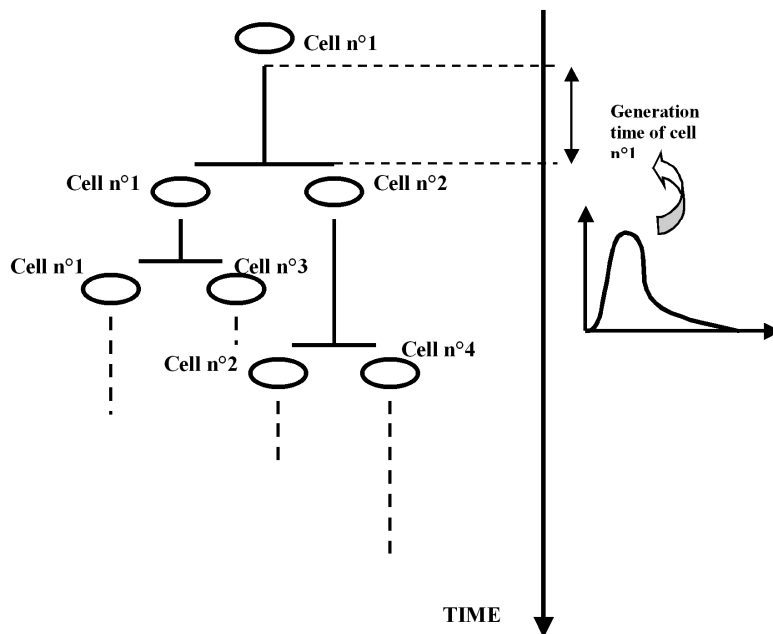

Figure 1 : schematisation of the stochastic microbial growth model according to a branching process. The procedure is illustrated in the case of a lone mother cell. For this cell and their daughters, the generation time is stochastically determined from a log-normal distribution

The bioreactor hydrodynamic effect on microbial growth constitute the background of this work. In the results and discussion section, several ways to implement the effect of the bioreactor mixing performance on the generation time probability distribution will be outlined. The simulation results will be confronted to experimental ones which have been obtained in a special bioreactor arrangement called scale-down reactor (SDR). The SDR has been described previously in this section and is used in order to reproduce hydrodynamic conditions encountered in large-scale bioreactors. In our case, the circulation of the microorganisms inside the bioreactor is the stochastic component of the system. Indeed, when considering a small population of 30,000 microorganisms travelling in a SDR, several fractions can be described in function of the specific displacement path taken by each individuals. For example, inside a given population, some individuals encounter large concentration fluctuations induced by the passage at the level of the nonmixed section of the SDR. Such individuals exhibit thus different growth behaviour according to the environmental stress experienced. The stochastic nature of the model and the relatively small size of the microbial population considered (typically, there are up to 10^9 cells par ml of broth in the reactor) induce strong fluctuations from a simulation result to another. According to this, the simulations performed in this work are made on the basis of an initial population of 30,000 cells in order to limit the effect of the standard deviation [16].

Variation of the parameters of the lognormal distribution and change point strategies

When observing the microbial growth curve of a fed-batch reactor, two distinct phases can be delimited (figure 2) : an exponential phase during the five first hours of culture corresponding to the batch culture and the beginning of the exponential fed-batch phase operating with a very low feed flow rate ; a linear phase during the fed-batch phase operating with a more elevated feed flow rate. When a scale-down effect is involved (in our case, this effect is induced by the appearance of a glucose concentration gradient in the late stage of the culture), a third linear phase can be

197

highlighted. Our stochastic microbial growth model is not able to capture by themselves these transitions from phase to phase.
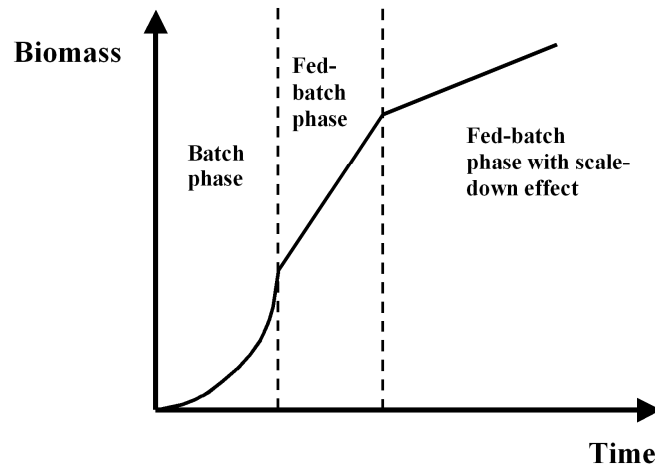
Figure 2 : illustration of the different microbial growth phases observed in scale-down fed-batch bioreactors

Typically, the concept of changing point model can be used here. The changing point concept allows to change the formulation of the model after a given time. In our case, we will adopt different strategies in order to reflect the phase transitions at the level of the simulated growth curves :

- First change point : during the first 3 hours of culture, corresponding to the initial batch phase, a probability distribution with given μ and σ parameters is considered in order to represent the microbial growth process. This assumption can be considered because the bioreactor is operating in batch mode and only a few perturbations are encountered. This is clearly not the case when operating in fed-batch mode for which homogenisation and oxygen transfer perturbations can occur. In the context of the stochastic model, this phenomena is traduced by a modification of the shape of the distribution. It has been considered that this perturbation depends on the importance of the microbial population (increasing the number of cells to be considered induces an increase of the probability to be submitted to growth perturbations) and the importance of the bioreactor environmental perturbations. The two parameters of the log-normal distributions, i.e. μ

and σ are both varying during the growth process. The proposed equations used to express the variation of these two parameters have the following form :

$$\sigma = \sigma_0 + \exp^{\alpha.t} \quad (2)$$

$$\mu = \mu_0 + \exp^{\beta.t} \quad (3)$$

with α and β being the variation factors and t the process time.

- Second change point : in order to allow the representation of the entire growth curve with the three distinct phases (figure 2), a second change point will be considered to simulate the appearance of the growth perturbations induced by the glucose concentration fluctuations. Two mathematical implementations will be considered in order to simulate the scale-down mechanism as it will be discussed below.

On the basis of these considerations, a single change point model and two kinds of multiple change point stochastic model will be evaluated in this work :

- Single change point model (SCPM) : only the transition between the initial batch phase and the beginning of the fed-batch phase will be involved in the SCPM. The simulation procedure involves the first change point described above. The aim of this preliminary SCPM is to evaluate the set of parameters α and β being the most suited to reproduce the initial states of the experimental growth curve before the appearance of the scale-down effect. This preliminary evaluation of the SCPM performances allows to simplify the non linear regression analysis.

- Multiple change point model 1 (MCPM 1) : in this case, two change points are considered. The second change point is related to the appearance of the scale-down effect (in our case, the appearance of glucose heterogeneities inside the broth) at a critical time, t_{crit}. This time corresponds to the time at which the interval between two injection pulses (t_{pulse}) of the feed pump is inferior or close to the global mixing time t_m of the system. Indeed, in these conditions it has been shown that a stable concentration gradient is established over the whole system at a given time when $t_{pulse} < t_m$ [1]. The

second change point consists to modify the α and β parameters when t_{crit} is reached according to the equations 2 and 3.

-   Multiple change point model 2 (MCPM 2) : the mathematical implementation of this model is similar to the one of the MCPM 1. The sole difference lies on the consideration of a probability for a microbial cell to encounter a gradient stress. This probability is calculated from a stochastic hydrodynamic model. Details will be given in the results and discussion section.

Non-linear regression analysis

In order to evaluate the simulations quality, a non linear regression analysis will be performed on the experimental and simulated growth curves. An efficient way to represent a population dynamics curve is to use the logistic equation :

$$\frac{dX}{dt}=r.X\left(1-\frac{X}{K}\right) \qquad (4)$$

With X being the microbial concentration (in number of cells or in g/L), r being the growth rate (h^{-1}) and K being the carrying capacity of the population (in number of cells or in g/L).

The differential equation can be solved by separation of variables and partial fractions :

$$X(t)=\frac{X(t_0).K}{\left(K-X(t_0)\right)e^{-r.t}+X(t_0)} \qquad (5)$$

The regression analysis will be performed on the basis of equation by using the *lsqcurvefit* function of MatLab. This algorithm is based on the Levenberg-Marquardt method and returns the values of the carrying capacity and the growth rate as well as the fitting error (or, more precisely, the sum of squared errors).

_____

Bioreactor hydrodynamic model

The stochastic microbial growth model will be confronted to bioreactor hydrodynamic data coming from some previously presented models [1]. These bioreactor mixing models are also stochastically expressed and will be briefly described here.

Two kinds of stochastic hydrodynamic model will be used :

-   A simplified flow model (figure 3A) for the determination of the passage probability at the level of the non-mixed part of the SDR : the two parts of the SDR are each modelized by a perfectly mixed compartment. The probabilities to shift from a compartment to another are calculated from the real flow rate promoted by the recirculation pump by the equation $P = Q_{recirc}/V$ (where Q_{recirc} represents the recirculation flow rate in m³/s and V the compartment volume in m³). The model is used here to perform microbial cells residence time experiment.

-   A complex flow model (figure 3B) to calculate the glucose concentrations experienced by the microbial cells in the reactor : in this case, both the mixed and the non-mixed part of the SDR are represented by several perfectly mixed compartments in series. A random number generation procedure permits to obtain the circulation of a set of microbial cells inside the reactor. On the other hand, a Markov chain procedure permits the representation of the concentration gradient inside the reactor according to the injection frequency of the feed pump. The superposition of the two phenomena permits to obtain the relative substrate concentration encountered by the microorganisms during their sojourn in the reactor.
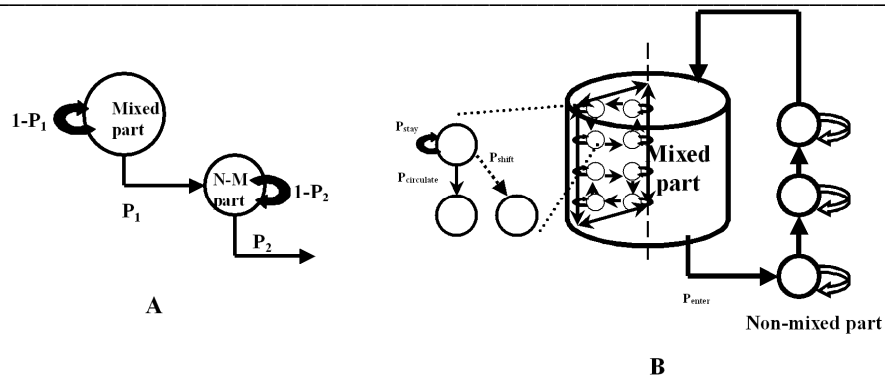
Figure 3 : stochastic flow models structure used for the calculation of the hydrodynamic data implemented at the level of the stochastic microbial growth model. A : simplified flow model of a SDR working in continuous mode ; B : complex flow model of the SDR

Exhaustive informations involving the calculation of the transition probabilities from a state to another (i.e., P_1, P_2, P_{stay}, $P_{circulate}$, P_{shift} and P_{enter} in figure 3) can be found in previous publications [1, 16].

Biological tracer experiments

Fluorescent stained cells have been used as a tracer in order to determine their respective residence time in the mixed and nonmixed part of the SDR. The cells are stained with a fluorescent dye (Vybrant CFDA SE cell tracer kit V-12883) which facilitates the detection by epifluorescent microscopy. The staining protocol consists to perform a preculture in a 500 ml Erlenmeyer flask in order to obtain the required amount of biomass for further staining. An aliquot of the preculture is centrifuged (5 minutes at 4000 rpm). The precipitate is washed with 10 ml of sterile PBS buffer (NaCl 8 g/l ; KCl 0.2 g/l ; K_2HPO_4 1.44 g/l ; KH_2PO_4 0.24 g/l ; adjusted to pH 7.5 with K_2HPO_4 and KH_2PO_4). Three successive centrifugation/washing sequences are performed. After this, microbial cells are stained by addition of 1mM of CFDA SE (carboxyfluorescein diacetate succinimidyl ester), followed by an incubation during 3 hours at 30°C. After incubation, the solution is centrifuged and the precipitate is washed with PBS buffer. When performing a biological tracer test, 5 ml of the stained cells suspension (>10^8 cells/ml, in order to detect a sufficient amount of cells

by microscopy) are poured at the level of the non-mixed part of the SDR, and samples are taken at the level of the mixed part and at the outlet of the nonmixed part. Cells are directly counted by fluorescent microscopy. For each sample, three aliquots of 10 µl each are placed on a microscopic plate for further counting. For each aliquot, three counts are performed for three widths of the microscopic plate. Mean and standard deviation are calculated for each sample.

3. Results and discussion

Growth behaviour of E. coli in SDRs

The *E. coli* cultivation tests are presented at figure 4. Two kinds of glucose feeding algorithm have been used. The feeding strategy 1 (figure 4A) induces an glucose excess in the whole reactor. In this case, there are no differences between the SDR tests. The feeding strategy 2 allows to limit the glucose excess and in this case, different growth evolution can be observed in function of the recirculation flow rate of the SDR. In a previous study [1], a hydrodynamic stochastic model has been used in order to determine the mean relative substrate concentration fluctuations experienced by *S. cerevisiae* in a fed-batch reactor. The analysis revealed that, in the case of a scale-down reactor, the exposure to higher substrate concentrations was increased when increasing the recirculation flow rate between the two parts of the reactor. The frequency distribution of the experienced concentration followed a log-normal law, the right side of this distribution corresponding to the fraction of microbial cells being the more exposed to concentration fluctuations, or in the case of a scale-down reactor, having the higher passage frequency at the level of the non-mixed part (these frequency distribution will be detailed in the section concerned with the MCPM 2).

203
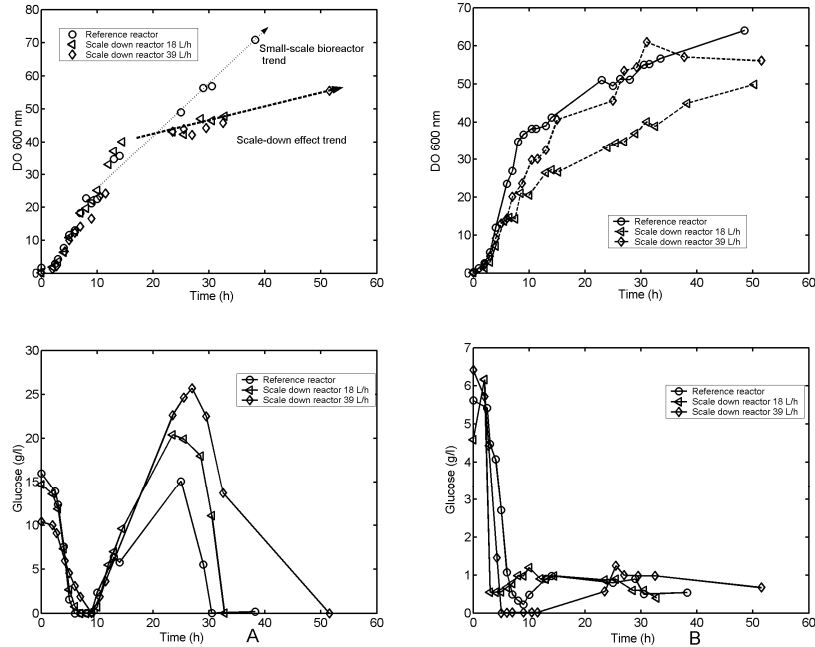
Figure 4 : microbial growth and glucose consumption curves obtained in scale-down and in classical small-scale reactors (reference reactor). A : feeding strategy 1 ; B : feeding strategy 2

Considering the problem related to the tests performed with the feeding strategy 1, only the tests carried out with the feeding strategy 2 will be used to validate the simulations results in the following sections.

Evaluation of the SCPM by non linear regression analysis

The initial batch phase of the culture (figure 2) has been modelled preliminary to the elaboration of the SCPM. The generation time probability distribution associated with this initial batch phase is easy to determine since we know that, in this case, the culture conditions are relatively constants. It will be thus assumed a mean generation time of 20 min that will be used as in the corresponding generation time distribution. We need thus to determine the value of the standard deviation allowing to reproduce the experimental growth curves. Figure 5 shows different case study in function of the value of the standard deviation of the lognormal generation time

distribution. We can see that for a standard deviation inferior to 0.2 hours, the simulated growth curves exhibit an oscillating behaviour (figure 5A). This phenomena can be explained by the fact that, in these cases, the corresponding generation time distribution is strongly centered around the mean. The whole microbial population is thus subjected to approximately the same generation time value. This case study do not reflect the microbial dynamics in bioreactors where cells taken at a given time are in different growing stages [11]. When the value of the standard deviation is below 1 (figure 5C), the stochastic nature of the process is so pronounced that unrealistic growth outburst can occurs. The experimental exponential growth curve can be simulated by considering standard deviation values comprised between 0.2 and 1 (figure 5B). A specific standard deviation value cannot be extracted from the results presented at figure 5B and the minimal value of 0.2 will be adopted for the rest of the study considering the small amount of perturbations encountered in the batch phase. In addition, this minimal value will allow a greater range of variation of the standard deviation for the validation of the single and multiple change point models.
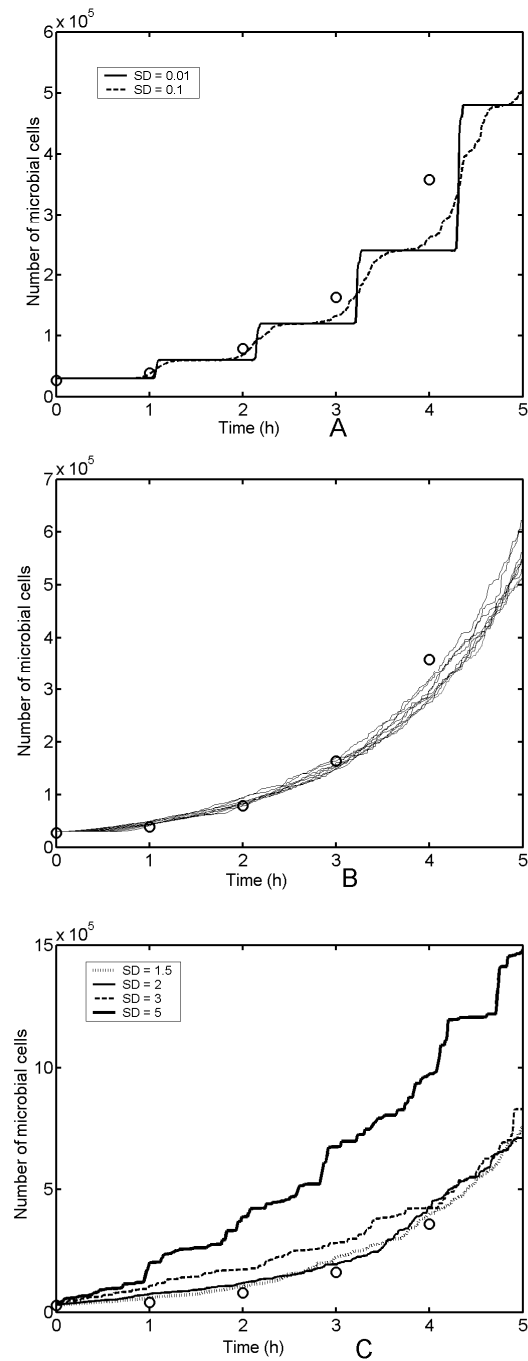
Figure 5 : comparison of the experimental (circle) and simulated results. A : sample paths obtained for σ ≤ 0.1 ; B : sample paths obtained for 0.2 ≤ σ ≤ 1; C : sample paths obtained for σ ≥ 1.5

The mean and the standard deviation will be thus assumed constant for the initial batch phase before an exponential change (equations 2 and 3) occurring in the earlier fed-batch phase. These changes of the probability distribution parameters can be modelled by the SCPM. In this case, the rate of change represented by the parameters (equations 2 and 3) must be determined. This determination has been done on the basis of a non-linear regression analysis involving the experimental and simulated data fits to the logistic equation (equation 5). The results of this analysis are presented at figure 6.

Figure 6 : non linear regression analysis performed on the simulated growth obtained by using the SCPM. The simulated growth curves have been fitted with a logistic equation and the carrying capacity of the population as well as the growth rate have been calculated in function of the α and β parameters of equations 2 and 3

The fitted parameters in the case of the experimental growth curve obtained in fed-batch reactors (feeding strategy 2) are presented in table1.

Table 1 : non linear regression results obtained from the experimental data (feeding strategy 2)

	Estimated growth rate (h^{-1})	Estimated carrying capacity (number of microbial cells)
Reference reactor	0.678	$1.19 \ 10^6$
SDR Q_{recirc} = 18 L/H	0.6	$8.07 \ 10^5$
SDR Q_{recirc} = 39 L/H	0.56	$9.55 \ 10^5$

The carrying capacity is the parameter showing the clearer evolution in function of the α and β parameters of equations 2 and 3. The regression results of the experimental data (table 1) are included in a zone comprises between 9.10^5 and 10^6 at the level of the carrying capacity contour plot (figure 6). The growth rate contour plot (figure 6) permits to determine that an increase of the α parameter is necessary to match both the carrying capacity and the growth rate of the experimental results. By superimposing the results of the two contour plots (figure 6), optimal values of the α and β parameters are determined. The values $\alpha = 0.2$ and $\beta = 0.1$ allows the SCPM to match the experimental ones. In all case, the sum of squared error was below 10^{10} microbial cells and the fit quality was good. The comparison of the experimental growth curve obtained from the fed-batch culture of *E. coli* in small-scale stirred bioreactor (feeding strategy 2) with the simulated growth curve obtained with the SCPM with the optimised parameters is presented at figure 7.
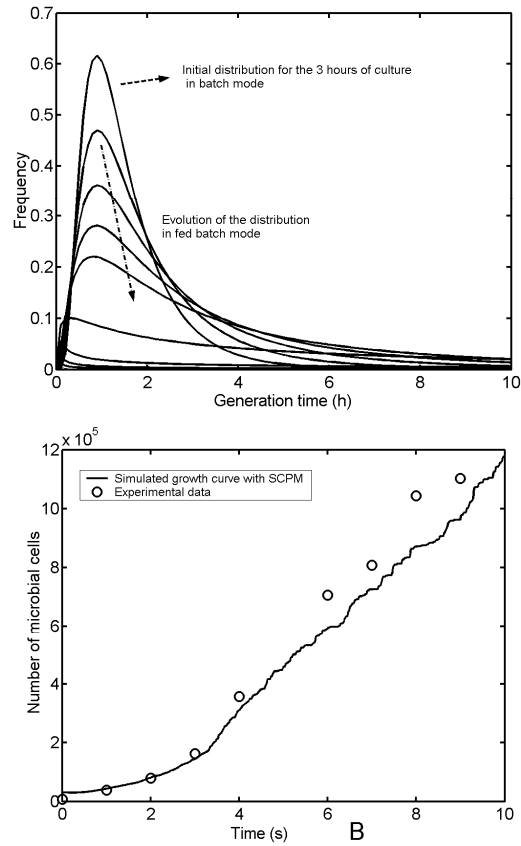
Figure 7 : evolution of the probability distribution shape during the simulation (top) and subsequent microbial growth curve (bottom) in the case of the fed-batch culture of *E. coli* in small-scale stirred bioreactor. The mean simulation results have been obtained on the basis of an initial population of 30,000 cells (solid line) and are compared with the experimental results (circle)

At the beginning of each simulation, 30,000 cells have been considered. Each simulation corresponds thus to the fate of a limited microbial population for a given sojourn time in a bioreactor running with given operating conditions.

The results presented at figure 7 permits to conclude that there is a significant modification of the microorganisms growth behaviour during the course of the culture, even in small-scale stirred bioreactor. These perturbations can be attributed to several factors such as the growth limitation by the sugar feed profile during the fed-batch mode, the inhibition by acetate excretion,... [17, 18]. It is important to

estimate the magnitude of these intrinsic perturbations in order to estimate further the mixing impact on the process. Another remark in relation with the results presented at figure 7 is that the log-normal shape of the distribution is more and more attenuated during the course of the process. In this case, it could be hypothesized that the cell size-generation time relationship is no longer valid due to the elongation of the cell generation time induced by environmental fluctuations.

Evaluation of the MCPM 1

In a second step, the impact of the scale-down effect has been included by considering a second change point. Indeed, it can be seen from figure that there is an abrupt change of the growth trajectory after approximately 10 hours of culture. As discussed previously, this time correspond to the critical time for which the feed pump frequency induces the appearance of a marked gradient concentration. The evaluation of the MCPM 1 has been done by focusing our attention at the level of the second change point. The simulated growth curve resulting from the use of the SCPM with the optimised parameters (figure 7) are used as a reference. The corresponding generation time distribution after 10 hours of culture has been considered at the beginning of each simulation. The change point at this level consists to increase the α and β parameters of equations 2 and 3. Several set of parameters have been tested and the results are presented at figure 8.
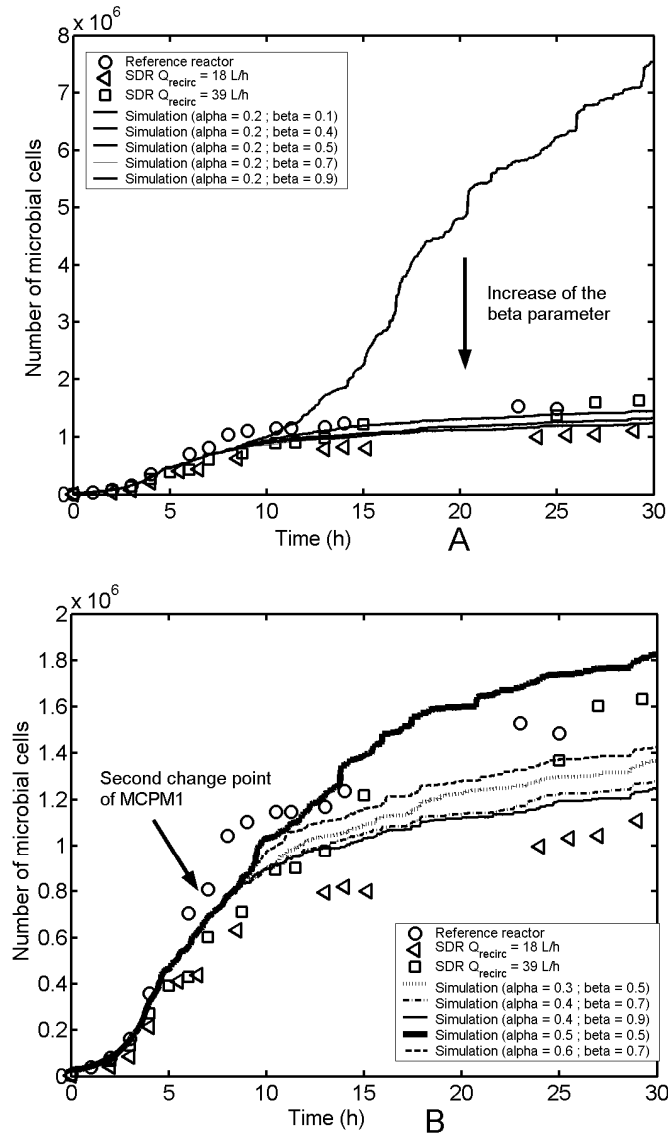
Figure 8 : comparison of the experimental results with the simulations performed with the MCPM1

Figure 8A shows that the increase of the β parameter of equations 3 is a necessary conditions in order to match the experimental data. This parameter induces an increase of the mean value of the generation time distribution used in the stochastic growth   model.

These simulations carried out with the MCPM 1 show that the attenuation of the cell size-generation time relationship is thus a necessary condition for the scale-down effect. This fact is also pointed out when varying the α parameter (figure 8B). Two problems have to be considered when dealing with the MCPM 1. Firstly, considering the discrete nature of the model, only the cells at the end of the generation time are affected by the second change point. Indeed, the cells keep the same generation time until the elongation and separation processes are unachieved. Secondly, it is difficult to extract informations about the bioreactor hydrodynamic impact on the microbial growth process. In addition to this two main problems, the MCPM1 is unable to reproduce the net change of growth trajectory observed in the case of the SDR test carried out at a recirculation flow rate of 18 L/h. In order to give more physical significance at the level of the second change point attributed to the scale-down effect, bioreactor hydrodynamic data will be considered.

Inclusion of bioreactor hydrodynamic data and evaluation of the MCPM2

In order to enhance the reliability of the microbial growth simulations, data coming from bioreactor hydrodynamic models will be implemented in a new version of the multiple change point model (i.e., MCPM 2). In previous studies [1, 16], the impact of mixing on a fed-batch culture of *S. cerevisiae* has been estimated by using a stochastic bioreactor hydrodynamic model taking into account the mixing and the microorganism circulation processes. It has been shown that the major fraction of the microorganisms that was exposed to large extracellular concentration fluctuations was linked to the passage at the level of the non-mixed part of the scale-down reactor. The probability of passage at the level of the non-mixed part is thus an important element that must be implemented at the level of the microbial growth model (and, more precisely, at the level of the second change point of this model). This probability of passage is obtained from a simplified stochastic compartment flow model and is validated by biological tracer tests (see materials and methods). Figure 9 shows the comparison of the simulated and experimental tracer curves for the scale-down reactor working in continuous mode (fresh water is added at the top of the mixed part and evacuated at the outlet of the non-mixed part) in order to

follow the residence time of the microbial cells at the level of the different parts of the SDR. It can be observed that there is a good agreement between the simulated and the experimental results, which permit the validation of the probability of passage between the mixed and the nonmixed sections of the SDR.
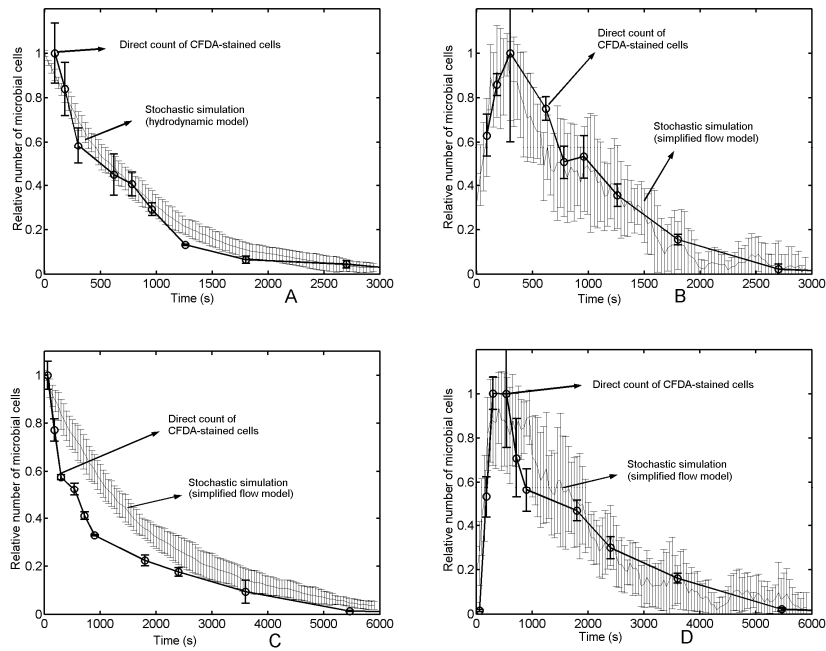
Figure 9 : comparison of experimental and simulated results of microbial cells dispersion inside the SDR running in continuous mode. The simulations have been performed by using a simplified stochastic flow model (see Material and Methods). A : Q_{recirc} = 39 L/h ; mixed part of the SDR. B : Q_{recirc} = 39 L/h ; nonmixed part of the SDR. C : Q_{recirc} = 18 L/h ; mixed part of the SDR. D : Q_{recirc} = 18 L/h ; nonmixed part of the SDR. The simulated results are presented as the mean and the standard deviation calculated from 10 simulations

The hydrodynamic data are then implemented at the level of the microbial growth model by considering, at the level of the second change point, the probability to enter in the non-mixed section of the SDR. As for the MCPM 1, the critical time is reached after approximately 10 hours of culture, when the global mixing time of the system is superior to the time between two pulses of the feed pump. After this time, microorganisms entering into the non-mixed section are considered to be perturbed by the fluctuating extracellular environment, which is traduced at the level of the microbial growth simulation by a drastic increase of the generation time.

213

The increase of the recirculation flow rat of the SDR leads to the increase of the passage frequency of microorganisms at the level of the nonmixed part of the reactor. This passage induces a hydrodynamic stress which is well represented both by the experimental and the simulated microbial growth curve. But it has been shown that the passage frequency at the level of the non-mixed part of the SDR is not the sole component playing a role at the level of the microorganisms exposure to gradient stress [1]. The probability for a microbial cell to encounter a stress must be related to the magnitude of the extracellular concentration fluctuation as well as the time of exposure. Such probabilities can be estimated by using a more refined bioreactor modelling procedure (complex stochastic flow model, see Material and Methods). In this procedure, the circulation path taken by a microorganism in a bioreactor is superimposed to the concentration gradient. The results are presented as a frequency distribution of the mean relative concentration experienced by each microbial cell of a given population on a given lapse of time [16]. Figure 10 presents such frequency distributions in the case of the two SDR operating conditions. From the observation of figure 10, we can reasonably assume that the fraction of the microbial population located at the right side of the frequency distribution is exposed to the more intensive substrate fluctuations in the nonmixed part of the SDR. Thus, at the level of the stochastic growth model, the probability to encounter a hydrodynamic stress will be calculated by estimating the fraction of the stressed population on the basis of these frequency distributions.
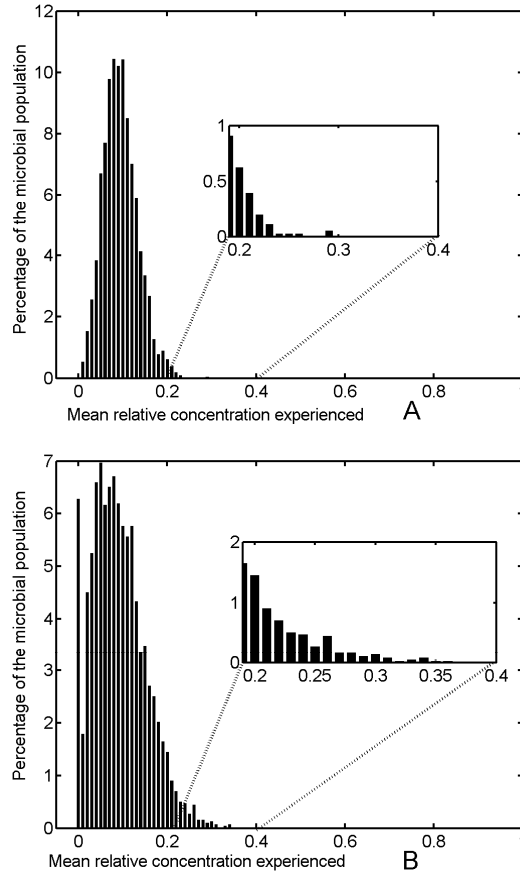
Figure 10 : frequency distributions of the mean relative concentration experienced by microbial cells obtained in the case of the SDR running with Q_{recirc} = 39 L/h (A), and with Q_{recirc} = 18 L/h (B). The simulations have been obtained by the superposition of a stochastic mixing model and a microbial cell circulation model (see complex model structure in Material and Methods)

In the case of the simulations showed at figure 10, only 3500 microbial cells have been considered in order to limit the computational time. Thus, the probability for a cell to encounter a stress is given by :

$$P_{stress} = \frac{\text{fraction of the population on the frequency distribution}}{3500} \qquad (5)$$

In order to accurately determine the fraction of the population encountering a stress, the percentage will be determined on a relative basis by comparing the two SDR tests. Indeed, the SDR test performed with a Q_{recirc} of 39 L/h presents approximately

the same biomass yield than the reference reactor (figure 4B). It can thus be assumed that for this SDR test no significant hydrodynamic stress is encountered. We will thus consider that the frequency distributions (figure 10) reflect a good image of the situation of the microbial population inside the SDR, and the percentage of the stressed population is thus determined by simply comparing the two frequency distributions relative to the SDR tests. For this purpose, several values of the critical relative concentration leading to a stress can be considered. It comes from the observation of the frequency distributions presented at figure 10 that the principal differences between the two frequency distributions arise beyond a relative concentration of 0.2. In order to facilitate the following discussion, the frequency distribution results of figure 10 have been reformulated in table 2. This table presents the number of microbial cells for each class of mean relative concentration experienced.

Table 2 : number of microbial cells per mean relative concentration class in the case of the two SDR tests performed with the feeding strategy 2

Mean relative concentration class	SDR Q_{recirc} = 39 L/h	SDR Q_{recirc} = 18 L/h
0.2	22	51
0.21	14	32
0.22	7	25
0.23	4	18
0.24	1	17
0.25	1	10
0.26	1	16
0.27	–	6
0.28	–	6
0.29	–	4
0.3	–	5
0.31	–	3
0.32	–	1
0.33	–	2
0.34	–	3
0.35	–	1
0.36	–	1

As shown in table 2, an amount of 26 microorganisms constitute the difference between the SDR test performed at Q_{recirc} = 39 L/h from the one performed at Q_{recirc} = 18 L/h. On the basis of this amount of microorganisms, a P_{stress} = 26/3500 = 0.0074 or 0.74% can be calculated. This probability will be then implemented at the level of the second change point of the MCPM 2 and reflects the probability for a microbial cell to experience a stress during its sojourn in the SDR. Figure 11 shows a comparison between the experimental growth curves and the simulated ones. It can be seen that the use of the MCPM 2 with a P_{stress} value of 0.0074 allows to reproduce the SDR results obtained with a Q_{recirc} = 18 L/h.

The culture time being long (several hours), even a small probability can have a strong impact on the global simulation results. Indeed, the microbial cells are submitted to the probability to encounter a stress at each time interval, suggesting that the scale-down effect is driven in our case by a cumulative process.
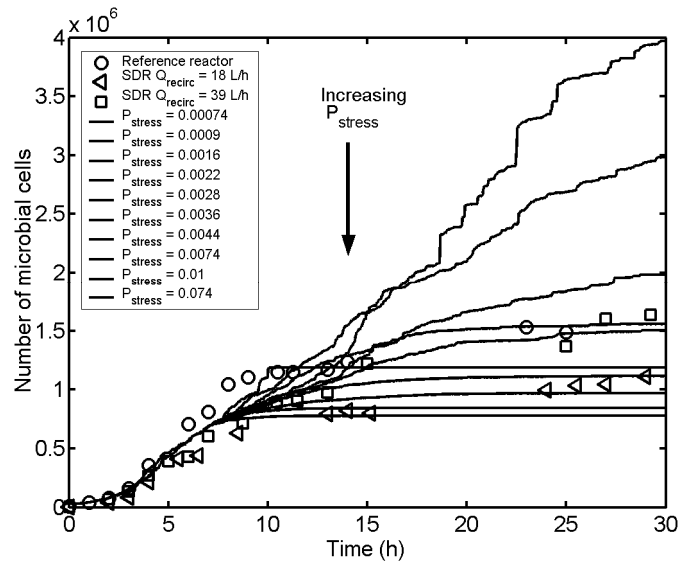
Figure 11 : comparison of the SDR tests with the simulated results obtained by using the MCPM 2

This conclusion is important for the reactor design procedure or in the context of a scaling-up operation, because a few modifications of the mixing performances of the system can induce strong ameliorations at the level of the bioprocess yield (or, on the contrary, can induces a drastic drop of the process performances if we have wrong with the scale-up calculation). This conclusion is validated by the experimental growth curves exposed in figure 4B which show a net increase of biomass yield when increasing the circulation intensity of the SDR.

Conclusion

We have presented a simple procedure to simulate the stochastic microbial growth of *E. coli* under bioreactor environment perturbations. In order to achieve this, a multiple change point model (MCPM) is necessary to simulate efficiently the transitions between growth phases, i.e. from the initial batch phase to the earlier fed-batch phase and to the late fed-batch phase with the occurrence of the scale-down effect. As previously determined [1, 3, 16], the stochastic component comes from the random nature of the microorganism displacement in the bioreactor where the

environment is fluctuating in function of space. This component has been entirely characterised in a previous study by a bioreactor hydrodynamic stochastic model allowing the superimposition of the concentration gradient field with the microorganisms displacements. The observation of the microbial growth simulations performed by the aim of the stochastic model leads to two main conclusions. First, the lognormal law is well-suited to represent the generation time distribution of *E. coli* cells in a bioreactor. Indeed, the stochastic growth model is able to simulate the entire growth curve of a fed-batch process in a small-scale bioreactor by modulating the parameters of the afferent lognormal probability distributions. Second, it has been observed that, even in small-scale stirred bioreactor, the growth process is not easy to interpret due to the numerous factors inducing variations at the level of the growth trajectory. This is expressed at the level of our model by continuously modifying the shape of the generation time distribution. This suggests that the law describing the growth of *E. coli* cells in fed-batch reactor is continuously changing leading to intrinsic perturbations. These intrinsic perturbations can be regarded as the adaptation mechanisms developed by the microbial cells in response to the continuously changing growth conditions encountered in a fed-batch reactor [19]. These intrinsic perturbations have been stochastically modelled in this study, which permit their isolation and the observation of the extrinsic perturbations. In our case, we have observed the impact of the bioreactor hydrodynamic, and more precisely the impact of the substrate concentration fluctuations induced by the fed-batch mode.

For the fermentation tests carried out with the feeding strategy 2, the scale-down effect is not systematically observed for all the SDR experiments and depends on the mixing and the circulation mechanisms induced by the bioreactor hydrodynamics. This fact has also been observed in the case of *S. cerevisiae*, suggesting that similar physiological mechanisms are involved in response to extracellular glucose fluctuations. In the case of the feeding strategy 2, a multiple changing point stochastic model (MCPM 2) is able to reproduce the microbial kinetic when connected to simulation results obtained from a hydrodynamic model involving mixing behaviour of the SDR and the circulation of the microorganisms.

In front of all these discussions, more general conclusions can be drawn :

- It has been shown that the increase of the recirculation flow rate of the SDR leads to an improvement of the biomass yield. This remark is only valid when the feeding strategy is designed to avoid glucose accumulation in the reactor. This observation leads to the conclusion that, in the case of large scale fed-batch bioreactor, the microbial kinetic can be improved by enhancing the circulation flow rate provided by the impeller system. If not possible, e.g. in the case of mechanical limitations, improvements can be achieved by redesigning the impellers geometry and combination.

- When the feed flow rate is well suited and allows to avoid glucose accumulation (feeding strategy 2), the impact of the bioreactor mixing performance on *E. coli* growth is similar to that previously observed for *S. cerevisiae* [1]. It suggests that the stress induction mechanism is similar for these two microorganisms. In spite of the fact that *E. coli* and *S. cerevisiae* are very different on the morphological point of view (we consider a prokaryotic and an eukaryotic organism), these organisms present several similarities at the level of the glucose metabolism. First, the two microorganisms exhibit a similar overflow metabolism when submitted to excessive glucose concentrations (traduced by an acetate production in the case of *E. coli* [17], and by an ethanol production in the case of *S. cerevisiae* [20]). Second, they both exhibit metabolism oscillations when the cells encounter fluctuating extracellular glucose concentration due to an adaptation of the glucose transporters [19, 21]. This fact suggests that the modelling strategy adopted during this work can be generalized to microorganisms exhibiting an overflow metabolism.

It is also important to point out some possible improvements of this work. Indeed, in order to enhance the reliability of the stochastic microbial growth model, it would be interesting to include experimental generation time distributions. The cell size distributions can be readily obtained by using modern techniques, such as image analysis and flow cytometry [22-24]. In the case of *E. coli*, the cell length can be correlated to the progression in the cell cycle, which allow to obtain the generation time distribution. However, it has been supposed that the cell size-generation time relationship is not valid for the late stage of the fed-batch culture due to the

inhibition mechanisms affecting cell growth and inducing a lag at the level of the generation time evolution, and this experimental validation would be only effective for the earlier stage of the microbial culture. Flow cytometry can be more efficiently used to determine more exactly the evolution of the fraction of the microbial population experiencing a hydrodynamic stress during the course of the culture [25].

Acknowledgement

References and Notes

1. Delvigne F., Lejeune A., Destain J., Thonart P., *Stochastic models to study the impact of mixing on a fed-batch culture of Saccharomyces cerevisiae.* Biotechnology progress, 2006. **22**: p. 259-269.
2. Vlaev D., Mann R., Lossev V., Vlaev S.D., Zahradnik J., Seichter P., *Macro-mixing and Streptomyces fradiae : modelling oxygen and nutrient segregation in an industrial bioreactor.* Trans IChemE, 2000. **78**: p. 354-362.
3. Delvigne F., Destain J., Thonart P., *Bioreactor hydrodynamic effect on Escherichia coli physiology : experimental results and stochastic simulations.* Bioprocess and biosystems engineering, 2005. **28**: p. 131-137.
4. Dorman K.S., Sinsheimer J.S., Lange K., *In the garden of branching processes.* SIAM review, 2004. **46**(2): p. 202-229.
5. Allen L.J.S., *An introduction to stochastic processes with applications to biology.* first ed. 2003, Upper Saddle River, New Jersey: Pearson Prentice Hall. 385.
6. Koch A.L., *The logarithm in biology. 1 : mechanisms generating the log-normal distribution exactly.* Journal of theoretical biology, 1966. **12**: p. 276-290.
7. Koch A.L., *The logarithm in biology. 2 : distributions simulating the log-normal.* Journal of theoretical biology, 1969. **23**: p. 251-268.
8. Furusawa C., Suzuki T., Kashiwagi A., Yomo T., Kaneko K., *Ubiquity of log-normal distributions in intra-cellular reaction dynamics.* Biophysics, 2005. **1**: p. 25-31.
9. Jain R., Ramakumar S., *Stochastic dynamics modeling of the protein sequence length distribution in genomes : implications for microbial evolution.* Physica A, 1999. **273**: p. 476-485.
10. Limpert E., Stahel W.A., Abbt M., *Log-normal distributions across the sciences : keys and clues.* Bioscience, 2001. **51**(5): p. 341-352.

11.   Kilian H.G., Gruler H., Bartkowiak D., Kaufmann D., *Stationary cell size distributions and mean protein chain length distributions of archea, bacteria and eukaryotes described with an increment model in terms of irreversible thermodynamics.* The european physical journal E, 2005. **17**: p. 307-325.

12.   Woldringh C.L., *Morphological analysis of nuclear separation and cell division during the life cycle of Escherichia coli.* Journal of bacteriology, 1976. **125**(1): p. 248-257.

13.   Grover N.B., Woldringh C.L., *Dimensional regulation of cell-cycle events in Escherichia coli during steady-state growth.* Microbiology, 2001. **147**: p. 171-181.

14.   Enfors S.O., Jahic M., Rozkov A., Xu B., Hecker M., Jürgen B., Krüger E., Schweder T., Hamer G., O'Beirne D., Noisommit-Rizzi N., Reuss M., Boone L., Hewitt C., McFarlane C., Nienow A., Kovacs T., Trägardh C., Fuchs L., Revstedt J., Friberg P.C., Hjertager B., Blomsten G., Skogman H., Hjort S., Hoeks F., Lin H.Y., Neubauer P., van der Lans R., Luyben K., Vrabel P., Manelius A., *Physiological responses to mixing in large scale bioreactors.* Journal of biotechnology, 2001. **85**: p. 175-185.

15.   Neubauer P., Häggström L., Enfors S.O., *Influence of substrate oscillations on acetate formation and growth yield in Escherichia coli glucose limited fed-batch cultivations.* Biotechnology and bioengineering, 1995. **47**: p. 139-146.

16.   Delvigne F., Lejeune A., Destain J., Thonart P., *Modelling of the substrate heterogeneities experienced by a limited microbial population in scale-down and in large-scale bioreactors.* Chemical engineering journal, 2006. **in press**.

17.   Xu B., Jahic M., Blomsten G., Enfors S.O., *Glucose overflow metabolism and mixed-acid fermentation in aerobic large-scale fed-batch processes with Escherichia coli.* Applied microbiology and biotechnology, 1999. **51**: p. 564-571.

18.   Xu B., Jahic M., Enfors S.O., *Modeling of overflow metabolism in batch and fed-batch cultures of Escherichia coli.* Biotechnology progress, 1999. **15**: p. 81-90.

19.   Ferenci T., *Growth of bacterial cultures' 50 years on : towards and uncertainty principle instead of constants in bacterial growth kinetics.* Res. microbiol., 1999. **150**: p. 431-438.

20.   Sonnleitner B., Käppeli O., *Growth of Saccharomyces cerevisiae is controlled by its limited respiratory capacity : formulation and verification of a hypothesis.* Biotechnology and bioengineering, 1986. **28**: p. 927-937.

21.   Reijenga K.A., Bakker B.M., van der Weijden C.C., Westerhoff H.V., *Training of yeast cell dynamics.* FEBS journal, 2005. **272**: p. 1616-1624.

22.   Métris A., LeMarc Y., Elfwing A., Ballagi A., Baranyi J., *Modelling the variability of lag times and the first generation times of single cells of E. coli.* International journal of food microbiology, 2005. **100**: p. 13-19.

23.   Elfwing A., LeMarc Y., Baranyi J., Ballagi A., *Observing growth and division of large numbers of individual bacteria by image analysis.* Applied and environmental microbiology, 2004. **70**(2): p. 675-678.

24.   Srienc F., *Cytometric data as the basis for rigorous models of cell population dynamics.* Journal of biotechnology, 1999. **71**: p. 233-238.

25.   Hewitt C.J., Nebe-Von Caron G., Axelsson B., Mc Farlane C.M., Nienow A.W., *Studies related to the scale-up of high-cell-density E. coli fed-batch fermentations using multiparameter flow cytometry : effect of a changing microenvironment with respect to glucose and dissolved oxygen concentration.* Biotechnology and bioengineering, 2000. **70**(4): p. 381-390.

CHAPITRE 9
Discussion générale et conclusions

La problématique sur laquelle repose ce travail concerne le dimensionnement et l'extrapolation des bio-réacteurs en respectant les contraintes liées aux micro-organismes. La stratégie de recherche exposée lors du premier chapitre de ce travail propose de se focaliser sur les deux composantes intervenant dans la problématique (le bio-réacteur et le micro-organisme) et le développement d'outils de modélisation pour chacune des composantes. Les différents niveaux d'étude abordés au cours du travail sont schématisés à la figure 1.
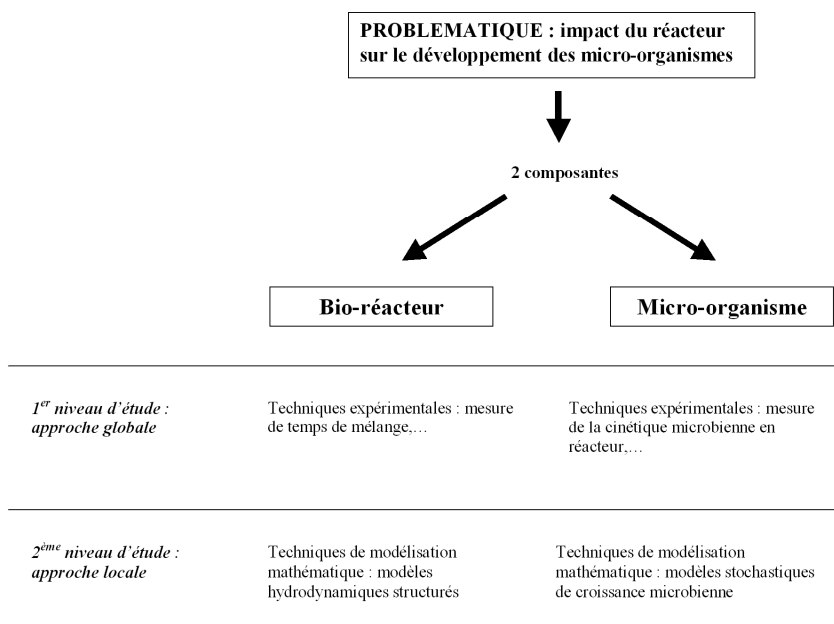
Figure 1 : présentation des deux composantes intervenant dans la problématique abordée au cours de ce travail, ainsi que des niveaux d'étude ayant été employés.

Les deux composantes de la problématiques, c'est-à-dire le micro-organisme et le bio-réacteur, présentent des paramètres propres et interagissent entre elles. En effet, le bio-réacteur possède un temps de mélange, une certaine capacité de transfert d'oxygène,…, alors que la population microbienne possède une vitesse de croissance. Tous ces paramètres vont interagir et vont conditionner les performances du bio-procédé. Le premier niveau d'étude met en œuvre une approche expérimentale qui permet de déterminer des paramètres globaux (comme par exemple, le temps de mélange pour la composante « bio-réacteur » et la vitesse de

224

---

croissance pour la composante « micro-organisme »). Afin de faciliter l'étude des deux composantes et de leurs interactions, des outils de modélisation ont été développés. Comme démontré lors du chapitre 1, il est nécessaire de développer des modèles de type structuré (ou ségrégé dans le cas de la cinétique microbienne) afin de scruter la dynamique interne des systèmes. C'est en effet cette dynamique interne qui permet d'expliquer de nombreux phénomènes d'interactions entre le bio-réacteur et les micro-organismes. Les outils de modélisation structurée ont fait l'objet d'un deuxième niveau d'étude. Il est important de noter que les données du premier niveau d'étude ont été nécessaires afin de valider les modèles. Les deux niveaux d'étude ont donc été utilisés en parallèle durant ce travail.

Pour rappel, la stratégie scientifique adoptée au cours de ce travail se résume comme suit :

- Développement des outils de modélisation de l'hydrodynamique du réacteur, ces aspects ayant été abordés au cours des chapitres 2 et 3.
- Dimensionnement d'un réacteur *scale-down* permettant de reproduire en laboratoire les conditions hydrodynamiques rencontrées à l'échelle industrielle, celui-ci ayant été effectué au cours du chapitre 4.
- Etude de l'impact des conditions hydrodynamiques du réacteur sur différents micro-organismes, celle-ci ayant été abordée au cours des chapitres 5, 6 et 7.
- Développement d'un modèle de cinétique microbienne prenant en compte les performances du bio-réacteur, abordé au cours du chapitre 7.

Les discussions principales et conclusions relatives à ces 4 points seront reprises dans ce chapitre.

9.1. Développement d'outils de modélisation pour l'hydrodynamique des réacteurs (chapitre 2 et 3)

La première partie du travail a été focalisée sur la composante « bio-réacteur » du problème. Dans une première étape, l'approche classique du génie chimique appliqué au mélange dans les bio-procédés a été confrontée à une approche plus élaborée (Chapitre 2). L'approche classique a consisté en l'étude des paramètres de

225

performance de l'opération de mélange ayant un impact sur le procédé considéré. Ces paramètres de performance sont :

- le taux de transfert d'oxygène, qui traduit la vitesse de transfert de l'oxygène des bulles gazeuses au milieu liquide contenant les micro-organismes.
- le temps de mélange, traduisant le temps que met le système agité pour revenir à un état d' équilibre suite à une perturbation.

Le procédé considéré étant la culture *fed-batch* d'une levure sauvage de *Pichia pastoris* en réacteur de 20 litres et de 500 litres.

Les deux opérations de mélange se sont avérées importantes dans les cultures réalisées, le taux de transfert d'oxygène ayant un impact plus important que le processus d'homogénéisation. En effet, les échelles de réacteur considérées sont restées modestes. Néanmoins, même à petite échelle des inhomogénéités peuvent survenir [1] et l'approche structurée a permis de mettre en évidence l'apparition de gradients de concentration suite à l'ajout de la source de carbone lors de la phase *fed-batch* du procédé. Certaines combinaisons d'agitateurs se sont avérées efficaces pour réduire ce gradient, et notamment le passage d'un système d'agitation purement radial à un système comprenant un ou deux agitateurs axiaux. La combinaison hybride (un agitateur radial + un agitateur axial) s'est avérée intéressante du fait de ses performances à la fois pour l'homogénéisation et le transfert d'oxygène. L'approche structurée a également permis de mettre en évidence l'impact de l'augmentation d'échelle du réacteur sur le gradient de concentration. En effet, les simulations ont montré une augmentation de l'intensité du gradient de concentration lors du passage d'un réacteur de 20 litres à un réacteur de 500 litres.

Cette première phase d'étude (chapitre 2) a mis en évidence :

- la nécessité de pouvoir réaliser des expériences dans des réacteurs de volume plus important afin d'observer un impact de l'homogénéisation plus marqué. En effet, ce phénomène d'homogénéisation va conditionner l'extrapolation du procédé. Afin de permettre la réalisation de telles expériences, la conception d'un réacteur *scale-down* sera une étape indispensable (voir chapitre 3 et suivants).

- l'intérêt de l'approche structurée, même si les modèles mathématiques relatifs à celle-ci doivent encore être améliorés. Ces améliorations ont été abordées au cours du chapitre 3.

En effet, au cours du chapitre 3, le modèle structuré classique (déterministe) a été confronté au modèle structuré stochastique. Il s'est avéré que ce dernier présente les mêmes performances que le modèle structuré classique. Néanmoins, le modèle stochastique permet également d'intégrer la circulation du micro-organisme et est plus facile à exprimer du point de vue mathématique, ce qui en fait un modèle de choix pour représenter l'hydrodynamique des bio-réacteurs

9.2. Dimensionnement d'un réacteur *scale-down* (chapitre 4)

Afin de permettre la réalisation de cultures de micro-organismes dans des conditions d'écoulement de réacteur industriel, un système de réacteur *scale-down* a été imaginé (celui-ci a été présenté au chapitre 1). Le modèle hydrodynamique stochastique a été utilisé afin de comparer les performances de mélange du réacteur *scale-down* par rapport à des réacteurs de taille industrielle. Lors de cette étude, il a été montré que la modification de la géométrie de la partie non mélangée du réacteur *scale-down*, ainsi que la modification du débit de la pompe de recirculation permettaient de retrouver les courbes de traceur (utilisées pour déterminer le temps de mélange, voir chapitre 1) de plusieurs réacteurs industriels. De plus, le modèle hydrodynamique stochastique a pu être employé pour reproduire ces courbes de traceurs. Néanmoins, la valeur du temps de mélange, voire même la forme de la courbe de traceur ne sont pas des paramètres suffisants pour comparer les performances hydrodynamiques des réacteurs dans le cadre des bio-procédés. Afin de comparer de manière plus fine l'effet du mélange sur la physiologie microbienne entre différents réacteurs, le modèle stochastique a été utilisé pour simuler le phénomène de mélange et l'apparition de gradient de concentration, mais aussi le phénomène de circulation des micro-organismes par rapport à ce gradient. Cette approche permet, par superposition des deux phénomènes, d'obtenir le profil de concentration rencontré par un micro-organisme lors de son séjour dans un réacteur. Il a été démontré au cours du chapitre 4 que cette approche constitue une base de

comparaison plus fiable. La même approche de superposition des deux modèles sera utilisée dans la suite du travail pour étudier l'impact de l'hydrodynamique du réacteur sur la physiologie et le développement de certains micro-organismes.

9.3. Impact des conditions hydrodynamiques du réacteur sur le développement des micro-organismes (chapitre 5, 6 et 7)

L'utilisation des modèles stochastiques relatifs au bio-réacteur permet l'obtention des profils de concentration rencontrés par les micro-organismes. En effet, ceux-ci permettent d'obtenir une représentation du gradient de concentration qui s'établit dans le réacteur, mais aussi la circulation des cellules microbiennes par rapport à ce gradient. Cette idée de détermination des variations de concentration perçues par une cellule microbienne durant son séjour dans un réacteur a déjà été proposée dans la littérature [2]. Celle-ci a été exploitée dans ce travail et à été étendue à une population microbienne de taille donnée (chapitres 6 et 7). De plus, une méthode de standardisation des résultats de simulation hydrodynamique a été proposée au cours du chapitre 6. De cette manière, les résultats de simulation sont exprimés sous forme d'un diagramme de fréquence représentant les différentes fractions de la population microbienne en fonction des profils moyens de concentration rencontrés. Un exemple de diagramme de fréquence est donné à la figure 2.
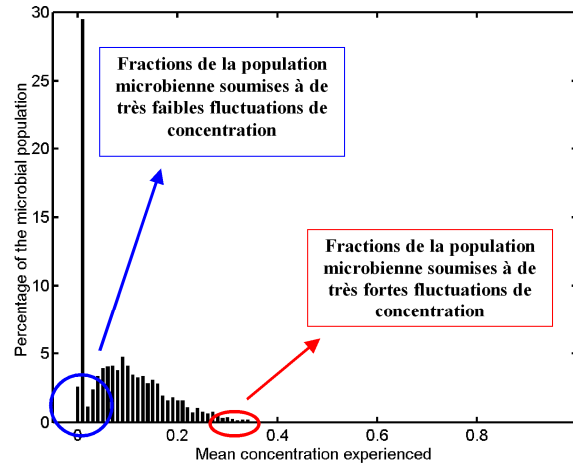
_____

Figure 2 : exemple de diagramme de fréquence obtenu par la méthode de standardisation des résultats de simulation hydrodynamique (chapitre 6). La simulation présentée ici met en œuvre une population microbienne de 3500 cellules circulant dans un réacteur dans lequel se développe un gradient de substrat.

L'histogramme de fréquence présenté à la figure 2 fait apparaître les différentes fractions la population microbienne soumises à des gradients de concentration plus ou moins importants. Cette approche a permis d'expliquer les chutes de rendements notées lorsque le débit de recirculation entre la partie mélangée et la partie non mélangée d'un réacteur *scale-down* était diminué. En effet, lorsque le débit de recirculation baisse, on note un étirement de l'histogramme de fréquence (figure 2) vers la droite, ce qui se traduit par une plus grande proportion de micro-organismes soumis à des gradients de concentration intenses.

9.4. Elaboration d'un modèle de cinétique microbienne prenant en compte les performances du bio-réacteur (chapitre 8)

La deuxième composante de la problématique (figure 1) était le micro-organisme lui-même. Afin d'étudier au mieux le comportement des micro-organismes face à l'hydrodynamique du réacteur, un modèle stochastique de cinétique microbienne a été proposé. L'expression d'un modèle de cinétique microbienne sous forme stochastique permet d'une part d'uniformiser les techniques de modélisation

utilisées au cours de ce travail, et d'autre part d'effectuer plus facilement la connexion entre le modèle de cinétique microbienne et les modèles hydrodynamiques élaborés précédemment.

Le modèle stochastique de cinétique microbienne proposé dans ce travail repose sur la détermination aléatoire des temps de génération de chaque cellule de la population considérée (dans notre cas, 3500 cellules microbiennes ont été considérées au début de chaque simulation). A ce niveau, la principale difficulté réside dans la détermination de la distribution de probabilité à partir de laquelle les temps de génération sont déterminés. Il a été démontré qu'une distribution de type log-normale était bien adaptée pour reproduire les courbes expérimentales de cinétique microbienne. En mode *batch*, la distribution possède une forme constante. Par contre, en mode *fed-batch*, l'allure de la distribution évolue de manière continue, ce qui reflète bien les contraintes physiologiques subies par la population microbienne lorsque celle-ci occupe de plus en plus de place dans le réacteur. Cela a été exprimé au niveau du modèle par une augmentation exponentielle de la moyenne et de l'écart-type de la distribution de probabilité.

Lorsque les contraintes hydrodynamiques deviennent prépondérantes, la distribution de probabilités a été remplacée par une probabilité pour chaque cellule microbienne de subir un stress hydrodynamique. Cette probabilité de ressentir un stress hydrodynamique a été déterminée à partir de données extraites des modèles hydrodynamiques stochastiques. Le modèle obtenu de cette manière permet de faire le lien entre la composante « micro-organisme » et la composante « bio-réacteur », et permet de mieux comprendre les facteurs influençant les rendements en biomasse lors d'un changement d'échelle de réacteur ou lors d'une modification de conditions opératoires. En effet, ce modèle permet de reproduire les courbes de cinétique microbienne obtenues lors des essais dans différents réacteurs *scale-down*.

9.5. Conclusion générale

Ce travail concerne la caractérisation de l'impact du bio-réacteur sur les performances des bio-procédés. Les deux composantes de la problématique, c'est-à-dire le bio-réacteur et le micro-organisme, ont été modélisées et des expériences de

cinétique microbienne en réacteur *scale-down* ont été menées afin de valider ces modèles. La conclusion de ce travail reprendra donc ces trois points.

- Le modèle hydrodynamique de bio-réacteur consiste a superposer un modèle de mélange et une modèle de circulation de manière a obtenir les profils de concentration rencontrés par les micro-organismes durant leur séjour dans le réacteur (Chapitres 3 et 4). Les résultats de simulation ont permis d'expliquer les différences de rendement en biomasse obtenues pour des réacteurs *scale-down* et des réacteurs agités classiques (Chapitres 5 et 6).

- Le modèle de cinétique microbienne repose sur la détermination stochastique des temps de mélange pour une population microbienne donnée (dans notre cas, une population microbienne initiale de 3500 individus a été considérée). Les données du modèle hydrodynamique ont été intégrées pour réaliser la détermination stochastique des temps de génération des cellules microbiennes (Chapitre 8). Cette approche a permis d'obtenir des courbes de cinétique microbienne aussi bien pour des cultures *batch*, que pour des cultures *fed-batch*. De plus, les résultats obtenus sont en accord avec les expériences réalisées en réacteur *scale-down*. Néanmoins, le modèle de cinétique microbienne peut encore être affiné de manière à obtenir des informations supplémentaires sur l'état physiologique des cellules. Ceci sera discuté plus en détail dans les perspectives de ce travail.

- Les expériences réalisées en réacteur *scale-down* ont permis de mettre en évidence un effet de l'hydrodynamique du réacteur sur les rendements en biomasse. Les expériences ont été réalisées en considérant deux micro-organismes : une bactérie de type *Escherichia coli* et une levure de type *Saccharomyces cerevisiae*. Dans les deux cas, une baisse des performances de circulation du réacteur *scale-down* a entraîné une chute importante du rendement en biomasse en fin de culture. Il est intéressant de noter qu'un effet hydrodynamique analogue a été observé à la fois pour *E. coli* et *S. cerevisiae*, qui sont pourtant deux micro-organismes éloignés du point de vue phylogénie. Néanmoins, ces deux organismes présentent certaines

similitudes au niveau de leur métabolisme du glucose qui pourraient expliquer l'analogie au niveau des effets hydrodynamiques observés. Premièrement, *E. coli* et *S. cerevisiae* sont tous deux des micro-organismes sensibles aux fortes concentrations en glucose qui entraînent chez eux l'induction de voies métaboliques « surverse » (l'excès de glucose est transformé en acétate dans le cas de *E. coli* et en éthanol dans le cas de *S. cerevisiae*). Deuxièmement, on observe pour ces deux micro-organismes des phénomènes d'oscillations métaboliques (surtout au niveau de la glycolyse et des voies annexes d'assimilation du glucose) lorsque la concentration en glucose extracellulaire fluctue. Lors de ce travail, il a été avancé que ce phénomène d'oscillations métaboliques pouvait être responsable de l'effet hydrodynamique noté lors des expériences.

9.6. Perspectives

Le présent travail ouvre de nouvelles perspectives d'approfondissement des connaissances relatives aux deux composantes de la problématique abordée dans ce travail : le bio-réacteur et le micro-organisme.

Au niveau de la composante « bio-réacteur » de la problématique, celle-ci a été abondamment abordée tant au niveau expérimental qu'au niveau de la modélisation mathématique. Cependant, deux problèmes ont été relevés concernant le modèle hydrodynamique stochastique. Le premier problème concerne le manque de résolution au niveau des gradients de concentration. En effet, la résolution dépend directement du nombre d'états utilisés pour représenter le réacteur. Plus ce nombre d'états est élevé et plus grande est la résolution au niveau du calcul des gradients de concentration locaux. Néanmoins, l'augmentation du nombre d'états implique une connaissance *a priori* du sens et de l'orientation des écoulements locaux, qui ne sont pas toujours connus, comme dans le cas notamment de la partie non mélangée des réacteurs *scale-down*. L'augmentation de la résolution spatiale du modèle implique donc la mise en œuvre de techniques avancées du génie chimique, comme par exemple la *Laser Induced Fluorecence* [3], qui permet de suivre avec une grande précision et une grande résolution spatiale (au niveau du pixel) la répartition de

molécules de fluorochrome au sein d'un réacteur. Le second problème concernant l'utilisation des modèles hydrodynamiques stochastiques décrits dans ce travail est le temps de simulation relativement élevé requis pour simuler la circulation des micro-organismes dans le réacteur. Malheureusement, ce problème ne peut pas être contourné à l'heure actuelle.

La modélisation mathématique de l'hydrodynamique du bio-réacteur est relativement bien détaillée dans ce travail. Néanmoins, outre l'homogénéisation, d'autres types d'opération de mélange peuvent s'avérer importants dans le cadre des bio-procédés. Citons par exemple le problème du transfert d'oxygène. Ce problème peut également être traité par une approche de modélisation structurée [4, 5] et la méthodologie présentée au cours de ce travail peut être appliquée à la caractérisation des fluctuations en oxygène dissous perçues par les micro-organismes.

Au niveau de la composante « micro-organisme » de la problématique, une des perspectives importantes de ce travail est l'élaboration d'un modèle de cinétique microbienne prenant en compte les fluctuations environnementales induites par l'hydrodynamique du réacteur. La complexité concernant ce type modélisation mathématique réside dans le fait que plusieurs sous-modèles sont requis afin d'obtenir un modèle réaliste du point de vue physique et biologique :

- un premier sous-modèle permettant de décrire la perception des fluctuations environnementales au niveau intracellulaire. En effet, des éléments de la littérature laissent à penser que le micro-organisme est capable de « filtrer » le bruit extracellulaire afin d'optimiser ses réactions biochimiques internes [6, 7]. Ce sous-modèle est particulièrement important dans le cadre de ce travail puisqu'il permet d'effectuer un lien direct entre la composante « bio-réacteur » et la composante « micro-organisme ».

- un deuxième ensemble de sous-modèles permettant de prendre en compte les aspects concernant les voies génétiques et métaboliques régulant l'activité de la cellule. Les systèmes d'induction et de répression des voies métaboliques peuvent être aisément modélisés par des techniques de « circuits intracellulaires » [8, 9]. Vu le nombre relativement restreint de molécules activatrices et inhibitrices, ainsi que des récepteurs intracellulaires, les systèmes d'induction et de répression sont également

soumis à des lois stochastiques [10]. La complexité de cette approche vient du nombre de voies ou de circuits à prendre en compte pour reproduire le phénomène visé.

- La troisième et dernière composante concerne la modélisation de la croissance cellulaire elle-même.

En rapport avec ce dernier sous-modèle, le modèle stochastique de cinétique microbienne mis au point au cours de ce travail (chapitre 8) permet d'intégrer les contraintes hydrodynamiques du réacteur et reflète bien l'impact de celles-ci sur la courbe de croissance microbienne. Néanmoins, ce type de modèle présente deux inconvénients :

- il est difficile à valider par des résultats expérimentaux, car il est basé sur les temps génération individuels des cellules microbiennes.

- il ne prend pas en compte l'état physiologique des cellules, ce qui comme nous l'avons vu précédemment doit faire l'objet d'un sous-modèle.

Ce dernier point est important pour la conduite d'un bio-procédé, les états physiologiques des cellules influençant la qualité finale du produit (dans le cas de la production de biomasse) ou la capacité de synthèse de molécules d'intérêt (dans le cas de la production de métabolites). Une des grandes perspectives de ce travail est le développement d'un modèle stochastique de cinétique microbienne ségrégé et structuré (c'est-à-dire prenant en compte les caractéristiques individuelles de chaque cellule et la dynamique interne de celle-ci) de manière à obtenir une représentation des différents états physiologiques des cellules de la population microbienne à un instant donné. Dans cette optique de caractérisation des états physiologiques des cellules microbiennes, les techniques de cytométrie en flux constituent un outil important [11]. Ces techniques ont d'ailleurs déjà été utilisées à de multiples reprises pour la mise en évidence de l'impact de l'hydrodynamique des réacteurs sur la physiologie microbienne [12, 13], ou sur l'impact du procédé sur la qualité technologique des cellules microbiennes [14].

La prise en compte de tout les phénomènes cités devraient permettre d'élaborer un modèle mathématique puissant permettant de simuler le comportement du micro-organisme (ou d'une population microbienne) face aux capacités hydrodynamiques du réacteur. D'une manière plus générale, ce type de modèle pourra être utilisé pour

234

décrire l'évolution d'une population microbienne dans n'importe quel type d'environnement (aliments, sols, cours d'eau,…). La difficulté pour parvenir à ce genre de résultat réside dans le nombre important de phénomènes à prendre en compte, ainsi que dans le manque de données au niveau de la dynamique des mécanismes intracellulaires.

Références

1. Patnaik P.R., *Can imperfections help to improve bioreactor performance ?* Trends in biotechnology, 2002. **20**(4): p. 135-137.
2. Vlaev D., Mann R., Lossev V., Vlaev S.D., Zahradnik J., Seichter P., *Macro-mixing and Streptomyces fradiae : modelling oxygen and nutrient segregation in an industrial bioreactor.* Trans IChemE, 2000. **78**: p. 354-362.
3. Fitch A.W., Ni X., *On the determination of axial dispersion coefficient in a batch oscillatory baffled column using laser induced fluorescence.* Chemical engineering journal, 2003. **92**: p. 243-253.
4. Mann R., Vlaev D., Lossev V., Vlaev S.D., Zahradnik J., Seichter P., *A network-of-zones analysis of the fundamentals of gas-liquid mixing in an industrial stirred bioreactor.* Récents progrès en génie des procédés, 1997. **11**(52): p. 223-230.
5. Zahradnik J., Mann R., Fialova M., Vlaev D., Vlaev S.D., Lossev V., Seichter P., *A network-of-zones analysis of mixing and mass transfer in three industrial bioreactors.* Chemical engineering science, 2001. **56**: p. 485-492.
6. Wolf D.M., Vazirani V.V., Arkin A.P., *Diversity in times of adversity : probabilistic strategies in microbial survival games.* Journal of theoretical biology, 2005. **234**(2): p. 227-253.
7. Rao C.V., Wolf D.M., Arkin A.P., *Control, exploitation and tolerance of intracellular noise.* Nature, 2002. **420**(14): p. 231-237.
8. Basu S., Karig D., Weiss R., *Engineering signal processing in cells : towards molecular concentration band detection.* Natural computing, 2003. **2**: p. 463-478.
9. Hasty J., McMillen D., Collins J.J., *Engineered gene circuits.* Nature, 2002. **420**(14): p. 224-230.
10. Santoso L., Booth H.S., Burden C.J., Hegland M., *A stochastic model of gene switches.* ANZIAM journal serie C, 2005. **46**: p. 530-543.
11. Srienc F., *Cytometric data as the basis for rigorous models of cell population dynamics.* Journal of biotechnology, 1999. **71**: p. 233-238.
12. Hewitt C.J., Nebe-Von Caron G., Axelsson B., Mc Farlane C.M., Nienow A.W., *Studies related to the scale-up of high-cell-density E. coli fed-batch fermentations using multiparameter flow cytometry : effect of a changing microenvironment with respect to glucose and dissolved oxygen concentration.* Biotechnology and bioengineering, 2000. **70**(4): p. 381-390.

13. Enfors S.O., Jahic M., Rozkov A., Xu B., Hecker M., Jürgen B., Krüger E., Schweder T., Hamer G., O'Beirne D., Noisommit-Rizzi N., Reuss M., Boone L., Hewitt C., McFarlane C., Nienow A., Kovacs T., Trägardh C., Fuchs L., Revstedt J., Friberg P.C., Hjertager B., Blomsten G., Skogman H., Hjort S., Hoeks F., Lin H.Y., Neubauer P., van der Lans R., Luyben K., Vrabel P., Manelius A., *Physiological responses to mixing in large scale bioreactors.* Journal of biotechnology, 2001. **85**: p. 175-185.

14. Müller S., Lösche A., *Population profiles of a commercial yeast strain in the course of brewing.* Journal of food engineering, 2004. **63**: p. 375-381.

ANNEXE

Principes d'élaboration des modèles stochastiques pour la simulation de l'hydrodynamique des bio-réacteurs mécaniquement agités

1. Introduction

Les modèles hydrodynamiques de bio-réacteurs utilisés au cours de ce travail possèdent deux caractéristiques principales :

- ils sont structurés : le bio-réacteur n'est pas considéré comme une boîte noire, mais comme un réseau de zones fluides considérées comme parfaitement mélangées[1]. Ce concept très important a été développé à l'origine pour simuler l'influence du mélange sur les réactions dans l'industrie chimique de base [1]. Il a été appliqué dans le cadre de cette étude pour calculer les gradients de concentration au sein des bio-réacteurs.
- ils sont stochastiques : en d'autres termes, cela signifie que le passage d'une molécule ou d'une particule d'une zone de fluide à une autre (appelée état dans le cas des modèles stochastiques) est gouverné par une probabilité. Le but de cette annexe est de décrire l'élaboration de ce type de modèle.

2. Exemple préliminaire

Pour faciliter la compréhension des principes mathématiques et algorithmiques utilisés pour l'élaboration des modèles stochastiques, un exemple concret est décrit dans les lignes qui suivent. La figure 1 montre un exemple simplifié de modèle hydrodynamique structuré de bio-réacteur comprenant deux zones de fluide (le modèle à deux zones constitue la configuration minimale pour un modèle structuré).

---

[1] Dans la littérature, ces zones de fluide sont appelées « zones », « compartiments », ou encore « états » dans le cas particulier des modèles stochastiques
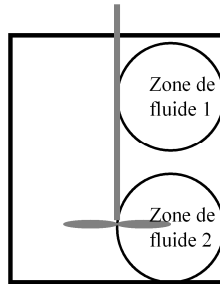
Figure 1 : modèle hydrodynamique structuré comprenant deux zones de fluide

Le processus stochastique qui est utilisé pour simuler l'homogénéisation d'un traceur au sein du réacteur est un processus de Markov (encore appelé chaîne de Markov). Le modèle à chaîne de Markov utilisé au cours de ce travail est discret au niveau temporel et au niveau spatial.

La discrétisation au niveau spatial implique un espace « d'états » S. Dans notre cas, ces états S_i correspondent aux zones de fluides au sein du réacteur agité. Une manière pratique de représenter ces états au sens de Markov est le graphe de transition [2, 3]. Dans le cas de la structure de modèle de la figure 1, le graphe de transition est le suivant :
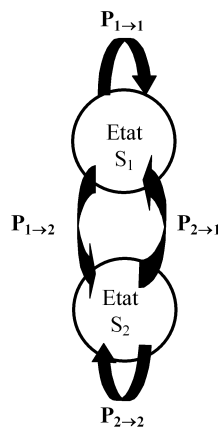

Figure 2 : graphe de transition correspondant au modèle d'écoulement de réacteur présenté à la figure 1

Le graphe de transition présenté à la figure 2 fait bien apparaître les probabilités de transition entre les états S_1 et S_2 du modèle. Les probabilités de transition d'une

chaîne de Markov à temps discret peuvent être rassemblées dans une matrice de transition T. Dans le cas du graphe de transition du modèle présenté à la figure 2, la matrice de transition est la suivante :

$$T = \begin{bmatrix} P_{1 \rightarrow 1} & P_{1 \rightarrow 2} \\ P_{2 \rightarrow 1} & P_{2 \rightarrow 2} \end{bmatrix} \qquad \text{(A-1)}$$

Avec $P_{i \rightarrow j}$ étant la probabilité de passer de l'état i à l'état j. Deux conditions sont requises au niveau de la valeur de ces probabilités :

- la somme des valeurs des probabilités d'une même ligne de la matrice T est égale à 1
- la valeur de chacune des probabilités est strictement inférieure à 1 (sauf dans le cas des états dits « absorbants », pour lesquels la valeur correspondante de probabilité est égale à 1)

La discrétisation au niveau spatial étant définie, il reste à décrire l'évolution du système au niveau temporel. Le modèle étant également discret en temps, une discrétisation temporelle est également requise et implique de considérer l'espace d'état de la chaîne de Markov à des temps donnés. La chaîne de Markov est alors représentée par l'équation suivante :

$$S_t = T \times S_{t-1} \qquad \text{(A-2)}$$

De manière développée :

$$\begin{bmatrix} S_{1,t} \\ S_{2,t} \end{bmatrix} = \begin{bmatrix} P_{1 \rightarrow 1} & P_{1 \rightarrow 2} \\ P_{2 \rightarrow 1} & P_{2 \rightarrow 2} \end{bmatrix} \times \begin{bmatrix} S_{1,t-1} \\ S_{2,t-1} \end{bmatrix} \qquad \text{(A-3)}$$

Ce qui signifie que le vecteur d'états S au temps t ne dépend que du vecteur d'états au temps t-1 et pas des vecteurs d'états précédents. En d'autres termes, un processus de Markov est un processus stochastique pour lequel le comportement futur du système ne dépend que du présent et pas de l'histoire passée du système. Cette propriété est connue sous s le nom de propriété de Markov [2, 3] et à des implications très importantes au niveau du présent travail. En effet, la simplicité du processus de Markov au niveau de la formulation mathématique en fait un algorithme rapide au niveau temps de simulation, mais ne permet pas de suivre le passage d'un élément particulier d'état en état au cours du temps. Le processus d'homogénéisation peut

donc être simulé, mais ce n'est pas le cas du processus de circulation ou du déplacement d'éléments[2] au sein du réacteur. Pour réaliser de telles simulations, un autre type de processus stochastique doit être utilisé. Dans ce cas, la matrice de transition et les différents états du modèle sont toujours valables, mais l'algorithme de développement temporel doit être modifié. Un algorithme simple pour ce type d'application et la simulation de Monte Carlo. Celui-ci sera décrit au cours du paragraphe 3.

Avant d'aller plus loin dans la discussion, il est important d'éclaircir un aspect conceptuel lié au modèle hydrodynamique stochastique. En effet, lors de l'introduction de cette partie annexe, les modèles hydrodynamiques structurés de réacteur ont été définis comme étant des réseaux d'éléments considérés comme étant parfaitement mélangés. A ce niveau, la question suivante se pose : l'état au sens de Markov (dans notre cas, une zone fluide) peut-il être considéré comme un élément parfaitement mélangé ? Pour répondre à cette question, il est utile de rappeler les deux types d'écoulement idéaux utilisés en génie chimique pour la modélisation des écoulements réels au sein des réacteurs :

- l'élément parfaitement mélangé, pour lequel un soluté est instantanément homogénéisé dans le volume de l'élément dès son entrée dans celui-ci
- l'élément piston, pour lequel un soluté entrant au temps t dans l'élément en ressort inchangé au temps t+r (r étant le temps de rétention au sein de l'élément piston)

Pour représenter une courbe de sortie de traceur dans un réacteur piston au niveau d'un état de Markov, les probabilités de transition de sortie de cet état doivent répondre à [4] :

$$P_{sortie} = \begin{cases} 0 & t \langle t+r \\ 1 & t=t+r \\ 0 & t \rangle t+r \end{cases} \quad (A-4)$$

---

[2] Par éléments, il est entendu des particules ou des micro-organismes dans le cas de la simulation d'un processus de circulation ou des molécules en solution dans le cas de la simulation d'un processus d'homogénéisation

Tout état ayant des valeurs de probabilités de sortie différentes de celles proposées dans cette équation peuvent être considérés comme parfaitement mélangés. Les probabilités de transition de sortie utilisées dans cette étude ont des valeurs strictement inférieures à 1, ce qui implique que les états du modèle peuvent être considérés comme parfaitement mélangés.

3.   Application de la procédure de modélisation stochastique à un cas concret

Les principes de base d'élaboration d'un modèle stochastique ayant été décrits, un exemple concret de modèle utilisé dans ce travail peut maintenant être abordé. La figure 3 reprend le schéma du modèle stochastique utilisé pour décrire l'hydrodynamique au sein d'un réacteur *scale-down*.
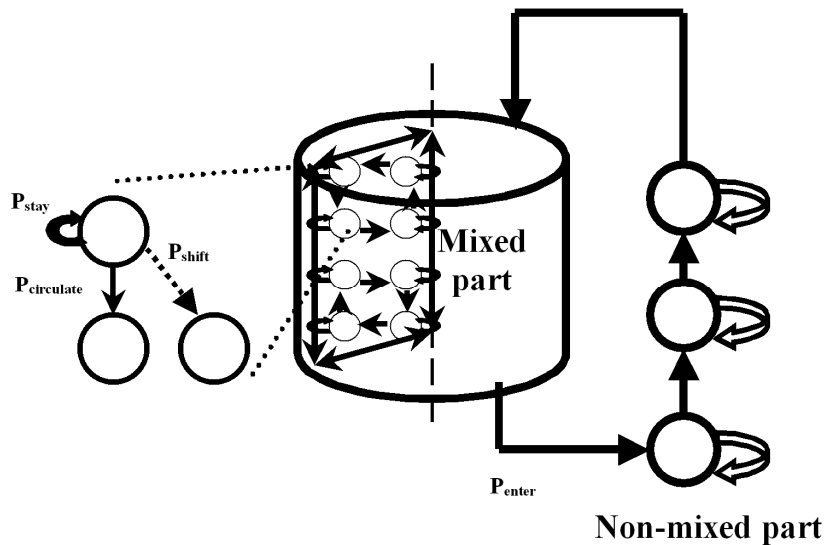
Figure 3 : schéma du modèle stochastique utilisé pour simuler l'hydrodynamique d'un réacteur *scale-down*. Huit plans comprenant chacun 8 états ont été mis en œuvre pour modéliser la partie mélangée du réacteur et trois états placés en série ont été utilisés pour modéliser la partie non mélangée

Dans ce cas, la matrice de transition est une matrice de 67 éléments sur 67 (le modèle comprenant 67 états ou zones de fluide) ayant la structure suivante :

$$T =$$

$$\begin{pmatrix}
1\text{-Pplug} & \text{Pplug} & 0 & 0 & \cdots \\
0 & 1\text{-Pplug} & \text{Pplug} & 0 & \cdots \\
0 & 0 & 1\text{-Pplug} & \text{Pplug} & \cdots \\
& & & \vdots & \\
\text{Pexit} & 0 & \cdots & & \text{Pcirc} \;\; \text{Pt3}
\end{pmatrix}$$

A partir de cette matrice, l'équation A-2 peut être utilisée pour simuler l'avancement du vecteur d'état du système au cours du temps. Au niveau numérique, cette procédure peut être représentée de la manière suivante[3] :

```
for i=1:t
S(1:67,i) = T^i*S(1:67,0);
end
```

Comme dit précédemment, cet algorithme ne peut être utilisé que pour simuler le processus d'homogénéisation. Pour simuler la circulation de particules ou de micro-

---

[3] Les notations pour les algorithmes sont valables dans le cas du logiciel MatLab

organismes, un processus de Monte Carlo reposant sur la génération de nombres aléatoires doit être employé. Cet algorithme fait intervenir plusieurs étapes :

- pour un élément en mouvement dans le réacteur et pour une transition, génération d'un nombre aléatoire à partir d'une distribution normale
- comparaison de ce nombre aléatoire avec les probabilités contenues dans la matrice de transition du modèle
- sur base de cette comparaison, prise de décision (procédure numérique du type : **if** rand > T(i,j),…, **elseif**,….,**end**)

Le grand avantage de l'algorithme de type Monte Carlo est la prise en compte de l'historique des éléments qui se déplacent d'état en état dans le modèle, ce qui permet de représenter le processus de circulation dans le réacteur. Le désavantage de cette approche est le temps de simulation qui est directement proportionnel au nombre de particules considérées. Dans le contexte du travail, l'algorithme a été utilisé pour simuler le déplacement des micro-organismes au sein du réacteur. Vu les concentrations cellulaires très importantes dans les bio-réacteurs (de l'ordre de 10^9 cellules par ml), seul un nombre limité de micro-organismes a pu être considéré afin de limiter le temps de simulation.

Références

1. Mann R., Pillai S.K., El-Hamouz A.M., Ying P., Togatorop A., Edwards R.B., Computational fluid mixing for stirred vessels : progress from seeing to believing. Chemical engineering journal, 1995. 59: p. 39-50.
2. Solaiman B., Processus stochastiques pour l'ingénieur. Collection technique et scientifique des télécommunications. 2006: Presses polytechniques et universitaires romandes. 241 p.
3. Allen L.J.S., An introduction to stochastic processes with applications to biology. first ed. 2003, Upper Saddle River, New Jersey: Pearson Prentice Hall. 385 p.
4. Pippel W., Philipp G., Utilization of Markov chains for simulation of dynamics of chemical systems. Chemical engineering science, 1977. 32: p. 543-549.